

INAUGURAL – DISSERTATION

zur

Erlangung der Doktorwürde

der

Naturwissenschaftlich – Mathematischen Gesamtfakultät

der

Ruprecht – Karls – Universität

Heidelberg

vorgelegt von

Dipl. Ing. Jakub Konrad Sypień

aus Warschau, Polen

Tag der mündlichen Prüfung:

21 Juli 2006

**"Struktur-Reaktivitäts-Beziehungen von Aluminiumalkoxiden bei
katalysierten Copolymerisations-Reaktionen:
Aluminium 2,2' methylenbisphenoxide in der Synthese von Poly(Ether-
Carbonaten) ausgehend von Cyclohexenoxid und Kohlendioxid"**

Gutachter: Prof. Dr Eckhard Dinjus

Priv. Doz. Dr. Markus Enders

**"Structure-reactivity relationships in aluminium alkoxides-catalysed
co-polymerisation reactions: aluminum 2,2' methylenebisphenoxide in the
synthesis of poly(ether-carbonate)s
from cyclohexene oxide and carbon dioxide"**

**Thesis
for the Doctoral Degree
at the Joint Faculty of Natural Science and Mathematics
of the University of Heidelberg**

**published by
Mr. Jakub Sypien, Chemistry MSc Eng
from Warsaw, Poland**

Die vorliegende Arbeit wurde in der Zeit von April 2003 bis April 2006 unter Anleitung von Herrn Prof. Dr. E. Dinjus im Forschungszentrum Karlsruhe am Institut für Technische Chemie angefertigt.

Ich erkläre hiermit an Eides statt, dass ich die vorliegende Arbeit selbständig und ohne unerlaubte Hilfsmittel durchgeführt habe.

.....
Jakub Konrad Sypień

Agnieszce, mojej żonie

1	ABSTRACT	3
2	KURZFASSUNG	5
3	ABBREVIATIONS:	7
4	INTRODUCTION AND AIM OF WORK	9
5	DISCUSSION OF THE RESULTS	25
5.1	Synthesis of ligands	25
5.2	Synthesis of catalysts	27
5.3	Copolymerisation processes	66
5.4	Comparison of the best results for self-synthesised and literature-known compounds	86
5.5	Spectroscopic characterisation of isolated polymers	88
6	CONCLUSION AND OUTLOOK	94
7	EXPERIMENTAL PART	98
7.1	General remarks	98
7.2	Syntheses of bisphenols ligands	100
7.3	Syntheses of the aluminium complexes	101
7.4	Synthesis of polymers	119
7.5	The use of catalyst-cocatalyst system as an initiator of copolymerisation	132
8	STRUCTURAL FORMULAS	136
8.1	Structural formulas of 1-based complexes	136
8.2	Structural formulas of 2-based complexes	137
8.3	Structural formulas of 3-based complexes	138
8.4	Structural formulas of 4-based complexes	139
8.5	Structural formulas of 5-based complexes	140
8.6	Structural formulas of 6-based complexes	141
8.7	Structural formulas of 7-based complexes	142

9	BIBLIOGRAPHY	143
10	APPENDIX 1 - CRYSTAL STRUCTURES	150
10.1	Crystallographic data of the ligand 1	150
10.2	Crystallographic data of the complex 1a	151
10.3	Crystallographic data of the complex 1c	152
10.4	Crystallographic data of the complex 1d	153
10.5	Crystallographic data of the complex 1e	154
10.6	Crystallographic data of the complex 2d	155
10.7	Crystallographic data of the complex 2g	156
10.8	Crystallographic data of the complex 3a	157
10.9	Crystallographic data of the complex 3c	158
10.10	Crystallographic data of the complex 3f	159
10.11	Crystallographic data of the complex 3g	160
10.12	Crystallographic data of the complex 4a	161
10.13	Crystallographic data of the complex 4b	162
10.14	Crystallographic data of the complex 6a	164
10.15	Crystallographic data of the complex 6c	165
10.16	Crystallographic data of the complex 7g	167
11	DANKSAGUNG	169

1 Abstract

The design of “single site” catalysts for the co-polymerisation of carbon dioxide and cyclohexene oxide (CHO), investigations on their structure/reactivity relations as well as the optimisation of the reaction parameters were main objectives of this work. The ligands for the catalyst design are based on 2,2'-bisphenol derivatives, bridged by either the methylene bridge (**1-6** based ones) or a sulphide moiety (**7** based one). Most of the ligands used were already described in the literature. Their reactions with aluminium precursors (AlEt_3 , AlEt_2Cl , AlEt_2I generated *in situ* and $\text{Al}(\text{OPr}^i)_3$) yield aluminum bisphenoxide complexes, displaying reactive Al-Cl, Al- C_2H_5 or Al- OPr^i moieties. The structures of the isolated complexes generally depend on the solvent used and the substituents in the ligand structure (either “bare” or sterically demanding). Reacting alkyl aluminium precursors with bulky *ortho*-substituted bisphenol ligands (**1 – 5**) in coordinating solvents (THF – **1-5 a-b** or Et_2O – **1-4 c-d**), the complexes formed are of monomeric structure but, in non-coordinating solvents (pentane or hexane) dimeric complexes are formed (**1-4 e-f**, **5f**). The geometry around the aluminium atoms in the methylene-bridged complexes display distorted, tetrahedral features and are independent on the solvent used. Reacting 2,2'-methylenebis(4-phenol), **6**, with AlEt_3 in ether solvents afforded oligomeric complexes with different coordination numbers at the aluminium centres. A monomeric alkoxide complex, **7a**, was obtained in course of the reaction of AlEt_3 with 2,2'-thiobis(4-*tert*-octylphenol), **7**, in THF as solvent; it displays a trigonal bipyramidal geometry; in hexane a dimeric complex **7c** and its Al-Cl counterpart, **7f**, are formed. The reaction of the bisphenol ligands with $\text{Al}(\text{OPr}^i)_3$ yielded dimeric complexes bridged by isopropoxy moieties (**1-7 g**). All new complexes were structurally characterised by single crystal X-ray diffraction and by NMR and IR spectroscopy.

The synthesised aluminium compounds were employed as catalysts in the co-polymerisation of carbon dioxide and CHO. Although despite several attempts for the optimisation of the reaction parameters only the formation of poly(ether-carbonate)s was observed. There are some general correlations that were found and could be summarised as follow:

1. The catalytic activity of the monomeric complexes generally depends on the presence of solvent in the coordination sphere (strong or weak Lewis base): Et_2O -aluminium alkoxide adducts, **1-4 c-d**, that were expected to be more reactive than their THF-counterparts display generally lower selectivity to the copolymer than **1-4 a-b**. Moreover, activity of complexes displaying an Al-Cl moiety seems to be enhanced in comparison to those with Al-Et moieties (results for 3-based complexes: **3a** – 20.49 % of the CO_2 incorporation; **3b**

- 21.37 %; **3c** – 12.07 %; **3d** – 17.83 %, the reactivity means the amount of incorporated carbon dioxide into copolymer backbone).
2. An analogous relation was found for the dimeric chloro-aluminium bisphenoxide complexes, **1-4 f**, they seem to be generally more active if compared to related Al-Et complexes, **1-4 e** (e.g. **1e** – 16.95 %; **1f** – 19.74 %; **4e** – 12.82 %; **4f** – 13.97 %, but **2e** – 21.74 %; **2f** – 20.92 %).
 3. The dimeric isopropoxy-bisphenoxide complexes are generally more active than their corresponding dimeric ethyl-aluminium counterparts (e.g. **1e** – 16.95 %; **1g** – 18.76 %; **2e** – 21.74 %; **2g** – 23.81 %; **3e** – 19.19 %; **3g** – 20.41 %). The reason of such behaviour might be rather the better solubility of the catalysts in the CO₂-expanded liquid phase whereas the bulkiness of the substituents in the ligand structure seems to play a minor role only.

Changing the coordination at the aluminium centre by replacing 2,2'-methylenebisphenol with 2,2'-thiobisphenol afforded the catalyst with the highest ability of CO₂ incorporation, **7c**, which promises further improvement.

Analogously to other reported Al-salen based catalysts, the new aluminium alkoxide catalysts were also investigated in conjunction with a series of co-catalysts – ionic compounds and neutral Lewis bases - in order to optimise catalytic activity and to improve copolymer selectivity. This part of studies was performed with monomeric and bridged dimeric alkoxide complexes (**1b** and **2g**, respectively). In contrast to literature reported results for Al-salen based catalysts, here the use of co-catalysts leads to deactivation, most probably owing to the unfavourable, tetrahedral geometry found around the aluminium atoms and thus making the coordination of epoxide / carbon dioxide to the active place of the catalyst more difficult. However, in some cases enhanced selectivity to monomeric *cis*-cyclohexene carbonate was found.

This work shows that the aluminium bisphenoxides are easy to synthesise, giving access quite easily to a broad class of Lewis acid catalysts able to promote the copolymerisation of CHO with CO₂. The gathered data indicate a rich chemistry of the investigated catalysts and determine potential paths of their future development.

2 Kurzfassung

Das Design und die Synthese von "Single-Site"-Katalysatoren für die Copolymerisierung von Kohlendioxid und Cyclohexenoxid (CHO), Untersuchungen zu ihrer Struktur-Reaktivitätsbeziehung sowie die Optimierung der Reaktionsparameter waren Hauptaugenmerk dieser Arbeit. Die Liganden für das Katalysator-Design beruhen auf 2,2'-Bisphenol-Derivaten, entweder Methylene- (**1-6** basierte Systeme) oder Sulfid-verbrückt (**7** basierte Systeme). Die meisten der verwendeten Liganden wurden bereits in der Literatur beschrieben. Ihre Reaktionen mit Aluminiumverbindungen (AlEt_3 , AlEt_2Cl , AlEt_2I erzeugt *in situ* und $\text{Al}(\text{OPr}^i)_3$) führen zu Aluminiumbisphenoxid-Verbindungen mit reaktiven Al-Cl-, Al- C_2H_5 - oder Al-OPrⁱ-Einheiten. Die Strukturen der isolierten Komplexe hängen im allgemeinen vom verwendeten Lösungsmittel und den Substituenten in der Ligandenstruktur ab (entweder klein oder sterisch anfordernd). Aus den Reaktionen von Al-Alkyl-Verbindungen mit in *ortho*-Position mit sterisch anspruchsvollen Substituenten ausgestatteten Bisphenolderivaten (**1-5**) in koordinierenden Lösungsmitteln werden monomere Komplexe gebildet (THF - **1-5 a-b** oder Et_2O - **1-4 c-d**); in nicht-koordinierenden Lösungsmitteln (Pentan oder Hexan) werden dimere Komplexe (**1-4 e-f**, **5f**) gebildet. Die Geometrie um die Aluminiumatome in den Methylene-verbrückten Komplexen zeigt verzerrt tetraedrische Eigenschaften und ist Lösungsmittel-unabhängig. Die Reaktion von 2,2'-Methylenebis(4-Phenol), **6**, mit AlEt_3 in Ether führt zu einem oligomeren Komplex mit verschiedenen Koordinationszahlen an den Aluminiumzentren. Ein monomeres Alkoxidekomplex, **7a**, wurde im Laufe der Reaktion von AlEt_3 mit 2,2'-Thiobis(4-*tert*-octylphenol), **7**, in THF als Lösungsmittel erhalten; er zeigt eine trigonal-bipyramidale Geometrie; in Hexan wird ein dimerer Komplex **7c** und sein Al-Cl Gegenstück, **7f**, gebildet. Die Reaktion der Bisphenol Liganden mit $\text{Al}(\text{OPr}^i)_3$ führt zu dimeren Komplexen, überbrückt durch Isopropoxid-Einheiten (**1-7 g**). Alle neuen Komplexe wurden strukturell charakterisiert mittels Einkristallröntgen-Beugung, und NMR- und IR-Spektroskopie.

Die synthetisierten Aluminiumverbindungen wurden als Katalysatoren in der Copolymerisierung von Kohlendioxid und CHO eingesetzt. In allen Experimenten zur Optimierung der Reaktionsparameter und der Selektivität wird nur die Bildung von Polyethercarbonaten beobachtet. Es gibt einige allgemeine Korrelationen, die folgendermaßen zusammengefasst werden könnten:

1. Die katalytische Aktivität der monomeren Komplexe hängt von der Anwesenheit von Lösungsmittel in Koordinationssphäre des Al-Zentrums ab (starke oder schwache Lewis-Basen): Et_2O -Addukte an Aluminiumalkoxide-Verbindungen, **1-4 c-d**, die als reaktiver

eingeschätzt wurden als ihre THF-Analoga (**1-4 a-b**) zeigen generell eine geringere Selektivität zum Copolymer als **1-4 a-b**. Außerdem scheint die Aktivität von Komplexen, die eine Al-Cl-Einheit aufweisen, im Vergleich zu denjenigen mit Al-Et-Einheiten erhöht (Ergebnisse für **3**-basierende Komplexe: **3a** – 20.49 % eingebauten CO₂; **3b** – 21.37 %; **3c** – 12.07 %; **3d** – 17.83 %, höherer Einbau von Kohlendioxid ins Copolymer-Rückgrat).

2. Eine analoge Beziehung wurde für die dimeren Chloro-Aluminium-Bisphenoxide, **1-4 f**, gefunden, sie scheinen allgemein, wenn verglichen mit ihren verwandten Al-Et-Komplexen, **1-4 e**, aktiver zu sein.
3. Die dimeren Isopropoxid-Bisphenoxide-Verbindungen sind allgemein aktiver als ihre entsprechenden dimeren Ethyl-Aluminiumverbindungen (z. B. **1e** – 16.95 %; **1g** – 18.76 %; **2e** – 21.74 %; **2g** – 23.81 %; **3e** – 19.19 %; **3g** – 20.41 %). Der Grund solchen Verhaltens könnte eher die bessere Löslichkeit der Katalysatoren in der CO₂-expandierten flüssigen Phase sein, wohingegen die Sperrigkeit des Substituenten in der Ligandstruktur nur eine untergeordnete Rolle zu spielen scheint.

Das Ändern der Koordination am Aluminiumzentrum durch Ersetzen von 2,2'-Methylenbisphenolderivaten durch 2,2'-Thiobisphenolen führt zum Katalysator mit der höchsten Fähigkeit zum CO₂-Einbau, **7c**, welcher Gegenstand für zukünftige Verbesserung sein könnte.

In Analogie zu Berichten zu Al-Salen-Katalysatoren wurden die neuen Aluminiumalkoxid-Katalysatoren auch untersucht in Kombination mit einer Reihe von Cokatalysatoren – ionischen Verbindungen und neutralen Lewis-Basen, um ihre katalytische Aktivität zu steigern und die Copolymer-Selektivität zu verbessern. Dieser Teil der Studien wurde mit monomeren und dimeren Alkoxidkomplexen (entsprechend **1b** und **2g**) durchgeführt. Im Gegensatz zu den in der Literatur berichteten Ergebnissen für Al-Salen-Katalysatoren führt hier der Einsatz der Cokatalysatoren zur Deaktivierung, am wahrscheinlichsten infolge der ungünstigen tetraedrischen Geometrie um die Aluminiumatome, die die Koordination von Epoxide / Kohlendioxid an der aktiven Seite des Katalysators erschwert. Jedoch wurde in einigen Fällen eine erhöhte Selektivität zum monomeren, cyclischen cis-Cyclohexencarbonat beobachtet.

Diese Arbeit zeigt, dass Aluminiumbisphenoxide einfach zu synthetisieren sind und einen effizienten Zugang zu einer ausgedehnten Klasse von Lewis-Säurekatalysatoren geben, die fähig sind, die CHO mit CO₂ co-zu-polymerisieren. Die erfassten Daten zeigen eine reiche Chemie der untersuchten Katalysatoren und stellen mögliche Wege für ihre zukünftige in Aussicht.

3 Abbreviations:

ax. H in Cy – axial hydrogen atoms in cyclohexane ring

eq. H in Cy – equatorial hydrogen atoms in cyclohexane ring

Me – methyl

Cy – cyclohexyl

^tBu – tertbutyl

MeCy – 1-methylcyclohexyl

ⁱPr – isopropyl

ⁱPrO – isopropoxy

sm – small

m – middle

s – strong

br – broad

d – doublet

d of mpl - doublet of multiplets

PDI – Polydispersity Index

MDBPH₂ – 2,2'-methylenebis(4,6-di-*tert*-butylphenol)

MDBP – 2,2'-methylenebis(4,6-di-*tert*-butylphenato)

MMBPH₂ – 2,2'-methylenebis(4-methyl-6-*tert*-butylphenol)

MMBP – 2,2'-methylenebis(4-methyl-6-*tert*-butylphenato)

MMCyPH₂ – 2,2'-methylenebis(4-methyl-2-(1-methylcyclohexyl)phenol)

MMCyP – 2,2'-methylenebis(4-methyl-2-(1-methylcyclohexyl)phenato)

MCIMePrPH₂ – 2,2'-methylenebis(4-chloro-6-isopropyl-3-methylphenol)

MCIMePrP – 2,2'-methylenebis(4-chloro-6-isopropyl-3-methylphenato)

MTMPH₂ – 2,2'-methylenebis(4,6-di-methylphenol)

MTMP – 2,2'-methylenebis(4,6-di-methylphenato)

MCIPH₂ – 2,2'-methylenebis(4-chlorophenol)

MCIP – 2,2'-methylenebis(4-chlorophenato)

TBOPH₂ – 2,2-thiobis4-(1,1,3,3-tetramethylbutyl)phenol) or 2,2'-thiobis(4-*tert*-octylphenol)

TBOP – 2,2-thiobis4-(1,1,3,3-tetramethylbutyl)phenato) or 2,2'-thiobis(4-*tert*-octylphenato)

TMBPH₂ – 2,2'-thiobis(4-methyl-6-*tert*-butylphenol)

TMBP – 2,2'-thiobis(4-methyl-6-*tert*-butylphenato)

HDBBAH₂ – 2-hydroxy-3,5-di-*tert*-butylbenzyl alcohol

HDBBA – 2-hydroxy-3,5-di-*tert*-butylbenzyl alcoholate

EDBPH₂ – 2,2'-ethylenebis(4,6-di-*tert*-butylphenol)

EDBP – 2,2'-ethylenebis(4,6-di-*tert*-butylphenato)

DHMBH₂ – 2,2'-di(hydroxymethyl)biphenol

DHMB – 2,2'-di(hydroxymethyl)biphenyl

MMPEPH₂ – 2,2'-methylenebis(4,6-di(1-methyl-1-phenylethyl)phenol)

MMPEP – 2,2'-methylenebis(4,6-di(1-methyl-1-phenylethyl)phenato)

TBMPH₂ – 2,2'-thiobis(6-*tert*-butyl-4-methylphenol)

TBMP – 2,2'-thiobis(6-*tert*-butyl-4-methylphenato)

CHO – cyclohexene oxide

PO – propylene oxide

SO – styrene oxide

salen – N,N'-bis(salicydene)-1,2-ethylenediamine

salcy – N,N'-bis(salicydene)-1,2-cyclohexyldiamine

N-MeIm – N-methylimidazol

PPh₃ – triphenylphosphine

TEAPTS – [(C₂H₅)₄N]⁺[C₇H₇SO₃]⁻ – tetraethylammonium-*para*-toluenesulphonic acid

[((*n*-C₄H₉)₄N]Br – tetra-*n*-butylammonium bromide

[PPN]Cl – bis(triphenylphosphoranylidene) ammonium chloride

[Et₄N][MeC₆H₄SO₃] – tetraethylammonium *p*-toluenesulphonate

DMAP – 4-(dimethylamino)-pyridine

% of -CO₃- – percent of carbonate linkages

CPC – cyclic propylene carbonate

HP NMR – High Pressure Nuclear Magnetic Resonance

NOESY – Nuclear Overhauser Effect Spectroscopy

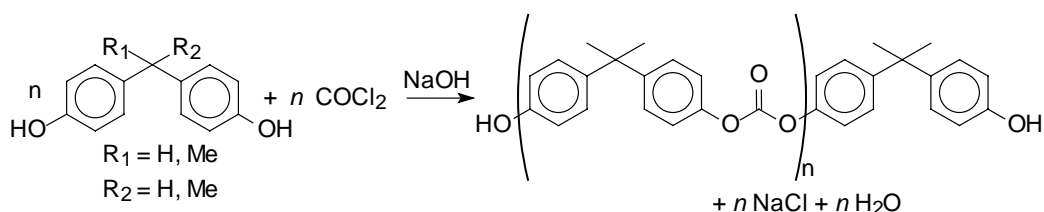
ROP – Ring Opening Polymerisation

M_n – Number Average Molecular Weight, [g / mole]

M_w – Weight Average Molecular Weight, [g / mole]

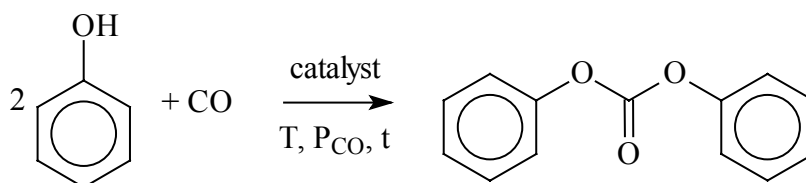
4 Introduction and aim of work

Polycarbonates as polymers in their commonly known form have been developed since 1930th, when Carothers run the first attempts to synthesise glycol esters of the carbonic acid.^{1,2} Polycarbonates as a result of the polycondensation reaction between reactive C₁-synthon (like e.g. phosgene) and aromatic diols (Scheme 1) are known since the end of 1950th.³ The most widely used diols are 2,2-bis(4-hydroxyphenyl)propane (Bisphenol A) and its derivatives. The investigated process is of paramount industrial importance, because of the advantageous properties of the isolated polymeric products, the low costs and availability of the reactants.

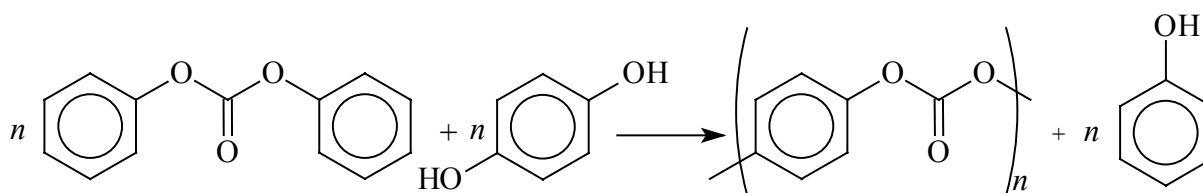


Scheme 1 Polycondensation reaction between reactive C₁-synthon (like e.g. phosgene) and aromatic diols.

Later, also carbon monoxide was used as a C₁-synthon on an industrial scale to produce diphenyl carbonate⁴⁻⁷ (Scheme 2), which is also widely used as a building block in polycarbonate chemistry, especially in its transesterification with bisphenol A derivatives (Scheme 3).

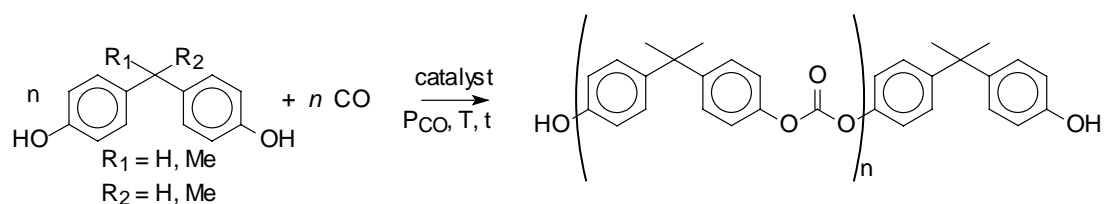


Scheme 2 Industrial production of diphenyl carbonate.



Scheme 3 Transesterification with diphenols giving poly(aromatic carbonates).

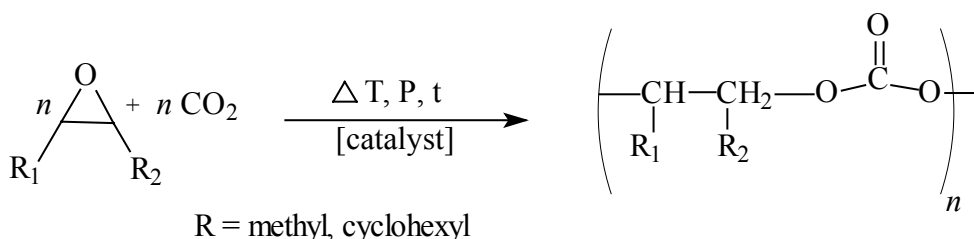
Owing to the high temperature required in the process (150 – 320°C) and the thermal instability of the reactants, this method is not as widely used as the polycondensation reaction. A direct synthesis of polycarbonates from carbon monoxide and aromatic diols like e.g. Bisphenol A is also possible, in the last decades the importance of that process increased regularly (Scheme 4).⁸



Scheme 4 *Direct synthesis of poly(aromatic carbonates) from carbon monoxide and aromatic diols.*

Taking into consideration the fact, that high-crystalline poly(aromatic carbonates) based on Bisphenol A have a high glass transition temperature (around 260°C) and display a very high versatility in the preparation of the final products, it is quite obvious that these polycarbonates find an ever-increasing use as engineering thermoplastics. With such characteristics as a high ductility, a very good transparency as well as a high heat and impact resistance poly(aromatic carbonates) are considered as special polymers and used for technological applications in many different fields.⁹

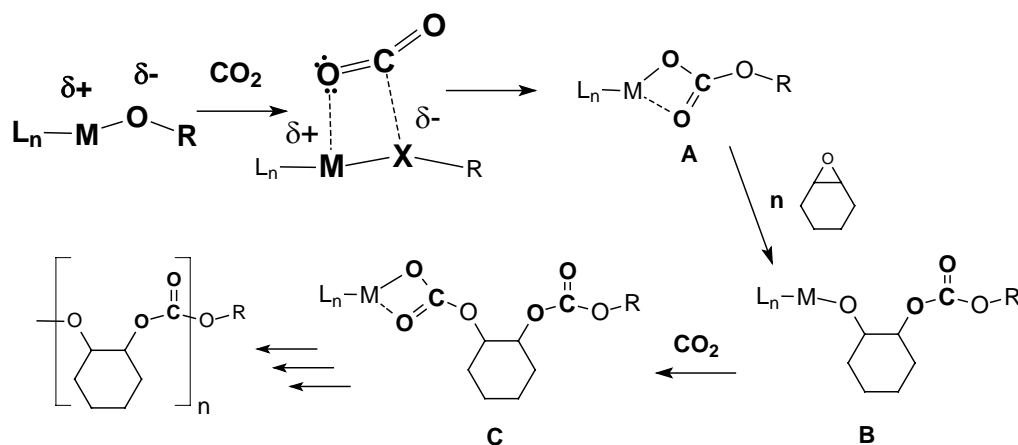
The replacement of hazardous organic solvents and chemicals by environmentally benign ones is a general growing tendency in chemical technology. Anastas and Warner¹⁰ have outlined the basic principle of a “Green Chemistry”, they listed general conditions, which each compound should fulfil, if it wants to be considered as a “green chemistry compound”. The carbon dioxide molecule fulfils some of these principles.¹¹ Its toxicity is lower than that of many organic solvents, it is naturally abundant and easy to handle. In the considered process, carbon dioxide can play the role of both solvent and reactant. It can be, after completion of the reaction, easily separated from the reaction mixture and released into the environment. In 1969 Inoue described for the first time that carbon dioxide and propylene oxide (PO) copolymerise to afford a poly(propylene carbonate) (Scheme 5).^{12,13} One more incentive is that the poly(aliphatic carbonates) obtained actually display promising characteristics such as a low toxicity and a good- to very good biodegradability¹⁴ making them a useful complement to the usual polycarbonates.^{15,16}



Scheme 5 *Synthesis of poly(aliphatic carbonates) from carbon dioxide and epoxides.*

Due to thermodynamic stability of carbon dioxide, the use of a catalyst for a copolymerisation reaction is necessary. There are some systems, mainly based on transition metals (such as monometallic systems based on Zn or Cr and bimetallic ones involving Zn-Co and Zn-Fe) and

main group elements (e.g. aluminium) alkoxides, which are interesting candidates as potential catalysts. A catalytic copolymerisation of epoxides with CO₂ requires two complementary coordination sites at the active centre. An acidic site (Lewis) allowing the epoxide to dock in (metallic core) and a nucleophilic site (oxygen of the alkoxide ligand) which is able to activate CO₂ and plays a role in the prolongation of the already-formed polycarbonate chain bound to the active centre of the catalyst (Scheme 6).

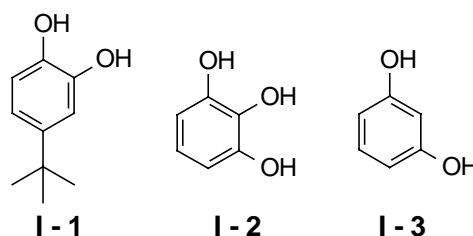


Scheme 6 *Schema of initiation of copolymerisation at the two complementary coordination sites at the active centre.*

On the basis of several mechanistic studies, it is proposed that the epoxide ring is firstly opened by a nucleophilic attack from the backside, several observations support this proposal: First of them is the fact that co-monomers susceptible to undergo only a cationic polymerisation (e.g. tetrahydrofuran, 7-oxabicyclo[2.2.1]heptane, oxepane) do not copolymerise with CO₂.¹⁷ Second, hydrolysing the copolymer produced from *cis*-cyclohexene oxide and CO₂ resulted in formation of *trans*-1,2-cyclohexanediol. The inversion of one of the C-O bonds in the epoxide indicates that the ring opening results from a S_N2 backside attack. Finally, studies with optically active epoxides established that the carbon atom, which is favoured for nucleophilic attack showed an inversion of configuration, again suggesting a nucleophilic S_N2 mechanism.^{18,19} The alternating character of the copolymer suggests that epoxide insertion is the rate-limiting step. Another important factor which has to be taken into account is that the investigated catalysts are also able to catalyse a ring opening polymerisation of the epoxide (homopolymerisation), however it is not a prerequisite for a successful copolymerisation that a catalyst has to be active toward both processes. If the CO₂ insertion were fast and the epoxide opening were slow, a CO₂ insertion would nearly always precede a subsequent epoxide opening, which is consistent with the observed alternating copolymer. On the other hand, if CO₂ insertion were the rate limiting step and epoxide opening were fast, the polymers would not be alternating, but instead, would have a high

percentage of ether linkages resulting from the sequential addition of the epoxide monomers as in an epoxide homopolymerisation. Morokuma mathematically confirmed through a theoretical approach (molecular modelling via DFT calculation) these considerations. Considering the most promising zinc(II) β -diiminate copolymerisation catalyst reported by Coates¹³⁶, the CO₂ insertion into the Zn–alkoxide bond and the formation of a Zn-alkylcarbonate bond is kinetically much more favourable than the thermodynamically favourable epoxide insertion, because of the high activation barrier for the latter. Only in the case of insertion of the sterically strained CHO into the Zn-carbonate bond, the barrier is low enough to compete against CO₂ insertion yielding alternating insertion, this is the rate-determining step of the discussed process.²⁰

Following the pioneering work of Inoue presented in 1969 dealing with complex hydroxo zinc complexes obtained from an hydrolysis of diethyl zinc, a number of papers exploring the catalytic activity of zinc(II) compounds in copolymerisation reactions were published. Scores of zinc(II) complexes were synthesised through the reaction of reactive zinc precursors with polyhydric ligands. The most investigated systems



were those based on ZnEt₂ and water, *tert*-butylcatechol **I-1**, pyrogallol **I-2**, or resorcinol **I-3**, prepared in different stoichiometrical ratios.^{17,21} Many epoxides and even some oxetanes were found to undergo a copolymerisation with CO₂, but owing to its low cost and good reactivity, propylene oxide became the most studied co-monomer of those days. An additional disadvantage of these catalysts was their usual insolubility, quite often the nature of the active species could not be elucidated. Despite some attempts of ligand's tuning²²⁻²⁷, the turnover numbers (TON) of these catalysts were rather low, varying between 5.9 for ZnEt₂/water^{12,13} and 13.8 for ZnEt₂/4-bromopyrogallol²², which appeared to be the most active system among the heterogeneous systems based on polyhydric phenols.

Studies dealing with differently substituted phenol derivatives were a natural continuation and development of Kuran's research. A major step in understanding and improving the zinc-catalysed polymerisation of CO₂ and epoxides was made in 1995 by Darensbourg, whose idea was to use a steric demanding phenol to obtain well-defined monomeric zinc bis(phenoxides) of the type [Zn(OAr)₂(Lewis base)₂]. These catalysts were based on 2,6-diphenylphenol and similar 2,6-disubstituted phenols.^{28,29} TONs obtained in copolymerisation reaction catalysed by the new zinc bis(phenoxide)s were far higher than the ones reported for the systems described by Kuran (TON up to the order of ca. 165, entry **I-4**, Table 1).²⁸ The use of well-

defined catalysts considerably facilitated the mechanistic studies of the copolymerisation process. When placed in a solution of cyclohexene oxide under CO₂, the 2,6-disubstituted zinc phenoxides produced high yields of the desired poly(cyclohexene carbonate), whereas it produced principally the monomeric, cyclic propylene carbonate when propylene oxide was employed as a substrate. The steric bulk of the poly(cyclohexene carbonate)'s backbone was said to prevent a zinc phenoxide-catalysed backbiting side-reaction necessary for a cyclic carbonate formation. In spite of being more expensive, the higher reactivity of cyclohexene oxide (a constrained bicyclic system) towards a CO₂ insertion and to the favoured formation of polymers over monomers has made CHO to the most common monomer for copolymerisation studies. A higher glass transition temperature of poly(cyclohexene carbonate) (~ 135 °C) compared to poly(propylene carbonate) (~ 33 °C) is one of its more advantages (higher stability of the final material, if required).

	Catalyst system	% of -CO ₃ -	M _n	PDI	TON	Ref
Copolymerisation of cyclohexene oxide with carbon dioxide						
I-4	Zn-(2,6-OC ₆ H ₃ Ph ₂) ₂ (Et ₂ O) ₂	91	38000	4.5	165.6	28
I-5	Zn-(2,6-OC ₆ H ₃ F ₂) ₂ (Py) ₂	> 99	no data	no data	no data	29
I-6	Zn-(2,4,6-OC ₆ H ₂ (Bu ^t) ₃) ₂ (PCy ₃)	> 99	no data	no data	472.0	32
I-7	[Zn-(2,6-OC ₆ H ₃ F ₂) ₂ (PCy ₃) ₂]	> 99	no data	no data	no data	30
I-8	[Zn-(2,6-OC ₆ H ₃ F ₂) ₂ (THF) ₂]	> 99	42000	6.0	280.1	30
I-9	[Zn-(O ₂ C-2,6-Cl ₂ C ₆ H ₃) ₂ (THF) ₃]	> 99	no data	no data	182.4	133
I-10	Zn precursor / HOOC-CH=CH-CH ₃	84	8.4- 15 * 10 ⁴	6.5-16.0	252.8 ^a	41
I-11	ZnO / HOCOCH=CHCOO(CF ₂) ₇ CF ₃	93	109000	6.4	161.2	42
I-12	[Al-(OC(Ph) ₃) ₂ (OPr ^t)]	no data	no data	no data	no data	63
I-13	[Al-(2,6-OC ₆ H ₂ (Bu ^t) ₂ (4-Me)(OPr ^t)]	no data	no data	no data	no data	63
I-14	[Al-(OC ₆ H ₁₃) ₂ Cl]	7.69	4531	2.62	287.8	128
I-15	[Al-(OCHC=HCOCOC ₈ H ₁₇) ₂ Cl]	21.74	4985	2.89	492.6	128
Copolymerisation of propylene oxide and carbon dioxide						
I-16	Zn(OH) ₂ / glutaric acid	>95	12000	no data	44.3	37
I-17	ZnO / glutaric acid	> 99	143000	2.4	134.0	36

Table 1 Comparison of reactivity of different phenoxide systems, a – yield given in g pol. / g cat.

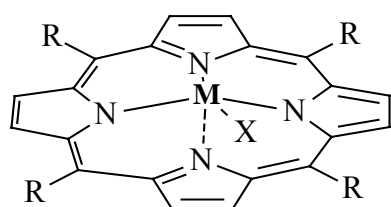
Several additives, also called co-catalysts, such as triphenyl phosphine (PPh₃), tricyclohexyl phosphine (PCy₃), 4-(dimethylamino)-pyridine (DMAP) as well as quaternary ammonium salts actually enhance the reactivity of the catalyst, leading to alternating copolymerisation even when the catalyst alone does not work efficiently. They could be used in a pure form, added to the reaction mixture together with the main catalyst, or as a co-ligands (procedure commonly used in case of phosphines) replacing for e.g. weaker Lewis base such as THF. Such ligand exchange resulted, depending on the reaction conditions, in the formation of monomeric zinc compounds, (ArO)₂Zn(PR₃)₂ (e.g. **I-5**)²⁸ or the corresponding dimeric ones like [Zn(OAr)₂(PR₃)₂]₂ (R = Cy, ^tBu, Me; e.g. **I-7**).³⁰ The variation of the phenolic substituents (e. g. fluorine atoms, tert-butyl and methyl groups in place of phenyl group) yielded catalysts with relatively high TONs of the order of magnitude of 470.^{31,32} The control of the

propagation reaction (as it can be seen in the Table 1, the efficiency of alternating polymerisation was almost 100%, entry **I 4-8**) was achieved through the use of catalysts, where only one coordination site was available for epoxide binding on each Zn centre and the most part of the zinc alkoxide was “shielded” by a ligand. Analysing the collected data, Darensbourg suggested that probably only one metal binding site is required for copolymerisation, but that two binding sites are needed for consecutive epoxide insertions to be competitive with the very rapid CO₂ insertion process. As it can be seen in that particular case, the chemical surroundings of the coordination centre directly influence the stereochemistry of the reaction.

The first attempts of use of different mono- and polycarboxylic acids employed as organic moieties have shown rather low yields, comparable to those obtained using ZnEt₂-polyhydric phenols systems (up to 9.8 g / g cat. for ZnEt₂ / *L*-mandelic acid).²⁷ Catalysts obtained via the reaction between the Zn precursor (such as ZnO, Zn(OH)₂, Zn(OAc)₂) with aliphatic carboxylic acids produced PPC copolymers with relatively low molecular weights and large polydispersities in a low yield over 2.5–15.4 g polymer per gram of catalyst.³³⁻³⁷ Recently Ree assumed that the preparation method of the catalyst has to play a significant role in its activity, and indeed, the preparation of zinc glutarate following four different reaction paths afforded the same product having completely different activities (the results for the best one are presented as **I-17** in the Table 1).³⁶ This polymer yield (64 g / g cat. or 134 TON) is marked as the highest value among the polymerisation yields that have been reported for this heterogeneous coupling of PO-CO₂ and is significantly higher than the maximum yield (ca. 34 g of polymer per gram of catalyst) ever reported in the literature.^{33-35,39,40} The use of unsaturated crotonic acid as a organic moiety of Zn-based catalyst **I-10** afforded product being active toward the copolymerisation of cyclohexene oxide and carbon dioxide with turnover frequencies approaching 252.8 g / g of Zn.⁴¹ Affording polymer with the weight average molecular weights (*M_w*) ranged from 84 000 to 150 000 and the corresponding polydispersities varied between 6.51 and 15.97; such high values of PDI are characteristic for coordinative anionic polymerisation system. In course of Darensbourg’s investigation it has been shown that only 10 % of the anticipated epoxide binding sites were available for catalysis. Darensbourg reported also new air-stable, well-soluble multi-centred zinc benzoate clusters utilising halogenated ligands. These new zinc carboxylates are able to copolymerise cyclohexene oxide with carbon dioxide with relative high TON (entry **I-9**, Tab. 1) as well as to catalyse a terpolymerisation with propylene oxide as subsequent epoxidic substrate. Additionally, Beckman functionalised the carboxylate ligand with perfluorinated rests by

reacting perfluorooctanol with maleic acid.⁴² The perfluoro zinc hemiesters obtained after reaction of the derivatised ligand with zinc oxide, **I-11**, were soluble in supercritical carbon dioxide, and displayed a high activity in the copolymerisation of CHO with CO₂. He indicated also that between two catalysts having the same carboxylic ligand but different metal cores – Al and Zn those based on Al afforded the highest yields of polymer but a fair-to-low carbon dioxide insertion, these results are reported as **I-14** and **I-15** (see Tab. 1).

Inoue suggested that owing to their structural similarity to chlorophyll, porphyrins should have a comparable ability to activate CO₂, and indeed, certain porphyrin-based compounds, like e.g. **I-18**-based were active.⁴³⁻⁴⁵ First attempts have shown that the reaction times required to complete the reactions were on a day-scale (up to 23 days were reported), the obtained yields were of the order of a few g of polymer / g of cat. Aluminium-based catalysts based on porphyrin framework appeared to be active toward copolymerisation of CO₂ and



- I-18a M = Al , R = -C₆H₅ , X = Cl
 I-18b M = Al , R = -C₆H₅ , X = OMe
 I-19a M = Cr , R = -C₆H₅ , X = Cl
 I-19b M = Cr , R = -C₆F₅ , X = Cl
 I-20 M = Mn , R = -C₆H₅ , X = OAc

different epoxides as presented in Table 2. Quaternary ammonium (such like Et₄NBr) and phosphonium (like

EtPh₃PBr) salts were successfully used as co-catalysts, interestingly these salts alone do not catalyse the reaction between carbon dioxide and epoxide under similar conditions.⁴⁶ These porphyrinic systems (specially **I-18a**) appeared to be able to activate PO, CHO as well EO.^{36,46}

	Co-catalyst	% of -CO ₃ -	M _n	PDI	TON	Ref.
Copolymerisation of cyclohexene oxide and carbon dioxide						
I-18a	EtPh ₃ PBr, 1	>99	6200	1.06	0.30 ^a	46
I-19a	DMAP, 1	low molecular weight, no additional data				49
I-19b	DMAP, 1	>97	9370	1.08	3120.0	50
I-20	None	99	6700	1.3	391.2	51
I-20	N-MeIm	84	700	1.9	no data	51
Copolymerisation of propylene oxide and carbon dioxide						
I-18b	none	40	3900	1.15	~ 0.20 ^a	45
I-18a	EtPh ₃ PBr, 1	>99	3500	1.09	0.18 ^a	46
I-18a	Et ₄ NBr, 1	75	1900	1.10	no data	46
Copolymerisation of ethylene oxide and carbon dioxide						
I-18	EtPh ₃ PBr, 1	70	5500	1.14	no data	46

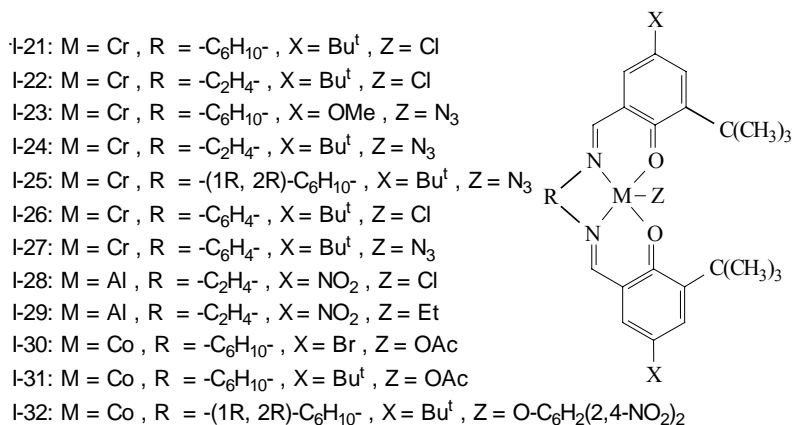
Table 2 Comparison of reactivity of different porphyrin-based systems, a – TOF, exact reaction times were not reported.

Based on the previous works of Inoue, Kruper^{48,49} investigated the reactivity of chromium porphyrinate complexes in the presence of amine cocatalysts (such as N-methylimidazole, N-MeIm, or (4-dimethylamino)pyridine, DMAP) toward a catalytic formation of cyclic carbonates from epoxides and CO₂. System **I-19a** catalysed the formation of monomeric

cyclohexene carbonate, in some screening runs stereochemically pure *trans*-PCHC could be isolated as a main product. Some years later Holmes developed a chromium porphyrin, **I-19b**, having perfluorinated phenyl rings making it soluble in supercritical CO₂.⁵⁰ Using this catalyst, high polymer yields and narrow polydispersities could be achieved with remarkably low catalyst loadings (see Table 2). Typical for polymers initialised by metalloporphyrinate systems, the narrow polydispersity of the copolymers suggests a living polymerisation, but unexpectedly low average molecular weights indicate that some mechanism limits the chain length. An unfavourable equilibrium between the polymer and monomers was suggested as a potential cause for the molecular weight limit. The obtained catalyst efficiencies (~3.9 kg of polymer/g of Cr or 3120 of TON) were greatly improved in comparison to the other porphyrin-based systems. Inoue reported recently the use of manganese as metal core of porphyrin-based compounds, which are highly active in copolymerisation reactions.⁵¹ **I-20** afforded PCHC with 99 % selectivity of carbonate in the isolated copolymers, obtained with moderate TONs (see Table 2). Attempts to increase the catalyst efficiency by using cocatalysts induced a decrease of the carbonate linkage content as well as of the length of polymer chain. Interestingly, contrary to all the reported catalysts, this one is able to catalyse this process under a remarkably low carbon dioxide pressure (one bar).⁵¹

In comparison to the rather complicated and low-yielding syntheses of the porphyrin metal complexes, a condensation reaction between diamines (aromatic and aliphatic: cyclic and linear) and non- and substituted salicylaldehydes yields compounds commonly known under the generic name “salens” (e.g. N,N'-bis(salicydene)-1,2-ethyldiamine), whose further conversions to the desired metal complexes are usually performed in high yields. The so-obtained transition metal salen derivatives were found to be active toward the asymmetric ring opening of epoxides to yield cyclic carbonates.⁵² Already the first catalytic test in the syntheses of poly(cyclohexene carbonate)s promoted by [(salen)CrCl] derivative, **I-21**, showed that even without any addition of Lewis bases as cocatalysts, copolymer can be obtained with relatively high TON, up to 250 (Table 3).⁵³ The isolated polycarbonate has more than 98 % of carbonate linkages, low polydispersity index and a relatively large average molecular weight, M_n (1.2 and ca. 8900 g mol⁻¹, respectively). An addition of 5 eq. of N-MeIm tripled the TON up to 774 (see entry 2, Table 3). Varying the electron density in the aromatic rings through the use of electron donating or withdrawing substituents and the kind of diamine used as spacer in the salen backbone allows the easy production of a large variety of highly active species. Combining these salens derivatives with Lewis base co-catalysts such as N-MeIm, DMAP, different phosphines or organic salts like e.g. quaternary ammonium

or phosphonium salts affords pure polycarbonates with high yields and conversion rates (**I 22-25**).⁵⁴⁻⁵⁶ The mixture of **I-25** with one equivalent of bis(triphenylphosphoranylidene) ammonium azide, [PPN⁺][N₃⁻], afforded system giving TOF as high as 2685.5, even higher than noted for **I-35b**, the best Coates' systems based on Zn(BDI) (TOF = 2290, entry 7, Table 4). Chromium-salen derivatives are active toward CHO-CO₂ (**I 21-25**) and PO-CO₂ (**I 26-27**) copolymerisation.^{54,57} The different co-catalysts used in these investigations are known to be inactive on their own, Nguyen showed that DMAP alone is not able to couple propylene oxide and carbon dioxide.⁵⁸

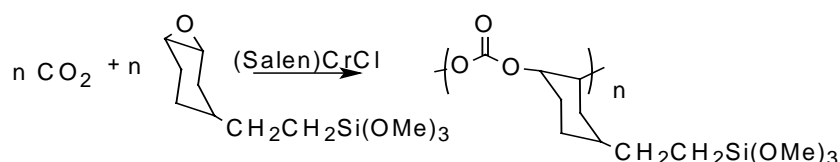


	Co-catalyst, [equiv.]	% of -CO ₃ -	M _n / [g/mol]	PDI	TON	Ref.
Copolymerisation of cyclohexene oxide and carbon dioxide						
I-21	none	>95	8900	1.2	250	53
I-21	N-MeIm, 5	>95	no data	no data	774	53
I-22	none	80	no data	no data	10.4 ^a	54
I-23	PPN ⁺ Cl ⁻ , 1	> 99	50000	1.1	1150 ^a	54
I-24	PPN ⁺ Cl ⁻ , 1	> 99	no data	no data	1022	55
I-25^b	PPN ⁺ Cl ⁻ , 1	> 99	50000	1.13	2462	56
I-25^b	PPNN ₃ , 1	> 99	50000	1.13	2685	56
I-28	none	75	25000	no data	194	131
I-28	(ⁿ Bu) ₄ NCl, 1	96	no data	no data	283	131
I-28	(ⁿ Bu) ₄ NN ₃ , 1	> 99	no data	no data	282	54
I-29	(ⁿ Bu) ₄ NN ₃ , 1	95	no data	no data	98	54
Copolymerisation of propylene oxide and carbon dioxide						
I-26	PPN ⁺ Cl ⁻ , 1	97	no data	no data	768	54
I-26	PPNN ₃ , 1	98	no data	no data	760	54
I-26	PCy ₃ , 1	94	no data	no data	596	54
I-27^c	DMAP, 1	98	16700	1.36	640	57
I-30	none	95	15300	1.22	243	132
I-31	none	99	6900	1.58	213	132
I-32	(ⁿ Bu) ₄ NBr, 1	> 99	23500	1.29	687	61
I-32	(ⁿ Bu) ₄ NCl, 1	> 99	24000	1.37	1113	61
Copolymerisation of [2-(3,4-epoxycyclohexyl)ethyl]trimethoxysilane and carbon dioxide						
I-22	N-MeIm, 2.5	99	no data	no data	862	62

Table 3 Comparison of the best salen catalytic systems basing on different metal cores. a – TOF, exact reaction times were not reported; b – coordinated THF molecule; c – TON of CPC was 240

Not only chromium can serve as a metal core for salen-based complexes active in copolymerisation processes. Since 1979, when Co(OAc)₂ was reported to couple PO and CO₂

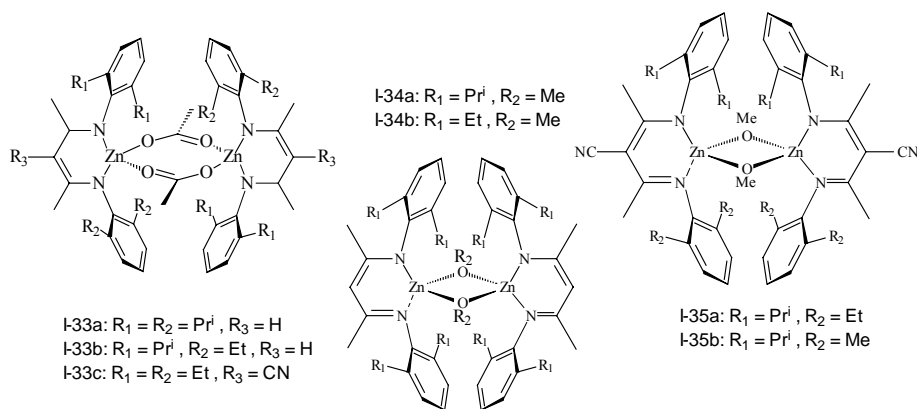
with extremely low TOF of 0.06 h^{-1} , some cobalt-based catalysts were reported to be active in copolymerisation reactions. Cobalt-salen systems based on naphthalene derivatives together with Lewis basic amines catalysed the synthesis of poly(propylene carbonate).⁵⁹ Moderate yield of PPC (TON 243 h^{-1}) was also obtained when the process was run with **I-30** as a promotor. Catalysts relying on this kind of structure are able to give an isotactic (S)-PPC with a moderate activity (TON of 213 obtained using **I-31**) but the highest selectivity of the head-to-tail coupling of the propylene oxide monomer (93% of head-to-tail linkages).⁶⁰ Coates has not investigated the use of cocatalysts, more recently Lu reported the successful use of binary catalyst system consisting of a chiral cobalt complex [(salcy)CoX] (X = different bulky phenoxides) and a quaternary ammonium salt $(^n\text{Bu})_4\text{NY}$ (Y = halogen or OAc) for completely alternating copolymerisation of CO_2 and aliphatic epoxides under extremely mild conditions (up to 4 MPa). Isolated polymers (see Table 3, **I-32**) displayed interesting characteristic (narrow PDIs, and rather high values of M_n , and TONs indicating high activities).⁶¹ Darensbourg suggested replacing the transition metal in the salen-based catalysts by a main group element. Although the isolated complexes were *iso*-structural with their transition metal-based counterparts, the observed activities were far below those typically observed the transition metal-based salens. **I 28-29** afforded polymers with relatively good TONs, [(salen)AlEt] were also reported to be less active than their chlorine-containing counterparts (see Table 3).^{54,131}



Scheme 7 Synthesis of poly(cyclohexene carbonate) modified oxide by silane groups.

Darensbourg reported an another interesting possibility to enhance the reactivity of the system: an optimisation of the epoxidic substrate to synthesise polymers soluble in supercritical carbon dioxide. This approach was investigated with Cr-salen catalyst (**I-21** was used in this case). Instead of modifying the ligand to make the catalyst soluble in the CO_2 -rich phase, the substrate was modified by grafting a silane group, what lead to a better solubility of the final polymer in scCO_2 or CO_2 -expended phases at a macromolecular level (see Scheme 7).⁶² Beckman studied the syntheses of scCO_2 -soluble copolymers containing both carbonate and ether linkages (ca. 25 % of carbonate). These copolymerisation were promoted by different aluminium alkoxide (**I 12-13**).⁶³

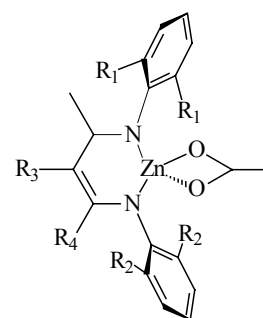
In 1998, as a systematic progress in the field of the zinc-based catalysed copolymerisation reactions was increasingly documented, Coates reported a complete new class of zinc-containing catalysts incorporating chelating electron-rich β -diimine ligands. These systems were as active as any other reported earlier and worked under interestingly mild P,T conditions and were able to produce pure poly(aliphatic carbonates) in good yields and very high TOFs. Some model catalyst systems were synthesised as model compounds of zinc alkoxides and zinc carboxylates. Similarly to the above described salens, subtle changes in the substituents, in steric demand as well as in the electronic density put on the ligand, could cause a drastic decrease of the catalytic activity of the isolated zinc β -diiminates derivatives. They were found as monomers and dimers in the solid state and solution, what depends on the sterics. For instance, playing with donating and withdrawing substituents of zinc acetate derivative complexes **I-33**, averaged molecular weight of 17900 by a polydispersity index of 1.11 and TOF as high as 917 were obtained (**I-33c**). Coates obtained the most active catalysts to date, **I-35b**, using asymmetric ligand with a electron-withdrawing CN group^{64,136}, what allowed to increase the TOF up to 2290 h⁻¹ (TON 382 indicating a reaction time as short as 10 - 20 min). The immobilisation of complexes of this type on silica afforded catalysts with moderate activities (of the order of 60 - 100 TOF) for CHO-CO₂ coupling.⁶⁵



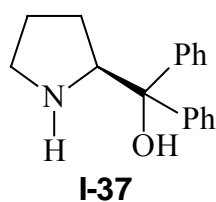
	M _n	PDI	TON	TOF	% of -CO ₃ -	Ref.
Copolymerisation of cyclohexene oxide and carbon dioxide						
I-33a	31000	1.11	494	247	96	122
I-34a	19100	1.07	449	224	95	66
I-34b	23700	1.14	447	239	96	66
I-33b	23300	1.15	364	729	99	134
I-33c	17900	1.15	306	917	90	134
I-35a	22000	1.11	362	2170	99	136
I-35b	22900	1.09	382	2290	90	136
Copolymerisation of propylene oxide and carbon dioxide						
I-36^p	36700	1.13	570	235	75:25 ^a , > 95	135
I-36^c	30600	1.15	276	138	93:7 ^a , > 95	135

Table 4 Comparison of the best Zn-BDI catalytic systems: a – selectivity PPC to PC ; b: T = 25°C, P = 6.9 bar ; c: T = 25°C, P = 34.5 bar

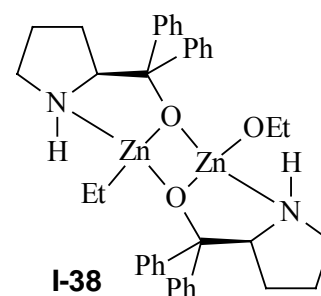
As already found for other catalytic systems, these complexes were found to be active towards a PO–CO₂ copolymerisation. Screening tests have shown that asymmetric ligands and reaction conditions have a significant impact on the form of isolated products. As it can be seen in the Table 4 for **I-36**, increasing the pressure of CO₂ from 6.9 to 34.5 bar suppresses the cyclic carbonate formation while simultaneously increasing the selectivity for polymer from 75 to 93 % and moderately decreasing the catalyst activity for PPC formation. This suggests that PC is formed by a backbiting reaction of the metal alkoxide. An interesting feature of the polymers synthesised using these catalysts are their remarkably low polydispersity indexes, with indices near 1.1 – 1.2. Further modification of ligand's substituents resulted in quite a number of catalysts having comparable reactivity, capable to initiate the syntheses of easy biodegradable polymers: poly(propylene carbonate), poly(lactid acid), polylactide and poly(3-hydroxybutyrate).⁶⁶⁻⁶⁸

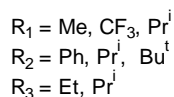
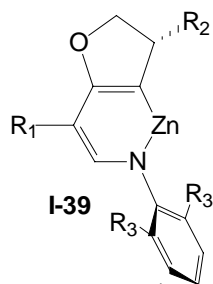


I-36: R₁ = Et, R₂ = Prⁱ,
R₃ = H, R₄ = CF₃

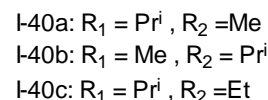
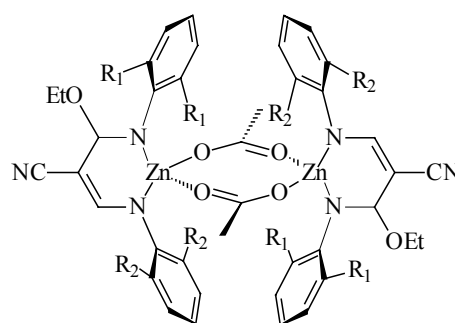


Similarly to many other polymerisation processes the use of asymmetric catalysts is of great importance as the only efficient method to control the stereochemistry of the final polymer obtained from chiral or *meso*-monomers. Considering the case of the *meso* monomer, cyclohexene oxide, the ring opening of the epoxide and the further polymerisation can produce either syndiotactic or isotactic poly(cyclohexene carbonate). Chiral catalysts influence the stereochemistry of the reaction at the active site of the catalyst, controlling the absolute configuration of the resulting polymers. Nozaki described the successful asymmetric copolymerisation of CHO and CO₂ using a chiral aminoalcohol **I-37** and ZnEt₂.⁶⁹ Isolated copolymers were hydrolysed, and the resulting *trans*-1*R*,2*R*-cyclohexane-1,2-diol was formed with an enantiomeric excess as high as 73%. Because only one enantiomer of the chiral alcohol was used, only the enriched *R,R*-diol was detected. More recently, she reported also an improved enantioselectivity (~ 80% ee) of the copolymerisation using a dimeric zinc complex **I-38**⁷⁰ in which one of the two ethyl groups was substituted by ethoxy group. The obtained copolymer has an EtOCOO- end group, indicating that the initiation reaction occurred by the insertion of CO₂ into the Zn–OEt bond. Despite of its high stereoregularity, the copolymer of ca. 80% ee shows a glass transition temperature at 117 °C, the value being very close to the ones previously reported for copolymers with lower stereoregularity.





Coates described another interesting system having an asymmetric structure in which the early reported β -diiminate catalysts were modified using an oxazoline part. The Zn(II) complex **I-39** with a so-obtained hybrid imine-oxazoline ligand gave an excellent catalyst having high activity.⁷¹ Furthermore, by varying the substituents on the oxazoline group (R_1), imine group (R_2), and N-phenyl group (R_3), an optimised catalyst displayed up to 86% ee with higher conversion and under milder conditions than those reported using the chiral alcohol. Most recently Kröger reported zinc acetate derivatives **I-40 a-c** of asymmetric, differently substituted 3-amino-2-cyanoimidoacrylate ligands.⁷² An innovation in the structures of presented systems was the presence of additional alkoxy group on the amine spacer. The presence of ethyl or methyl substituents on *ortho* position of the phenyl ring enhanced the selectivity and activity of isolated compounds. Copolymerisations were carried out at the pressure as low as 4 MPa, but at significantly higher temperature (see Tab 5) (for comparison: T and P for **I-33a** were 50°C and 6.50 bar, respectively). PCHC was isolated as resulting polymer with narrow polydispersities (<1.26) number averaged molecular weights above 10000 g/mole and more than 75 % of carbonate linkages. It was shown that the kind of substitution by methyl and ethyl groups either on the side of the imido ester or on the side of the anilines does not significantly influence the activities obtained. However similar ligands with a combination of methyl and isopropyl groups on the anilines seem to be more active than the ones combining ethyl and isopropyl groups (see Table 5).



	% of -CO ₃ -	M _n	PDI	TON	TOF	Ref.
I-40a ^a	88	24500	1.15	367	183	72
I-40b ^b	75	15800	1.21	396	198	72
I-40b ^a	88	10000	1.16	210	210	72
I-40c ^b	72	20000	1.26	327	164	72

a - T = 90°C, b - T = 100°C

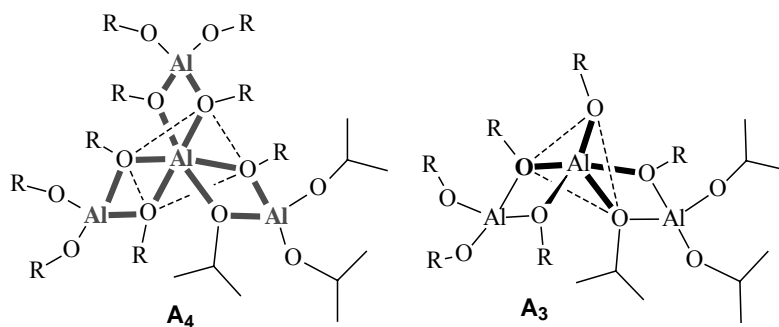
Table 5 Comparison of (3-amino-2-cyanoimidoacrylate) Zn acetate derivatives.

The problem of the isolation of polymers with an absolute stereochemistry employing non-chiral catalysts is attracting more and more attention. Chisholm reported recently some interesting studies dealing with the stereochemistry of different polymers catalysed by common catalysts. He investigated the regioregularity of poly(propylene carbonate) obtained with zinc glutarate as a catalyst, and focused on the diads produced by a head-to-head, tail-to-

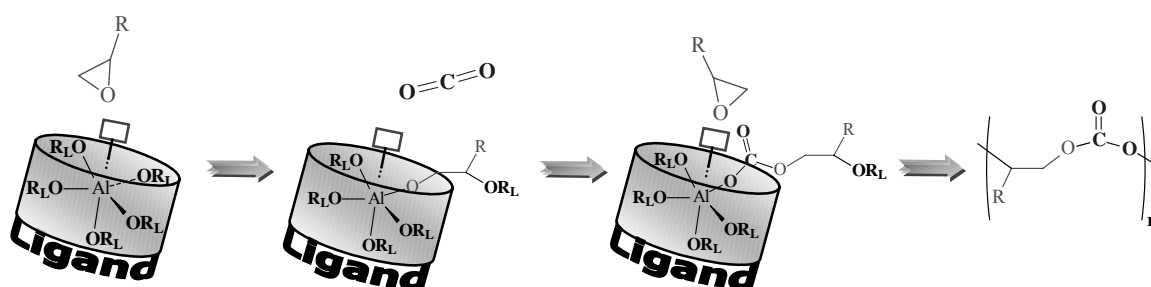
head and tail-to-tail connection of the monomers.⁷³ Likewise the stereochemistry of polylactides was comprehensively investigated by the Chisholm's group, some transition and main group metals bisphenoxides were reported as being not able to convert *rac*-LA (lactic acid) to the stereoplex of isotactic PLA (L + D).⁷⁴ By the mean of different NMR techniques, the structures of oligoether-carbonates, logical models for the poly(ether carbonates) regions found in the polymeric poly(propylene carbonate), were examined at the diads, triads and tetrads level.^{75,76} Investigating the differences found in the ring opening polymerisation of lactides and propylene oxide, Chisholm and co-workers showed that some aluminium chloride-based complexes are inactive in initiating the ROP of lactides (*L* and *rac*) but that, upon addition of propylene oxide, these aluminium compounds are able to form block-copolymers of the form (PPO)_n(PLA)_m.⁷⁷ On the other side, isopropoxy-bridged and porphyrine-based catalysts, although active in the ROP of PO at room temperature, required higher temperature (up to 80°C) to efficiently catalyse the ring opening polymerisation of LA. Such results together with kinetic studies suggested two different reaction mechanisms: a single-site catalysis being favoured for lactides polymerisation and a dimolecular catalysis involving a Lewis base and two metal sites to activate the substrate and allow an efficient linking of the epoxidic monomers.

Almost all catalysts presented in this work are able to alternatively copolymerise epoxides with CO₂, that of course within a wide efficiency's range. Although a very rich variety of ligands has been already investigated (only few Al-based catalysts, e.g. Al-porphirins. Al-salens displayed the sought after capability to afford pure poly(aliphatic carbonate)s. As it was already mentioned above (see Table 1, **I 11-15**), using basic aluminium phenoxides Beckman has cursorily investigated the mechanism of this copolymerisation, mainly focusing on the solubility of the isolated polymers in scCO₂. Owing to their high Lewis acidity and potential reactivity, aluminium alkoxides are a promising catalysts group. Usual homoleptic aluminium tri-alkoxides are known to exist at least as dimers, trimers and tetramers.⁷⁸⁻⁸⁰ The commercially available aluminium isopropoxide was used as a catalyst for Meerwein-Ponndorf-Verley Reduction (MPV Reduction)⁸¹ and Ring Opening Polymerisation (ROP) of lactones^{82,83}; notwithstanding the fact that it exists in two forms – the thermodynamically stable tetramer (A₄) and the unstable trimer (A₃) obtainable via distillation of A₄.⁸² The low reactivity of the A₄ structure is the reason for the large difference in catalytic activity between A₃ and A₄, where a coordinatively saturated Al atom occupy the centre of the alkoxide oligomer. The presence of a pentacoordinated, coordinatively unsaturated, aluminium atom in the centre of the A₃ oligomer makes this aggregate much more reactive. It was confirmed that

within a A_4/A_3 mixture only A_3 is responsible for the presence at the end of the polymer of isopropoxide end groups, whereas A_4 remains unreacted within the time required for complete ϵ -CL consumption.^{82,83} Owing to its dual nature (complex equilibrium between two isomers) and the low tunability of the catalyst the search for new catalysts for ROP polymerisation was necessary.



Taking as an origin the results of Duda and Jerome's investigations^{82,83} dealing with the ROP of ϵ -caprolactone catalysed with $Al(OPr^i)_3$ we wanted to evaluate its reactivity in the copolymerisation of epoxides with CO_2 . The first screening tests, involving aluminium isopropoxide and cyclohexene oxide, have shown that the optimal conditions to allow a catalytic cycle to take place and to isolate significant amounts of copolymers are between 80 – 110 bar of carbon dioxide and in a temperature region ranging from 50 to 80°C. Operating with an epoxide – catalyst ratio of 300 to 1, it was possible to isolate copolymers with a carbonate-ether ratio of ca. 3.3 to 1, with a polydispersity index of 1.2-1.5 and an average molecular weight of ca 8600 g/mole.⁸⁵ Longer reaction's time, higher temperature lead to liberation of undesirable cyclic monomer: cyclohexene carbonate. Similarly as in case of lactones, up to three polymers chains may grow simultaneously at the coordination centre.



Scheme 8 *Schema of prolongation of polymer chain – docking of comonomers at the active centre.*

The disadvantages of aluminium isopropoxide as a catalyst – complex mechanism, several different active sites in the solution, low polydispersity and CO_2 incorporation might be overcome by shielding the aluminium atom with bulky substituted bisphenolate ligands. **The aim of this work** was to find catalytic systems involving aluminium alkoxides, where only one definite reaction site at the metal centre (see Scheme 8) remains accessible to the two co-

monomers: epoxide and carbon dioxide. The most part of the aluminium alkoxide has to be “shielded”, protected by a ligand, which should be of the alkoxidic type, but which also has to be quite inert relative to a carbon dioxide insertion. Good candidates to fulfil this task seem to be 2,2'-methylene-bisphenol ligands owing to the chelating capabilities of the ligand on its own (formation of a stable eight-member ring system with the Al-centre) and to the general lower reactivity of metal aryloxides toward CO₂. The remaining ligand at the aluminium centre, having then a definite geometry, would allow an easier study of the insertion of the monomers and might also allow a fine-tuning of this incorporation toward the formation of pure polycarbonates. One main incentive was the fact that a lot of studies involving aluminium 2,2'-methylene-bisphenoxides as efficient catalysts were reported. For instance, these complexes were successfully used in regioselective Diels Alder reactions⁸⁶, in the Meerwein Ponndorf Verley Reduction^{87,88}, in ROPs of lactones^{77, 89-91} (mainly ϵ -CL) as well as propylene oxide⁷⁷, and in the polymerisation of glycidyl acetate to poly(ortho ester)⁹².

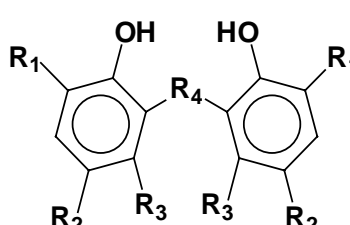
5 Discussion of the results

In this work we wanted to focus on aluminium alkoxide-based catalytic systems and to establish some basic correlations between structure and catalytic activity. In order to gain more information on the active species involved in different catalytic reactions and to have a better control on the reactions' course, a "simplification" of the catalytic systems is often necessary. The use of chelating alkoxo-ligands can elegantly provide a structurally well defined aluminium catalysts. Bulky 2,2'-methylene-bisphenols constitute a versatile and easy-to-handle toolbox for the coordination chemist. The synthesis on a larger scale of these chelating ligands from formaldehyde and the corresponding bulky phenols is relatively easy and allows the rapid development of a ligand library.^{93, 96}

The bulky 2,2'-methylene-bisphenols allow through a definite substitution of the aromatic ring at location 6 (*ortho*) and 4 (*para*) (see Table 6) to directly investigate the steric and electronic influence of these substituents on the structure and the activity of the aluminium bisphenoxides in copolymerisation reactions. Generally, two important parameters have to remain in sight for a further industrial up-scaling of any catalytic process: the final price of the catalyst (from the bulk reagents to the final purification) and its efficiency. For this work we firstly evaluate the practicability of the catalyst's synthetic method with some already known bisphenols and consequently tested their catalytic activity with cyclohexene oxide and CO₂.

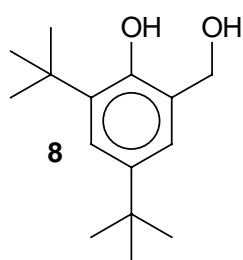
5.1 Synthesis of ligands

In our study we wanted to find catalytic systems, which would be relatively cheap, easy to synthesise and would give high yields of the desired catalyst product in two or three reaction's steps. Bisphenols seem to be ideal candidates to fulfil this program. **2**, **3**, **6** and **7** presented in Table 6 were purchased from the commercial sources, three of them (**1**, **4** and **5**) were synthesised.



Ligand	R ₁	R ₂	R ₃	R ₄
1	<i>tert</i> -Bu	<i>tert</i> -Bu	H	-CH ₂ -
2	<i>tert</i> -Bu	Me	H	-CH ₂ -
3	1-methylcyclohexyl	Me	H	-CH ₂ -
4	Pr ^{iso}	Cl	Me	-CH ₂ -
5	Me	Me	H	-CH ₂ -
6	H	Cl	H	-CH ₂ -
7	H	<i>tert</i> -octyl	H	-S-

Table 6 Substituents of used bisphenols.



The synthesis of such bisphenolic compounds through the condensation of the adequate substituted phenols with formaldehyde as formalin (37% formaldehyde aqueous solution) or paraformaldehyde is easy and was already described in the literature.⁹³⁻⁹⁵ Initially, the synthesis of **1** was realised with formalin, as a two-step reaction⁹³ (see Figure 1) according

to the procedure reported by Ohba, but owing to the laborious and time-consuming isolation of the final bisphenol (very low yield) the “formalin-way” was abandoned. However, the first step of this synthesis generates, in good yields an aromatic diol, 2-hydroxy-3,5-di-*t*-butyl benzylic alcohol **8**, which can be also used as a versatile chelating ligand in our search for new aluminium catalysts. Although **8** is not a bisphenol, its hybrid structure displaying a narrower steric hindrance than the corresponding bisphenol makes it another interesting candidate for our reactivity study. Nevertheless, the use of pure, solid formaldehyde, “paraformaldehyde” with small amounts of sulphuric acid as catalyst, was successful and allowed the isolation in high yields of the desired bisphenols.⁹⁶

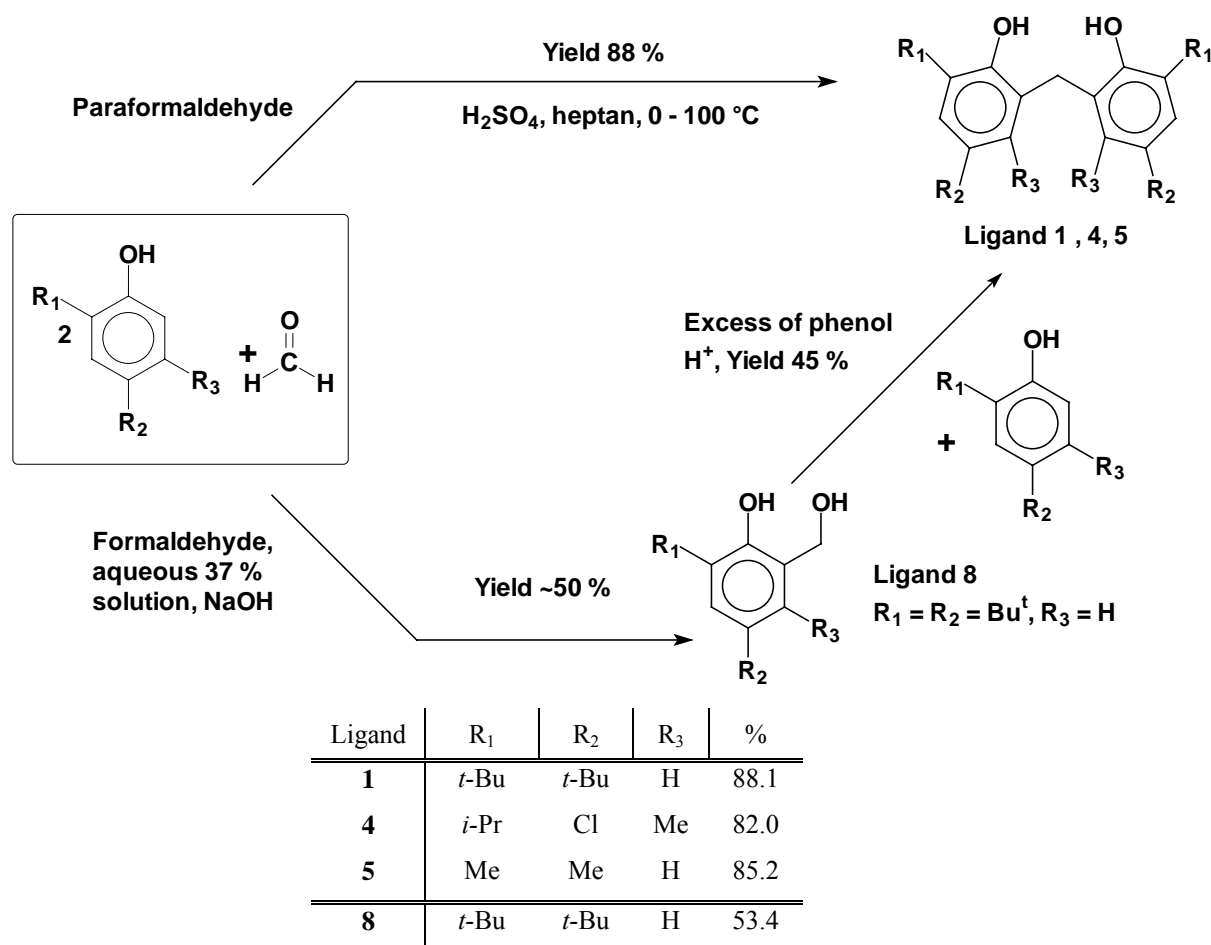
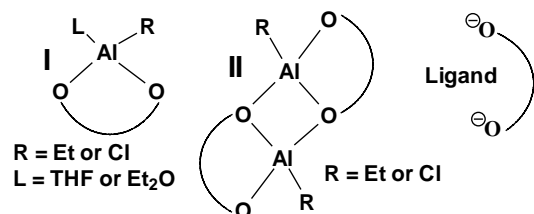


Figure 1 Possible reaction paths of bisphenols synthesis. Yields of self-synthesised ligands given for “paraformaldehyde path” (**1,4,5**) and for formalin-path in case of **8**.

5.2 Synthesis of catalysts

The reactions of $XAlEt_2$ ($X = Et, Cl$ or I) with the aromatic diols presented in Table 6 were realised in the presence of non-coordinating solvents like hexane and pentane and



coordinating ones like diethyl ether and THF, affording the desired aluminium alkoxides, whose general structure is schematically represented as **I** and **II** (*vide supra*). Depending on the solvent used and the presence of bulky

substituent in *ortho*-position of the diols, differently coordinated products were isolated. When steric demanding *ortho*-substituted ligands were present, the coordination number of aluminium was always four and was independent from the solvent used. In comparison, using ligands without any substituents at the *ortho* position, afforded different coordination numbers depending on the ether used. Table 7 presents the nomenclature used for the isolated catalysts and the resulting obtained polymers. The solvent used and the leaving nucleophile bound to the aluminium centre are summarised in the headline of the table. A comprehensive list of the exact structures of all the isolated compounds is presented in Appendix 1.

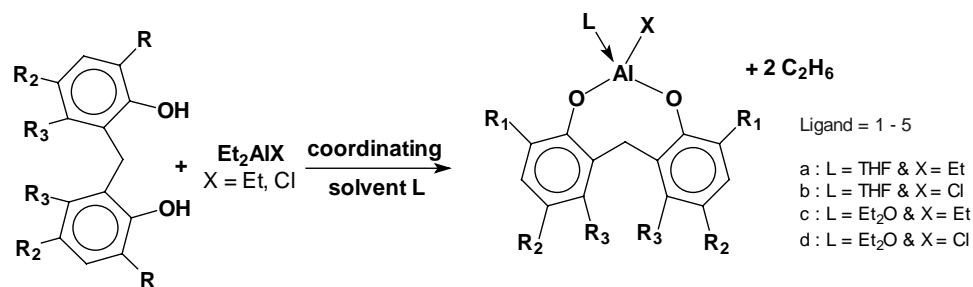
		THF/Et	THF/Cl	Et ₂ O/Et	Et ₂ O/Cl	Hex/Et	hex/Cl	hex/OPr ⁱ	hex/I
1	cat.	1a	1b	1c	1d	1e	1f	1g	
	pol.	P-1a	P-1b	P-1c	P-1d	P-1e	P-1f	P-1g	
2	cat.	2a	2b	2c	2d	2e	2f	2g	2h
	pol.	P-2a	P-2b	P-2c	P-2d	P-2e	P-2f	P-2g	P-2h
3	cat.	3a	3b	3c	3d	3e	3f	3g	
	pol.	P-3a	P-3b	P-3c	P-3d	P-3e	P-3f	P-3g	
4	cat.	4a	4b	4c	4d	4e	4f	4g	
	pol.	P-4a	P-4b	P-4c	P-4d	P-4e	P-4f	P-4g	
5	cat.	5a	5b				5f	5g	
	pol.	P-5a	P-5b				P-5f	P-5g	
6	cat.	6a		6c				6g	
	pol.	P-6a		P-6c				P-6g	
7	cat.	7a		7c			7f	7g	
	pol.	P-7a		P-7c			P-7f	P-7g	
8	cat.			8c				8g	
	pol.								

Table 7 Designation of isolated catalysts and polymers.

5.2.1 Reaction of aluminium precursors with bisphenols run in the presence of ethers: formation of monomeric species

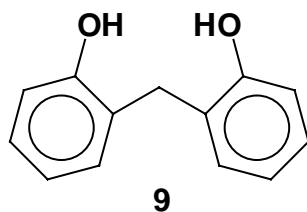
As it was already mentioned above, fourfold coordinated aluminium compounds were isolated as a result of the reaction of *ortho*-substituted ligands with aluminium precursors. In the presence of ether the products formed are monomers, with dative coordinated THF or diethyl ether molecule (see Figure 2). The identification of the products was performed using

different NMR spectroscopy techniques, the structures of crystals were determined by the X-ray structural analysis on single crystal.



Ligand	R ₁	R ₂	R ₃	%	Ligand	R ₁	R ₂	R ₃	%
1a	<i>t</i> -Bu	<i>t</i> -Bu	H	82.9	1b	<i>t</i> -Bu	<i>t</i> -Bu	H	78.9
1c	<i>t</i> -Bu	<i>t</i> -Bu	H	90.8	1d	<i>t</i> -Bu	<i>t</i> -Bu	H	80.5
2a	<i>t</i> -Bu	Me	H	quant.	2b	<i>t</i> -Bu	Me	H	quant.
2c	<i>t</i> -Bu	Me	H	89.1	2d	<i>t</i> -Bu	Me	H	79.0
3a	1-MeCy	Me	H	77.5	3b	1-MeCy	Me	H	83.2
3c	1-MeCy	Me	H	86.0	3d	1-MeCy	Me	H	77.6
4a	<i>i</i> -Pr	Cl	Me	71.1	4b	<i>i</i> -Pr	Cl	Me	67.8
4c	<i>i</i> -Pr	Cl	Me	quant.	4d	<i>i</i> -Pr	Cl	Me	76.7
5a	Me	Me	H	84.6	5b	Me	Me	H	78.1

Figure 2 General scheme of monomeric alkyl and halide aluminium complexes synthesis.



The structure of 2,2'-methylene(bisphenol) **9** is the structural backbone common to all the bisphenol ligands used in this study and the chemical shifts recorded in ¹H and ¹³C NMR for the coordinated forms do not vary significantly from one specie to the other. Almost all of the aliphatic substituents give rise to signals which do not overlap the distinctive signals of the bridging methylene group. In the free ligand, the phenyl rings can freely rotate around the bond involving the bridging methylene group – hence the two hydrogen atoms of the bridging group are chemically equivalent affording only one peak at 3.95–3.98 ppm as it presented in Figure 3. In comparison, the ¹H NMR spectra of the aluminium bisphenoxides **1–3 a–d** show, that these two hydrogen atoms are chemically non-equivalent (AB pattern), one hydrogen atom pointing away and the second towards the Al atom. For all complexes having **1–3** as a ligand and displaying a coordinated solvent molecule the two doublets are located at about 3.35 and 3.88–3.95 ppm. In the case of **4a** the two hydrogen atoms of the methylene are magnetically equivalent. There is a significant upfield shift of the chemical shift for the methylene bridge signals in **4c** and **4d**, which is too strong to be completely attributed to the electron-withdrawing properties of

the chlorine atoms in *para*-position. Unfortunately, no single crystals could be isolated for **4c** and **4d** and it was not possible to correlate the uncommon upfield shift with a potential structural characteristic. Table 8 shows a comparison of chemical shifts of groups contained hydrogen atoms presented in the investigated complexes, Table 9 presents the values of the geminal coupling constants of monomeric compounds, as well.

	AlCH ₂ CH ₃	AlCH ₂ CH ₃	C(7)(H _{EXO})	C(7)(H _{ENDO})	R ₁	R ₂	C ₃ -H	C ₅ -H
1a	0.08	1.07	3.39	3.88	1.22	1.31	7.05	7.22
1b	-	-	3.39	3.97	1.22	1.31	7.05	7.18
1c	0.07	1.09	3.38	3.98	1.22	1.30	7.07	7.21
1d	-	-	3.36	3.73	1.08	1.20	7.05	7.20
2a	0.01	1.08	3.31	3.85	1.08	2.16	6.96	7.07
2b	-	-	3.42	3.95	1.40	2.26	6.91	7.07
2c	0.08	1.09	3.30	3.90	1.28	2.16	6.82	6.97
2d	-	-	3.42	3.80	1.31	2.17	6.85	6.97
3a	0.05	1.04	3.31	3.83	1.28-1.88	2.17	6.82	6.97
3b	-	-	3.42	3.80	1.21-1.99	2.19	6.84	6.97
3c	0.05	1.05	3.29	3.87	1.19-1.91	2.20	6.86	6.98
3d	-	-	3.36	3.76	1.21-2.03	2.18	6.86	6.98
4a	0.00	0.98	3.98		1.08, 3.39	-	-	6.94
4b	-	-	3.89	3.95	1.08, 3.17	-	-	6.98
4c	0.00	1.00	2.87	invisible	1.12, 3.16	-	-	6.98
4d	-	-	3.00	3.54	1.08, 3.19	-	-	6.98
5a	0.12	0.98	3.29	3.90	2.14	2.19	6.70	6.86
5b	-	-	3.32	4.57	2.14	2.19	6.71	6.87

Table 8 Comparison of chemical shifts of characteristic hydrogen atoms.

	C(7)(H _{EXO})	J _{H-H} [Hz]	C(7)(H _{ENDO})	J _{H-H} [Hz]
1a	3.39	13.55	3.88	13.70
1b	3.39	13.72	3.97	13.72
1c	3.38	13.55	3.98	13.55
1d	3.36	13.55	3.73	13.55
2a	3.31	13.72	3.85	13.72
2b	3.42	13.72	3.95	13.72
2c	3.30	13.59	3.90	13.59
2d	3.42	14.09	3.80	14.09
3a	3.31	13.60	3.83	13.60
3b	3.42	14.33	3.80	14.25
3c	3.29	13.74	3.87	13.74
3d	3.36	13.74	3.76	
4a	3.98			
4b	3.89	Invisible	3.95	invisible
4c	2.87	14.08	invisible, probably hidden	
4d	3.00	13.80	3.54	13.80
5a	3.29	13.55	3.90	13.70
5b	3.32	13.50	4.57	13.70

Table 9 Comparison of chemical shifts and geminal coupling constants of hydrogen atoms bound to C(7) carbon atom.

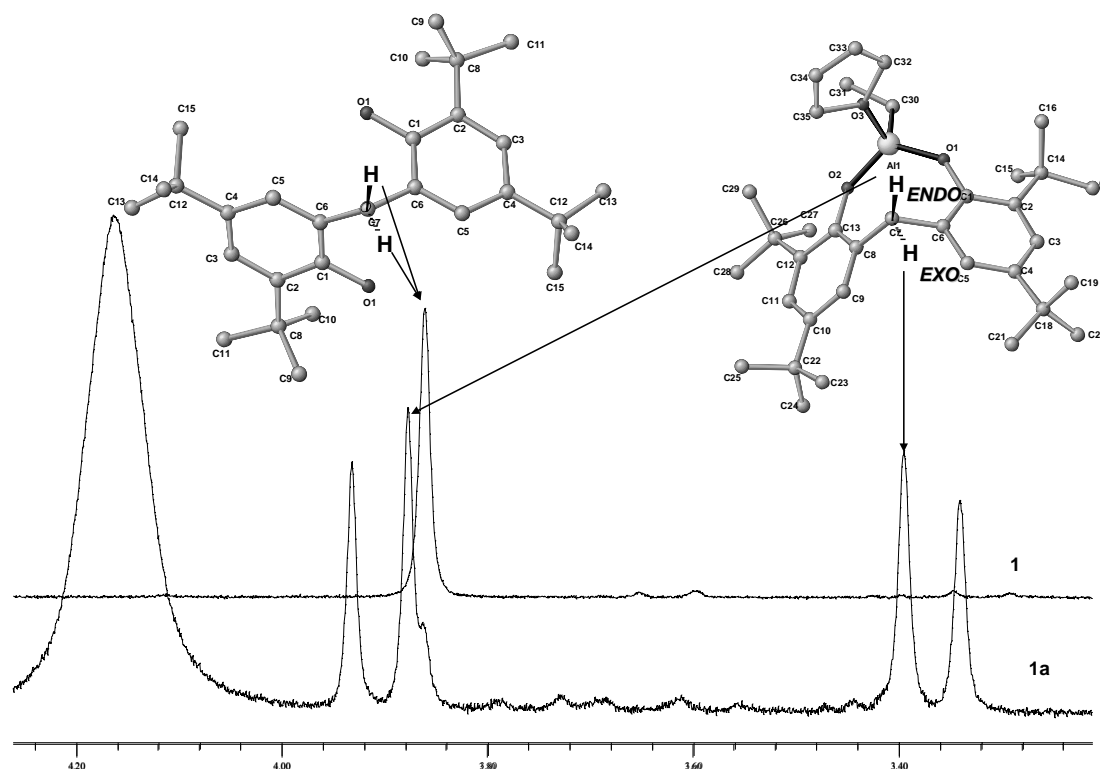
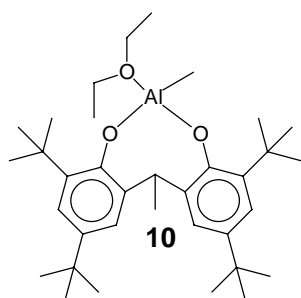


Figure 3 Chemical shift of equivalent and non-equivalent hydrogen atoms in ligand **1** and Al complex **1a**.



The magnitude of the geminal-coupling constant of ${}^2J_{\text{HCH}}$ ranges from 13.55 to 14.33 Hz, indicating the non-equivalence of the methylene hydrogen atoms (see Table 9). These values are comparable to the values reported in the literature for similar compounds like e.g. [(EDBP)(Et₂O)AlMe], **10**.⁹⁷ Such a feature is also found in titanium based compound like the bis(amido)titanium complexes of MMBPH₂ displaying chelating bisphenol ligands.⁹⁸ Incidentally, the use of 2,2'-methylene-bisphenols as chelating ligands ended up usually forming eight-membered rings system. Five different ground conformations have been reported in the literature (*crown*, *chair*, *boat-boat*, *boat-chair* and *chair-chair*) in which the distorted *boat-chair* conformation is usually found in the case of aluminum 2,2'-methylene-bisphenoxides.⁹⁹ Considering the general structures of the aluminium bisphenoxides it can be seen that the structure of the eight-membered ring via the bonding to the aluminium atom is quite predetermined and it explains both the non-equivalence of the methylene hydrogen atoms and the observation that the two *ortho*-substituents are generally in a similar environment. The BC conformations found in the different isolated complexes (monomers, dimers and trimers) are most of the time slightly distorted (see Figure 4).

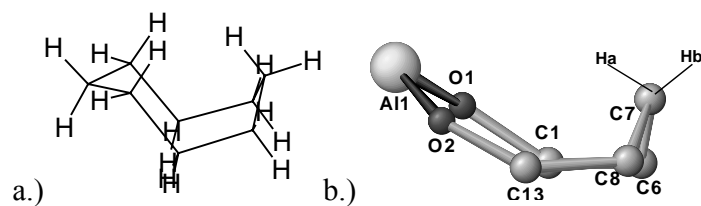


Figure 4 The ideal and distorted BC conformations of cyclohexane and **1a**.

The assessment of the endo-exo character (endo: pointing towards the Al atom; exo: not pointing towards Al) for the non equivalent hydrogen atoms of the methylene bridge was performed via 2D-NOESY (Nuclear Overhauser Effect Spectroscopy) experiments. (see Figure 5). As an example, such measurements were performed with the aluminium bisphenoxide **1b** with a mixing time of 800 ms and a relaxation delay of 1.5 second. The different NOE contacts between hydrogen atoms of the *para-tert-Butyl* group and the hydrogen CH_{EXO} of the methylene bridge, between *para-* and *ortho-tert-Butyl* groups and between *ortho-tert-Butyl* group and hydrogen atoms of the THF bound to the metal (respectively represented as **a**, **b** and **c** in Figure 5) can be seen on the 2D NOESY spectrum as cross-peaks). Analysing the influence of the solvent used during the syntheses, it was already shown, that for the case of bulky *ortho*-substituted complexes synthesised in non-coordinating solvents, both H_{EXO} and H_{ENDO} are shifted downfield (to about 3.55 and 4.40 ppm, respectively), as shown in Figure 6. Such phenomenon might be explained by a weak interaction of the H_{ENDO} with the oxygen atom of the coordinated THF as it can be noticed in the X-ray structure with a rather short C-H...O interaction (of the order of 2.75 Å). Table 10 summarised the detailed data relevant to weak hydrogen bond found in the different structures (bond lengths and angles) and we can see that only the **4**-based monomeric compounds do not display such an interaction between coordinated solvent and hydrogen of the methylene bridge.

Catalyst	Hydrogen bond angle, [°]	Hydrogen bond length, [Å]	Lit.
[(MDBP)(THF)AlEt] 1a	C(7)-H(7A)-O(3) 164.1	H(7B)-O(3) 2.583	a
[(MDBP)(Et ₂ O)AlEt] 1c	C(7)-H(7A)-O(3) 164.2	H(7B)-O(3) 2.704	a
[(MDBP)(Et ₂ O)AlCl] 1d	C(7)-H(7A)-O(3) 159.5	H(7B)-O(3) 2.840	a, 86
[(MMBP)(Et ₂ O)AlCl] 2d	C(7)-H(7A)-O(3) 164.7	H(7B)-O(3) 2.655	a, 86
[(MMMCyP)(THF)AlEt] 3a	C(7)-H(7A)-O(3) 157.5	H(7B)-O(3) 2.821	a
[(MMMCyP)(Et ₂ O)AlEt] 3c	C(7)-H(7A)-O(3) 158.7	H(7B)-O(3) 2.817	a
[(MCIMePrP)(THF)AlEt] 4a	C(7)-H(7A)-O(3) 110.6	H(7B)-O(3) 4.430	a
[(MCIMePrP)(THF)AlMe]	C(7)-H(7A)-O(3) 109.62	H(7B)-O(3) 4.462	90
[(EDBP)(THF)AlMe]	C(7)-H(7A)-O(3) 167.8	H(7B)-O(3) 2.419	97

Table 10 Distances and angles of hydrogen bonds, a – this work

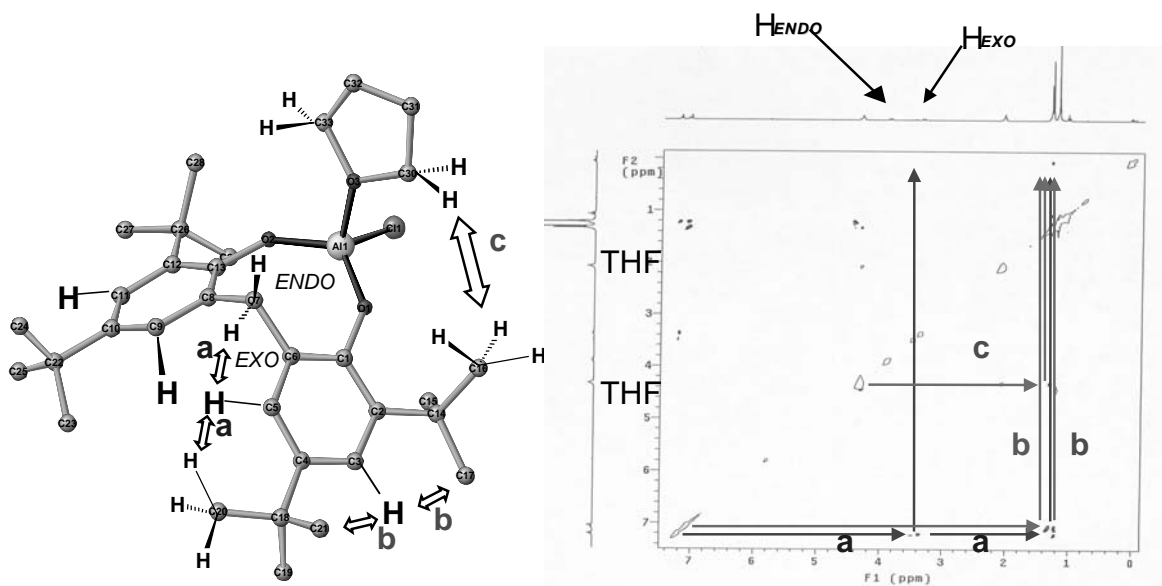


Figure 5 Identification of hydrogen atom signals of **1b** using ^1H - ^1H NOESY NMR spectroscopy.

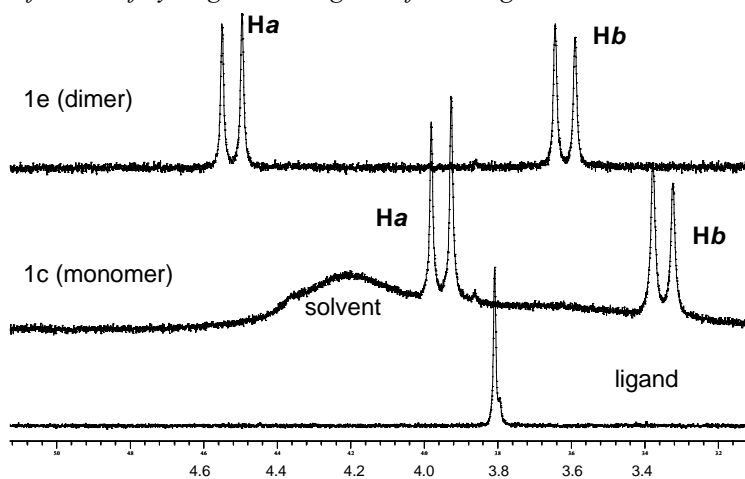


Figure 6 Comparison of chemical shifts of H_{ENDO} and H_{EXO} peaks for free ligand, monomeric (**1c**) and dimeric (**1e**) compounds.

Generally the monomeric aluminium compounds herein investigated easily crystallise from the corresponding solvent (THF or diethyl ether), forming colourless crystals within 24 h from concentrated solutions at low temperature. The crystallisation of monomeric aluminium bisphenoxides-THF or aluminium bisphenoxide- Et_2O adducts can also be performed in non-coordinating solvent (like e.g. hexane), the process occurred rapidly (ca. 30 min.), although the obtained crystals were of lower quality. An another crystallisation method successfully used was to dissolve the aluminium bisphenoxide in hot toluene (concentrated solutions, at ca. 85°C) and allowing it to slowly cool down to room temperature giving usually well shaped colourless crystals. This method was used in the case of dimers and there, where other purification ways appeared to be unsuccessful. Isolated complexes crystallise in the monoclinic system e.g. space groups Cc for **1c**, P2(1)/c for **1a** and **4a** and P2(1)/n for **1d**, **3a** and **4b** as well as in the orthorhombic system with e.g. Pnam for **2d**. In comparison, the

methyl analogue [(MMBP)AlMe(Et₂O)]⁹⁷ also crystallises in the orthorhombic system, although with Pbc_a crystal group. **3c**, another aluminium bisphenoxide structurally characterised in this study, also crystallises in this uncommon space group.

Considering the special case of the 1-methyl-cyclohexyl (1-MeCy) substituted bisphenol, there are, surprisingly, no reports in the literature concerning the structural characterisation of bulky bisphenoxide complexes displaying an *ortho* 1-methyl-cyclohexyl moieties (**3**-based complexes). To our knowledge only one compound, an ionic complex [(MMMCyP)Al(OPrⁱ)₂][NEt₄] was scarcely documented by Braune.¹⁰⁰ Similarly to other aryloxides described in the literature, the X-ray structure analyses on single crystal confirmed that the geometry around the central Al(1) is distorted tetrahedral, the distances and angles are sum up in Tables 11 and 12. In the case of complexes containing an Al-Cl bond (**1d** and **2d**) the lengths of aluminium-oxygen bonds are shorter than the corresponding lengths found in the aluminium bisphenoxides displaying an Al-C bond (for instance: **1d** with Al(1)-O(1) of 1.695(5) Å and Al(1)-O(2) of 1.681(5) Å vs. **1c** with Al-O distances of 1.721(2) Å and 1.721(3) Å for Al(1)-O(1) and Al(1)-O(2), respectively), this feature can be explained by a higher Lewis acidity of the aluminium centre. The bond lengths involving phenolic oxygen atoms and aluminium atom in other aluminium alkyl bisphenoxides are very close and do not vary significantly (1.703(3) Å for Al(1)-O(1) bond of **3c** and 1.756(3) Å for Al(1)-O(2) of the ionic complex [(MMMCyP)Al(OPrⁱ)₂][NEt₄]). The bond between aluminium atom and the oxygen of the coordinated ether (Et₂O or THF) is significantly longer than corresponding distance involving metal core and phenolic oxygen atoms, which is fully consistent with a dative bonding. Despite the ionic character of the compound isolated by Braune, the corresponding bond lengths and angles are comparable to the values found in the neutral species described in this study and in the related literature.

Catalyst	Length of bonds, [Å]		Length of bonds, [Å]		Lit.
[(MDBP)(THF)AlEt] 1a	Al(1)-O(1)	1.7217(18)	O(1)-C(1)	1.349(3)	a
	Al(1)-O(2)	1.7156(18)	O(2)-C(13)	1.352(3)	
	Al(1)-O(3)	1.8850(19)	O(3)-C(32)	1.436(4)	
	Al(1)-C(30)	1.950(3)	O(3)-C(35)	1.497(4)	
[(MDBP)(Et ₂ O)AlEt] 1c	Al(1)-O(1)	1.721(2)	O(1)-C(1)	1.349(4)	a
	Al(1)-O(2)	1.721(3)	O(2)-C(13)	1.351(4)	
	Al(1)-O(3)	1.884(3)	O(3)-C(34)	1.434(6)	
	Al(1)-C(30)	1.946(4)	O(3)-C(32)	1.534(6)	
[(MDBP)(Et ₂ O)AlCl] 1d	Al(1)-O(1)	1.695(5)	O(1)-C(1)	1.3662(19)	a, 86.
	Al(1)-O(2)	1.681(5)	O(2)-C(13)	1.3605(19)	
	Al(1)-O(3)	1.830(6)	O(3)-C(30)	1.452(4)	
	Al(1)-Cl(1)	2.1270(8)	O(3)-C(32)	1.461(4)	
[(MMBP)(Et ₂ O)AlCl] 2d	Al(1)-O(1)	1.6948(15)	O(1)-C(1)	1.361(2)	a, 86
	Al(1)-O(1#)	1.6948(15)	O(2)-C(13)	1.469(3)	
	Al(1)-O(2)	1.849(2)	O(2)-C(13)#1	1.469(3)	
	Al(1)-Cl(1)	2.1252(13)			

[(MMMCyP)(THF)AlEt] 3a	Al(1)-O(1)	1.713(2)	O(1)-C(1)	1.351(3)	a
	Al(1)-O(2)	1.720(2)	O(2)-C(13)	1.362(4)	
	Al(1)-O(3)	1.870(2)	O(3)-C(32)	1.41(2)	
	Al(1)-C(30)	1.955(4)	O(3)-C(35)	1.46(2)	
[(MMMCyP)(Et ₂ O)AlEt] 3c	Al(1)-O(1)	1.703(3)	O(1)-C(1)	1.342(5)	a
	Al(1)-O(2)	1.722(3)	O(2)-C(13)	1.360(5)	
	Al(1)-O(3)	1.882(3)	O(3)-C(32)	1.473(5)	
	Al(1)-C(30)	1.945(5)	O(3)-C(34)	1.455(5)	
[(EDBP)(THF)AlMe]	Al(1)-O(1)	1.715(6)	O(1)-C(1)	1.358(9)	97
	Al(1)-O(2)	1.713(5)	O(2)-C(17)	1.359(5)	
	Al(1)-O(3)	1.864(6)	O(3)-C(32)	1.418(12)	
	Al(1)-C(31)	1.924(8)	O(4)-C(33)	1.437(12)	
[(MMMCyP)Al(OPr ⁱ) ₂][NEt ₄]	Al(1)-O(1)	1.734(3)	O(1)-C(1)	1.341(5)	100
	Al(1)-O(2)	1.756(3)	O(2)-C(17)	1.347(5)	
	Al(1)-O(3)	1.728(3)	O(3)-C(30)	1.407(5)	
	Al(1)-O(4)	1.739(3)	O(4)-C(33)	1.431(5)	

Table 11 Comparison of selected bond lengths [\AA] for [(bisphenol-*H*₂)(solvent)AlX] (*X*=Et and Cl) complexes, a – this work

Correlating the distances and bond angles involving the key atoms of the coordination sphere around the aluminium atom in the investigated structures (Al(1), O(1), O(2), O(3) and Cl(1) as well as carbon atom bound to the metal core) (see Tables 11 and 12) it can be seen that all the complexes display a high symmetry (symmetry plane or inversion point) and that the values found are within the ranges reported for similar aluminium bisphenoxides.^{86,97}

Catalyst	Bond angle, [°]		Bond angle, [°]		Lit.
[(MDBP)(THF)AlEt] 1a	O(1)-Al(1)-O(2)	115.76(9)	O(1)-Al(1)-C(30)	112.33(11)	a
	O(2)-Al(1)-O(3)	100.50(9)	O(3)-Al(1)-C(30)	106.36(11)	
	O(1)-Al(1)-O(3)	105.22(9)	C(1)-O(1)-Al(1)	140.71(15)	
	O(2)-Al(1)-C(30)	114.92(11)	C(32)-O(3)-C(35)	109.2(2)	
	C(3)-C(2)-C(1)	117.5(2)	C(35)-O(3)-Al(1)	125.08(18)	
[(MDBP)(Et ₂ O)AlEt] 1c	O(1)-Al(1)-O(2)	116.89(12)	O(3)-Al(1)-C(30)	111.90(17)	a
	O(2)-Al(1)-O(3)	103.17(14)	C(1)-O(1)-Al(1)	142.9(2)	
	O(1)-Al(1)-O(3)	102.67(13)	C(32)-O(3)-C(35)	109.2(2)	
	O(2)-Al(1)-C(30)	114.13(16)	C(35)-O(3)-Al(1)	127.5(4)	
	O(1)-Al(1)-C(30)	112.33(11)	C(3)-C(2)-C(1)	118.1(3)	
[(MDBP)(Et ₂ O)AlCl] 1d	O(1)-Al(1)-O(2)	119.93(6)	C(13)-O(2)-Al(1)	144.01(11)	86
	O(2)-Al(1)-O(3)	104.21(6)	C(1)-O(1)-Al(1)	138.34(11)	
	O(1)-Al(1)-O(3)	104.51(6)	C(30)-O(3)-Al(1)	19.66(19)	
	O(2)-Al(1)-Cl(1)	110.82(5)	C(32)-O(3)-Al(1)	116.46(19)	
	O(3)-Al(1)-Cl(1)	103.52(6)	C(1)-C(2)-C(14)	121.19(15)	
[(MMBP)(Et ₂ O)AlCl] 2d	O(1)-Al(1)-O(2)	104.55(7)	O(1)-C(1)-C(6)	120.08(19)	86
	O(1)-Al(1)-Cl(1)	110.14(6)	C(1)-C(6)-C(7)	122.5(2)	
	O(2)-Al(1)-Cl(1)	106.11(8)	C(2)-C(9)-C(12)	109.6(2)	
	C(1)-O(1)-Al(1)	140.82(14)	C(2)-C(9)-C(11)	111.17(18)	
	C(13)-O(2)-Al(1)	121.77(15)	C(14)-C(13)-O(2)	112.0(2)	
[(MMMCyP)(THF)AlEt] 3a	O(1)-Al(1)-O(2)	117.08(11)	O(3)-Al(1)-C(30)	104.21(19)	a
	O(1)-Al(1)-O(3)	103.17(11)	C(1)-O(1)-Al(1)	149.2(2)	
	O(2)-Al(1)-O(3)	101.11(12)	C(13)-O(2)-Al(1)	136.52(19)	
	O(1)-Al(1)-C(30)	112.77(16)	C(32)-O(3)-C(35)	114.7(15)	
	O(2)-Al(1)-C(30)	115.83(17)	O(1)-C(1)-C(2)	120.4(3)	
[(MMMCyP)(Et ₂ O)AlEt] 3c	O(1)-Al(1)-O(2)	116.29(17)	O(3)-Al(1)-C(30)	105.96(19)	a
	O(1)-Al(1)-O(3)	100.79(16)	C(1)-O(1)-Al(1)	147.4(3)	
	O(2)-Al(1)-O(3)	104.60(16)	C(13)-O(2)-Al(1)	138.8(3)	
	O(1)-Al(1)-C(30)	113.20(19)	C(34)-O(3)-C(32)	115.1(4)	
	O(2)-Al(1)-C(30)	114.04(19)	O(1)-C(1)-C(2)	119.8(4)	

[(EDBP)(THF)AlMe]	Al(1)-O(1)-C(1)	136.5(5)	O(3)-Al(1)-C(31)	106.4(3)	97
	Al(1)-O(2)-C(13)	148.3(5)	O(1)-Al(1)-O(2)	116.5(3)	
	O(1)-Al(1)-C(31)	117.2(3)	O(1)-Al(1)-O(3)	99.6(3)	
	O(2)-Al(1)-C(31)	111.1(3)			

Table 12 Comparison of selected bond angles [$^{\circ}$] for [(bisphenol- H_2)(solvent)AlX]
(X=Et and Cl) complexes, a – this work

5.2.1.1 Reactions of Et₃Al and Et₂AlCl with MCIMePrPH₂ in the presence of THF – formation of two different products

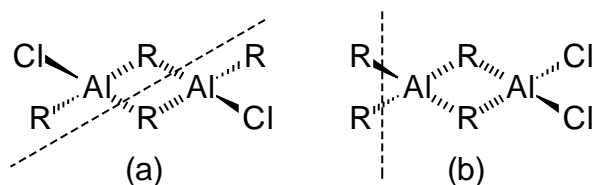
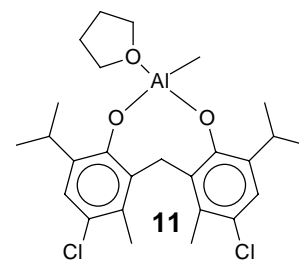


Figure 7 Symmetrical and asymmetrical cleavage of alkyl-halide aluminium compounds.

Aluminium compounds are known to form neutral donor-acceptor complexes with bisphenols through symmetrical dissociation of the aluminium alkyl dimer (Figure 7, a).¹⁰¹ A scarcely documented reaction route is the asymmetrical cleavage (Figure 7, b) of the aluminium alkyl dimer to produce ionic species. As for the moment only AlCl₃ and EtAlCl₂ afforded compounds having ionic structures. The EtAlCl₂ dimer treated with a pentadentate macrocyclic ether and THF yields two cationic complexes: [AlCl₂ (benzo-15-crown-5)][AlCl₃Et] and [AlCl₂(THF)₂][AlCl₃Et], respectively.^{102,103} Atwood isolated a similar *iso*-structural [AlCl₂(THF)₄][AlCl₄] analogue.^{102,104} Keeping in sight the synthesis and isolation of neutral [(MCIMePrP)(THF)AlCl] complex as a supplement to our catalyst library (see Table 7), we performed its synthesis, and unexpectedly isolated an ionic compound, in which the cation has the same structure as the one reported by Atwood (see Figure 10). It was confirmed by X-ray single crystal analysis. In order to confirm that the obtained product was not serendipitously synthesised, this reaction was repeated yielding again the same product, despite the fact, that two different solvents (THF and hexane) were used for the washing of the obtained solid. Interestingly, this is to date the only ionic compound isolated from AlEt₂Cl.¹⁰²⁻¹⁰⁴

Both X-ray structures of **4**-based Al-complexes as well as the structure of the methyl analogue of **4a**, [(MCIMePrP)AlMe(THF)]⁹⁰ **11**, differ from other isolated monomeric compounds. The presence of 3,3'-methyl substituents has a significant influence on the geometry of phenyl rings bonded to C(7) carbon.



Looking from the side and comparing with **1a**, we can see that due to the steric repulsion between the 3,3'-methyl groups of the MCIMePrP ligand the relative symmetry of the bisphenoxide ligand is disordered in **4a**. Comparing the values for the angles Al(1)-O(1)-C(1): 131.9° and Al(1)-O(2)-C(13): 122.8° in **4a** and Al(1)-O(1)-C(1): 140.7° and Al(1)-O(1)-C(13): 145.2° for **1a**, it can be seen, that these second values are much larger as those for **4a** and suggest that the symmetric complexes have a bigger potential docking site for an epoxide than the asymmetric one. In case of others

monomeric structures these angles are also of that order of magnitude close to **1a**. The torsion angle between C(1)C(6) and C(8)C(13) is 38.9°, what is very close to value of 40.4° for methyl analogue of **4a**.⁹⁰

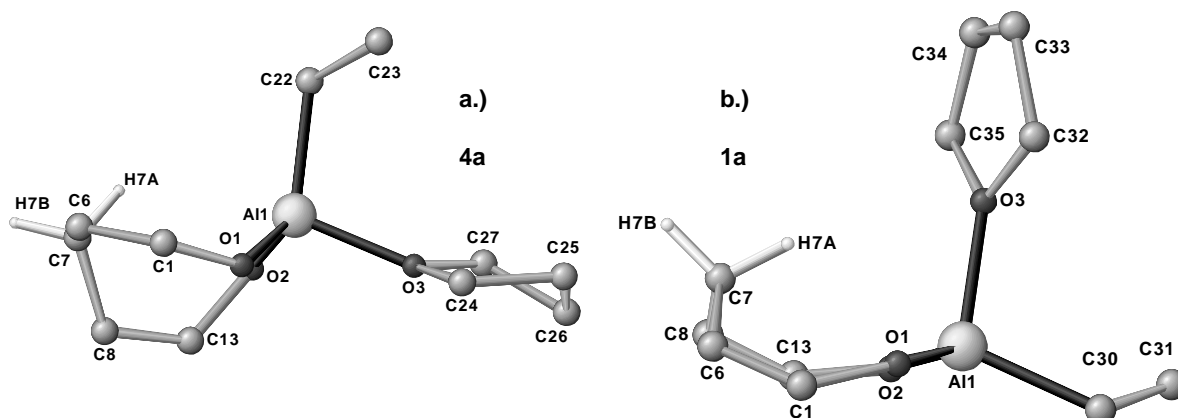


Figure 8 Influence of 3,3'-methyl substituent on distortion of bisphenol ligands. a.) highly distorted **4a**, b.) slightly distorted **1a**

Another interesting feature is the system of two mutually perpendicular eight-membered ring present in the anion of **4b** (see Figure 8). Aluminium atom of $[\text{Al}(\text{MCIPr}^i\text{MP})_2]^-$ anion is fourfold coordinated and is located inside of the slightly distorted tetrahedron formed by the bisphenoxides' oxygen atoms. The cation $[\text{AlCl}_2(\text{THF})_4]^+$ of the isolated ionic compound consists of an octahedrally coordinated aluminium atom with four equatorial THF's oxygen atoms and two axial chlorine ones. Distances between Al(1) and oxygen atoms of bisphenol O(1-4) and Al(2) and O(5-8) of THF rings vary hardly, but the first ones are significantly shorter (see Table 13). Lengths of bonds between aluminium atom Al(2) and oxygen atoms of coordinated THF molecules (O5-8) are 0.07 Å longer than corresponding bond between Al(1) and O(3) of THF in **4a** (ca. 1.949 Å and 1.877(2), respectively). Both eight-membered rings in anion are distorted, as seen in the following bonds angles: Al(1)-O(1)-C(1) 144.9(4)°, Al(1)-O(2)-C(9) 126.6(4)°, Al(1)-O(3)-C(22) 123.3(4)° and Al(1)-O(4)-C(30) 129.6(4)°. Bonds angles between oxygen and carbon atoms of phenol rings are much more regular (O(1)-C(1)-C(6): 120.4(5); O(2)-C(9)-C(8): 121.6(5)°; O(3)-C(22)-C(27): 120.1(5)° and O(4)-C(30)-C(31): 118.0(5)° respectively), although lengths of bonds O(1)-C(1) and O(2)-C(9) are shorter than the corresponding bonds of second ring (1.336(6) and 1.349(7) Å and 1.357(7) Å and 1.361(7) Å vs. O(3)-C(22) and O(4)-C(30), respectively). $[\text{AlCl}_2(\text{THF})_4][\text{Al}(\text{MCIPr}^i\text{MP})_2]$ revealed to crystallise in monoclinic system. To our best knowledge, there are no data in literature about aluminium diolates compounds displaying such a structure.

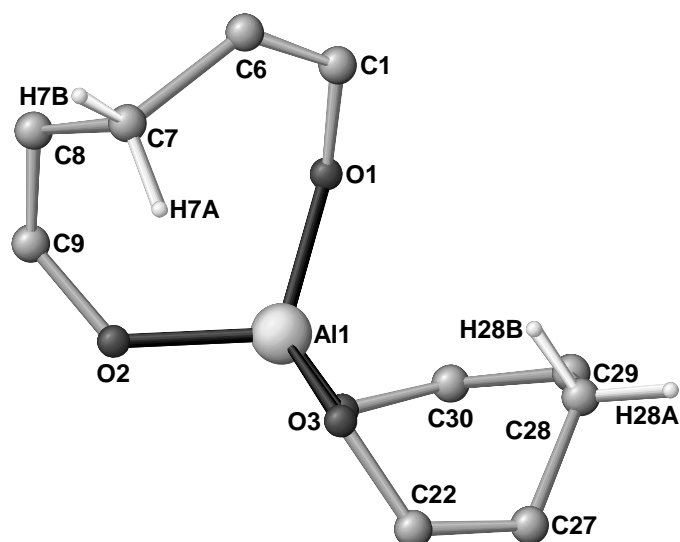


Figure 9 Distorted eight-member rings of anion of **4b**. Phenol rings were omitted for clarity.

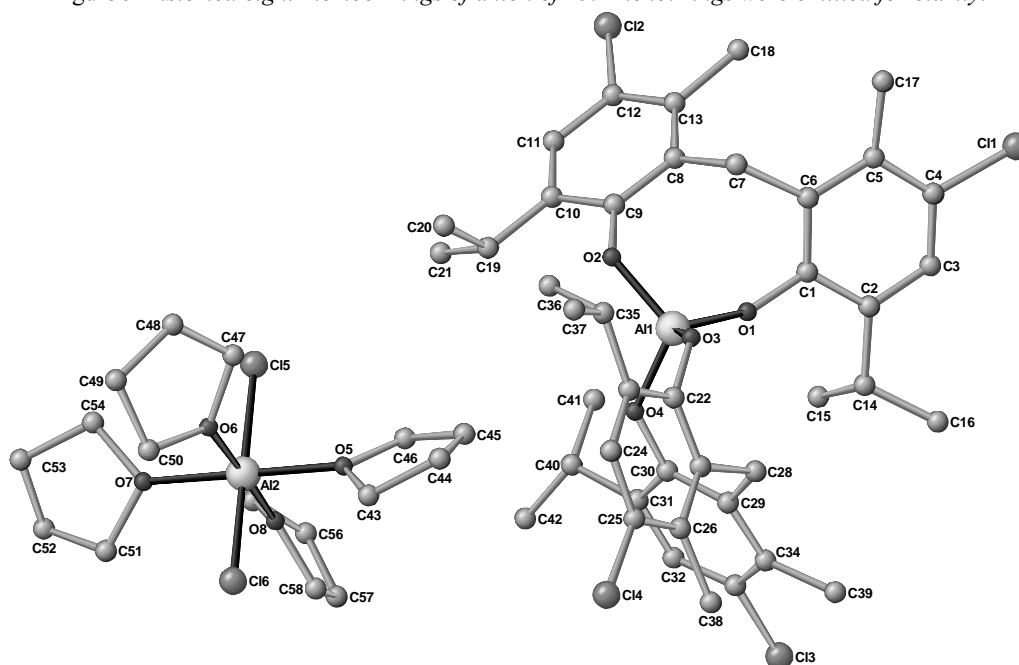


Figure 10 Crystal structure of $[AlCl_2(THF)_4][Al(MCIPr^iMP)_2]$.

Catalyst	Length of bonds, [Å]		Bond angle, [°]		Lit.
[(MCiMePrP)(THF)AlEt] 4a	Al(1)-O(1)	1.728(2)	O(1)-Al(1)-O(2)	109.16(10)	a
	Al(1)-O(2)	1.735(2)	O(1)-Al(1)-O(3)	98.63(10)	
	Al(1)-O(3)	1.877(2)	O(1)-Al(1)-C(22)	119.73(13)	
	Al(1)-C(22)	1.941(3)	C(27)-O(3)-Al(1)	121.56(18)	
	O(1)-C(1)	1.353(3)	C(1)-O(1)-Al(1)	131.90(18)	
	O(2)-C(13)	1.364(3)	C(24)-O(3)-Al(1)	126.01(19)	
	O(3)-C(24)	1.475(4)	O(2)-C(13)-C(12)	118.0(3)	
	O(3)-C(27)	1.484(4)	C(24)-O(3)-C(27)	109.4(2)	
			O(1)-C(1)-C(6)	120.5(3)	
			O(1)-C(1)-C(2)	118.4(3)	
[(MCiMePrP)(THF)AlMe]	Al(1)-O(1)	1.728(3)	O(1)-Al(1)-O(2)	108.11(12)	90
	Al(1)-O(2)	1.738(2)	O(1)-Al(1)-O(3)	100.96(12)	
	Al(1)-O(3)	1.885(3)	O(2)-Al(1)-O(3)	103.15(13)	
	Al(1)-C(22)	1.940(4)	O(2)-Al(1)-C(22)	118.36(17)	

	O(1)-C(1)	1.389(3)	C(1)-O(1)-Al(1)	127.9(2)	
	O(2)-C(13)	1.381(3)	C(13)-O(2)-Al(1)	120.8(2)	
	O(3)-C(24)	1.473(1)	C(23)-O(3)-Al(1)	120.5(3)	
	O(3)-C(26)	1.445(4)	C(26)-O(3)-Al(1)	126.7(3)	
			C(23)-O(3)-C(26)	108.9(3)	
			C(23)-O(3)-Al(1)	120.5(3)	
			C(26)-O(3)-Al(1)	126.7(3)	
			O(1)-C(1)-C(2)	117.5(3)	
[AlCl ₂ (THF) ₄][Al(MCIPr ⁱ MP) ₂] 4b	Cl(5)-Al(2)	2.246(3)	O(1)-Al(1)-O(2)	108.3(2)	a
	Cl(6)-Al(2)	2.225(3)	O(1)-Al(1)-O(4)	107.9(2)	
	Al(1)-O(1)	1.726(4)	O(2)-Al(1)-O(4)	111.4(2)	
	Al(1)-O(2)	1.739(4)	O(1)-Al(1)-O(3)	115.7(2)	
	Al(1)-O(3)	1.747(4)	O(2)-Al(1)-O(3)	107.7(2)	
	Al(1)-O(4)	1.746(4)	O(4)-Al(1)-O(3)	105.7(2)	
	Al(2)-O(5)	1.955(5)	O(6)-Al(2)-O(8)	178.4(2)	
	Al(2)-O(6)	1.944(5)	O(6)-Al(2)-O(5)	90.4(2)	
	Al(2)-O(7)	1.955(5)	O(8)-Al(2)-O(5)	91.3(2)	
	Al(2)-O(8)	1.949(5)	O(6)-Al(2)-O(7)	89.8(2)	
[AlCl ₂ (THF) ₄][EtAlCl ₃]	Cl(1)-Al(1)	2.2443(9)	O(1)-Al(1)-O(2)	89.53(7)	103
	Cl(2)-Al(1)	2.2429(9)	O(1)-Al(1)-O(4)	89.69(7)	
	Al(1)-O(1)	1.9409(16)	O(2)-Al(1)-O(4)	179.20(7)	
	Al(1)-O(2)	1.9450(16)	O(1)-Al(1)-O(3)	179.12(7)	
	Al(1)-O(3)	1.9371(16)	O(2)-Al(1)-O(3)	89.71(7)	
	Al(1)-O(4)	1.9331(16)	O(4)-Al(1)-O(3)	91.07(7)	
	Al(2)-C(17)	1.951(3)	C(17)-Al(2)-Cl(4)	112.00(8)	
	Al(2)-Cl(3)	2.1608(10)	C(17)-Al(2)-Cl(3)	111.41(8)	
	Al(2)-Cl(4)	2.1506(9)	Cl(4)-Al(2)-Cl(3)	106.89(4)	
	Al(2)-Cl(5)	2.1701(10)	C(17)-Al(2)-Cl(5)	111.50(9)	

Table 13 Comparison of selected lengths of bonds [\AA] and bonds angles [$^\circ$] for self-synthesised **4a** and **4b** and literature-known [(MCIMePrP)(THF)AlMe] and [AlCl₂(THF)₄][EtAlCl₃], a – this work

The unusual features of the described structure generate interesting features of ¹H NMR spectra. Owing to significant steric repulsions of methyl groups attached on 3 position of phenyl rings two sets of resonances would be expected. At 20 °C only one set of resonances of substituted phenyl rings is visible, two hydrogen atoms in the bridging methylene are observed to be magnetically equivalent with a chemical shift of 3.98 ppm (see Figure 11). This magnetic equivalence can be attributed to the rapid twisting of the MCIPrⁱMP ligand and recombination of THF on the aluminium centre.⁹⁰ Another result of this rapid dissociation is a lack of observable C-H...O interaction, what can be seen in the hydrogen bond length and the hydrogen bond angle of **4a** are 4.43 Å and 110.6°, respectively.

The isolated ionic compound is well soluble in THF and chlorinated solvents. Both ligand moieties bound to tetrahedral Al atom are spectroscopically equivalent. Despite a significant different distances between aluminium and hydrogen atoms H(7A) and H(7B) bound to bridging carbon (2.671 Å and 4.315 Å, respectively), there is no observable shift in chemical shifts of these two hydrogen atoms (3.89 ppm and 3.95 ppm, respectively), so one can assume that they are also equivalent (see Figure 12).

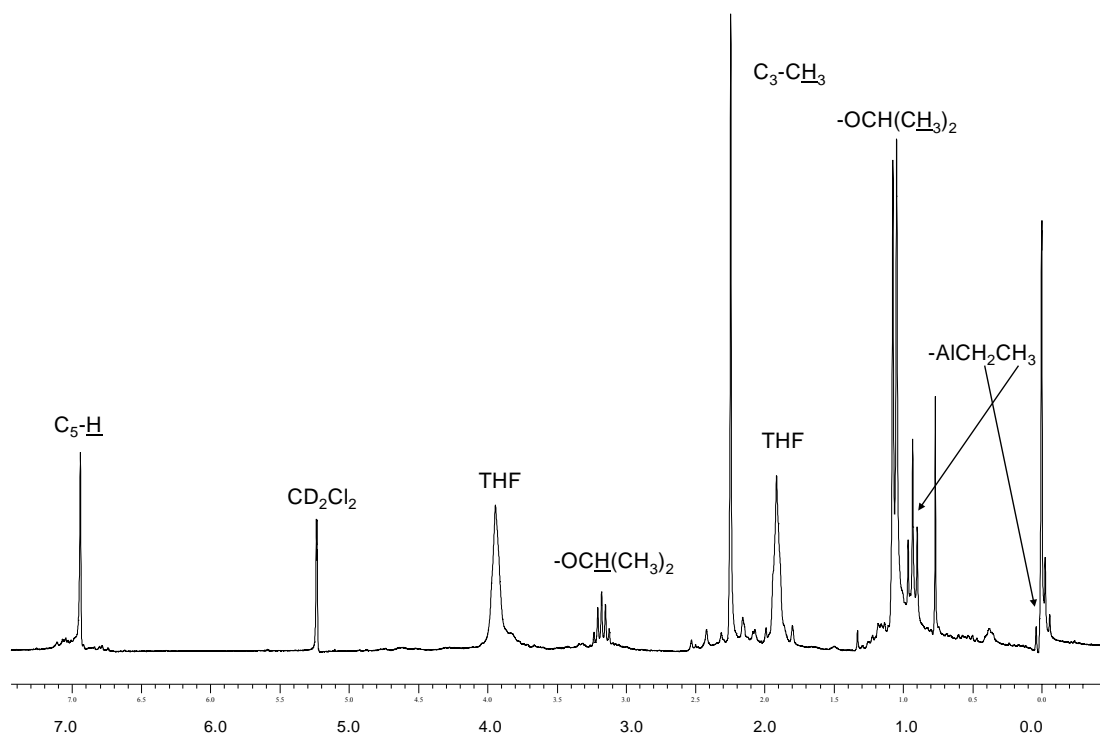


Figure 11 ^1H NMR spectrum of complex **4a**.

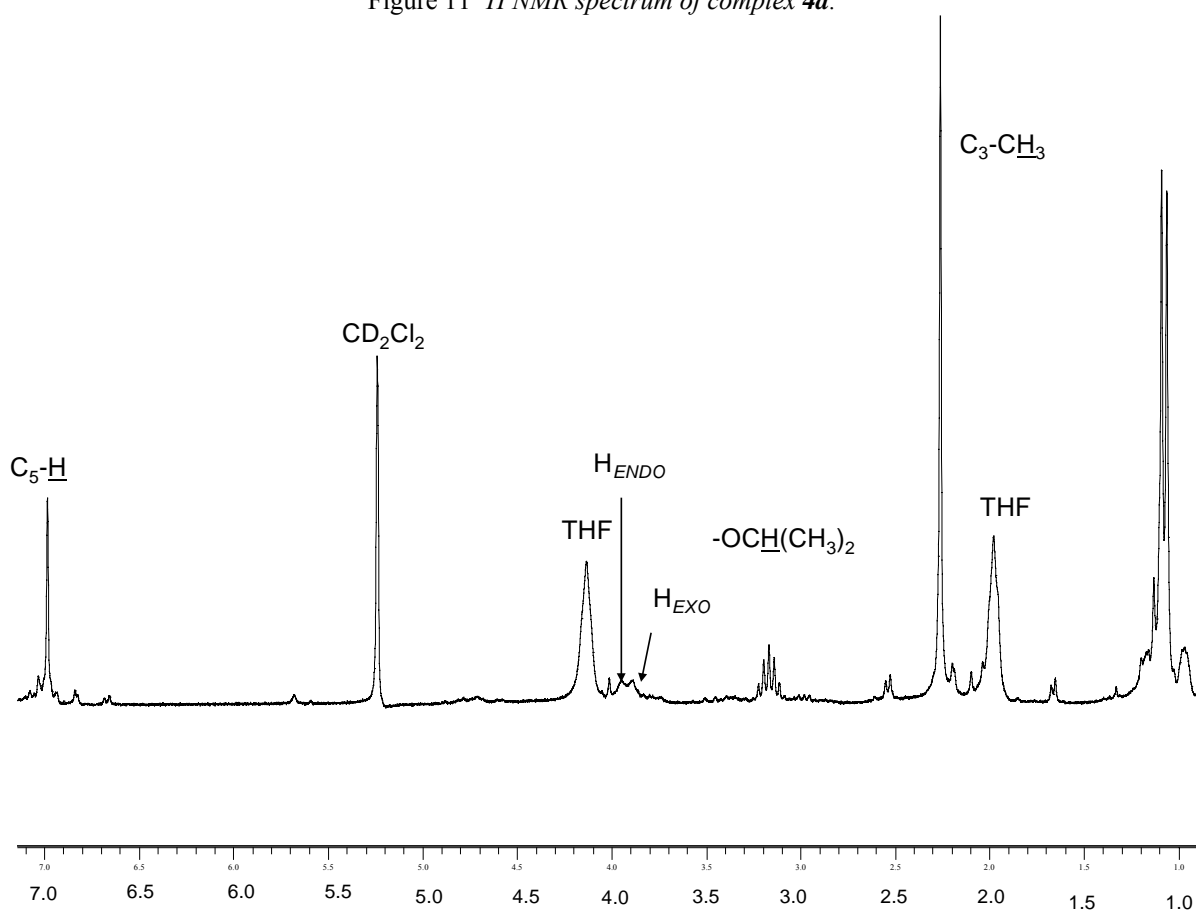


Figure 12 ^1H NMR spectrum of **4b** complex.

5.2.2 Reactions realised in the absence of ethers. Influence of ortho-substituent on the reaction path. Formation of dimers and trimers

The reactions of differently substituted aromatic diols with aluminium precursors performed in non-coordinating hexane result in the formation of dimeric compounds. All the reactions reported here, were carried out in a one to one stoichiometry (ligand : aluminium precursor) (see Figure 13). The purification of these products and their spectroscopic identification were performed in the same manner as it was done in the case of monomers. In this part of our investigation AlEt_3 , AlEt_2Cl and AlEt_2I made *in situ* were used as aluminium precursors. In order to compare the influence of the halide used on the catalytic activity, it was decided to synthesise a **2h**, an iodine analogue of chlorine contained **2f**, whose synthesis was realised in a two-step approach.¹⁴⁴ Firstly the reaction of Et_3Al with iodine performed in hexane resulted in the formation of diethylaluminium iodide and then a solution of MMBPH_2 was drop-wise added.

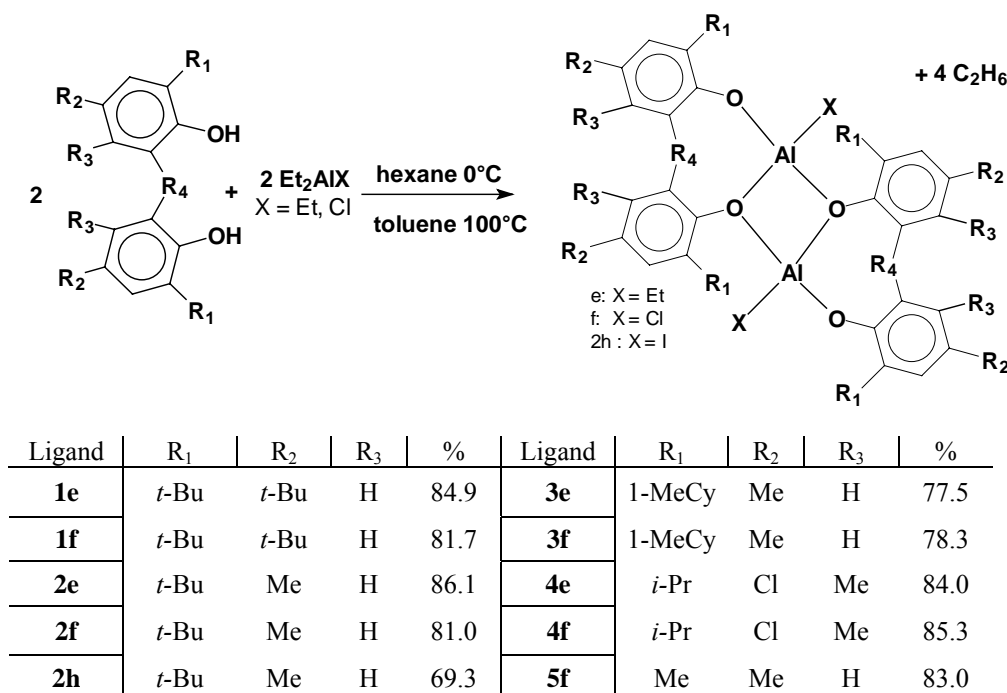
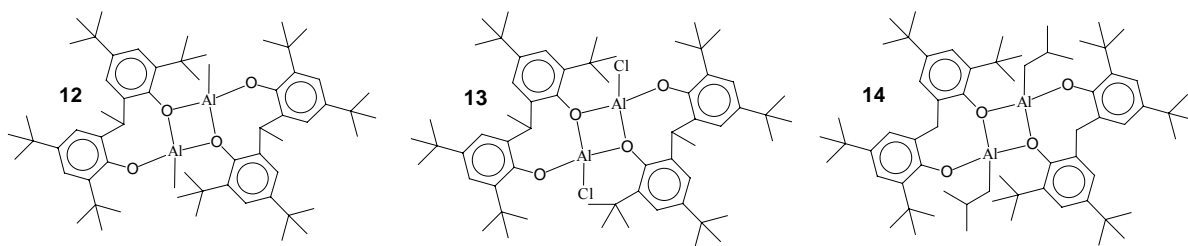


Figure 13 General scheme of synthesis of dimeric alkyl (signed as **e**) and halides (signed as **f** and **h**) aluminium complexes.

In order to obtain crystals suitable for the X-ray analysis, the crystallisation procedure was performed either with a concentrated hexane solution or a hot toluene. The coordination around the Al can be described as a distorted tetrahedron geometry with the largest angle being associated with the eight-membered ring of the bisphenoxide ligand. The ^{27}Al NMR can easily confirm this geometry, in the case of **1e** giving broad large peak with maximum at ca. 53 ppm (5595 mm Hz). Isolated dimeric compound crystallised either in the monoclinic (**1e**) or triclinic (**3f**) crystal systems. The dimeric compound already reported in the literature like e.g. **13** (analogue of **1f**) crystallises in the same manner as **3f**. Although no detailed X-ray structural analysis has been

reported concerning the other known aluminium bisphenoxides like e.g. [(EDBP)AlMe]₂, **12**, and [(MDBP)AlBu^{iso}]₂, **14**, these compounds, belonging to the same group of dimeric bisphenoxide compounds, should display analogous structural characteristics in both solid state and solution.



Catalyst	Length of bonds, [Å]		Length of bonds, [Å]		Lit.
[(MDBP)AlEt] ₂ 1e	Al(1)-C(30)	1.938(4)	Al(1)-O(2)	1.700(2)	a
	Al(1)-O(1)	1.862(3)	O(1)-C(1)	1.428(4)	
	Al(1)-O(1a)	1.874(3)	O(2)-C(13)	1.363(4)	
[(MMMCyP)AlCl] ₂ 3f	Al(1)-Cl(1)	2.0898(12)	Al(1)-O(2)	1.674(2)	a
	Al(1)-O(1)	1.844(2)	O(1)-C(1)	1.434(3)	
	Al(1)-O(1a)	1.845(2)	O(2)-C(13)	1.367(3)	
[(EDBP)AlCl] ₂ 13	Al(1)-Cl(1)	2.060(3)	Al(1)-O(2)	1.637(4)	86, 107
	Al(1)-O(1)	1.826(4)	O(3)-C(4)	1.434(4)	
	Al(1)-O(1a)	1.817(4)	C(18)-C(20)	1.515(5)	

Table 14 Comparison of selected bond distances for [(diolate)AlX]₂ (X=Me, Et and Cl) complexes, a – this work.

The NMR spectroscopy is one of the most powerful spectroscopic method to investigate the structure of complexes in solution. It is of course relevant to gather information on the compounds' structure before studying these compounds under catalytic experimental conditions (e.g. with an epoxide and under CO₂ pressure). In the case of the aluminium bisphenoxides obtained from the reaction of bisphenols derivatives and triethylaluminium, it can be noticed that the ethyl group directly bound to the aluminium centre has a constrained geometry (no rotation around the Al-C bond, the methylene hydrogen atoms directly bond to the aluminium appear as a complex multiplet). It indicates furthermore that the bisphenolic chelating ligand meets the requirement for a constrained, definite geometry at the active centre. Moreover, there is significant difference in the bond lengths involving phenoxy rings and aluminium atom (ca. 3.28 Å for Al(1)-O(1)-C(1) vs. 3.05 Å for Al(1)-O(2)-C(13)); also bond angles Al(1)-O(1)-C(1) and Al(1)-O(2)-C(13) differ significantly (ca. 124 vs. ca. 156 degree). Collected data for the “home-made” **1e** and **3f** are in good agreement with those collected for [(EDBP)AlCl]₂ **13** (1.637(4), 1.826(4) and 1.817(4) Å, respectively). Due to this difference Al(1)-O(1)-C(1) bond might be considered as a bridging ligand with bridging oxygen atom, it can be seen at the ¹H NMR spectrum of each isolated product as a slight magnetic non-equivalence of phenyl rings (and their substituents) (see Figure 14 as well as Tables 14 and 15). Owing to such dimeric structure each group of hydrogen atoms appears as a doublet of signals of equal intensity, hydrogen atoms bounds to the bridging carbon appear as an AB spectrum. Due to broad peaks generated by

cyclohexene moieties of **3**-based catalysts an aliphatic part of spectrum seems the same as in the case of their monomeric counterparts.

Catalyst	Bond angle, [°]		Bond angle, [°]		Lit.
[(MDBP)AlEt] ₂ 1e	O(1)-Al(1)-C(30)	121.69(15)	Al(1)-O(2)-C(13)	156.1(2)	a
	O(1)-Al(1)-O(2)	112.62(12)	O(2)-C(13)-C(8)	118.5(3)	
	O(2)-Al(1)-C(30)	108.02(15)	C(6)-C(1)-O(1)	116.8(3)	
	Al(1)-O(1)-C(1)	123.9(2)			
[(MMMCyP)AlCl] ₂ 3f	O(1)-Al(1)-Cl(1)	121.47(8)	Al(1)-O(2)-C(13)	155.1(2)	a
	O(1)-Al(1)-O(2)	112.59(10)	O(2)-C(13)-C(8)	117.8(3)	
	O(2)-Al(1)-Cl(1)	106.68(8)	O(1)-C(1)-C(6)	116.7(2)	
	Al(1)-O(1)-C(1)	122.11(16)			
[(EDBP)AlCl] ₂ 13	Cl(1)-Al(1)-O(1)	119.0(2)	Cl(1)-Al(1)-O(2)	108.1(2)	86, 107
	O(1)-Al(1)-O(2)	113.1(2)	Cl(1)-Al(1)-O(1A)	111.0(1)	
	O(1)-Al(1)-(1A)	81.1(2)	O(2)-Al(1)-O(1A)	123.1(2)	
	Al(1)-O(1)-C(1)	121.0(3)	Al(1)-O(2)-C(13)	157.3(4)	

Table 15 Comparison of selected bond angles [°] for self-synthesised and literature-known [(diolate)AlX]₂ (X=Et and Cl) complexes, (listed for monomer), a – this work

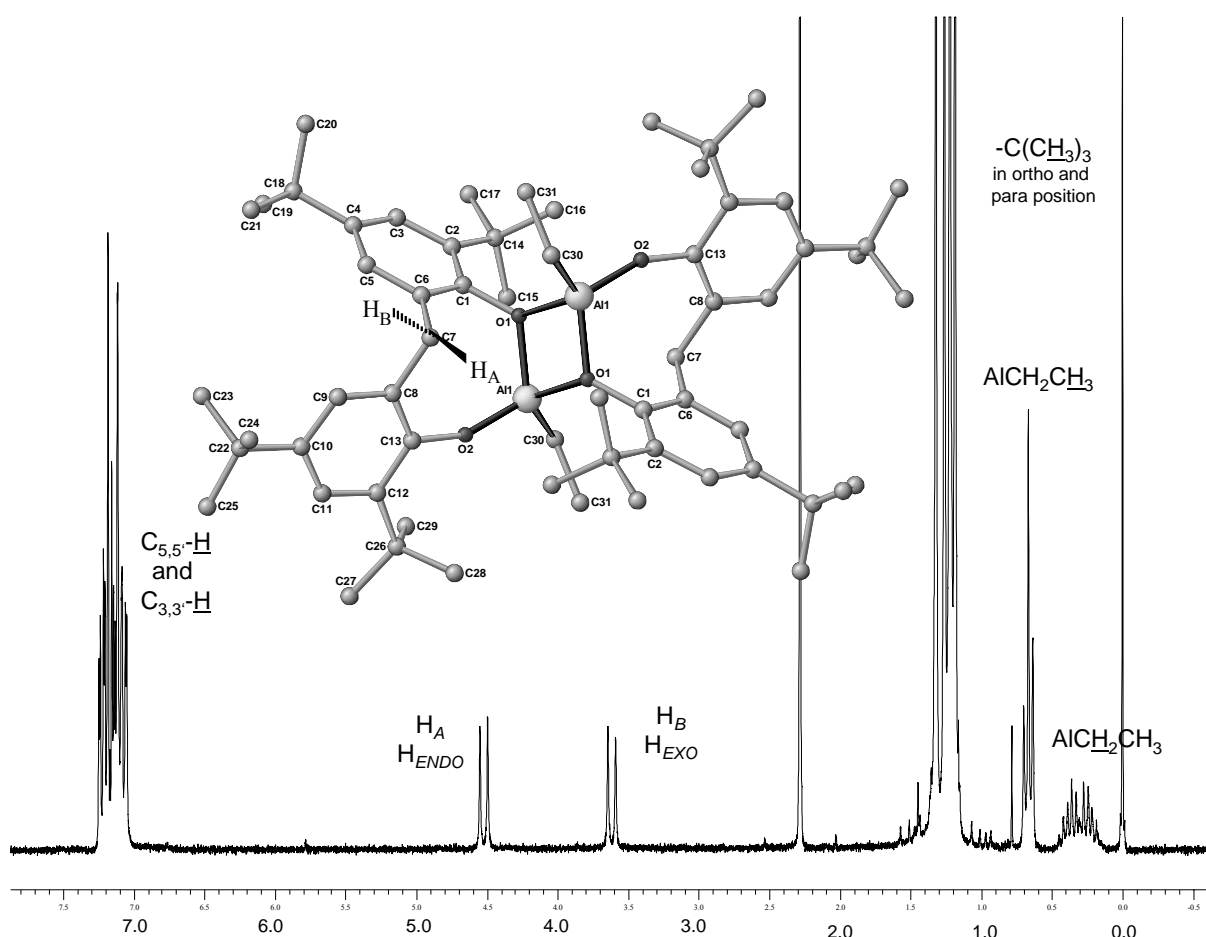


Figure 14 Identification of product by use of ¹H NMR spectroscopy. Confirmation of existence of dimer in its hydrocarbon solution.

The ¹H NMR spectra of **1–4 e–f** show, that the two hydrogen atoms bound to carbon C(7) of the methylene bridge are non-equivalent (AB pattern) in which one hydrogen atom is pointing away and the second towards Al atom (see Figure 14). For all compounds having **1 – 4** as a ligand the two doublets are located at about 3.48–3.55 and 4.35–4.45 ppm. In opposition to the monomeric bisphenoxides, where the presence of a weak interaction between oxygen of the neutral O-donor

ligand and one of the hydrogen atoms of the methylene bridge C(7) resulted in an upfield shift of the hydrogen located closer to the aluminium atom (see Table 9), the dimeric bisphenoxides did not display such a phenomenon (see Table 16).

	C(7)H ₂ (H _{EXO})	J _{H-H} [Hz]	C(7)H ₂ (H _{ENDO})	J _{H-H} [Hz]
1e	3.48	13.64	4.39	13.64
1f	3.65	13.42	4.38	14.38
2e	3.55	13.55	4.44	13.70
2f	3.48	13.55	4.39	13.70
2h	3.58	14.65	4.34	14.41
3e	3.55	13.74	4.40	13.74
3f	3.55	13.72	4.40	13.72
4e	3.51	13.68	4.35	13.42
4f	3.51	13.42	4.38	13.72
5f	3.76	invisible	4.50	invisible

Table 16 ¹H NMR data of hydrogen atoms bounded to C-7 atom in dimer molecule.

As found in the case of the monomeric bisphenoxides, the magnitudes of the geminal coupling constant, ²J_{HH}, range from 13.40 to 14.70 Hz, confirming the non-equivalence of the C-7 methylene hydrogen atoms. These values are comparable to the ones previously reported for [(EDBP)AlMe]₂^[105] **12**, [(EDBP)AlCl]₂^[106] **13** and [(MDBP)AlBu^{iso}]₂^[107] **14**. In all considered aluminium bisphenoxides, the NMR data are in agreement with the structural data recorded by X-ray crystallography on single crystals.

	AlCH ₂ CH ₃	AlCH ₂ CH ₃	C(7)(H _{EXO})	C(7)(H _{ENDO})	R ₁	R ₂	C ₃ -H	C ₅ -H
1e	0.11, 0.15	0.51, 0.65	3.48	4.39	1.22	1.31	6.95	7.05
1f	-	-	3.65	4.38	1.21	1.38	7.18	7.24
2e	0.36	0.75	3.55	4.44	1.20, 1.28	2.14, 2.25	6.90	6.98, 7.03
2f	-	-	3.48	4.39	1.22	2.18	6.99	7.03
2h	-	-	3.58	4.34	1.22	2.17	6.93	7.17
3e	0.25	0.84	3.55	4.40	1.11-1.75	2.15, 2.25	6.88, 6.96	7.01
3f	-	-	3.55	4.40	1.11-1.69	2.15, 2.25	6.88, 6.97	7.01
4e	0.11, 0.21	0.51	3.51	4.35		-	-	7.04
4f	-	-	3.31	4.40	1.18	-	-	7.04
5f	-	-	3.76	4.50	2.13-2.20 (broad peak)		6.75-6.80	7.01

Table 17 Comparison of chemical shifts of hydrogen atoms.

The infrared spectroscopy, unfortunately, cannot serve as an effective tool for a unambiguous characterisation of the obtained aluminium complexes. The different substituents grafted to the 2,2'-methylenebisphenoxide backbone generate complex vibration modes yielding spectra where C=C, C-O and C-C stretching bands as well as C-H bending band overlap making a quick attribution quite difficult. However, there are some distinctive absorption bands, which can provide some information. For a number of alkoxides with different metal cores (such as Al, Ti, Zr, Hf, Nb, Tn) metal alkoxides bands of ν(C-O)M appear in the region between 1150 and 900 cm⁻¹, the position of the absorption bands depends on the nature of the alkoxy group.¹⁰⁸ For instance, isopropoxy derivatives show bands at 1170, 1150, 950 cm⁻¹ corresponding to ν(C-H) as well as a strong doublet at 1375 and 1365 cm⁻¹, corresponding to

stretching $\delta(\text{O-H})$ vibrations. Bands above 1000 cm^{-1} were assigned to stretching $\nu(\text{C-O})$ vibrations¹⁰⁸, a set of intensive bands in the region of $699 - 650\text{ cm}^{-1}$ can be attributed to to $\nu(\text{Al-O})$ stretching (see band at 663 cm^{-1} , see Figure 15.) The stretching bands at $900 - 720$ as well as at about 550 cm^{-1} confirm the kind of substitution (*ortho*-, *meta*-, *para*-, and mixed) in phenol rings (bending C-H).^{109,110}

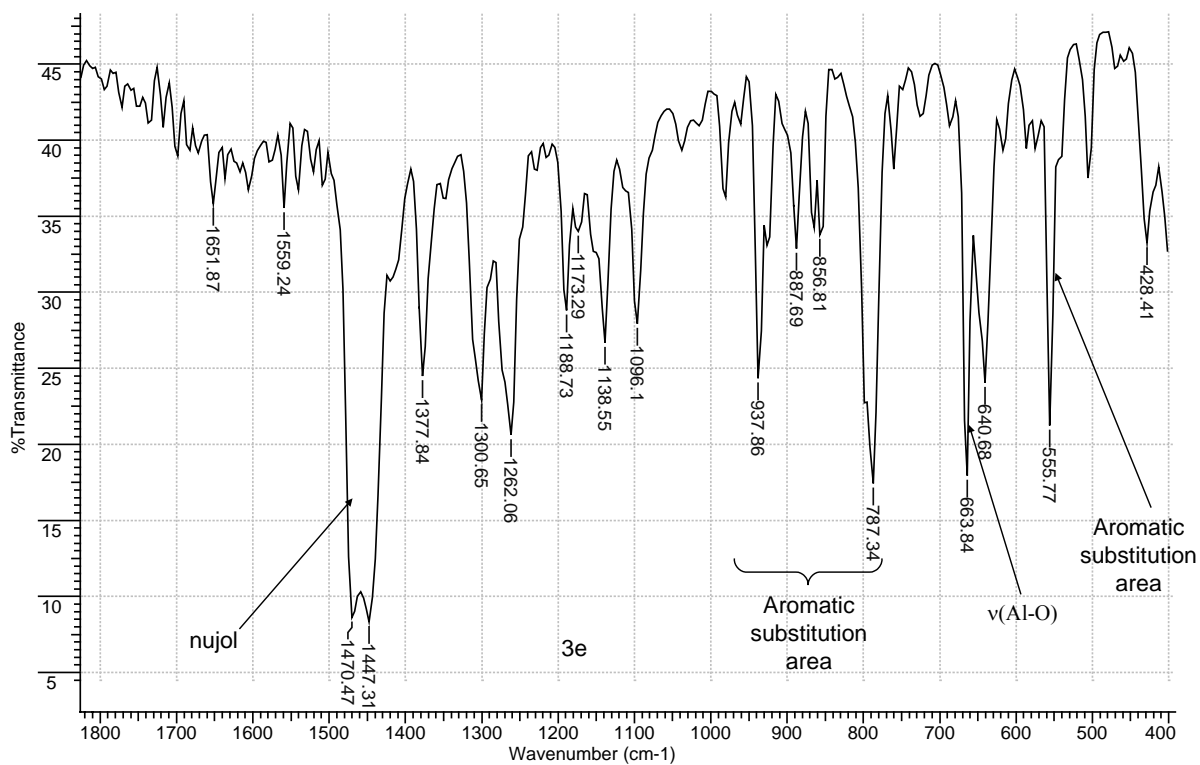


Figure 15 IR Spectrum of **3e** ($1800 - 400\text{ cm}^{-1}$).

5.2.3 Reactions of aluminium isopropoxide with ligands

The dimeric isopropoxy-bisphenoxy aluminium derivatives can be synthesised according to three different reaction's paths (see Figure 16), what was illustratively studied using 2,2'-methylenebis(4,6-di-tert-butylphenol), **1**. The first one is a one-step reaction of the bisphenol with aluminium isopropoxide under liberation of isopropanol. The second one is a two-step reaction, where an Al-ethyl-bisphenoxide dimer reacts with isopropanol. The last way of reaction was confirmed during an attempt of isolation of monomeric isopropoxy-diethyl ether complex of **1**, which yielded a dimeric specie without any Lewis base coordinated to the aluminium centers. Owing to larger basicity of alcoholate than Et₂O the stabilisation of dimeric structure is even possible in weak coordinating solvents, such like e.g. diethyl ether, this basicity does not allow on formation of solvent adducts.

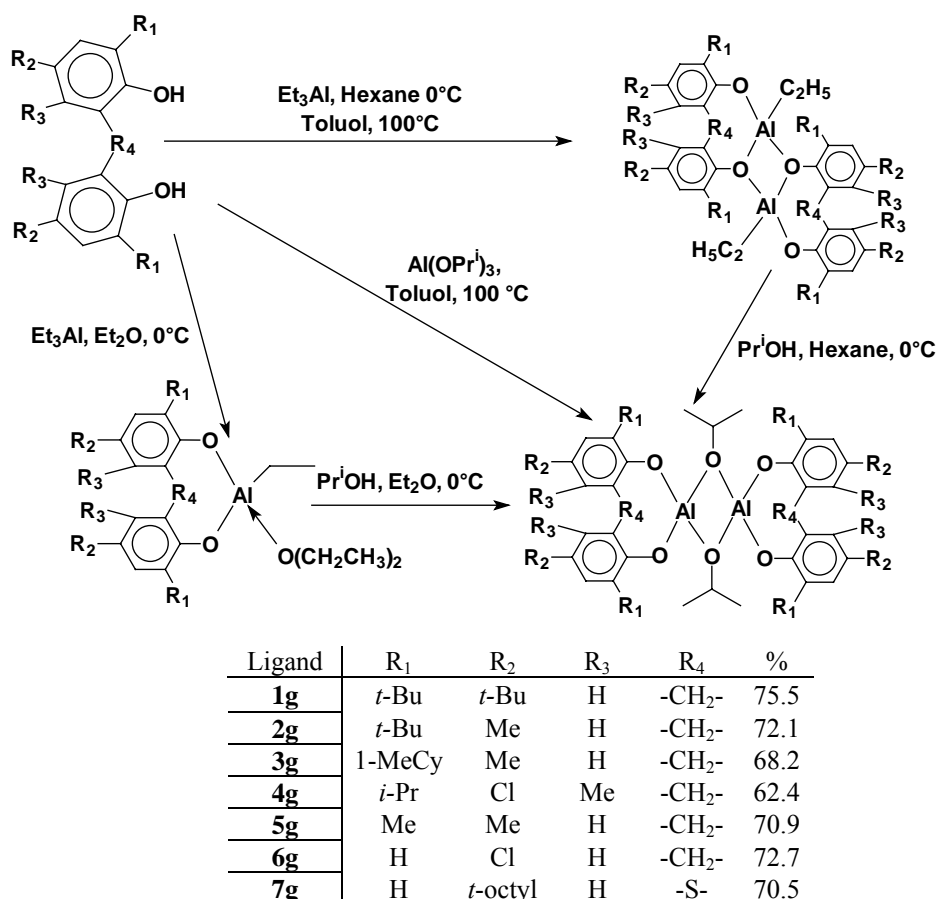


Figure 16 Three possible reaction paths of aluminium isopropoxy-bisphenolate syntheses. Reaction yields are given for direct, one-step conversion of ligand with aluminium isopropoxide.

Another method mentioned by Braune¹⁰⁰, having only a laboratory significance is a reaction of dialkyl alkoxy aluminium compound with aromatic diol, with simultaneous liberation of gas (in most of the cases, ethane), as it is shown at the Figure 17.

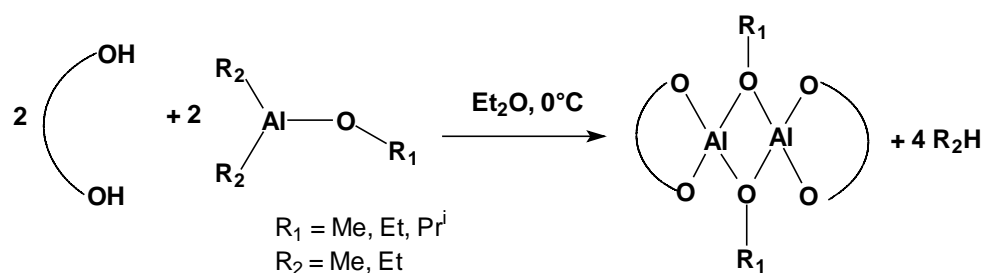


Figure 17 Schema of reaction of dialkyl alkoxy aluminium compound with aromatic diol giving bridging alkoxy bisphenoxides.

Catalyst	Bond	Length of bonds, [Å]	Bond	Length of bonds, [Å]	Lit.
[(MDBP)Al(μ -OPr ⁱ) ₂ 2g	Al(1)-O(1)	1.6954(12)	O(1)-C(1)	1.3618(18)	a, 89
	Al(1)-O(2)	1.7048(12)	O(2)-C(13)	1.3776(19)	
	Al(1)-O(3)	1.8156(12)	O(3)-C(24)	1.4654(19)	
	Al(1)-O(3)#1	1.8157(11)			
[(MMCyP)Al(μ -OPr ⁱ) ₂ 3g	Al(1)-O(1)	1.690(4)	O(1)-C(1)	1.365(6)	a
	Al(1)-O(2)	1.712(4)	O(2)-C(13)	1.383(6)	
	Al(1)-O(3)	1.816(4)	O(3)-C(30)	1.455(6)	
	Al(1)-O(3)#1	1.824(4)			
[(MCIMEPRP)Al(μ -OPr ⁱ) ₂ 4g	Al(1)-O(1)	1.695(2)	O(1)-C(1)	1.367(12)	90
	Al(1)-O(2)	1.707(2)	O(2)-C(13)	1.369(24)	
	Al(1)-O(3)	1.805(2)	O(3)-C(22)	1.472(8)	
	Al(1)-O(3)#	1.804(2)			
[(EDBP)Al(μ -OBz) ₂	Al(1)-O(1)	1.689(2)	O(1)-C(1)	1.379(4)	137
	Al(1)-O(2)	1.683(2)	O(2)-C(13)	1.368(3)	
	Al(1)-O(3)	1.812(2)	O(3)-C(31)	1.452(4)	
	Al(1)-O(3)#	1.816(2)			
[(EDBP)Al(<i>i</i> -OPr ⁱ) ₂	Al(1)-O(1)	1.693(3)	O(1)-C(1)	1.378(5)	87
	Al(1)-O(2)	1.694(3)	O(2)-C(13)	1.380(4)	
	Al(1)-O(3)	1.813(3)	O(3)-C(31)	1.462(5)	
	Al(1)-O(3)#	1.816(3)			
[(MMPEP)Al(<i>i</i> -OPr ⁱ) ₂	Al(1)-O(1)	1.6955(16)	O(1)-C(1)	1.367(2)	88
	Al(1)-O(3)	1.8062(16)	O(2)-C(13)	1.360(2)	
	Al(1)-O(2)	1.6970(16)	O(3)-C(50)	1.461(3)	
	Al(1)-O(3)#	1.8136(16)			
[(TBOP)Al(μ -OPr ⁱ) ₂ 7g	Al(1)-O(1)	1.744(2)	S(1)-C(7)	1.777(3)	a
	Al(1)-O(2)	1.736(2)	S(1)-C(6)	1.780(3)	
	Al(1)-O(3)	1.813(2)	O(1)-C(1)	1.342(3)	
	Al(1)-O(3)#1	1.8428(19)	O(2)-C(12)	1.350(3)	
	Al(1)-S(1)	2.6798(11)	O(3)-C(29)	1.473(3)	
[(TBMP)Al(μ -OPr ⁱ) ₂	Al(1)-O(3)	1.742(8)	S(1)-C(5)	1.788(11)	114c
	Al(1)-O(2)	1.750(8)	S(1)-C(15)	1.797(11)	
	Al(1)-O(1)	1.794(7)	O(1)-C(1)	1.444(12)	
	Al(1)-O(1)#1	1.864(7)	O(2)-C(4)	1.337(11)	
	Al(1)-S(1)	2.552(5)	O(3)-C(16)	1.343(12)	

Table 18 Comparison of selected bond distances for self-synthesised and literature-known [(bisphenoxide)Al(μ -OPrⁱ)₂] complexes, a – this work.

In order to isolate isopropoxy-bisphenoxides, we used the first of the above-discussed reaction paths, which resulted in moderate-to-relatively high yields of the desired aluminium complexes. In each case an easy purification via crystallisation is possible, although the obtained yields are not as high as in cases of monomeric and dimeric “non-bridging” bisphenoxides.

All reaction products obtained after an equimolar reaction between aluminium isopropoxide and 2,2'-methylene-bisphenols display a dimeric feature based on a characteristic Al₂O₂-rhombus core, the two molecules's halves being bridged via the oxygen atom of the isopropoxy group. Depending on the kind of bridging element between the two phenolic rings of the bisphenol ligand (methylene group or sulphur atom) the geometry around the aluminium atom is either distorted tetrahedral (methylene bridge) or distorted trigonal bipyramidal (sulphide moiety). The distances between Al-O(3)(μ-OPrⁱ) and Al-O(3)#1(μ-OPrⁱ) are shown in the Table 18 and indicate that the bridging oxygen atoms are roughly symmetrically bonded to the two Al centres. The lengths of these two bonds are significantly longer than the distances involving aluminium and oxygen atoms of the bisphenoxides (ca. 1.80-1.83 Å vs. 1.69-1.71 Å, respectively). The values of bond angles are roughly comparable and differ on 1.0 – 1.5° from each other (for instance for O(2)-Al(1)-O(1) bond angle this values vary between 117.53(6) for [(MDBP)Al(μ-OPrⁱ)]₂ **2g** and 119.04(15)° for [(EDBP)Al(μ-OPrⁱ)]₂, an exception is **4g**, where due to the steric repulsion between the 3,3'-methyl groups of the MCIMEPrP ligand the relative symmetry of the bisphenoxide molecule is more disordered. [(TBOP)Al(μ-OPrⁱ)]₂, **7g**, is the special case of isopropoxy derivatives isolated in course of our investigations, because sulphur atom replaces the methylene group affording new features and geometry, what will be described separately (see Chapter 5.2.4.2). As it can be seen analysing data in the Tables 18 and 19, distances between aluminium and oxygen atoms of both sulphide bridged ligands are longer for ca. 0.03 – 0.05 Å than corresponding lengths of bonds in methylene bridged ligands.

Catalyst	Bond angle [°]		Bond angle [°]		Lit.
[(MDBP)Al(μ-OPr ⁱ)] ₂ 2g	O(1)-Al(1)-O(2)	117.53(6)	O(1)-Al(1)-O(1)#1	79.61(12)	a, 89
	O(1)-Al(1)-O(3)	115.78(6)	O(1)-C(1)-C(2)	119.50(14)	
	C(1)-O(1)-Al(1)	140.39(10)	O(2)-C(13)-C(12)	119.61(15)	
	C(13)-O(2)-Al(1)	134.62(11)	O(1)-C(1)-C(6)	119.73(14)	
	C(24)-O(3)-Al(1)	136.40(10)	C(9)-C(8)-C(7)	118.33(15)	
[(MMMCyP)Al(μ-OPr ⁱ)] ₂ 3g	O(1)-Al(1)-O(2)	118.5(2)	O(1)-C(1)-C(2)	120.5(5)	a
	O(1)-Al(1)-O(3)	116.06(18)	O(2)-C(13)-C(12)	120.5(5)	
	C(1)-O(1)-Al(1)	144.2(3)	O(1)-C(1)-C(6)	119.1(5)	
	C(13)-O(2)-Al(1)	130.7(3)	C(9)-C(8)-C(7)	117.7(5)	
	C(30)-O(3)-Al(1)	133.9(4)	C(22)-O(3)-Al(1)	128.01(15)	
[(MCIMEPRP)Al(μ-OPr ⁱ)] ₂ 4g	O(1)-Al(1)-O(2)	114.98(9)	O(1)-Al(1)-O(3)#	112.82(9)	90
	O(1)-Al(1)-O(3)	117.91(9)	O(2)-Al(1)-O(3)	109.88(9)	
	O(2)-Al(1)-O(3)#	115.43(9)	O(3a)-Al(1)-O(3)	81.68(8)	
	C(13)-O(2)-Al(1)	123.27(15)	O(1)-C(1)-C(2)	117.3(2)	
[(EDBP)Al(μ-OBz)] ₂	O(2)-Al(1)-O(1)	118.16(12)	O(2)-Al(1)-O(3)	108.30(10)	137
	O(1)-Al(1)-O(3)	111.58(10)	O(2)-Al(1)-O(3)#	117.57(11)	
	O(1)-Al(1)-O(3)#	114.07(12)	O(3)-Al(1)-Al(1)#	80.52(10)	
	O(2)-Al(1)-Al(1)#	120.61(9)	O(1)-Al(1)-Al(1)#	120.54(10)	
	O(3)-Al(1)-Al(1)#	40.32(7)	O(3)#-Al(1)-Al(1)#	40.20(7)	
[(EDBP)Al(i-OPr ⁱ)] ₂	O(1)-Al(1)-O(3)	114.75(16)	O(2)-Al(1)-O(3)#1	112.03(19)	87
	O(1)-Al(1)-O(2)	119.04(15)	O(3)-Al(1)-O(3)#1	80.55(14)	

	O(2)-Al(1)-O(3)#	110.37(15)	O(1)-Al(1)-O(3)#	110.50(14)	
	C(1)-O(1)-Al(1)	119.1(4)	C(13)-O(2)-Al(1)	139.4(3)	
	O(3)-Al(1)-Al(1)#	40.31(9)	O(3)#-Al(1)-Al(1)#	40.24(9)	
$[(\text{MMPEP})\text{Al}(\text{i-OPr}^i)]_2$	O(1)-Al(1)-O(2)	118.43(8)	O(1)-Al(1)-O(3)	109.75(8)	88
	O(2)-Al(1)-O(3)	108.43(8)	O(1)-Al(1)-O(3)#	116.07(8)	
	O(2)-Al(1)-O(3a)	115.97(8)	O(3)-Al(1)-O(3)#	81.31(8)	
	C(50)-O(3)-Al(1)	124.46(14)	C(50)-O(3)-Al(1)	136.68(15)	
	Al(1)-O(3)-Al(1)#	98.69(8)			
$[(\text{TBOP})\text{Al}(\mu\text{-OPr}^i)]_2$ 7g	C(7)-S(1)-C(6)	105.40(13)	O(2)-Al(1)-O(3)	122.35(10)	a
	C(7)-S(1)-Al(1)	89.09(9)	O(1)-Al(1)-O(3)	117.73(10)	
	C(6)-S(1)-Al(1)	88.43(9)	O(2)-Al(1)-O(3)#1	100.18(9)	
	O(2)-Al(1)-O(1)	118.21(10)	O(3)-Al(1)-O(3)#1	79.99(9)	
	O(1)-Al(1)-O(3)#1	102.93(9)	O(2)-Al(1)-S(1)	81.43(7)	
	O(1)-Al(1)-S(1)	81.78(7)	O(3)-Al(1)-S(1)	93.65(6)	
	O(2)-Al(1)-Al(1)#1	116.64(8)	O(3)#1-Al(1)-S(1)	173.32(7)	
	O(3)-Al(1)-Al(1)#1	40.39(6)	O(1)-Al(1)-I(1)#1	117.56(8)	
	O(3)#1-Al(1)-Al(1)#1	39.60(6)			
$[(\text{TBMP})\text{Al}(\mu\text{-OPr}^i)]_2$	C(5)-S(1)-C(15)	106.4(5)	O(3)-Al(1)-O(2)	118.7(4)	120c
	C(5)-S(1)-Al(1)	91.2(5)	O(3)-Al(1)-O(1)	121.7(4)	
	C(15)-S(1)-Al(1)	90.7(6)	O(2)-Al(1)-O(1)	119.2(4)	
	O(2)-Al(1)-O(1)	119.2(4)	O(3)-Al(1)-O(1)#1	99.4(4)	
	C(1)-O(1)-Al(1)	137.8(7)	O(3)-Al(1)-S(1)	83.1(3)	
	O(1)-C(1)-C(3)	110.4(11)	O(2)-Al(1)-S(1)	83.3(3)	
	C(16)-O(3)-Al(1)	128.9(9)	O(1)-Al(1)-S(1)	97.3(3)	

Table 19 Comparison of selected bond angles for self-synthesised and literature-known $[(\text{diolate})\text{Al}(\mu\text{-OPr}^i)]_2$ complexes, a – this work.

Despite several attempts of crystallisation, **8g** resulting as the product of reaction of 2-hydroxy-3,5-di-*tert*-butylbenzyl alcohol, **8**, with $\text{Al}(\text{OPr}^i)_3$ did not afford crystals allowing to establish its exact structure. Owing to unsymmetrical structure of ligand **8g** can exist as a *cis*- and *trans* form, but large steric repulsion between of Bu^t and Pr^i groups make a *trans*-isomer more preferable than its *cis* counterpart (see Figure 18).

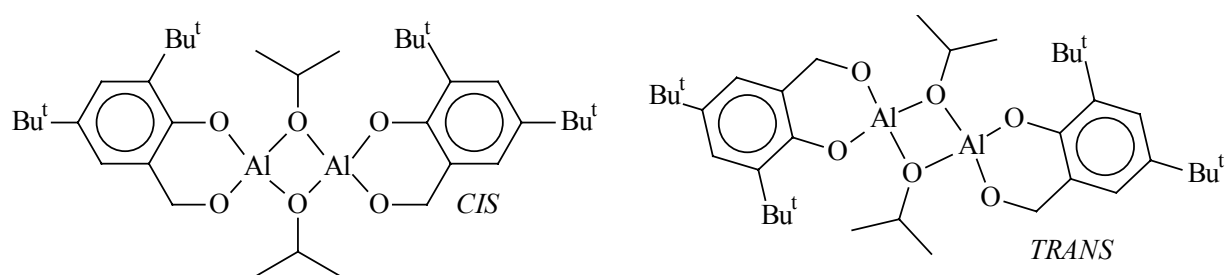


Figure 18 Two possible isomers of **8g**.

Each investigated compound displaying dimeric feature in the solid state (such as the isopropoxy-bridged aluminium bisphenoxides) has also dimeric form in apolar solvents (like C_6D_6 , CDCl_3 , CD_2Cl_2). Table 20 presents a short overview of the chemical shifts recorded in $^1\text{H-NMR}$ for the isolated compounds. Due to the slightly constrained geometry of the bridging isopropoxy group in the dimeric structures, the methine hydrogen atoms of the isopropoxy groups appear as complex multiplets at 1.30, 1.40-1.48 ppm (respectively, **5g**, **7g**, **3g**) and ca. 1.55 ppm (**1g** and **2g**) whereas the methyl groups of the bridging ligands come out as split doublets over a broad range (4.13 – 4.77 ppm).

Only in some cases the ^1H NMR signal of the isopropoxy groups (methine as well as methyl, in our case **6g** and **4g**) are significantly shifted upfield, what can be correlated to the presence of a chlorine atom at carbon 4 of the phenyl ring which, via resonance and induction effects, influence the electron density in the Al_2O_2 structural fragment and consequently the chemical shift of the iso-propoxo ligand.

	R ₁	R ₂	-OCH(CH ₃) ₂	C(7)(H _{EXO})	C(7)(H _{ENDO})	-OCH(CH ₃) ₂	C ₃ -H	C ₅ -H
1g	1.23	1.33	1.55	3.77	3.97	4.62	7.11	7.25
2g^a	1.39	2.18	1.57	3.78	4.10	4.62	6.95	7.11
3g^a	1.11–1.75	2.19	1.48	3.67	3.75	4.54	6.96	7.01
4g^b	1.11, 3.24	-	1.17, 1.19	3.91		4.33	2.32	7.02
5g	2.00-2.05		1.30	3.50-3.55	invisible	4.54	6.84	7.02
6g	7.12	-	1.13, 1.15	invisible	3.24	4.13	6.92	7.09
7g	7.12 - 7.19	0.61, 1.24 1.61,	1.40, 1.43,	sulphur moiety		4.77	7.52	6.72, 6.75

Table 20 Chemical shifts of hydrogen atoms groups in isoporopoxy derivatives, a – Ref. 100; b – Ref. 90

5.2.4 Investigation of the influence of only *para*-substituted ligands on the catalytic activity of isolated complexes

5.2.4.1 Reactions of aluminium precursors with 2,2'-methylenebis(4-chlorophenol), **6**, in different solvents

In order to investigate the influence of the *para*-substituents alone on the potential catalytic activity, we used 2,2'-methylene-bisphenol with only one substituent at carbon C4 of the aromatic ring. As already reported in the former cases, all reactions were carried out in a one to one stoichiometry (ligand : aluminium component). The structure of the isolated aluminium compounds strongly depends on the solvent used during the reaction and also on the kind of *ortho*-substituent. Taking 2,2'-methylenebis(4-chloro-phenol), **6**, as starting ligand and performing the reaction with triethylaluminum in the presence of diethyl ether, allowed us to isolate a trinuclear compounds with two bridging ligand molecules¹¹¹ (product's stoichiometry 3 to 2, see Figures 19 and 21), although the reaction stoichiometry was 1 to 1. Using THF as solvent, the reaction yields binuclear aluminium bisphenoxides with fivefold coordinated aluminium atoms and coordinated solvent molecules, as presented in Figures 19 and 20.

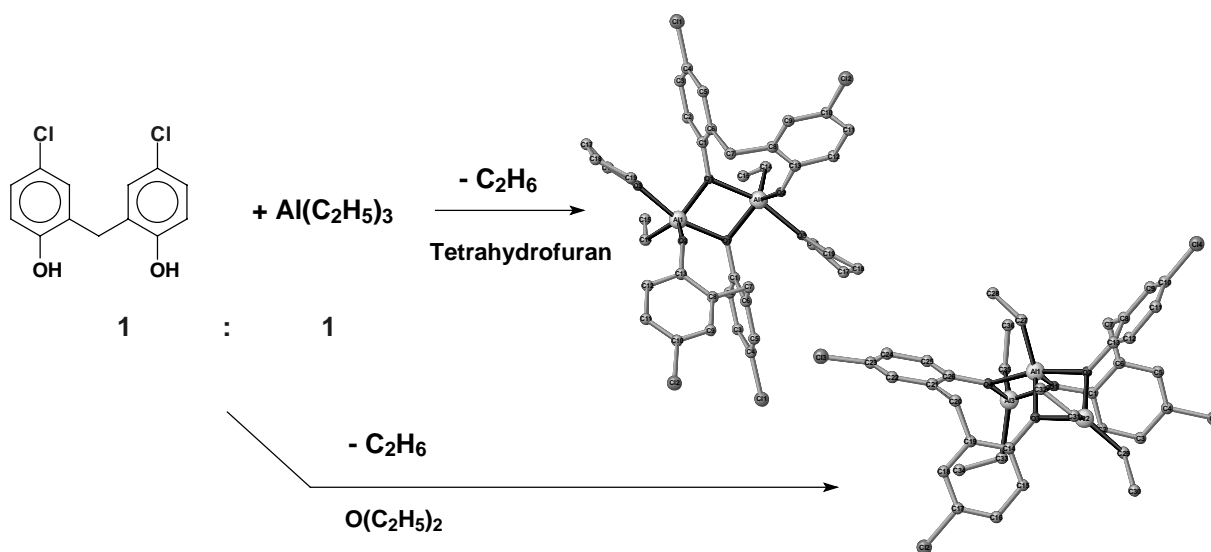


Figure 19 Influence of solvent on reaction's path

The structure of **6a** shows dimeric features with five-coordinated aluminum atoms displaying a distorted trigonal bipyramidal geometry, with the phenoxydic oxygen atoms occupying axial and equatorial positions and the oxygen atom of THF occupying the remaining axial positions [$\text{O}(1)\text{-Al}(1)\text{-O}(3)=163.7^\circ$], as shown at the Figure 20. 1.958(4) Å of the Al(1)-C(14) bond length is exactly within a range expected for terminal bond distances. As expected, bisphenoxide **6a** displays a boat-chair conformation of the aluminium-bisphenol-ring like the

other bisphenoxides presented in this study. The coordinated THF molecules are placed in *trans* position relative to a virtual plane including the two aluminium atom. In ^1H NMR spectrum the hydrogen atoms of the bridging methylene group cannot be clearly detected at room temperature, most probably overlapped by the NMR-signal of the methylene groups of THF in α -location of the oxygen atom. Recording the spectra at lower temperature ($-40\text{ }^\circ\text{C}$) yield better resolved spectra with discernible bridging methylene groups and the expected splitting of the NMR signal. Likewise considering the ^{13}C NMR spectra of **6a** recorded at $-40\text{ }^\circ\text{C}$, the Al-bound ethyl groups can be noticed as broad signals at 33 ppm (methyl) and -1 ppm (methylene), whereas the spectra recorded at RT delivered few informations. In the $^{13}\text{C}\{^1\text{H}\}$ and DEPT 135 NMR spectra recorded at RT, 4 broad signals (at 122.1, 125.1, 130.3, 132.6 and 154.7 ppm) for the carbons of the phenoxy groups and signals of THF (68.7 and 25.3 ppm) can be noticed. Recording at $-40\text{ }^\circ\text{C}$ did not yield better resolved spectra in the aromatic region.

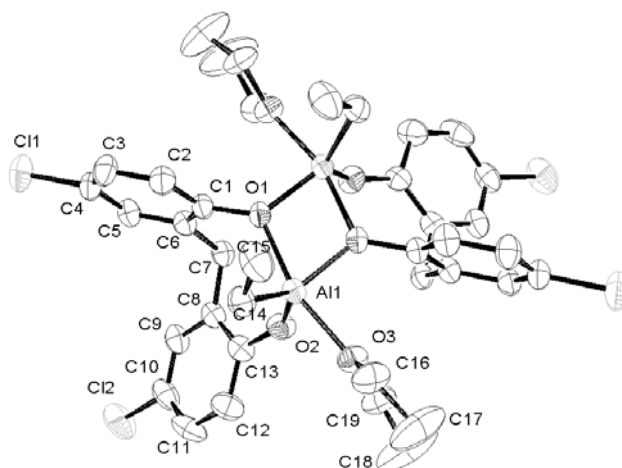


Figure 20 The distorted trigonal bipyramidal geometry of Al atoms in **6a**.

Catalyst	Length of bonds, [Å]				Lit.
		Al(1)-O(1)#1	1.829(2)	O(1)-C(1)	
	Al(1)-O(2)	1.729(3)	O(2)-C(13)	1.338(5)	
	Al(1)#1-O(1)	1.829(2)	O(3)-C(19)	2.938(3)	
	O(3)-C(16)	1.463(5)	Al(1)-C(14)	1.958(4)	
	Bond angle, [°]				
[(MCIP)(THF)AlEt] ₂ 6a	O(2)-Al(1)-O(1)#1	112.37(15)	O(3)-Al(1)-O(4)	94.52(17)	a
	O(2)-Al(1)-C(14)	122.71(18)	O(1)-Al(1)-O(3)	163.72(11)	
	Al(1)#1-O(1)-Al(1)	105.23(11)	C(16)-O(3)-C(19)	108.8(3)	
	C(13)-O(2)-Al(1)	144.0(3)	C(3)-C(4)-Cl(1)	119.4(4)	
	O(1)#1-Al(1)-C(14)	124.84(18)	C(1)-O(1)-Al(1)#1	129.2(2)	
	O(2)-Al(1)-O(3)	88.56(15)	C(1)-O(1)-Al(1)	125.0(2)	

Table 21 Selected bond distances and bond angles for **6a**, a – this work

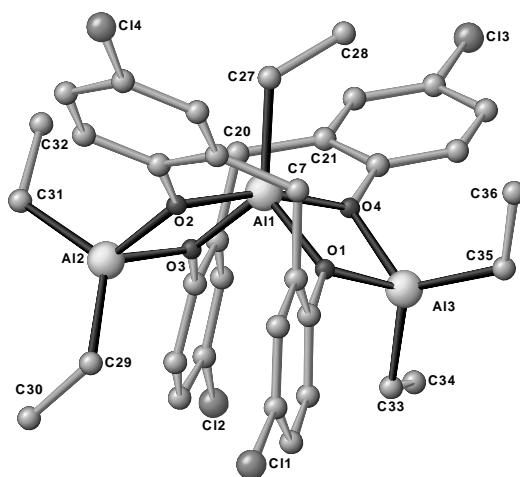


Figure 21 The **6c** backbone displaying a trinuclear feature with the distorted trigonal bipyramidal geometry of the central aluminium atom and the distorted tetrahedral one characterising the terminal ones.

The structure of **6c** exhibits a trinuclear feature, the core of the complex is based on two Al_2O_2 rhombuses mutually bound to a third central aluminium atom displaying a trigonal bipyramidal coordination geometry, O(1), O(3) and C(27) representing the equatorial sites and O(2) and O(4) occupying the axial positions (O(1), O(3), C(27) and Al(1) within the same plane, mean deviation from the main plane: 2.15; O(2)-Al(2)-O(4): 165.6°). The two terminal aluminium atoms adopt a slightly distorted tetrahedral coordination geometry. The bisphenoxide ligands are coordinated in a bridging mode through both oxygen atoms (O(1), O(2)) of the ligand. The backbone of **6c** can be also described as based on two four-membered and two eight-membered rings (see Figure 21). The distances involving terminal tetrahedrally coordinated aluminium atoms and oxygen atoms of the bridging phenoxides vary only slightly (1.853(4), 1.883(4) for Al(2)-O(2), Al(2)-O(3) and 1.867(4) and 1.856(4) Å for Al(3)-O(1) and Al(2)-O(4), respectively). The sums of the angles around the O(1), O(2), O(3) and O(4) atoms amount to 359.0, 358.8, 359.7 and 356.9°, respectively, which indicate a lack of strain in the eight-membered cycles. Compounds displaying such structural features were reported in the literature in some few cases like, e.g. the reaction of alkyl-aluminium with 2,2'-di(hydroxymethyl)biphenyl, DHMBH₂, (161.43 and 156.07° for the ethyl and methyl derivatives, respectively)¹¹², and with some other aromatic diols such as 4-tert-butyl-1,2-catechol, 1,2-catechol, 2,2'-di(hydroxymethyl)biphenol^{111b,c}.

Catalyst	Length of bonds, [Å]		Length of bonds, [Å]		Lit.
[(MCIP) ₂ Al ₃ Me ₃] 6c	Al(1)-O(1)	1.850(4)	Al(1)-O(3)	1.852(4)	A
	Al(1)-O(2)	1.962(4)	Al(1)-O(4)	1.960(4)	
	Al(2)-O(2)	1.853(4)	Al(2)-O(3)	1.883(4)	
	Al(3)-O(1)	1.867(4)	Al(3)-O(4)	1.856(4)	
	Al(2)-C(29)	1.945(6)	Al(2)-C(31)	1.952(6)	
	Al(3)-C(33)	1.989(7)	Al(3)-C(35)	1.910(7)	
[(HDBBA) ₂ Al ₃ Et ₃] 8	Al(1)-O(1)	1.840(9)	C(39)-O(3)	3.275(82)	A
	Al(1)-O(4)	1.836(8)	O(1)-C(1)	1.393(11)	

	Al(2)-O(4)	1.810(58)	C(7)-O(2)	1.443(7)	
	Al(2)-O(1)	2.003(5)	C(16)-O(4)	2.970(5)	
	O(2)-Al(2)	1.808(11)	C(37)-Al(3)	1.963(1)	
	Al(1)-C(31)	1.966(13)	Al(2)-O(3)	1.990(0)	
	Al(1)-C(33)	1.966(6)	Al(2)-C(35)	1.940(5)	
[(DHMB) ₂ Al ₃ Me ₅]	Al(1)-O(1)	1.854(2)	Al(3)-O(4)	1.820(2)	112
	Al(1)-O(3)	1.834(2)	Al(3)-O(1)	1.858(2)	
	Al(1)-O(2)	1.921(2)	Al(2)-O(2)	1.816(3)	
	Al(1)-O(4)	1.928(2)	Al(2)-O(3)	1.836(2)	
[(OC ₆ H ₄ O) ₂ Al ₃ Bu ^t ₅]	Al(1)-O(1)	1.869(5)	Al(3)-O(3)	1.871(5)	111c
	Al(2)-O(2)	1.884(5)	Al(3)-O(2)	1.850(5)	
	Al(1)-O(4)	1.853(5)	Al(2)-O(3)	1.843(4)	
	O(4)-C(27)	1.328(8)	Al(2)-O(4)	1.884(5)	
	O(1)-C(21)	1.355(8)	O(2)-C(26)	1.356(9)	

Table 22 Comparison of selected bond angles for [(diolate)₂Al₃R₅] (R=Me, Et and Bu^t) complexes, a – this work

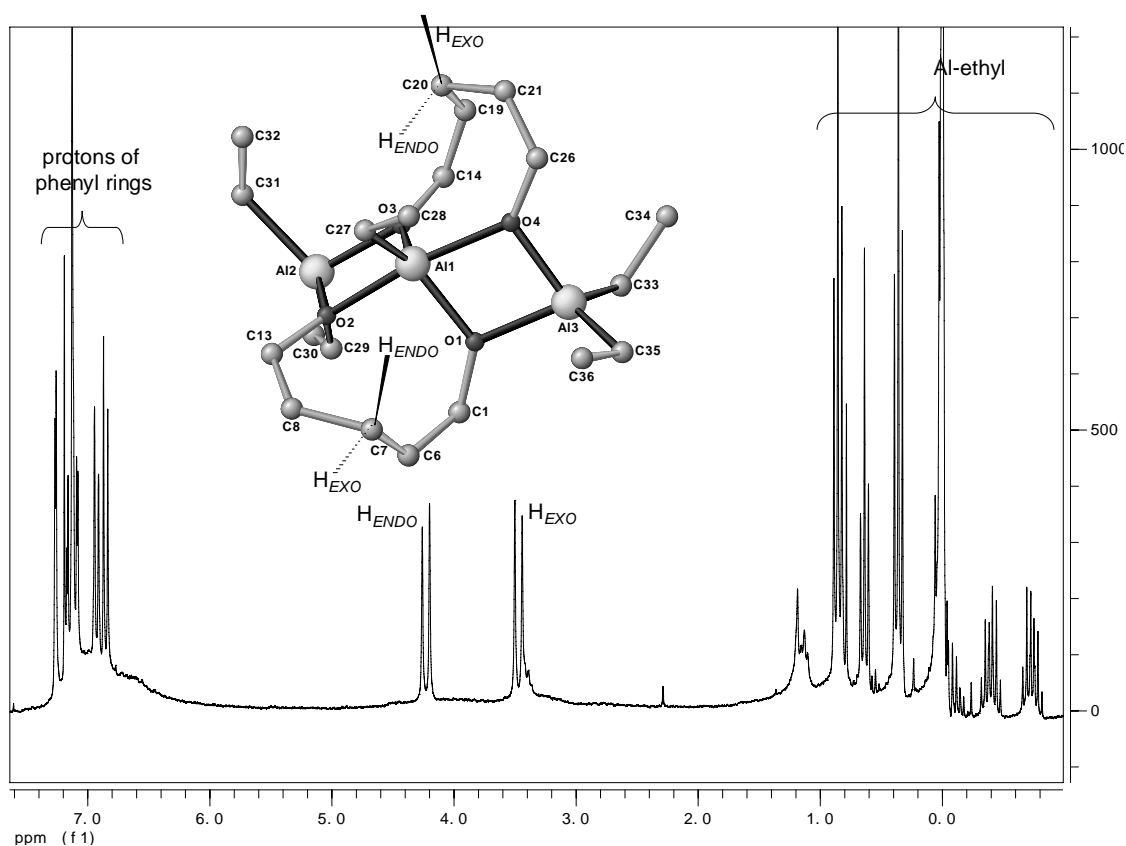


Figure 22 ¹H NMR spectrum and X-ray structure of **6c** molecule. For clarity, shown only as consisting of two four-membered and two eight-membered rings.

The two eight-membered rings may be described as adopting a distorted boat-chair conformation (see Figure 22), analogously to the aluminum bisphenoxides reported by Lin.⁸⁶ The hydrogen atoms of the methylene bridge display the usual pattern in ¹H-NMR: a doublet of doublets with the coupling constant of 15.04 Hz (this value is within the usually observed range for aluminium bisphenoxides). Compared to **6a**, the trinuclear compound **6c** reveals good resolved, albeit complex, NMR-spectra clearly showing in ¹³C/DEPT 135 spectra two sets of resonances for the phenyl rings in the 2,2'-methylenebis(4-chlorophenoxide) ligands (two set of 6 narrow signals at 120.53/121.17, C-H; 128.31/130.39, quaternary C;

129.01/129.36, C-H; 130.82/131.59, quaternary C; 131.74/131.89, C-H and 147.9/151.4 ppm, quaternary C; recorded in CD₂Cl₂). Considering the solid state structure of compound **6c**, one set of resonances can be attributed to the phenol rings located perpendicular to the pseudo-C₂ symmetry axis and the other to the phenyl rings oriented along the pseudo-C₂ symmetry axis (see Figure 21). Accordingly, only one signal was recorded at 32.1 ppm for the bridging methylene of the bisphenoxide ligand. For compound **6c** several ¹³C NMR signals are found for the ethyl groups bound to the aluminum atoms, as expected at high-field, at 0.65 ppm, and 1.39 ppm for the methylene groups and 8.15, 8.7 and 10.0 for the methyl groups. This suggests a structure in solution with 3 different types of ethyl group. In comparison, the ethyl groups bound to the aluminium atoms produce a complex pattern in ¹H NMR. The Al(2)-C(31)-C(32) and Al(3)-C(35)-C(36) ethyl groups located in *syn*-position (on the same side of a virtual medium plane containing the three aluminium as well as the four oxygen atoms of the bisphenoxide) to the ethyl group bonded to the central aluminium atom reveals as a triplet at 0.85 and multiplets at -0.40 ppm, the ethyl groups located in position *anti* (Al(2)-C(29)-C(30) and Al(3)-C(33)-C(34)) give a triplet at 0.36, and multiplet at -0.725 ppm. The ethyl group bound to the central aluminium atom gives a triplet at 0.64 and a multiplet at -0.06 ppm.

Catalyst	Bond angle, [°]		Bond angle, [°]		Lit.
[(MCIP) ₂ Al ₃ Et ₅] 6c	O(1)-Al(1)-O(3)	103.09(17)	O(1)-Al(1)-O(2)	94.13(16)	a
	O(1)-Al(1)-C(27)	129.9(2)	O(3)-Al(1)-O(2)	76.76(15)	
	O(3)-Al(1)-C(27)	127.0(2)	C(27)-Al(1)-O(2)	95.0(2)	
	O(1)-Al(1)-O(4)	76.29(15)	O(4)-Al(1)-O(2)	165.59(16)	
	O(3)-Al(1)-O(4)	94.71(16)	O(1)-Al(1)-Al(3)	37.98(11)	
	C(27)-Al(1)-O(4)	99.4(2)	O(3)-Al(1)-Al(3)	99.65(13)	
	O(4)-Al(1)-Al(3)	38.38(10)	O(2)-Al(1)-Al(3)	130.78(12)	
[(HDBBA) ₂ Al ₃ Et ₅] 8	Al(2)-O(3)-Al(3)	97.7(11)	O(3)-Al(3)-C(37)	111.4(9)	a
	Al(2)-O(3)-C(16)	117.4(10)	C(16)-O(3)-Al(3)	138.9(8)	
	Al(2)-O(3)-Al(3)	97.7(8)	C(35)-Al(2)-O(2)	124.4(12)	
	Al(2)-O(2)-Al(3)	104.9(4)	C(1)-O(1)-Al(2)	118.2(7)	
	O(1)-Al(1)-C(33)	111.4(14)	O(1)-Al(2)-O(4)	77.6(2)	
	O(1)-Al(1)-C(31)	118.1(1)	O(1)-Al(1)-O(4)	81.3(4)	
	C(7)-O(2)-Al(2)	124.0(0)	C(35)-Al(2)-O(1)	99.5(6)	
[(DHMB) ₂ Al ₃ Me ₅]	O(4)-Al(1)-O(2)	111.99(19)	O(4)-Al(1)-O(3)	92.36(17)	112
	O(2)-Al(1)-O(3)	77.03(17)	O(4)-Al(1)-O(1)	76.56(18)	
	O(1)-Al(3)-O(4)	79.74(19)	O(3)-Al(1)-O(1)	161.43(19)	
	O(2)-Al(1)-O(1)	93.15(18)	O(3)-Al(2)-O(2)	79.48(18)	
[(OC ₆ H ₄ O) ₂ Al ₃ Bu ^t ₅]	O(4)-Al(1)-O(1)	78.7(2)	C(26)-O(2)-Al(2)	110.8(4)	111c
	O(4)-Al(1)-C(1)	112.6(3)	O(3)-Al(2)-C(9)	118.9(3)	
	O(1)-Al(1)-C(1)	118.6(3)	Al(3)-O(2)-Al(2)	101.4(2)	
	O(2)-Al(2)-C(9)	107.3(3)	O(4)-Al(2)-C(9)	108.2(3)	
	C(28)-O(3)-Al(2)	112.7(3)	O(2)-Al(3)-O(3)	78.2(2)	

Table 23 Comparison of selected bond angles for [(diolate)₂Al₃R₅] (R=Me, Et and Bu^t) complexes, a – this work

Such a noticeable influence of the solvent on the final structure of the aluminum alkoxide was also observed during the reaction involving 2-hydroxy-3,5-di-*t*-butylbenzyl alcohol, HDBBAH₂ **8**, and triethyl aluminium. Using diethyl ether as a solvent affords a trinuclear aluminium phenoxide as final product (see Figure 23). Unfortunately, the crystallisation attempts for the related product synthesised in coordinating THF were unsuccessful, however considering the NMR data gathered for the isolated amorphous solid, a symmetric binuclear structure comparable to the structure of **6a** could be proposed.

Both trinuclear aluminium bisphenoxide **6c** and **8c** crystallise in the same space group. The X-ray structure parameters are listed together with the experimental data of **6c** in Tables 22 and 23. As it can be seen in Figure 23, the fivefold coordinated aluminium centre adopts a distorted trigonal bipyramidal geometry, with two oxygen atoms of the benzylic alkoxide moieties and a carbon of the aluminium-bound ethyl group occupying the equatorial positions, whereas the remaining two phenoxy oxygen atoms are in apical position. Two terminal aluminium atoms are significantly distorted from the ideal tetrahedral geometry. The total angles measured around the oxygen atoms in the 6-membered rings do not imply any special stresses in the rings (for O(1), O(2), O(3), O(4) 356.1, 354.0, 354.4 and 356.1 were noted, respectively).^{111,112}

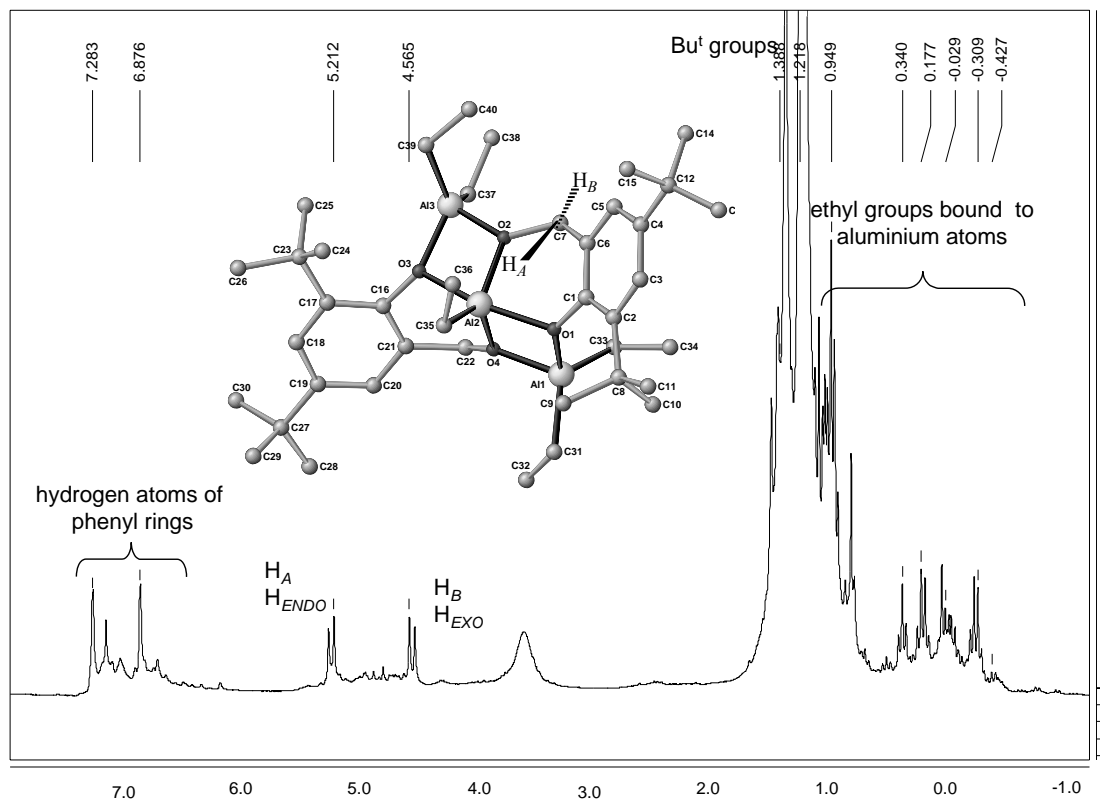


Figure 23 Reaction's product of 2-hydroxy-3,5-di-*t*-butylbenzyl alcohol HDBBAH₂ and triethyl aluminium - ¹H NMR spectrum and X-ray structure of **8c** molecule – assessment of signals.

The hydrogen atoms of methylene bridge are magnetically non-equivalent and appear as a pattern of doublet of doublets in the ^1H NMR spectrum, which is shifted more downfield (H_{EXO} at 4.56 ppm, $^2J_{\text{HH}} = 13,55$ Hz and H_{ENDO} at 5.21 ppm). the geminal coupling constant are comparable to those usually obtained for aluminium bisphenoxides).^{86-88,90-91,97} Owing to the unsymmetrical structure of the ligand used, the product obtained, **8c**, can exist in two forms, a *trans*- and a *cis*- isomer, although the formation of the latter seems to be thermodynamically unfavourable, considering the steric hindrance of the bulky *tert*-butyl group.^{111a,b} Complex presented in the Figure 23 is a *trans*-isomer. In the ^1H NMR spectrum, the signals of the ethyl groups bound to aluminium atoms are seen as a complex system, with triplet at 0.34 ppm, quadruplets (0.18, -0.28 ppm) and a broad multiplet between 0.03 and -0.17 ppm.

The reaction of **6** with AlEt_2Cl in Et_2O was not performed, owing to the fact that it would most probably yield a mixture of *trans* and *cis* products whose separation would have been time-consuming. Considering compound **8** the number of possible isomers would have been even higher with four possible isomers: *trans*-ligand-*trans*-chlorine, *trans*-ligand-*cis*-chlorine, *cis*-ligand-*cis*-chlorine and *cis*-ligand-*trans*-chlorine.

5.2.4.2 Reaction of aluminium precursors with 2,2'-thiobis(4-*tert*-octylphenol) in different solvents

In the relevant literature there is a large variety of transition metal and main group element alkoxides having a chelating sulphur-bridged bisphenols as ligand and displaying a catalytic activity toward various polymerisation reactions. Some works dealing with e.g. the formation of polyethylene and other polyolefins¹¹³ and the Ring Opening Polymerisation of epoxides (propylene oxide, ethylene oxide)¹¹⁴ were reported. To our best knowledge, up to now, no application of these catalysts in the copolymerisation of epoxides with carbon dioxide was reported. As it was already shown with such modified bisphenols, the replacement of the bridging methylene group by a sulphide moiety yields a significant change in the electronic as well as in the steric properties of the ligand and, logically, a significant change in the structure of the obtained aluminium complexes. Hence, in comparison with the methylene-bridged bisphenols, 2,2'-thiobisphenols are potentially O,S,O-tridentate. With a more versatile sulphide bridge, which additionally possesses electron pairs able to coordinate to a Lewis acid (Al), we have an other tool to optimise the direct surrounding of the metal centre and influence the catalytic activity of the aluminum complexes.

The sulphur atom via its lone electron pairs yield a fivefold coordinated aluminium atom, instead of the usually observed tetrahedral coordination geometry.⁸⁶⁻⁸⁹ Interestingly, the B-C (boat-chair) conformation of the above-mentioned eight-member ring remains the same as in the case of carbon-bridged compounds.¹⁰⁰

For our investigation we have chosen 2,2'-thiobis(4-*tert*-octylphenol), TBOPH₂ **7**, whose reactions with AlEt₃ and Al(OPrⁱ)₃ resulted in the formation of the corresponding aluminium thiobisphenoxides. We performed the reaction with different aluminium precursors, keeping the same stoichiometries as in the case of the **6**-based catalysts in order to obtain, when possible, iso-structural products to complete our catalysts' library.

Reactions performed in THF afforded **7a** in good yield as a white amorphous powder. Despite several attempts of recrystallisation, even after using the usually successful slow cooling down of a THF-toluene solution, no single crystals could be separated and the isolated solid remains an amorphous powder. Taking into consideration the results reported by Braune (using bulky-*ortho*-substituted thiobisphenol, 2,2'-thiobis(6-*tert*-butyl-4-methylphenol TBMPH₂) which yield monomers with fivefold coordinated metal core), one could reasonably assume that the isolated compound is a monomer, (bisphenoxide-O,S,O)AlEt(THF), although without clear structural information the formation of dimers cannot be completely ruled out. In the case of the dimeric form, the aluminium atom should display a six-fold, more or less

octahedrally coordinated aluminium centre which would give a characteristic ^{27}Al -NMR signal around zero ppm (related to $\text{AlCl}_3 \cdot 6 \text{H}_2\text{O}$, ^{27}Al -NMR standard). The recorded ^{27}Al NMR spectra displayed only a broad signal at 55 ppm (5813 Hz) (**7a**) in the region characteristic of tetra- and penta-coordinated (respectively tetrahedral and trigonal bipyramidal geometries) aluminium species indicating the absence of hexacoordinated aluminium species.¹⁴¹ (see Figure 24).

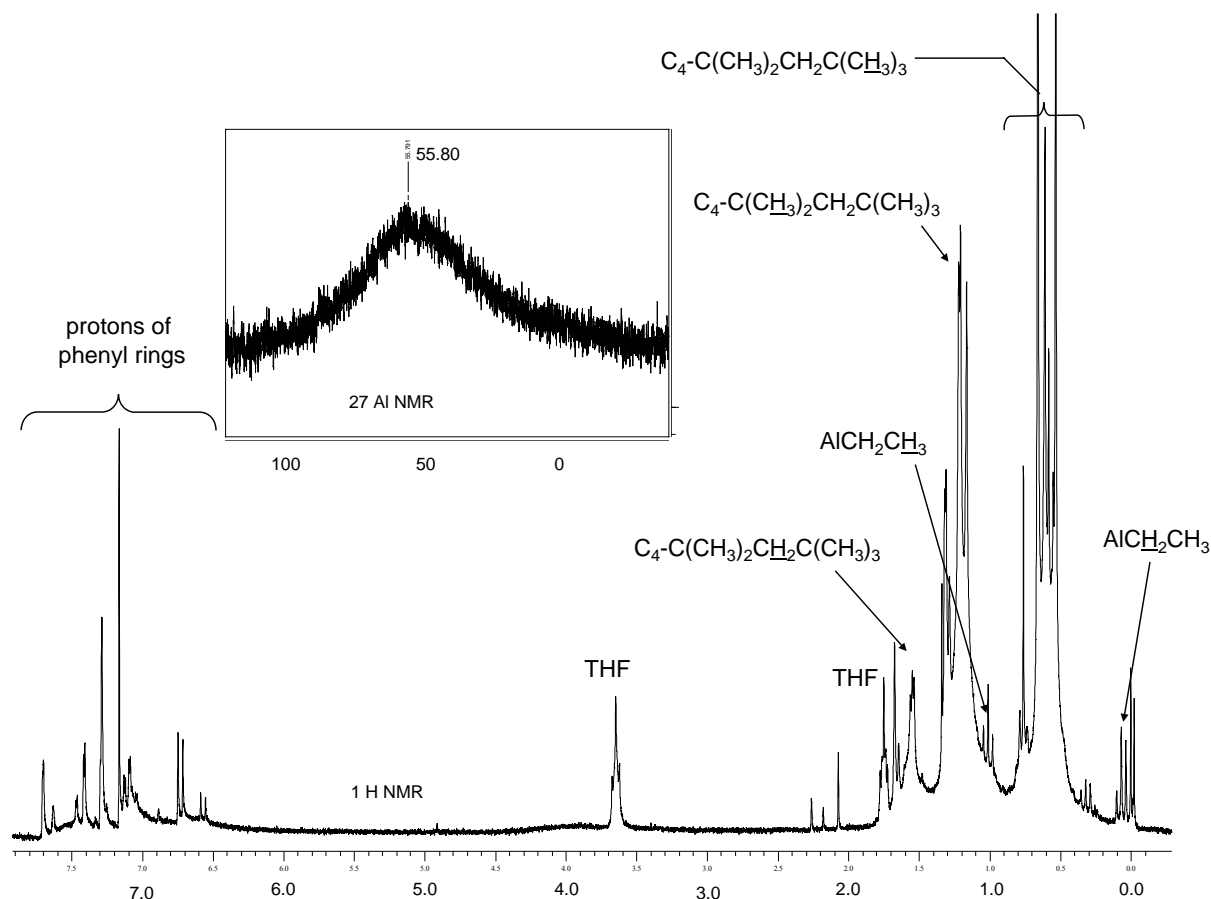


Figure 24 ^1H NMR spectrum of **7a**.

In the ^1H NMR spectrum a broad set of aromatic hydrogen atoms as well as three sets of broad signals corresponding to aliphatic hydrogen atoms are visible. The methylene group of the Al-bound ethyl ligand can be seen as a single quadruplet indicating, contrary to dimeric alkyl derivatives, a non-constrained geometry around the aluminium atom. In its crystal form, it should display trigonal bipyramidal geometry around the aluminium atom, with the oxygen atoms of ligand occupying the equatorial positions and the sulphur atom at the apical one. A related study reported in the literature by Janas and Sobota, deals with the reaction of 2,2'-thiobisphenol **7** with AlMe_3 in non-coordinating toluene.^{113c} We carried out a similar reaction in diethyl ether with AlEt_3 as starting compound in order to obtain either a complex having an analogue structure to **6c** or a compound with coordinated solvent molecule. This reaction was performed in a 3 to 2 stoichiometry (aluminium to ligand). Several attempts of crystallisation

of the isolated white solid were unsuccessful, only amorphous powders could be isolated. In the ^1H NMR spectrum, no signals related to diethyl ether could be detected, the signals of the methyl and methylene parts of the ethyl groups appear at 1.00 and 0.06 ppm, respectively. The ^1H NMR-signal of the *tert*-octyl chains in *para*-position as well as the signals of the aromatic protons do not overlap, what suggest a dimeric structure for the isolated compound. This strongly suggests that the complex exists as a dimer in aprotic media with fivefold coordinated aluminium atoms, the complex can be seen as an ethyl analogue of the complex reported by Sobota.^{113c} In our case even a significant excess of the aluminium precursor does not influence the stoichiometry of the final product (see Figure 25).

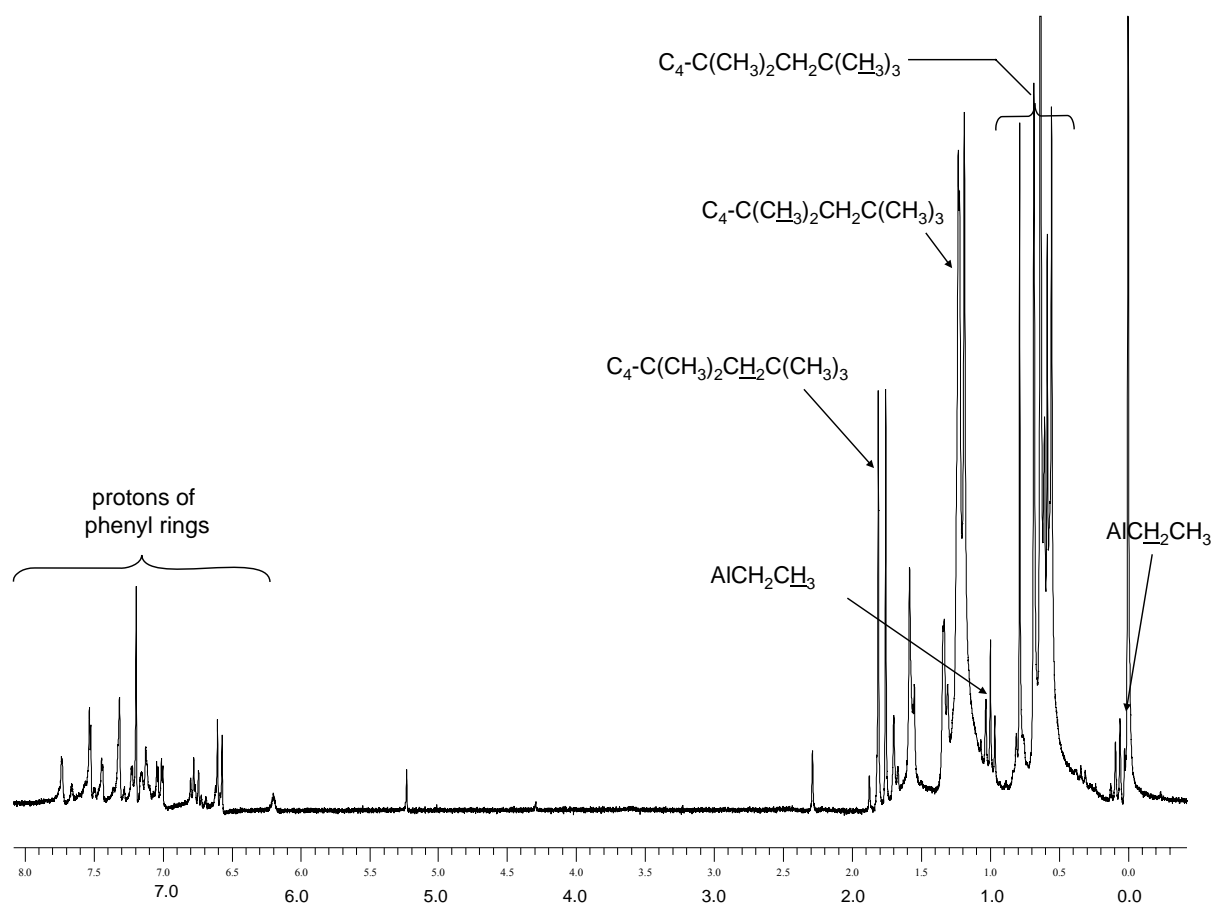


Figure 25 ^1H NMR spectrum of **7c**.

Braune isolated a sulphide-bridged *para*-substituted analogue of **2g** in high yields, having a similar structure to bisphenoxide **7g** presented in this study. Both compounds were completely characterised by NMR spectroscopy and X-ray crystallography (**2g**: monoclinic, P2(1)/c; **7g**: triclinic, P-1, see Figure 26) and display symmetrical structures featuring two bridging $\mu\text{-OPr}^i$ ligands. Recently, Janas and Sobota^{113c} reported the synthesis of ethoxy-bridged analogue of **7g**, but no X-ray data were reported. The metal centres in each of these compounds (**2g** and **7g**) display a trigonal-bipyramidal coordination geometry with the

bridging sulphide group of the thiobisphenols and one isopropoxy group occupying the apical positions. The standard length reported in the literature¹¹⁵ for aluminium-sulphur bond range from 2.2565(8)¹⁴⁰ to 2.675(2) Å^{113c}, the Al(1)-S(1) distance of 2.6798(11) Å measured in the molecular structure of **7g** lies slightly over the range of these interactions. Distances between Al and phenoxy oxygen atoms are slightly shorter than Al–O bond of OPrⁱ group, similarly as in case of other isopropoxy bridged complexes (see Tables 25 and 26), what is to be correlated to the delocalisation of the electron over the aromatic ligand.

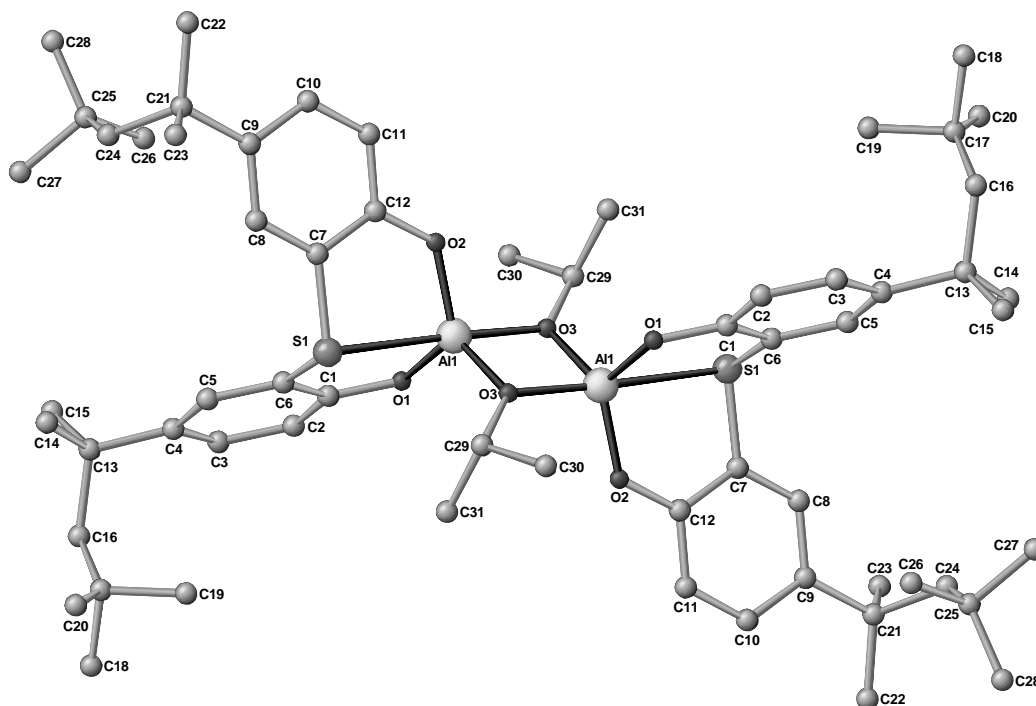


Figure 26 The X-ray structure of $[(TBOP)Al(\mu-OPr^i)]_2$ **7g**.

Catalyst	Length of bonds, [Å]		Length of bonds, [Å]		Lit.
$[(TBOP)Al(\mu-OPr^i)]_2$ 7g	Al(1)-O(1)	1.744(2)	S(1)-C(7)	1.777(3)	a
	Al(1)-O(2)	1.736(2)	S(1)-C(6)	1.780(3)	
	Al(1)-O(3)	1.813(2)	O(1)-C(1)	1.342(3)	
	Al(1)-O(3)#1	1.8428(19)	O(2)-C(12)	1.350(3)	
	Al(1)-Al(1)#1	2.8005(16)	O(3)-C(29)	1.473(3)	
	Al(1)-S(1)	2.6798(11)			
$[(TBMP)Al(\mu-OPr^i)]_2$	Al(1)-O(3)	1.742(8)	S(1)-C(5)	1.788(11)	114c
	Al(1)-O(2)	1.750(8)	S(1)-C(15)	1.797(11)	
	Al(1)-O(1)	1.794(7)	O(1)-C(1)	1.444(12)	
	Al(1)-O(1)#1	1.864(7)	O(2)-C(4)	1.337(11)	
	Al(1)-Al(1)#1	2.828(7)	O(3)-C(16)	1.343(12)	
	Al(1)-S(1)	2.552(5)			

Table 24 Comparison of X-ray data collected for self-synthesised **7g** and literature-known $[(TBMP)Al(\mu-OPr^i)]_2$ (these data are also presented as a part of Table 18), a – this work.

The ¹H NMR spectrum of **7g** reveals six sets of resonances (see Figure 26), three sets for the aromatic hydrogen atoms of the phenol rings (in the range of 6.72 – 7.52 ppm) and three for the hydrogen atoms of the *para*-substituted *tert*-octyl groups, found in the spectrum within the

range 0.60 – 1.60 ppm. Such an overlapping of different signal sets suggests a non-equivalence of the ligands within the aluminum bisphenoxide. Both methine and methyl hydrogen atoms of the bridging isopropoxy groups are shifted downfield compared to the methylene-bridged aluminum bisphenoxides and appear at 4.77 ppm, 1.40 and 1.43 ppm, respectively instead of 4.13-4.62 ppm, 1.48-1.55 (in **1-3 g**) in the methylene-bridged (see Table 20).

Catalyst	Bond angle, [°]		Bond angle, [°]		Lit.
[(TBOP)Al(μ -OPr ⁱ)] ₂ 7g	C(7)-S(1)-C(6)	105.40(13)	O(2)-Al(1)-O(3)	122.35(10)	a
	C(7)-S(1)-Al(1)	89.09(9)	O(1)-Al(1)-O(3)	117.73(10)	
	C(6)-S(1)-Al(1)	88.43(9)	O(2)-Al(1)-O(3)#1	100.18(9)	
	O(2)-Al(1)-O(1)	118.21(10)	O(3)-Al(1)-O(3)#1	79.99(9)	
	O(1)-Al(1)-O(3)#1	102.93(9)	O(2)-Al(1)-S(1)	81.43(7)	
	O(1)-Al(1)-S(1)	81.78(7)	O(3)-Al(1)-S(1)	93.65(6)	
	O(2)-Al(1)-Al(1)#1	116.64(8)	O(3)#1-Al(1)-S(1)	173.32(7)	
	O(3)-Al(1)-Al(1)#1	40.39(6)	O(1)-Al(1)-l(1)#1	117.56(8)	
[(TBMP)Al(μ -OPr ⁱ)] ₂	C(5)-S(1)-C(15)	106.4(5)	O(3)-Al(1)-O(2)	118.7(4)	114c
	C(5)-S(1)-Al(1)	91.2(5)	O(3)-Al(1)-O(1)	121.7(4)	
	C(15)-S(1)-Al(1)	90.7(6)	O(2)-Al(1)-O(1)	119.2(4)	
	O(2)-Al(1)-O(1)	119.2(4)	O(3)-Al(1)-O(1)#1	99.4(4)	
	C(1)-O(1)-Al(1)	137.8(7)	O(3)-Al(1)-S(1)	83.1(3)	
	O(1)-C(1)-C(3)	110.4(11)	O(2)-Al(1)-S(1)	83.3(3)	
	C(16)-O(3)-Al(1)	128.9(9)	O(1)-Al(1)-S(1)	97.3(3)	

Table 25 Comparison of X-ray data collected for self-synthesised **7g** and literature known [(TBMP)Al(μ -OPrⁱ)]₂ (these data are also presented as a part of Table 24), a - this work

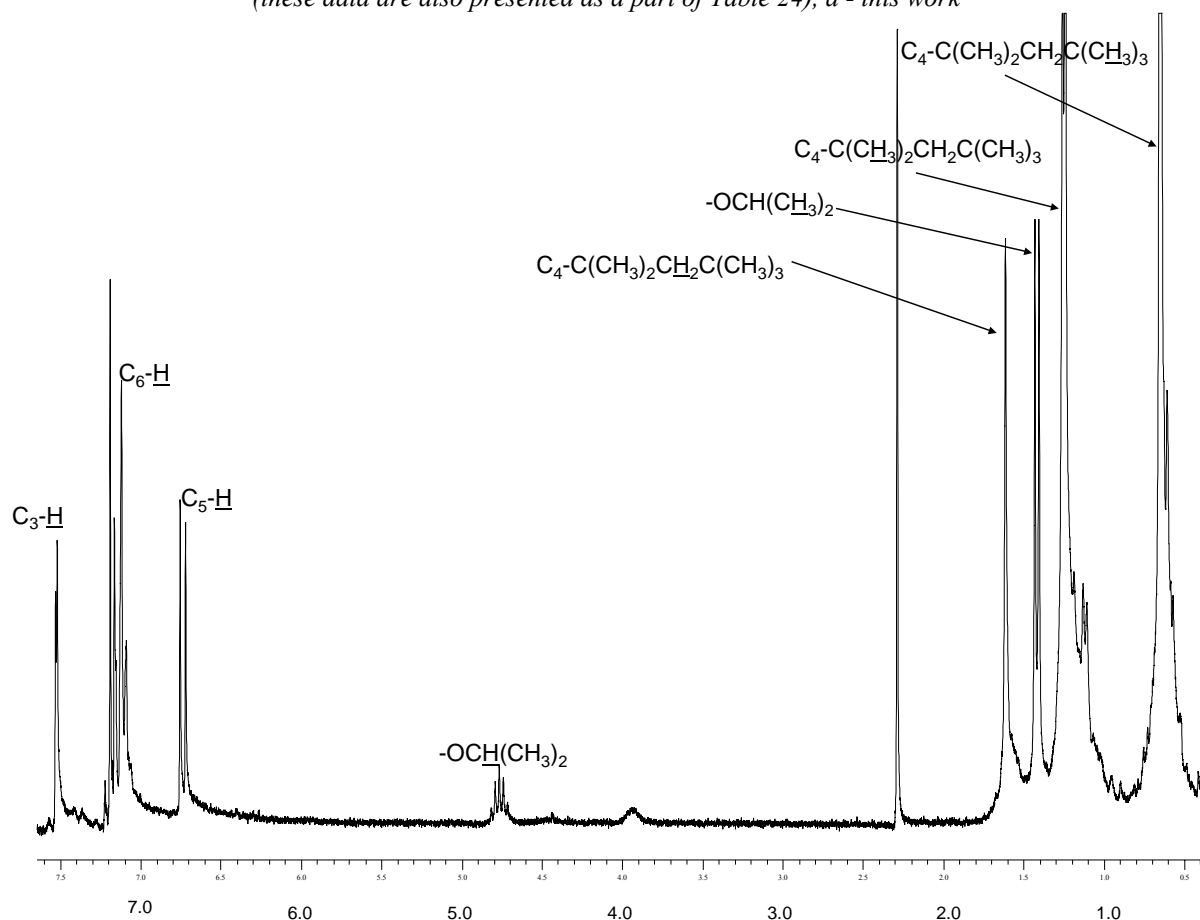


Figure 27 ¹H NMR spectrum of **7g**.

*** **

To summarise the synthetic part of this work, we can see that the aluminum bisphenoxides are principally suitable to elaborate a catalyst's library. Complementing the aluminum-bisphenoxide pool already reported by Okuda and Lin we were able to easily synthesise, purify and structurally characterise new aluminum bisphenoxide. These new compounds were also with FT-IR and NMR methods spectroscopically characterised.

5.2.5 ^{27}Al NMR as a tool in the identification of organometallic compounds

^{27}Al -NMR spectroscopy which, thanks to, allows an easy and rapid assessment of the coordination geometry of the aluminium atom(s) involved in the copolymerization.

Due to its high sensitivity, the ^{27}Al -NMR spectroscopy can be used to assess the coordination geometry and symmetry around the aluminium atom(s) as well as to gain some mechanical information during a reaction involving aluminum-based reactive species. Aluminium atom has a spin number as high as $5/2$ what yields a significant broadening of the NMR-signals. There are two following drawbacks of ^{27}Al NMR spectroscopy: (i) depending on the symmetry of the Al-containing species, the line width can vary from 3 Hz to several thousand Hz and in some case might be that broad that the signal cannot be ascertained as a signal any more, and (ii) that the “information density” of the recorded ^{27}Al spectra remains relatively low even though the NMR-data are backed-up by relevant literature data.

Some data have been compiled by Benn¹¹⁶ and later on, in the more detailed work of Barron dealing with π -bonding in tetrahedrally coordinated aluminium alkoxides.¹¹⁷ According to Barron's work carried out in 1983, who has investigated four- and fivefold coordinated aluminium compounds, we can attribute chemical shifts between 180 and 140 ppm to tetracoordinated aluminium derivatives. In the fivefold coordinated aluminium atoms the δ -values are placed in the 120 – 110 ppm range, in the fivefold coordinated AlCl_3 and AlBr_3 adducts the δ -values are located between 65 and 35 ppm.¹¹⁸ The sixfold coordinated aluminium compounds are found in the range of +20 – -40 ppm. As Barron reported, the ^{27}Al NMR shifts of tetrahedrally coordinated aryloxides (phenoxides) cover a wide range, between 140 and 45 ppm¹¹⁷, according to his suggestion this region can be divided into three sub-areas: the mono aryloxides δ 140-134 ppm; the bis aryloxides δ 72-69 ppm; and the tris aryloxides δ 50-47 ppm. Most of the reported aluminium compounds can be found within these three regions. So, we can see that we can categorise the chemical shifts of aluminium atom, according to the degree of substitution about the metal core.¹¹⁹

An additional difficulty encountered in the recording of ^{27}Al NMR spectra is the fact that most of the commercial probehead (Varian Bruker, Jeol) are based on diamagnetic aluminium-based alloys which deliver also a background signal. This very broad signal might dominate in some cases, especially in dilute solutions, and complicate the attribution of the different NMR signals.^{142,143} This broad “probe head signal” cover the range of 150 to 0 ppm, with maximum at ca. 60 ppm. All performed measurements were made with the suitable concentrations for ^1H , ^{13}C and ^{27}Al NMR and background spectra were also recorded accordingly.

		^{27}Al NMR [δ]	Assignment	Ref.
1	$[(\text{MDBP})(\text{THF})\text{AlEt}]$, 1a	52.8	t	a
2	$[(\text{MDBP})(\text{THF})\text{AlCl}]$, 1b	59.2	t	a
3	$[(\text{MDBP})(\text{Et}_2\text{O})\text{AlEt}]$, 1c	57.5	t	a
4	$[(\text{MDBP})(\text{Et}_2\text{O})\text{AlCl}]$, 1d	60.1	t	a
5	$[(\text{MDBP})\text{AlEt}]_2$, 1e	53.0	t	a
6	$[(\text{MMBP})(\text{Et}_2\text{O})\text{AlEt}]$, 2c	58.6	t	a
7	$[(\text{MMBP})\text{AlEt}]_2$, 2f	53.4	t	a
8	$[(\text{MMBP})\text{Al}(\text{OPr}^i)]_2$, 2g	58.0	t	a
9	$[(\text{MCIBP})(\text{THF})\text{AlEt}]_2$, 6a	70.6	tbp	a
10	$[(\text{MCIBP})_2\text{Al}_3\text{Et}_3]$, 6c	55.9	t, tbp	a
11	$[(\text{TOBP})(\text{THF})\text{AlEt}]$, 7a	56.5	tbp	a
13	$[(\text{TBMP})(\text{THF})\text{AlMe}]$	59.0	tbp	114c
14	$[(\text{TBMP})\text{Al}(\text{OPr}^i)]_2$	59.0	tbp	114c

Table 26 Chemical shifts of ^{27}Al NMR measured for different aluminium compounds, t – tetrahedral; tbp – trygonal bipyramidal, a - this work

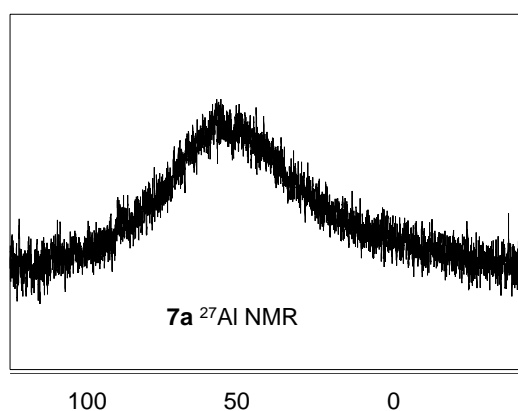


Figure 28 ^{27}Al NMR spectrum of **7a**, 56.5 ppm.

All measured complexes presented in the Table 26 appear in the narrow range between 63 and 50 ppm, regardless of their coordination and substitution of carried ligand. In case of **6c** signals of four- and fivefold coordinated aluminium atoms overlap each other; the chemical shift of fivefold coordinated aluminium atom in **7a** (see Figure 28) is in a good agreement with the value reported by Okuda for its bulky-*ortho*-substituted analogue (respectively 56.5 and 59.0 for **7a** and $[(\text{TBMP})(\text{THF})\text{AlMe}]$). This analytic technique requires a tidy experience, because in such cases as discussed above each observed chemical shift is a relevant of different factors (sterics, intramolecular effects $\pm M$, $\pm I$, kind of substitution) and the oftenest an additional support of e.g. the X-ray structure is recommended.

5.3 Copolymerisation processes

5.3.1 Description of the experimental set-up and preparation of tests

We developed a kind of "multi-reactor" system involving four high pressure reactors equipped with magnetically coupled stirring systems and electrical heating mantles (magnetic stirrer + aluminium block + thermoelement). Temperature and pressure were monitored via a digital multimeter (HP 34970A) connected to a personal computer. One of the high-pressure reactors we used is schematised in Figure 29. The copolymerisation was typically conducted in 70 cm³ stainless steel (SS 316) autoclaves equipped with standard Swagelock fittings and a separate loop made of stainless steel tubing which can be operated independently of the main reactor body. Because of the general moisture sensitivity of metal alkoxides and in order to get reproducible results, the reactors were heated at 100 °C and purged with argon prior to use. Cyclohexene oxide (5-20 cm³) was transferred (with or without co-solvent) into the autoclave, the reactor was then pressurised with CO₂ (60 bar) for a few minutes under stirring and afterwards weighed, the procedure was repeated until the desired CHO/CO₂ molar fraction was reached (18-35 g CO₂). Owing to the general high Lewis acidity of aluminium alkoxides and the ability to also catalyse a homopolymerisation of the epoxides, the catalyst was firstly dissolved under argon into ca. 1 cm³ toluene (or CH₂Cl₂) introduced into the separate loop and was then, establishing the communication with the epoxide/CO₂ mixture in the autoclave, allowed to diffuse into the reaction mixture through gravity. This procedure though time-consuming was necessary to get reproducible results and clearly evaluate the reactivity of the catalyst in pure copolymerisation reactions. Each copolymerisation process has been going on for 18 hours. In order to evaluate the practicality of this "catalyst-in-the-loop" method, we firstly run a couple of copolymerisation reactions in a stainless steel autoclave fitted with Borosilicate windows (MPI für Kohlenforschung, Mülheim, SS-316, 220 cm³, T_{max} = 220°C, P_{max} = 200 bar) and could see that the forming copolymer under the chosen experimental condition remained a thick solution at the bottom of the reactor. Slowly decompressing the autoclave yields the poly(ether-carbonate) as a white foam which can be easily dissolved in CH₂Cl₂. After the reaction time the autoclaves were cooled down to RT (water bath) and the carbon dioxide slowly vented, under stirring, in a fume hood. After opening the remaining solid / syrupy solution was dissolved in CH₂Cl₂ and the aluminium catalyst was then hydrolysed with 10% HCl aqueous solution (50-100 cm³) and separated from the copolymers via a separating funnel. The organic extracts were washed two times with saturated NaHCO₃ and dried with MgSO₄. The short-chained copolymers were then separated from the long-chained ones via repeated dissolving in CH₂Cl₂ and consecutive

precipitation in methanol. The white amorphous solids, which have at the end of the purification process a talcum-like appearance, are easily soluble in CHCl_3 , benzene and toluene and are insoluble in acetone or water.

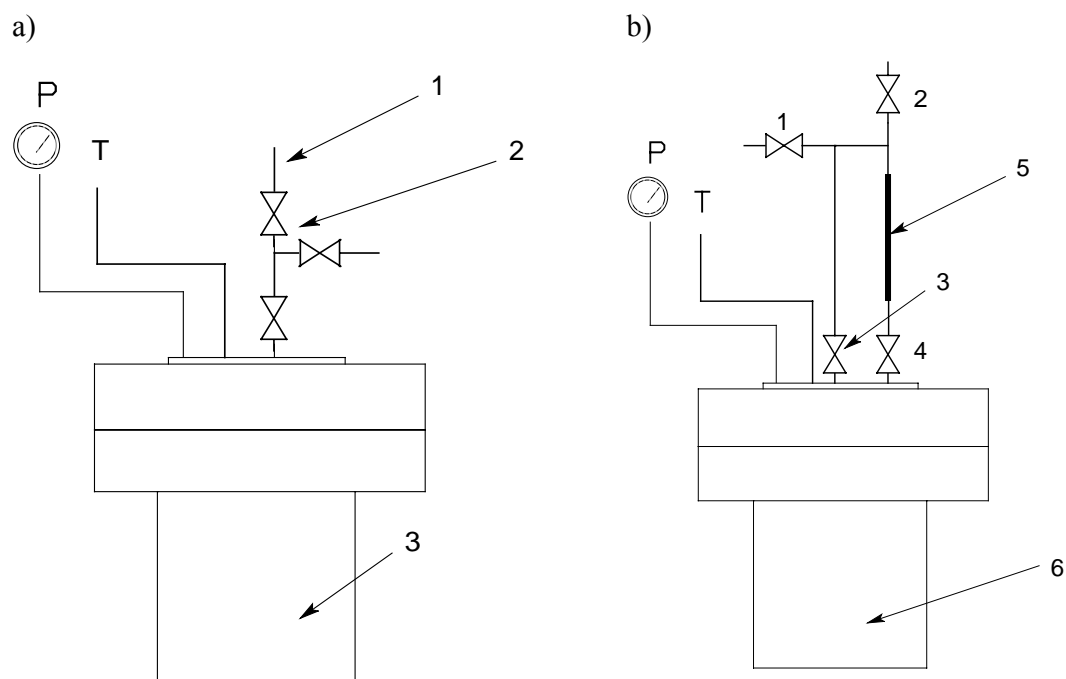


Figure 29 Scheme of the autoclaves. a.) Standard autoclave: 1-inlet of gases (Ar , CO_2), 2 – system of pressure valves, 3 – mixture of reactants; b.) 1-4 – pressure valves, 5 – 1 cm^3 cell for catalyst solution, 6 – mixture of reactants

5.3.2 Structure-reactivity relationships in the aluminium-bisphenoxide-catalysed copolymerisation of cyclohexene oxide with carbon dioxide: first results

One of the aims of this investigations was to firstly find if the aluminium bisphenoxides are suitable candidates to catalyse the copolymerisation of CHO with CO_2 and optimise the reactions parameters to have a possibly the highest amounts of carbonate linkages in the final copolymers. Considering the general structure of the chosen aluminium bisphenoxides catalysts, we have three majors keys which might influence their reactivity in the investigated copolymerisation reaction: i) the nature of the starting compound (AlEt_3 , AlEt_2Cl or AlOPr^i) and consequently the nature of the aluminium-nucleophile bond (Al-C , Al-Cl or Al-O) which has a direct influence on the generation of the first alkoxo-species actually active in the copolymerisation; ii) the nature of the substituents bound to the 2,2'-methylene bisphenoxide backbone as well as iii) the presence or not of neutral ligands in the coordination sphere of the reactive aluminium centre. Working with those three structural parameters in combination with temperature, pressure, molar epoxide / CO_2 ratio and potential co-catalysts would produce a huge matrix of potential experiments, what taking into account the relatively short duration of this study we had to limit the first copolymerisation experiments to a narrow

series of experiments. A secondary “target” was to find a highly reactive catalytic system allowing the production of copolymers with high molecular weights AND a low molecular weight distribution (or polydispersity indexes) in order to deliver copolymers with reproducible mechanic properties. In this regard the absence of remaining catalysts’ traces in the copolymers is of tremendous importance. Although the separation of the catalyst from the copolymer via hydrolysis and subsequent extraction of the polymer with an organic solvent is reasonably working, the search for the highest e catalyst / substrate ratio remains in focus of interest. The available literature provides some information about the synthesis of poly(propylene oxide) PPO using aluminium bisphenoxide **1f**¹¹², but the ratio used was relatively small (ca. 200-300 to 1; epoxide to catalyst). In the work of Beckman and co-workers dealing with the copolymerization of CHO and CO₂, this ratio was comparably small (100 / 1). Using Al(OPrⁱ)₃ CHO / CO₂ copolymerisation was catalysed with the 300 to 1 molar ratio.⁸⁵ The majority of the report dealing with the more documented zinc- and cobalt-based catalytic system, state a substrate/catalyst ratio of ca. 1000 to 1 This the reason why we adopted this standard. Before we found that with as high epoxide-to-catalyst molar ratio as 1000 to 1 using aluminium bisphenoxides only CHO is able to cleave we run a couple of unsuccessful copolymerisations involving CO₂ and PO or SO.

Experimental conditions in which the different reaction’s partners (epoxide/CO₂ and catalyst) are able to easily interact with each other are a prerequisite for an effective catalysis. The use of supercritical carbon dioxide as medium and reactant might seem an elegant solution to efficiently run copolymerisation reaction involving CO₂. However the preliminary tests we performed did not yield a notably better incorporation of CO₂ into the copolymer. This might be tentatively explained by a lower solubility and hence, reactivity, of the bisphenoxide-based catalysts in pure carbon dioxide. We found that using near-to-supercritical fluid conditions is enough to observe an optimum in the formation of polyether-carbonate from CO₂ and cyclohexene oxide. Operating in a so-called “CO₂-expanded” liquid phase (pressure from 90 to 120 bar, temperatures ranging from 80 to 110°C, with a CHO to CO₂ molar ratio of 1 to 3) the probability of successful work in optimal conditions is the greatest and the aluminium catalyst might react with both co-monomers.

The influence of different bisphenol-grafted substituents on reactivity and selectivity of the bisphenoxide catalysts having the same structural features (see Tables 27 – 33) is presented. Some comparisons concerning the nature of the nucleophile directly bound to the aluminium centre (C, O-R, Cl and in one case I), keeping the bisphenol ligand constant are provided as well. Similarly to catalytic systems based on Al⁵⁴, Cr^{53,54,56} and Co¹⁴⁷⁻¹⁵¹ reported in the

literature, we have eventually performed two series of screening tests involving Lewis bases, ammonium and phosphonium salts as co-catalysts in order to influence the selectivity of the copolymerization of some bisphenoxide catalysts.

Yield of polymer is given in percents and was defined as a weight of isolated polymer divided by the theoretical weight of isolated pure carbonate which might be isolated. The content of carbonate linkages is also given in percents. The number average molecular weight of isolated polymers is given in g per mole.

5.3.2.1 Catalysts with a general structure [(bisphenol-2H)(THF)AlEt]

The results of the copolymerisation screening performed with aluminium bisphenoxides containing a coordinated solvent molecule (in this case THF) and obtained from the reaction of AlEt₃ with the investigated bisphenols are summarised in Table 27. Different correlations between aluminium bisphenoxides' structures and catalytic activities can be discerned from the data gathered in this table. The most reactive aluminium complexes relative to a copolymerisation of CO₂ with CHO seem to be the bisphenoxides bearing a sterically demanding group at location 6 of the phenyl rings like e.g. **3a** with a 1-methyl-cyclohexyl group (20.49 %). At a lesser extend **2a** and **4a**, with respectively a *tert*-butyl and an *iso*-propyl rests at carbon 6 of the phenyl, corroborated this assumption and produced long-chained copolymers but with a lower CO₂-incorporation. (11.36 % and 12.03 % for **2a** and **4a**, respectively). **3a** and **2a** display almost the same tetrahedral coordination geometries around the aluminium atom whereas **4a** shows a markedly distorted tetrahedral environment owing to the presence of a supplementary methyl group at carbon 3 of the phenyl and the resulting twisting of the bisphenoxy ligand. The presence of a third substituent at carbon 3 although complicating the evaluation of the structure-reactivity relationships seems to have in that particular case no considerable influence on the reactivity.

Cat.	Yield [%]	-CO ₃ - [%]	M _n	PDI	TON	TOF
1a	39	6.81	16156	1.58	464	26
2a	18	11.36	5525	3.09	259	14
3a	55	20.49	7069	1.84	673	37
4a	46	12.03	10255	2.41	660	37
5a	0.4	1.59	16402	1.54	6	0.3
6a	The reaction did not take place.					
7a	1.2	4.57	14937	1.57	6	0.3

Table 27 Copolymerisation results for monomeric [(bisphenol-2H)(THF)AlEt] catalysts. ($\eta_{CHO} = 0.2 - 0.3$, $P = 75 - 95$ bar, $T = 80-95$ °C, for **6a**: $P = 100$ bar, $T = 110$ °C).

The presence of chlorine atoms at location 4 of the phenyl rings in the case of **4a** and **6a** should have a significant influence on the reactivity of the aluminium bisphenoxides. A chlorine atom bound to an aromatic system plays an ambivalent role: through its electron-

withdrawing capabilities (so called -I effect), it can narrow the electron density in the phenyl rings and enhance the Lewis acid character of the aluminium bisphenoxide whereas through resonance-phenomena (so called +M effect) it can stabilize the bisphenoxide ligand and lower the reactivity of the final aluminium complex. Considering a pure inductive effect of the chlorine, the related aluminium bisphenoxide-THF adducts would be quite stable and not compete efficiently with an epoxidic substrate to initiate the copolymerisation reaction. That is most probably what we observed in the case of **6a**, where the THF molecule cannot be displaced by the epoxide, this also under hard conditions (100 bar and 110 °C).¹²⁴ In comparison, **4a** possesses two electron-donating alkyl groups: respectively a methyl and an *iso*-propyl one at locations 3 and 6 of the phenyl rings, which may compensate a low electron density in the aromatic system and allow a coordination of the epoxide to take place. It seems that the distorted tetrahedral environment found around the aluminium in **4a** has a narrow influence on the catalytic activity of the complex. The presence of different substituents at carbon 4 has a direct impact on the reactivity as it can be seen considering the sub-groups **1a** (4,6-di-*tert*-Bu), **2a** (4- Me, 6- *tert*-Bu), and **5a** (4,6-di-Me). Surprisingly compound **1a** with a second *tert*-butyl group in position 4 instead of a methyl group as in **2a** displays a narrow reactivity suggesting that the presence of a bulky, electron donating (+I effect) alkyl substituents at carbon 4 deactivate somehow the aluminium bisphenoxide. This is correlated by the very low reactivity (yield: ca. 1 %) found in the case of **7a** which has a *tert*-octyl groups at the carbons at location 4 of phenyl rings affording long-chained copolymer with a very low CO₂ insertion. In comparison **5a** with a second methyl group in position 6 instead of a *tert*-butyl one as in **2a** delivered the lowest reactivity of this catalyst's series. It seems, in a first approximation, that the presence of a sterically demanding alkyl group at carbon 6 AND the presence of a small alkyl group at carbon 4 (e.g. **2a**) promote the formation of copolymer with a better CO₂-incorporation (higher amounts of CO₃-linkages).

5.3.2.2 Catalysts with a general structure [(bisphenol-2H)(THF)AlCl] and **4b**

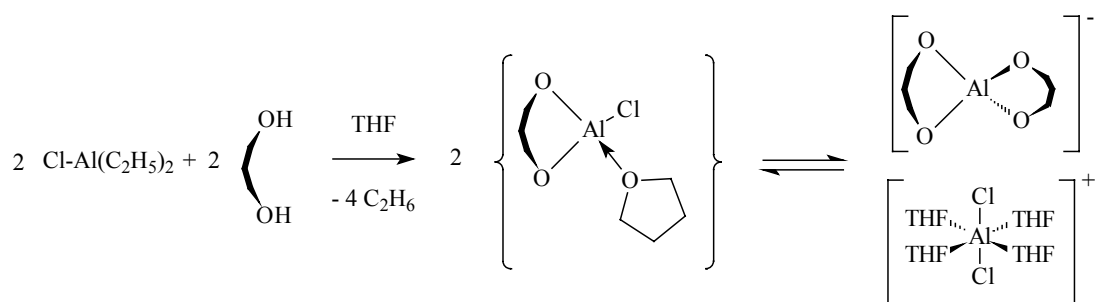
It was interesting to evaluate more precisely the influence of the nucleophile bound to the aluminium atom on the efficiency of the copolymerisation. The synthesis of the corresponding [(bisphenol-2H)(THF)AlCl] analogues from (C₂H₅)₂AlCl is straightforward and the copolymerisation's results obtained with some of these compounds are summarised in Table 28. The most reactive aluminium complexes is anew the bisphenoxide having a sterically demanding 1-methyl-cyclohexyl group at location 6 of the phenyl rings like e.g. **3b**. The CO₂-insertion and the copolymer chain length are in the same range (M_n and CO₃ amount) than the data found using **3a** as a catalyst. At a lesser extend **1b**, with a *tert*-butyl

fragments at carbons 6 of the phenyl rings, displayed a fair reactivity producing longer copolymer chains with a lower CO₂-incorporation than **3b** (respectively, 11.36 % for **1b** and 21.37 % for **3b**). Considering **2b**, with a methyl groups at carbons 4 of the phenyl rings, the reactivity found was lower than **1b**, what seems to be in contradiction to the trend found in the precedent chapter where the presence of a methyl groups at carbon 4 of the phenyl rings had a positive influence on the CO₂-insertion. However if we more generally consider the bisphenoxides **3b**, **2b** and **1b** and their Al-ethyl analogues: **3a**, **2a** and **1a**, all displaying a comparable tetrahedral coordination geometries, it can be seen that: i) compounds **3a** and **3b** produced medium-sized copolymer chains with the highest CO₂-incorporation, ii) compounds **1a** and **1b** produced the longest copolymer chains with fair CO₂-incorporations, and iii) compounds **2a** and **2b** produced the shortest copolymer chains with also fair CO₂-incorporations. Surprisingly compound **5b** with methyl groups at carbon 6 and 4 of the phenyl rings showed no reactivity at all.

Cat.	Yield [%]	-CO ₃ - [%]	M _n	PDI	TON	TOF
1b	52	11.36	10472	1.77	705	39
2b	21	7.01	4633	3.37	292	16
3b	64	21.37	8332	2.30	836	44
4b	42	14.81	10160	2.41	378	21
5b	The reaction did not take place.					

Table 28 Copolymerisation results for monomeric [(bisphenol-2H)(THF)AlCl] catalysts.
($\eta_{CHO} = 0.2 - 0.3$, $P = 85 - 95$ bar, $T = 85 - 95$ °C, for **2b**: $P=110$ bar, $T = 105$ °C)

Bisphenoxide **4b** that bears a third ancillary group at carbon 3 of the phenyl presents a kind of discrepancy between structure in the solid state and catalytic activity. **4b** was found to display in the solid state a complete different structure than its Al-Et counterpart, **4a**: while **4a** remains a neutral bisphenoxide with a markedly distorted tetrahedral environment, **4b** rearrange to form a crystalline ionic compound: $[\text{Al}(\text{THF})_4(\text{Cl})_2]^+[\text{Al}(\text{MCIMePrP})_2]^-$. However considering the catalytic test involving **4b**, it can be seen that the reactivity is comparable to the reactivity recorded for the corresponding neutral $[(\text{MCIMePrP})(\text{THF})\text{AlEt}]$, **4a**. Considering the fact that we used a freshly made, amorphous catalyst for these tests, the similar reactivity in the catalysis found for **4a** and **4b** strongly suggests that bisphenoxide **4b** exists originally as a neutral aluminium-THF adduct which slowly rearrange to form the isolated crystalline ionic aluminium bisphenoxide (see Scheme 9). This transient neutral bisphenoxide $[(\text{MCIMePrP})(\text{THF})\text{AlCl}]$ displaying at the aluminium centre enough room for a coordination of the epoxide is most likely the active specie in the copolymerisation reaction.



Scheme 9 The rearrangement of neutral **4b** specie into an ionic one.

5.3.2.3 Catalysts with a general structure [(bisphenol-2H)(Et₂O)AlEt]

As evoked in the introduction of this chapter, the nature of the coordinated solvent (strong or weak Lewis base) or its absence in the coordination sphere of the catalyst plays a role in the catalysis. The synthesis of relevant aluminium bisphenoxides was relatively easy and derived from the usual synthesis way by substituting THF with diethyl ether or n-hexane. The solid state structures of the complexes involving diethyl ether as neutral ligands were similar to the structures found for the related THF-bisphenoxide adducts, what is important to draw parallels between the different aluminium bisphenoxide classes. The copolymerisation's results obtained with some of these compounds are summarized in Table 29. Considering that a diethyl ether-aluminium alkoxide adduct (weak Lewis base/strong Lewis acid) should not be as stable as a THF-aluminium alkoxide adduct (strong Lewis base/strong Lewis acid), we expected a higher catalytic activity of the diethyl ether-aluminium bisphenoxides. Surprisingly the reactivity's trend found for the last two aluminium bisphenoxide classes was somehow disproved by the tests run with the bisphenoxide-diethyl ether adducts: the highest catalytic activity was noted for **1c** catalyst based on the bisphenol bearing four *tert*-butyl groups. It afforded copolymers in high yield (45 %) and with carbonate amounts comparable to the ones obtained with aluminium bisphenoxides bearing 1-methyl-cyclohexyl groups and THF (**3a** and **3b**). In comparison **3c** produced in low yields medium-sized copolymer chains with a fair CO₂-incorporation. Compound **2c** based on a bisphenol with *tert*-butyl group at carbons 6 and methyl at carbon 4 of the phenyl rings displayed no reactivity at all and draw a parallel to the related compounds **2a** and **2b** which produced the shortest copolymer chains with a low CO₂-incorporation. Interestingly compound **4c** seems to satisfy the criteria for an efficient ROP catalyst, considering cyclohexene oxide as substrate of the homopolymerisation. This is underlined by the high number average molecular weight, the low polydispersity index and low content of carbonate linkages in the isolated polymers. This

trend is confirmed in the case of the related chlorinated bisphenoxide **4d**, [(MCIMePrP)(Et₂O)AlCl], as it will be described in the next chapter.

Cat.	Yield [%]	-CO ₃ - [%]	M _n	PDI	TON	TOF
1c	45	20.49	6030	2.40	628	35
2c	The reaction did not take place.					
3c	0.8	12.05	4179	2.35	11	0.6
4c	38	4.11	19789	1.57	544	30
5c	6	2.12	14060	1.54	214	12

Table 29 Copolymerisation results for monomeric [(bisphenol-2H)(Et₂O)AlEt] catalysts. ($\eta_{CHO} = 0.3$, $P = 80 - 90$ bar, $T = 90 - 110$ °C)

5.3.2.4 Catalysts with a general structure [(bisphenol-2H)(Et₂O)AlCl]

Keeping in sight the catalytic results involving the THF-based adducts, in order to complete this first series of experiments we had to run similar catalytic tests with their diethyl ether counterparts, the ethyl ones were described in the last chapter, here we want to focus on the chlorine derivatives (see Table 30).

Cat.	Yield [%]	-CO ₃ - [%]	M _n	PDI	TON	TOF
1d^a	50	11.47	8190	1.61	683	85
2d	The reaction did not take place.					
3d	30	17.83	5724	2.00	408	23
4d	18	11.14	34543	1.28	144	8

Table 30 Copolymerisation results for monomeric [(bisphenol-2H)(Et₂O)AlCl] catalysts. ($\eta_{CHO} = 0.2-0.3$, $P = 75 - 100$ bar, $T = 90 - 100$ °C), *a* – reaction time 8 h.

The synthesis was relatively straightforward and performed in diethyl ether from AlClEt₂ and the related bisphenols. Considering the copolymerisation screening, it can be noticed that within this catalyst's series the catalyst allowing a good CO₂-insertion into the copolymer is anew the catalyst bearing a 1-methyl-cyclohexyl groups at carbons 6 of the phenyl rings, **3d**, even though the copolymer chain obtained are rather short (**3d** – yield: 30 %, -CO₃-: 12.03 %, M_n, 5724). Compound **1d** with *tert*-butyl group instead of 1-methyl-cyclohexyl although producing copolymers with higher averaged molecular weights displayed a lower CO₂-incorporation (17.83 and 11.47 % for **3d** and **1d**, respectively), the same trend was observed for **3b** and **1b** (21.37 and 11.36 % for **3b** and **1b**, respectively). Compound **2d** shows non reactivity at all the same as its organometallic Al-Et counterpart **2c**, suggesting that the combination 2,2'-methylenebis(4-methyl-6-*tert*-butylphenol) and diethyl ether as a neutral ligand bound to the aluminium atom is not working for some unclear reasons. It would have been interesting to study more closely the catalytic activity of the connected combination 2,2'-methylenebis(4,6-di-methylphenol) and diethyl ether, but unfortunately owing to the limited duration of this study, it was not possible to prepare and test this bisphenoxide. As previously reported in the case of **4c**, compound **4d**, involving diethyl ether and aluminium-chlorine reactive bond, is a very efficient catalyst to generate long-chained copolymers from

cyclohexene oxide, although with a low CO₂-insertion (**4d** – yield: 18 %, -CO₃-: 11.14 %, M_n, 34543). A remarkable fact stand out for this catalyst: the very narrow molecular weight distribution (PDI: 1.28) which might be attributed either to the presence of a definite, single reaction site at the catalyst or to a very rapid growing polymer chains exchange at the aluminium centre (more rapid than the increasing of the polymer chain through successive insertion into the Al-O bond).

5.3.2.5 Catalysts with a general structure [(bisphenol-2H)AlEt]₂

Cat.	Yield [%]	-CO ₃ - [%]	M _n	PDI	TON	TOF
1e	52	16.95	5650	2.43	352	19
2e	44	21.74	8592	2.01	278	15
3e	80	19.19	8261	1.79	542	30
4e	27	12.82	9004	2.43	187	10
6c	27	1.98	19663	1.53	257	14
7c	42	24.39	6243	1.50	287	16

Table 31 Copolymerisation results for dimeric **1-4 e** and **7c** as well as trinuclear **6c** catalysts. ($\eta_{CHO} = 0.2 - 0.3$, $P = 75 - 100$ bar, $T = 90 - 95$ °C)

After having considered monomeric aluminium alkyl derivatives with neutral THF or diethyl ether molecules waiting to be displaced by the epoxide at the active coordination site, we logically focused on bisphenoxide systems having no neutral ligands in the coordination sphere, hoping to see a significant difference in the catalytic activity. It was not clear whether the dinuclear feature of these aluminium bisphenoxides remains the same upon addition of the epoxide or the epoxide (CHO) would be nucleophilic enough to break down these oligomeric bisphenoxides to form monomers similar to the compounds reported in the preceding chapters. The monomers (epoxide and CO₂) would then coordinate to the acidic centres and undergo a copolymerisation reaction with an efficiency comparable to the one obtained with monomeric bisphenoxide. Owing to the absence of neutral O-donors bound to aluminium, which stabilise the monomeric structure, different coordination geometries at the aluminium centres were observed, sometimes within the same oligomeric molecular structure. Analysing the data summarised in Table 31 we can see, that the ethyl-aluminium bisphenoxides displaying the highest catalytic activity are again based on the 2,2'-methylenebis(4-methyl-6-*tert*-butylphenol) (**2e** – yield: 44 %, -CO₃-: 21.74 %, M_n: 8592) and 2,2'-methylenebis(4-methyl-2-(1-methylcyclohexyl)phenol) (**3e** – yield: 80 %, -CO₃-: 19.19 %; M_n: 8261) and display in the solid state similar features. The replacement of the methyl group at carbon 4 of the phenyl rings by a *tert*-butyl in compound **1e** brought 16.95 % of carbonate linkages and medium-chained copolymers (M_n: 5649) and the catalytic selectivity was significantly worse than in the case of **3e** and **2e**. Compound **4e** with its three-fold substitution at the aromatic ring (3-Me, 4-Cl, 6-Pr^{iso}) and twisted structural feature delivered, the same as in the case of

the related monomeric O-donors-substituted derivatives, the worse results of this series. Interestingly, the trend pointing towards efficient ring opening polymerisation catalysts found earlier for this ligand could anew be corroborated (**4e**, -CO₃-: 12.82 %; M_n: 9004, **4f**, -CO₃-: 13.97 %; M_n: 12159).

Solely considering the CO₂ incorporation into the copolymer, the ethyl aluminium bisphenoxide, **7c**, with a sulphide- instead of a methylene bridge, was the most efficient catalyst of our bisphenoxide “library” (yield: 42 %, -CO₃-: 24.39 %; M_n: 6243) followed by the ethyl-aluminium bisphenoxides based on the 2,2'-methylenebis(4-methyl-6-*tert*-butylphenol) (**2e**, see above). This high CO₂ incorporation was obtained despite a lousy solubility of **7c** in common solvents (like toluene, CH₂Cl₂ or hexane) and the fact that the catalyst had to be used more as a suspension at room temperature. The difference in the reactivities found for **7c** (and **7f**, as it will be shown in the next chapter, both dimer) and **7a** (monomer) are quite unexpected and call for a more thorough investigation. This results and, more generally, a comparison of the copolymers obtained with mononuclear and binuclear bisphenoxides suggest that binuclear aluminium bisphenoxides remain binuclear also in presence of a O-donor like an epoxide, what will be discussed more in details in the Chapter 5.3.3.

5.3.2.6 Catalysts with a general structure [(bisphenol-2H)AlCl]₂

Considering the trend found in the last chapter it was interesting to investigate the related dimeric aluminium bisphenoxides possessing an aluminium-chlorine bond with respect to the copolymerisation efficiency and compare the results with those obtained with the monomeric chloro-aluminium bisphenoxide containing a Lewis base in the coordination sphere.

The higher efficiency of the dimeric bisphenoxides was anew confirmed and the best results were obtained with the chloro-aluminium bisphenoxides based on the following bisphenols. For the 2,2'-methylenebis(4-methyl-6-*tert*-butylphenol), for dimeric **2f** the polymer displayed the following parameters: yield: 49 %, -CO₃-: 20.92 %; M_n: 12522, for monomer **2b** – yield: 20 %, -CO₃-: 7.01 %; M_n: 4633. In cases of 2,2'-methylenebis(4,6-di-methylphenol) and the 2,2'-methylenebis(4,6-di-*tert*-butylphenol) these parameters were as follow: dimer **5f** – yield 32 %, -CO₃-: 20.75 %; M_n: 6216; monomer **5b** displayed no reactivity at all; and dimer **1f** – yield: 56 %, -CO₃-: 19.46 %; M_n: 10585; monomer **1b** – yield: 52 %, -CO₃-: 11.36 %; M_n: 10472, respectively.

Another correlation can be also taken for Table 32 summarising the polymerisation results: the dimeric chloro-aluminium bisphenoxides seem to be generally more active than the corresponding dimeric ethyl-aluminium bisphenoxides. Hence chloro-dimer **1f** is more

reactive than ethyl-dimer **1e** (**1f** – see above; **1e** – yield 52 %, -CO₃⁻: 16.95 %; M_n: 5650), **2f** has comparable reactivity with **2e** (**2f** – see above; **2e** – yield: 27 %, -CO₃⁻: 21.74 %, M_n: 8592) despite slightly lower carbonate content it yields longer polymer chains. **4f** is also more reactive than **4e** (**4f** – yield: 32 %, -CO₃⁻: 13.97 %; M_n: 12159; **4e** – yield: 27 %, -CO₃⁻: 13.82 %, M_n: 9004). One exception to this rule was found in the catalytic activity of aluminium bisphenoxides based on the 2,2'-methylenebis(4-methyl-2-(1-methylcyclohexyl)phenol): the chloro-aluminium bisphenoxide **3f** is less active than the ethyl-aluminium bisphenoxide **3e** (**3f** – yield: 63 %, -CO₃⁻: 17.01 %; M_n: 4885; **3e** – yield 80 %, -CO₃⁻: 19.19 %; M_n: 8261). This seems to be related to steric interactions between chlorine atom and the bulky steric demanding 1-methyl-cyclohexyl moiety.

Cat.	Yield [%]	-CO ₃ ⁻ [%]	M _n	PDI	TON	TOF
1f	56	19.46	10585	1.99	380	21
2f	49	20.92	12522	1.55	330	18
2h	The reaction did not take place.					
3f	63	17.01	4885	2.33	469	26
4f	32	13.97	12159	2.34	407	22
5f	32	20.75	6216	1.84	210	12
7f	54	22.42	6377	1.51	366	20

Table 32 Copolymerisation results for dimeric [(bisphenol-2H)AlCl]₂ catalysts.
(η_{CHO} = 0.2-0.3, P = 75 – 100 bar, T = 90 - 95 °C)

Considering more generally the chloro-aluminium bisphenoxides based on the 2,2'-methylenebis(4-methyl-2-(1-methylcyclohexyl)phenol), it can be noticed that the selectivity of the dimeric species, **3f**, is unexpectedly lower than that of the corresponding monomeric THF-adduct **3b** (**3f** – see above; **3b** – yield 64 %, -CO₃⁻: 21.37 %; M_n: 8332). The same trend can be found, though not so clear, studying the related ethyl-aluminium bisphenoxides **3e** and **3a** (**3e** – see above; **3a** – yield 55 %, -CO₃⁻: 20.49 %; M_n: 7069). This lower reactivity of the dimeric species seems to be related to the high steric demand of the 1-methyl-cyclohexyl substituent in the discussed ligand (rotation around the C(2)-C(16) and C(12)-C(23) axes). Comparing the X-ray structure of the dimeric bisphenoxide **3f** with that of the monomeric bisphenoxide **3a** (see Figure 30), it can be noticed that in dimeric species, 1-methyl-cyclohexyl substituents belonging to two different bisphenol ligands display together a higher steric hindrance than in the case of the monomeric bisphenoxide and would hamper therefore the coordination of the monomers to the aluminium centre.

Interestingly, the presence of an additional substituent bound to carbons 3 of the phenyl rings as found in the tri-substituted 2,2'-methylenebis(4-chloro-3-methyl-(1-isopropyl)phenol) results in a significant distortion of the bisphenol ligand. It can be seen that the aluminium compounds based on this ligand delivered similar catalytic results for the dimeric and monomeric species (**4f** – yield: 32 %, -CO₃⁻: 13.97 %, M_n: 12159; **4b** – yield: 42 %, -CO₃⁻:

14.81 %, M_n : 10160). It can be also remarked that the related dimeric and monomeric chloro- and ethyl-bisphenoxides display also similar reactivities (dimers: **4f** – see above; **4e** – yield: 27 %, $-\text{CO}_3^-$: 13.82 %, M_n : 9004; and monomers: **4b** – see above; **4a** – yield: 46 %, $-\text{CO}_3^-$: 12.03 %, M_n : 10255).

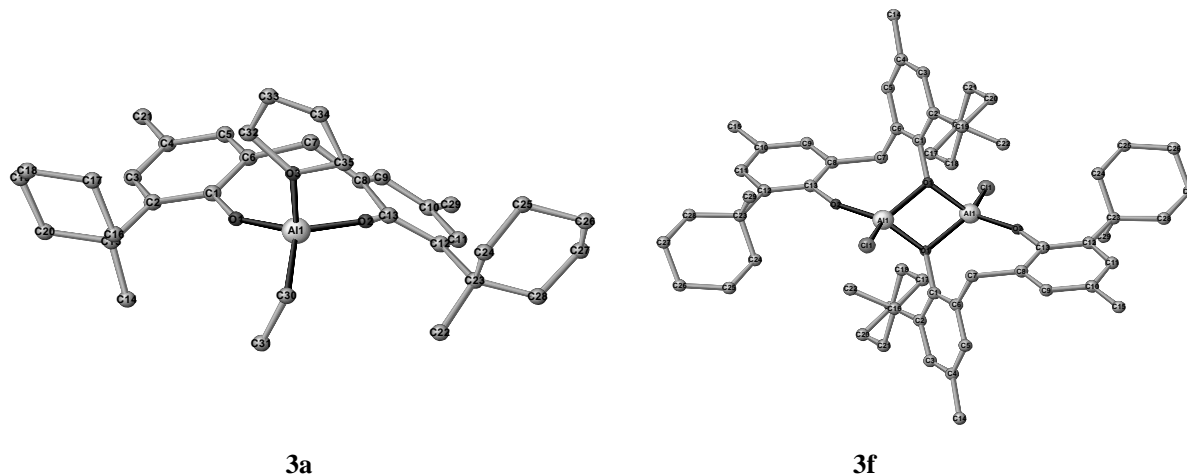


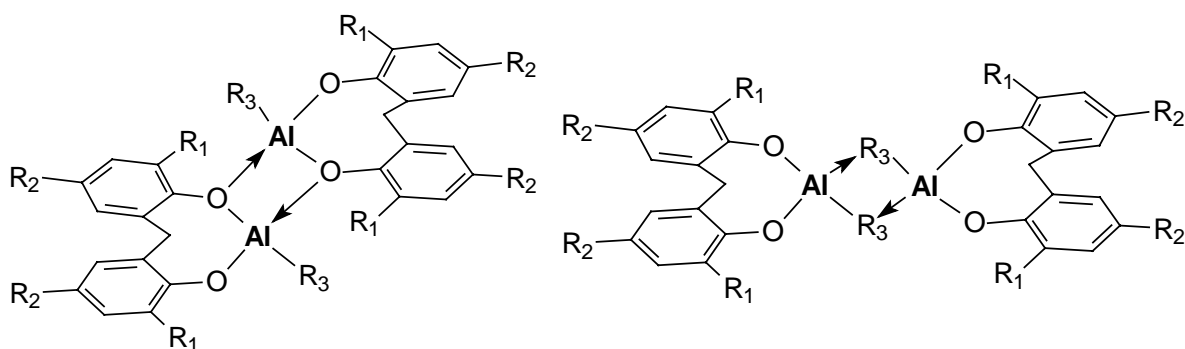
Figure 30 The X-ray structure of the monomeric [(Tetrahydrofuran)-ethyl-{2,2'-methylenebis(4-methyl-2-(1-methylcyclohexyl)phenoxide)} aluminium (III)], **3a**, and dimeric bis[chloro-aluminium 2,2'-methylenebis(4-methyl-6-(1-methyl-cyclohexyl)phenoxide)], **3f**

Solely considering the CO_2 incorporation into the copolymer, the chloro-aluminium bisphenoxide, **7f**, with a sulphide- instead of a methylene bridge, was the one of the most efficient catalyst of our bisphenoxide “library” (yield: 54 %, $-\text{CO}_3^-$: 22.42 %; M_n : 6377) and the most active within the “dimer halide group”. **7f** is followed by the chloro-aluminium bisphenoxides based on the 2,2'-methylenebis(4-methyl-6-*tert*-butylphenol) (**2f**, see above) and by the one based on 2,2'-methylenebis(4,6-di-methylphenol) (**5f**, see above). This latter result was completely unexpected, because it illustrates that bulky *ortho*-substituents are not essential to ensure the high CO_2 incorporation, but owing to the relatively short duration of this study further investigations explaining this phenomenon could be not performed.

A brief evaluation of the influence of the halide bound to the aluminium on the catalytic activity was performed. **2h**, an iodine analogue of **2f**, was synthesised according to the work of Lin¹⁴⁴, in a two-steps reaction, from elementary iodine and Et_3Al followed by the reaction with the corresponding bisphenol. The so-obtained amorphous iodo-aluminum-bisphenoxide was filtered, dried and then employed as catalyst. The absence of reactivity of this catalyst suggests that the aluminium-iodine bond is significantly stronger than the aluminium-chlorine one in such halogeno-aluminium-bisphenoxides. This can tentatively explained by a suitable coordination geometry around the aluminium centre allowing a stronger iodine-aluminum back-bonding. The epoxide might be able to coordinate to the iodo-aluminum-bisphenoxide, but would not displace the iodine atom to lead to the formation of an alkoxide.

5.3.2.7 Catalysts with a general structure $[(\text{bisphenol-2H})\text{Al}(\mu\text{-OPr}^i)]_2$

Up to now we considered aluminium bisphenoxides with aluminium-carbon or aluminium-chlorine reactive bonds. The formation of the actual active catalytic species, an aluminium-alkoxide ($\text{Al-O}_{\text{epoxide-T}}$, where T stands for chlorine or ethyl) resulting from the first insertion of an epoxide molecule into the Al-Cl or Al-C bond implies a latency time before a copolymerisation reaction actually starts. It is a logical outcome to synthesise and test pure alkoxo-aluminium bisphenoxides. Alkoxo-bisphenoxides we synthesised displayed also a dimeric structure in the solid state differing from the dimeric chloro- and alkyl-bisphenoxides because that the bisphenoxides ligands do not act as bridging ones any more. The bridging element in this class of aluminium bisphenoxides is the ancillary alkoxide R_3 (in the considered case an isopropoxide) which is basically part of the catalytic active site (see Scheme 10).



Scheme 10 *Schema of dimeric compounds: a.) non-bridged and b.) bridged structure*

As reported earlier the synthesis of this bisphenoxide class is easy and was performed from the commercially available aluminium tri-isopropoxide and the relevant substituted bisphenoxides. The copolymerisation's results obtained with these bridged alkoxo-aluminium bisphenoxides are summarised in Table 33. As anticipated, the catalytic activity of most of these compounds is higher than the alkyl- and chloro-aluminium bisphenoxides.

Interestingly the positive reactivity's trend found earlier for the three bisphenols with bulky substituent in ortho position, namely 2,2'-methylenebis(4-methyl-6-*tert*butylphenol), ligand **2**, 2,2'-methylenebis (4,6-di-*tert*-butylphenol), ligand **1**, and 2,2'-methylenebis(4-methyl-2-(1-methylcyclohexyl)phenol), ligand **3**, was also found for the related dimeric isopropoxo-bridged bisphenoxides. The highest catalytic activity was noted for **2g** which afforded copolymers in good yield, with 23.81 % carbonate linkages in long-chained copolymer (M_n : 9980). A very promising feature of **2g** is the relatively narrow molecular weight distribution measured for the obtained copolymers (**2g** – yield 56 %, $-\text{CO}_3^-$: 23.81 %; M_n : 9980; PDI: 1.37). This suggests that, under the conditions used, either the catalyst acts as a pure single

site catalyst (one active site: one growing polymer chain) or that the transfers of the growing polymers chains between metallic centres is so quick that the averaged polymers isolated at the end of the reaction have comparable length.¹⁴⁵

Bisphenoxide **3g** and **1g** were close second (yield: 35 %, -CO₃⁻: 20.4 %; M_n: 7474) and third (yield: 42 %, -CO₃⁻: 18.8 %; M_n: 8605) in this catalyst ranking. The copolymerisation results obtained with these three catalysts were in the same range if no better than those obtained with the related dimeric ethyl aluminium bisphenoxides **2e** (yield: 54 %, -CO₃⁻: 24.7 %; M_n: 8592), **3e** (yield: 42 %, -CO₃⁻: 19.2 %; M_n: 8261) and **1e** (yield: 42 %, -CO₃⁻: 16.9 %; M_n: 5650). Incidentally, it could be observed, taking bisphenoxide **1g** as an example, that the reaching of an optimal P/T region as well as the homogeneity of the reaction mixture logically play an important role in the success of the CO₂-insertion. Running the test at ca. 90 bar and 80 °C, no reactivity of **1g** was observed. Increasing the pressure up to about 120 bar and performing the test at 80 °C yield an amorphous solid containing up to 18.75 % of carbonate linkages (yield: 42 %, -CO₃⁻: 18.75 %; M_n: 8605).

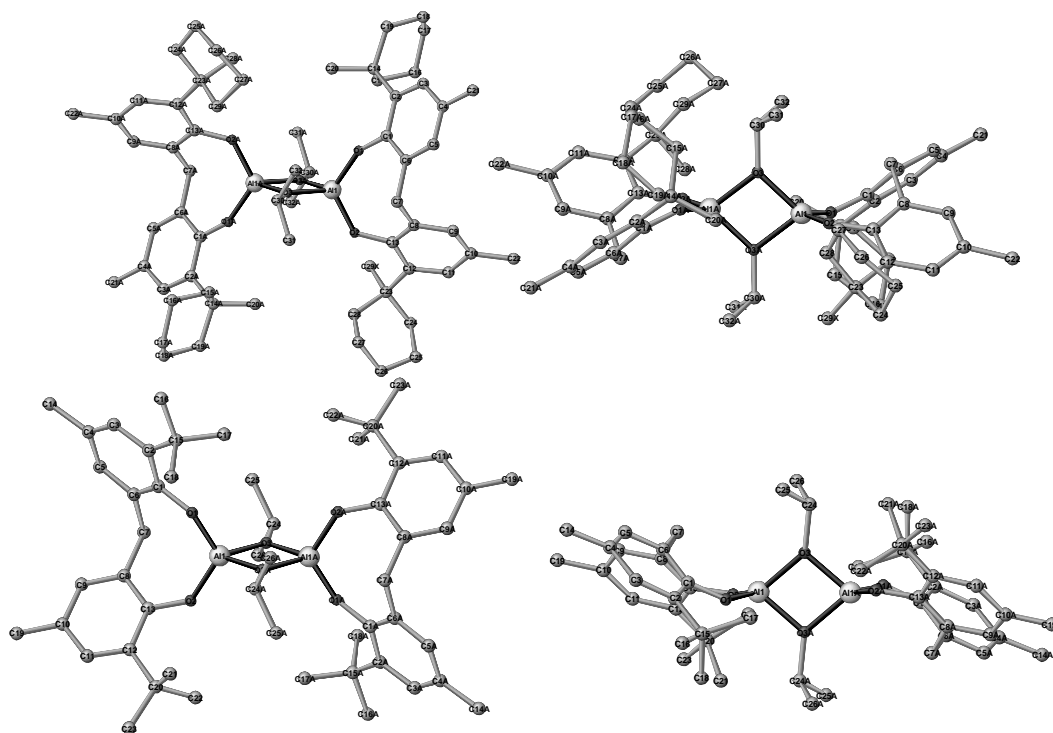


Figure 31 The X-ray structures of bridged: *bis[isopropoxy-{2,2'-methylenebis(4-methyl-2-(1-methylcyclohexyl)phenato)} aluminium (III)], 3g, and bis[isopropoxy-{2,2'-methylenebis(4,6-di-tert-butylphenato)} aluminium (III)], 1g*

As already noticed earlier in the case of the monomeric **5a** and **5b**, the substitution of the bulky substituent in ortho position by a smaller one like a methyl group (ligand **5**, bisphenoxide **5g**) leads to a significantly lower carbon dioxide incorporation (yield: 58 %, -CO₃⁻: 5.87 %; M_n: 13816). It seems also in the case of the isopropoxo bridged bisphenoxides

that the presence of a sterically demanding alkyl group at carbon 6 also promote the CO₂-incorporation into the copolymer as already suggested by catalyst bearing ligand **3** (1-MeCy *ortho*-substituent), ligand **2** and **1** (*tert*-butyl *ortho*-substituent). The presence of such bulky *ortho*-substituent seems to block one side of the aluminium bisphenoxide, weather the bisphenoxide is in a monomeric or dimeric form, and actually shield one side of the catalyst to provide a rather narrow coordination site for the co-monomers: epoxide and carbon dioxide (see Figure 31).

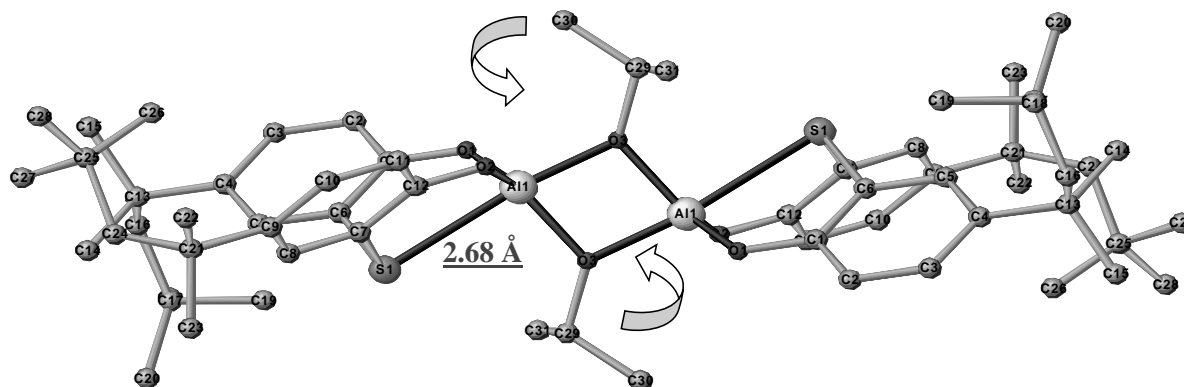


Figure 32 X-ray structures of bridged bis[isopropoxy-2,2'-methylenebis(4-methyl-2-(1-methylcyclohexyl)phenato)] aluminium (III), **7g**

This assumption seems on the other hand to be contradicted by catalyst **7g** which bears no *ortho* substituent at carbon 6 of the phenyl at all. Only considering the CO₂ incorporation into the copolymer, **7g** containing a sulphide bridge was anew one of the most efficient catalyst of our bisphenoxide “library” (yield: 37 %, -CO₃-: 24.21 %; M_n: 4542) although delivering rather short-chained copolymers. One has to remember that the presence of a sulphur atom serving as a bridging in the bisphenol instead of a methylene group involves significant changes of the coordination sphere around the aluminium atom and in the Lewis acidity of the aluminium centre, what has a significant impact on the obtained results. Most of the complexes relying on a 2,2'-methylene-bisphenol display a tetrahedral geometry around aluminium atom (**1-6 g**), whereas in the case of the sulphide bridged bisphenol (**7g**) a trigonal bipyramidal geometry is observed. It can be seen in Figure 32 that the obstruction usually brought about by the bulky substituent in *ortho* position might be in some extent assumed by the coordinating sulphide bridge (Al-S distance: 2.68 Å). The presence of such a narrow contact seems to also shield one side of the catalyst and offer on the other site a rather narrow coordination site for epoxide and carbon dioxide.

To draw an other parallel between the dimeric isopropoxy-bridged bisphenoxides at hand and the aluminium bisphenoxides studied in the previous parts, it can be noticed that the isopropoxy-bridged bisphenoxides based on chlorinated bisphenol, 2,2'-methylenebis(3-

methyl-4-chloro-6-isopropylphenol), ligand **4**, and 2,2'-methylenebis(4-chlorophenol), ligand **6**, delivered also rather unspectacular catalytic results. Compound **4g** with its three-fold substitution at the aromatic ring (3-Me, 4-Cl, 6-Pr^{iso}) delivered, similarly as e.g. in the case of the related monomeric THF-substituted derivatives, rather long copolymers with a fair CO₂-insertion (**4g**, -CO₃-: 15.6 %; M_n: 11290). Moreover **4g** seems to be more able to efficiently catalyse a ring opening polymerisation as it was already found for its related dimeric ethyl- and chlorinated analogues **4f** and **4e** (**4e**, -CO₃-: 12.82 %; M_n: 9004, **4f**, -CO₃-: 13.97 %; M_n: 12159) and monomeric bisphenoxides with Lewis bases in the coordination sphere like **4 a-b** and **4 c-d**. The last bisphenoxide of this class, compound **6g** based on the 2,2'-methylenebis(4-chlorophenol) gave better catalytic results than its oligomeric ethyl counterparts **6a** and **6c**, what should be directly ascribed to the presence of a reactive Al-OiPr bond within the catalyst (**6g**: -CO₃-: 11.5 %; M_n: 6058 ; **6a**: no reaction; **6c**: -CO₃-: 1.98 %; M_n: 19663). However due to its moderate catalytic activity, bisphenoxide **6g** cannot compete with the other isopropoxy-bridged bisphenoxides.

Cat.	Yield [%]	-CO ₃ - [%]	M _n	PDI	TON	TOF
1g^a	42	18.76	8605	1.94	289	16
2g^b	56	23.81	9980	1.37	432	24
3g^b	35	20.41	7474	2.04	205	11
4g^b	41	15.58	11289	1.91	271	15
5g^b	58	5.87	13816	2.10	405	22
6g^b	38	11.51	6058	2.95	390	22
7g^b	37	24.21	4542	1.46	251	14

Table 33 Copolymerisation results for [(bisphenol-2H)Al(μ-OPr^{iso})]₂ catalysts. (η_{CHO} = 0.2-0.3, a: P=120 bar, T = 80 °C; b: P = 80 – 100 bar, T = 80 - 95 °C)

5.3.3 Generalities on aluminium bisphenoxides presenting dimeric structures

As it was said in the Chapter 5.3.2.5, the results of copolymerisation tests performed with dimeric catalysts suggest that binuclear aluminium bisphenoxides remain binuclear also in presence of a O-donor like an epoxide. This seems in contradiction with the results reported by Lin⁹⁷ for the case of aluminium bisphenoxides as well as with the reports of D. Darensbourg's group dealing with bulky cadmium and zinc phenoxides^{30,32,133}. These studies state that dimeric alkyl aluminium bisphenoxides undergo in the presence of Lewis base like THF, Et₂O or O=PPh₃ a rearrangement to form monomeric species with the Lewis base logically coordinated to the aluminium centre like, e.g. [R-Al(bisphenoxide)(THF)]. Likewise dimeric cadmium 2,6-disubstituted phenoxides, like e.g. [Cd(2,6-di-*tert*-Bu-phenoxide)₂]₂, react with cyclic ethers to form stable monomeric species with two coordinated THF or, far more unusually, with two coordinated epoxides like [Cd(2,6-di-*tert*-Bu-phenoxide)₂(CHO)₂]. The corresponding zinc phenoxides have a much higher catalytic activity in copolymerisation reaction than the cadmium-based ones and produce polycarbonates in higher yields with low amounts of ether linkages. Darensbourg proposed that

the lack of alternating epoxide ring-opening/CO₂-insertion steps observed in some cases and responsible for the presence of polyether regions is the result of the catalyst's possessing two THF coordinated, i.e. two epoxide binding sites, and the ensuing deficient control of the stereochemistry of the coupling reaction.

However one counter example, also reported by Darensbourg³⁰, seems to support our conjecture and involves a dimeric zinc phenoxide which remains a dimer in solution and catalyses the copolymerisation of CO₂ with CHO with a high efficiency. The dimeric 2,6-di-fluorophenoxide **1-8**, [Zn(2,6-OF₂C₆H₃)₂(THF)]₂, was synthesised from the reaction of the zinc bistrimethylsilylamide with two equivalents of 2,6-difluorophenol in tetrahydrofuran to form a stable dimer with one coordinated THF per metallic centre. The copolymers obtained with this catalyst contained almost no polyether linkages. This absence of ether linkages in the copolymers together with the fact that related monomeric zinc phenoxides very often afford polyether regions in the final copolymer strongly supports the fact that its dimeric structure with one epoxide binding site per metallic centre remains inert during the catalysis.

Cat.	Yield [%]	-CO ₃ - [%]	M _n	PDI	TON	TOF
1e	52	16.95	5650	2.43	352	20
2e	44	21.74	8592	2.01	278	16
3e	80	19.19	8261	1.79	543	30
4e	27	12.82	9004	2.43	187	10
6a	The reaction did not take place.					
7c	56	22.88	5894	1.55	781	43

Table 34 Copolymerisation results for dimeric alkyl-aluminium bisphenoxides.

Getting back to “our” aluminium bisphenoxides, we succeeded in isolating a dimeric aluminium 2,2'-methylenebis(4-chlorophenoxide) [(MMCyP)(THF)Al(C₂H₅)₂]₂, **6a**, structurally comparable to the successful Darensbourg's zinc fluorophenoxides, what in consequence showed that aluminium bisphenoxides can remain dimeric with a coordinated Lewis base using, of course, the appropriate chelating ligand. However the structure found in the solid state differs markedly from other dimeric bisphenoxide in displaying the THF molecules in *cis*- instead of in *trans* position (relative to the plane formed by the two aluminium atoms and the two bridging phenoxy oxygen atoms) (see (see Figure 20 and Table 34). This might explained why the catalytic performances of compound **6a** and its “Lewis-base-free” counterpart **6c** were so drastically low or even not possible (**6a** – no reaction; **6c** – -CO₃-: 1.98 %; M_n: 19663) and, clearly, could not match with our best aluminium bisphenoxide systems.

The dimeric feature of the aluminium bisphenoxides in solution as well as the nature of the substituents at position 6 of the bisphenol ligands seem to have a direct influence on the way

the monomers, CHO and carbon dioxide, coordinating to the aluminium centres and then undergoing a partly alternating connection to yield the isolated poly(ether-carbonate)s.

This might explain the discrepancy between the efficient CO₂-insertion noticed with catalyst **7c** and the high reactivity of mononuclear **7a** in ring opening polymerisation (**7c**: -CO₃-: 22.88 %; M_n: 5894 vs. **7a**: -CO₃-: 4.57 %; M_n: 14937). Same similarities were found in the case of **1e** and **1a** (**1e**: -CO₃-: 16.95 %; M_n: 5649 vs. **1a**: -CO₃-: 6.81 %; M_n: 16156) as well as in the case of **2e** and **2a** (**2e**, -CO₃-: 21.74 %; M_n: 8592 vs. **2a**, -CO₃-: 11.36 %; M_n: 5526). Once again the bisphenoxide bearing a 1-methyl-cyclohexyl group in ortho position of the phenyl seems to hold a special place in our study as noticed in the copolymerisation tests which delivered comparable results for the dimeric **3e** and for the monomeric **3a** (**3e**, -CO₃-: 19.19 %; M_n: 8261 vs. **3a**, -CO₃-: 20.49 %; M_n: 7069). The same trend was observed in the case of the three-fold aromatic-substituted (3-Me, 4-Cl, 6-Pr^{iso}) bisphenoxides **4e** and **4a** which conveyed similar results (**4e**, -CO₃-: 12.88 %; M_n: 9004 vs. **4a**, -CO₃-: 12.03 %; M_n: 10255).

5.3.4 Deactivation of catalyst upon addition of cocatalyst – unexpected results

Considering the numerous studies on different catalytic systems involving the use of electron-donating Lewis bases as co-catalysts to improve the CO₂-incorporation into the copolymer^{54,139}, it was interesting to assess the influence of some co-catalysts together with one representative aluminium bisphenoxide on the course of the copolymerisation. As representing compounds monomeric **1b** and dimeric isopropoxy-bridged **2g** were chosen. These co-catalysts were neutral Lewis bases like 1-methylimidazole 1-MeIm, triphenyl phosphine PPh₃ and 4-(N,N-dimethylamino)pyridine DMAP as well, or ionic derivatives like tetraethylammonium p-toluenesulphonate, [Et₄N][MeC₆H₄SO₃], TEAPTS; tetrabutylammonium bromide [(n-C₄H₉)₄N]Br and bis(triphenyl phosphoranylidene) ammonium chloride [PPN]Cl. According to the literature, using a Lewis base should facilitate the formation of the first active alkoxo-species by coordination and subsequent labilizing of the aluminium-nucleophile bond in the catalyst (Al-C, Al-Cl or Al-O-Prⁱ). Another activation path proposed in different contributions relies on the activation of the epoxide by the co-catalyst (Lewis base or halide anion of the ionic salts). This activation of the aluminium-nucleophile bond as well as the promoting of the prolongation of the copolymer chain via an insertion of a monomer into the active aluminium-O_{Polymer} bond.

Entry	CHO/cat/ cocat	Co-catalyst	% of carbonate	M _n	PDI	TON		
1	1b	1000	none	17.45	10472	1.77	705.5	
2	1b	300	N-MeIm		CHC tr. ^a			
3	1b	1000	PPh ₃		CHO			
4	1b	1000	TEAPTS		CHO			
5	1b	1000	[(C ₄ H ₉) ₄ N] ⁺ Br ⁻		CHC tr. ^a			
6	1b	1000	[PPN]Cl		CHC			
7	2g	1000/1/0	none	23.81	9980	1.37	432	1 cm ³ toluene
8	2g	300/1/0	none	26.53	6258	1.77	131	10 cm ³ CH ₂ Cl ₂
9	2g	1000/1/0	none	16.39	7274	2.52	329	no solvent
10	2g	1000/1/0	none	20.16	8047	2.28	359	3 cm ³ CH ₂ Cl ₂
11	2g	1000/1/0	none		CHO			10 cm ³ CH ₂ Cl ₂
12	2g	300/1/1	TEAPTS	25.64	4548	1.42	194	
13	2g	1000/1/1	[PPN]Cl		CHO			
14	2g	300/1/1	[PPN]Cl	Polyether	8502	1.18	-	
15	2g	300/1/1	[PPN]Cl		CHO			1 cm ³ toluene
16	2g	300/3/3	[PPN]Cl		cyclic carbonate only			1 cm ³ toluene
17	2g	1000/1/1	N-MeIm		CHO			
18	2g	300/1/1	N-MeIm	23.31	2083	1.48	64.36	
19	2g	300/1/1	N-MeIm		CHO			1 cm ³ toluene
20	2g	1000/1/1	[(C ₄ H ₉) ₄ N] ⁺ Br ⁻		CHC tr. ^a			
21	2g	300/1/1	[(C ₄ H ₉) ₄ N] ⁺ Br ⁻		CHO			
22	2g	1000/1/1	DMAP		CHO			
23	2g	300/1/1	DMAP	25.38	3776	1.46	214	
24	2g	300/3/3	DMAP		CHO			1 cm ³ toluene

Table 35 Copolymerisation of cyclohexene oxide and carbon dioxide using **2g** with with / without cocatalysts;
^a CHC tr.– traces of cyclic carbonate.

Considering the copolymerisation run with bisphenoxide **1b** as catalyst, the experiments involving phosphine or amine as co-catalysts proved to be unsuccessful, producing no polycarbonates and only traces of cyclic carbonate. The ammonium salts delivered only small amounts of cyclic carbonate (entries 4,5, Table 35). Interestingly the reaction carried out with bis(triphenyl phosphoranylidene) ammonium chloride as a co-catalyst produced significantly more cyclic carbonate than the ammonium salts and no copolymers (up to 50% yield, via ^1H NMR) (entry 6). Altogether the reactivity of the ammonium salts follows the trend $\text{TEAPTS} < [\text{n-Bu}_4\text{N}][\text{Br}] \ll [\text{PPNCl}]$.

In catalytic tests run with bisphenoxide **2g** (catalyst/substrate: 1/1000 molar ratio) no formation of polymer was observed if the reaction mixture was too diluted (entry 11), in other cases polymer with a significant amount of carbonate linkages was isolated (entries 7 – 10). Performing the same test with catalyst/co-catalyst/substrate: 1/1/1000 molar ratio, with an ionic ammonium co-catalyst yield traces of cyclic carbonate only in the case of $[(\text{C}_4\text{H}_9)_4\text{N}]^+\text{Br}^-$ (entry 20). The increase of the catalyst/substrate ratio to 1/300 and the simultaneous use of co-catalyst afforded polymers with slightly lower amounts of carbonate linkages (23.31 % for N-MeIm and 25.38 % for DMAP, entries 18 and 23 respectively), comparing to the blank reaction without co-catalyst (26.53 %, entry 8), but with significantly decreased the number average molecular weights (even to 2083.3). Considering the strong Lewis base DMAP, a further increase of the co-catalyst (up to 3 eq.) does not yield formation of polymer, although depending on the catalyst/co-catalyst ratio of the used ionic $[\text{PPN}]\text{Cl}$ either the significant amount of cyclic carbonate CHC (entry 16) or only polyether (entry 14) were isolated. Altogether the reactivity of the ammonium salts follows the trend $[\text{Bu}_4\text{N}][\text{Br}] \sim < \text{DMAP} < [\text{PPN}]\text{Cl} \ll [\text{TEAPTS}]$.

Such a low co-operation between catalyst and co-catalyst is most probably due to the tetrahedral coordination geometries around the aluminium atom. Considering the aluminium salen derivatives newly reported by Darenbourg¹³¹, which display a good catalytic activity and allow a further fine tuning by using a co-catalyst, it can be seen that the typical square pyramidal geometry found in these salen complexes plays a predominant role. This constrained geometry allows a co-catalyst to coordinate in trans position of either the starting nucleophile (Cl, Et or -O-Prⁱ) or the growing polymer chain and thus to efficiently activate the Al-nucleophile bond. Such a favourable interaction cannot be found in the tetrahedral coordination geometry of the aluminium bisphenoxides.

5.4 Comparison of the best results for self-synthesised and literature-known compounds

Considering the ever increasing interest in catalytic systems able to promote the formation of aliphatic carbonates and the resulting increasing number of contributions dealing with this topic, it was relevant to weigh “our” catalytic system against the other systems. Surprisingly, maybe owing to the common high Lewis acidity of aluminium alkoxide, comprehensive studies dealing with an aluminium-catalysed copolymerization of epoxides and carbon dioxide are relatively scarce. Beckman described some copolymerisations catalysed by monodentate aluminium tri-alkoxides, but the properties of the isolated copolymers have been not in detail investigated, as e.g. in case of **I-12** and **I-13** (Table 1). In case of **I-14** and **I-15** (see Table 1) these data were provided, so these copolymers can be compared with our results.⁶³

	[%] pol. y.	% of -CO ₃ -	M _n	PDI	TON	Ref.
2g^b	14	26.53	6258	1.77	131	A
7c	42	24.39	6243	1.50	287	A
7g	37	24.21	4542	1.46	251	A
2g	56	23.81	9980	1.37	432	A
7f	54	22.42	6377	1.51	366	A
2e	44	21.74	8592	2.01	278	A
3b	64	21.37	8332	2.30	834	A
2f	49	20.92	12522	1.55	330	A
5f	31	20.75	6216	1.84	210	A
3a	55	20.49	7069	1.84	673	A
3g	35	20.41	7474	2.04	205	A
3e	80	19.19	8261	1.79	542	A
I-14, Table 1^c		7.69	4531	4.15	288	128
I-15, Table 1^c		21.74	4985	2.89	493	128
I-28, Table 3		75.0	25000		196	131

Table 36 Comparison of our best results with literature known data, a – this work, b – [CHO/cat.] = 300 : 1, c – [CHO/cat.] = 100 : 1, all other 1000: 1

Almost all the catalysts (with the exception of **2c**, **2d**, **2h**, **5b** and **6a**) were able to initialise copolymerisations already with a tenfold smaller epoxide / aluminium molar ratio (1000 to 1 vs. Beckman’s 100 to 1). Also, with the exception of **7g**, all catalysts delivering copolymers with more than 19 % of carbonate linkages afforded these polymers with significantly lower polydispersity indexes and higher molecular weights than those noted for **I-14** and **I-15**. However the molecular weight distribution remain generally quite broad, ranging from 1.37 to 2.30, suggesting that the “single-site character” of the catalysis involving the aluminum bisphenoxides is not as high as anticipated. Interestingly, with exception of **3b**, the catalysts displaying the highest activity in the copolymerisation of cyclohexene oxide with CO₂ have a dimeric form (bridging and non-bridging bisphenol ligand as well). Diminishing the epoxide / catalyst molar ratio does not lead to a significant enhancement of the reactivity and to an increase of the carbon dioxide insertion (compare value for **2g** and **2g^b**). Also with exception

of 7-based compounds, for which the trigonal bipyramidal geometry was noted, all isolated compounds display a tetrahedral coordination environment around the aluminium atom.

In comparison, the literature known bulky tetradentate *salen* derivatives of group 13¹³¹ display a distorted square pyramidal geometries⁵⁴, with a significantly narrower docking site for the epoxide or CO₂ molecule. The presence of sterically demanding groups in these compound, without the help of a supplementary co-catalyst, hinders a potential binuclear side-reaction.

5.5 Spectroscopic characterisation of isolated polymers

5.5.1 IR spectroscopy investigations

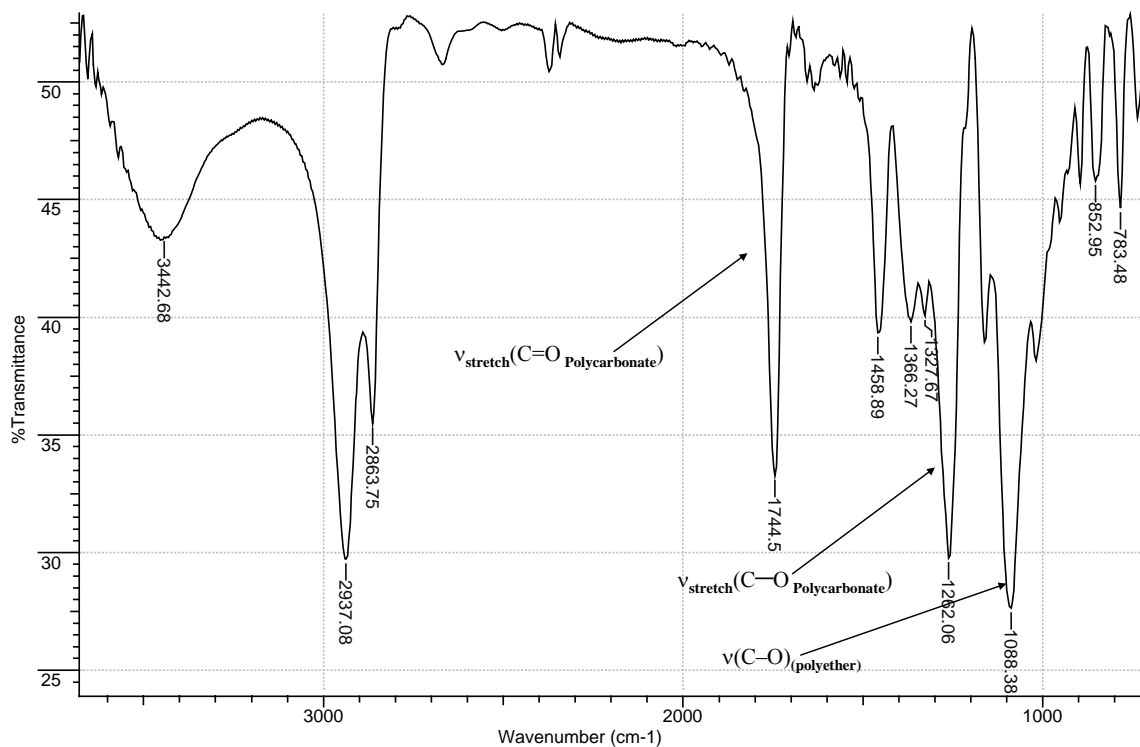


Figure 33 IR Spectrum of P-3e.

The activation and insertion of carbon dioxide into an epoxidic C-O bond with formation of a carbonate can be easily assessed via IR spectroscopy which also allows to distinguish between polycarbonate ($\nu_3(\text{C}=\text{O})$ at 1740 cm^{-1} ($\nu(\text{C}-\text{O})$ at 1280 cm^{-1})⁴⁶ as well as *trans*-cyclohexyl carbonate at 1823 cm^{-1} or *cis*-cyclohexyl carbonate at 1806 cm^{-1} (Figure 33).¹³⁸

5.5.2 NMR spectroscopy investigations

Using ¹H- and ¹³C-NMR spectroscopy we can identify the stereochemistry of the polymer and estimate the amount of CO₂ bound into the copolymer as carbonate linkages. The "carbonate signal" – signal of methine hydrogen atoms located in *alpha*-location of the carbonate fragment, (-CR(H)-CR(H)-O-CO₂-), appears at 4.70 – 5.15 ppm, the "ether's signal" – signal of the methine hydrogen atoms in *alpha*-location of the ether linkages, (-CR(H)-CR(H)-O), is located at 3.2 – 4.0 ppm. The signals of the methylene fragment of the cyclohexene ring appear between 0.9 and 2.1 ppm (see Figure 34). Generally, the signals of the methine protons appear in the form of two or three overlapping signals (3.2 – 4.0 ppm) which can be attributed according to the literature dealing with poly(cyclohexene oxide)¹⁴⁶ to syndiotactic (RR), heterotactic (MR and RM), and isotactic (MM) triads. Comparably to ¹H spectra, three main peaks were found for the methine carbons at 78.6, 78.0 and 76.6 ppm confirming the presence

of several regions of different tacticity in the polymers. In addition, the remaining methylene groups of the cyclohexane moieties were found in two main groups ranging from 29.0 to 30.1 ppm and 23.4 and 22.2 ppm (see Figure 35). The ^{13}C NMR spectroscopy of the final products confirmed the CO_2 incorporation into the polymer: the isolated poly(ether-carbonate)s display one broad signal at ca. 154–155 ppm (benzene D_6) in the carbonate region of the spectrum. This broad signal results most likely from the superposition of different discrete carbonate signals coming from different carbonate fragments separated by pure polyether regions as it can be expected for a statistical copolymer.

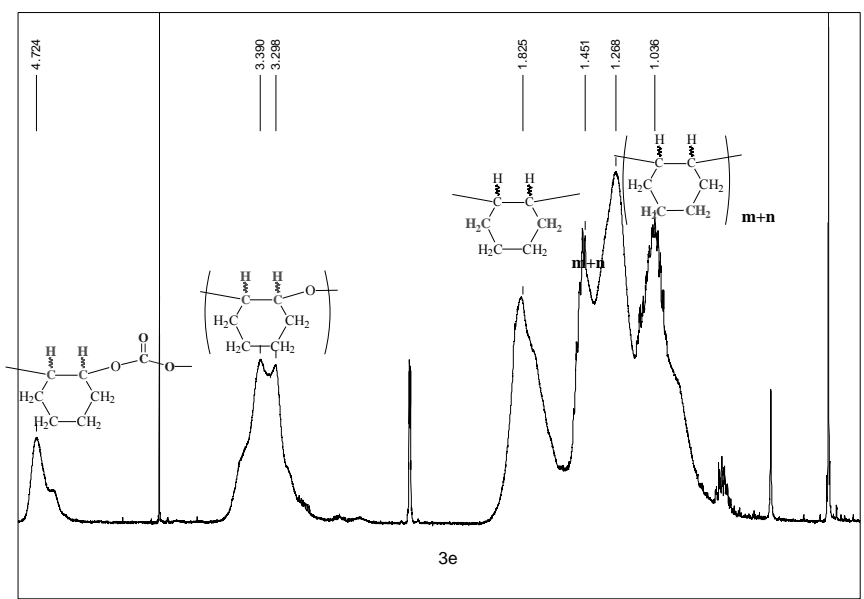


Figure 34 ^1H NMR spectrum of isolated polymer.

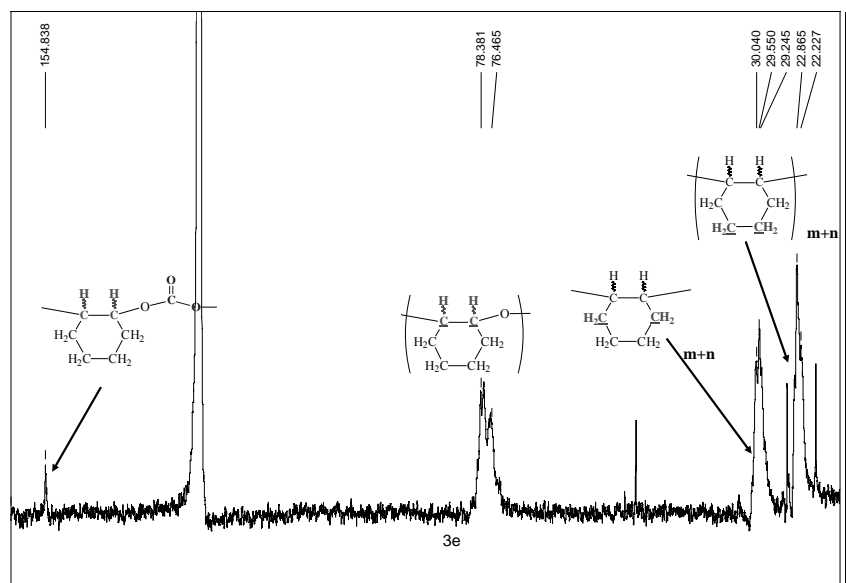


Figure 35 ^{13}C NMR spectrum of isolated polymer.

Using a High Pressure NMR-tube (sapphire tube / titanium upper body with titanium valve), we wanted to gain some information on the reaction mechanism and run different NMR-experiments under CO₂-atmosphere. We took one of our most promising candidates, the dimeric bis[isopropoxy- $\{2,2'$ -methylenebis(4-methyl-6-*tert*-butylphenato)} aluminium (III)], **2g**, and recorded 1D- and 2D-¹H spectra under high pressure condition (up to 60 bar). Firstly, it was interesting to identify the alkylcarbonate formed from the reaction of the isopropoxo-alumino-bisphenoxide with carbon dioxide alone. **2g** was pressurised with pure carbon dioxide to about 25 bar and yielded reversible formation of aluminium isopropylcarbonate. Compared to the ¹³C-spectrum of the copolymer, the signal of the formed isopropyl-carbonate is shifted downfield and appeared to be sharper than the carbonate signal of the copolymer. and appears at about 159 ppm (see Figure 36).

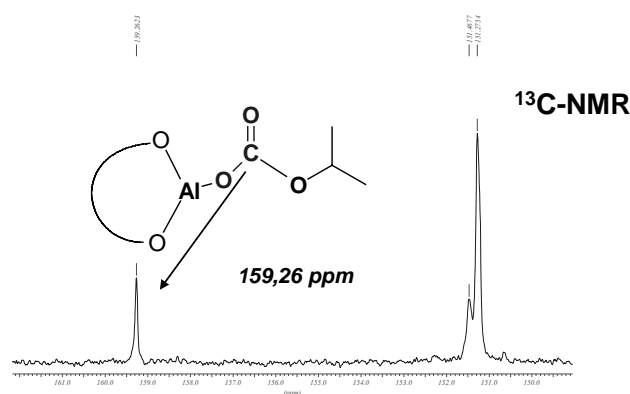


Figure 36 ¹³C NMR study of reactivity of **2g** with CO₂.

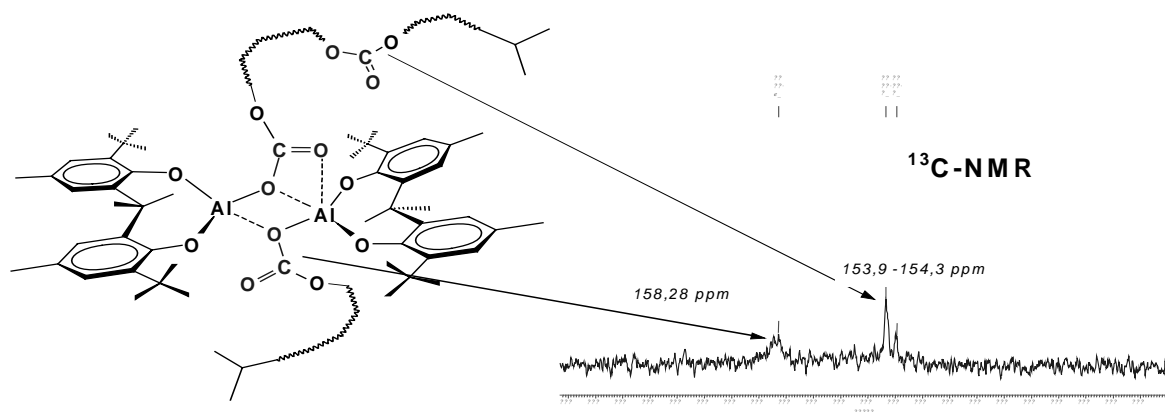


Figure 37 Proposed structure of the active site of the catalyst in the copolymerization of CO₂ with CHO

Recording a ¹³C-spectrum, under experimental conditions (ca. 80°C and under 30–40 bar CO₂), of a mixture CHO/CO₂ with **2g** as catalyst, revealed two sets of carbonate's signals a broad signal at ca. 160 ppm attributed to the carbonate directly bound to the aluminium-site (attribution made after comparison with the spectrum of the lone catalyst under CO₂-atmosphere) and several signals attributed to the carbonate groups included in the the growing

copolymer chain (see Figure 37). The ^{27}Al NMR spectra of the reaction mixture delivered low information and showed the presence of two different co-ordination geometries for the aluminium centres: a tetrahedral and an octahedral one (see Figure 38).

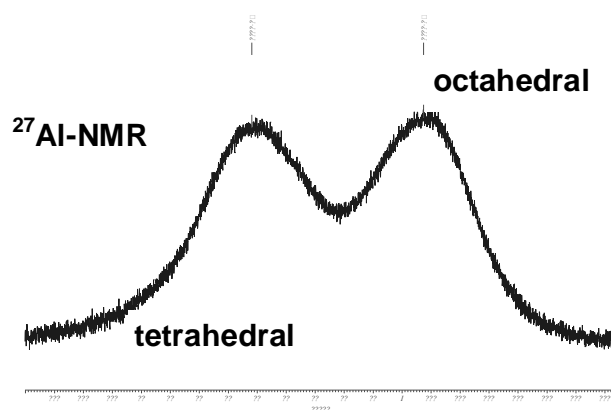


Figure 38 The H-P ^{27}Al NMR study of reactivity of CO_2 with CHO.

5.5.3 Stereochemistry of formed carbonate linkages

Generally speaking, controlling the absolute stereochemistry of a given polymerisation process is of paramount importance to control the qualities of the final material. It is commonly known, that microstructure directly affects the polymer properties. On the other hand, the kinetic resolution of racemic epoxides or desymmetrization of *meso*-epoxides by copolymerisation is a potential route to valuable chiral building blocks and is the scope of an ever increasing interest. Using the ^{13}C NMR spectroscopy and thanks to the pioneering works of Nozaki^{69,126}, Coates⁷¹ and Chisholm^{73,75,76} we are able to assess in some extent the absolute stereochemistry of copolymers based on epoxides and CO_2 and find the way the different monomers were linked together. Concerning more precisely poly(cyclohexene carbonate), Kuran firstly attributed the carbonate signal found at 153.7 ppm to syndiotactic diad (-S-RR-, [r]) and the one found at 153.1 ppm to isotactic diad (-SS-SS- or -RR-RR-, [m]),¹²⁵ drawing a parallel to 2,2'-oxydicyclohexanol. This molecule can be practically seen as a model having an ethereal linkage instead of a carbonate moiety. Only a few years ago, the research groups of Nozaki^{69,126} and Coates⁷¹ proposed a new interpretation of the ^{13}C NMR spectra of poly(cyclohexene carbonates) and could precisely attribute the different ^{13}C signals to different carbonate fragments' geometries. The ^{13}C NMR signal for the sp^2 carbons of the isotactic carbonate fragments is observed at 153.7 ppm whereas the signals for the syndiotactic carbonate fragments are observed at higher field between 153.3 and 153.1 ppm. In our case, the ^{13}C NMR analysis of the purified copolymers (see Figure 34) showed a broad signals ranging from 154.8 to 155.1 ppm in the carbonate region of the spectrum (with

exceptions of **P-2e**, **P-2f**, **P-3d** affording signals between 153.5 and 153.9 ppm) (see Table 38). Unfortunately it is not easy to ascertain the stereochemistry of the reaction as easily as in the case of a complete CO₂ insertion yielding pure poly(cyclohexene carbonate). To the best of our knowledge, no comprehensive study dealing with (cyclohexene ether-carbonate) were reported. Only a few reports addressed this topic incidentally, Chisholm for instance newly reported the chemical shifts of carbonate region for poly(propylene carbonate)¹²⁷ (depending on the catalyst used the signals appeared between 154.10 and 154.80.ppm) and oligoether carbonates (154.10 – 154.20.ppm).⁷⁶

We proposed that the broad signals we observed result most likely from the superposition of different discrete carbonate signals. These carbonate signals are the sum of several carbonate signals belonging to different polycarbonate regions of different lengths (diad, triad or tetrad), these polycarbonate regions being separated by pure polyether regions. This way of polymerising tends to show that the final co-polymer is in fact a statistical copolymer. However, comparing the NMR spectra of purified poly(ether-carbonate)s like e.g. **P-2e**, **P-2f** or **P-3d** to the models reported by Nozaki¹²⁶, it seems, solely considering the chemical shift found for the carbonates, that the polycarbonate regions of the copolymer display an isotactic structure.

Cat.	¹ H NMR of polymer	¹³ C NMR of polymer	Cat.	¹ H NMR of polymer	¹³ C NMR of polymer
P-1a	5.10	Peak is invisible	P-3f	5.07	154.6 – 155.0
P-1b	5.10	154.6 – 154.9	P-3g	5.14	154.9 – 155.3
P-1c	4.93	154.6 – 154.9	P-4a	4.93	154.9 – 155.3
P-1d	5.13	154.7 – 155.1	P-4b	5.14	154.9
P-1e	5.13	154.6 – 155.0	P-4c	5.06	peak is invisible
P-1f	5.13	154.8 – 155.1	P-4d	5.15	peak is invisible
P-1g	5.09	154.8 – 155.1	P-4e	5.08	155.1 – 155.5
P-2a	4.95	peak is invisible	P-4f	5.13	154.8 – 155.1
P-2b	5.12	peak is invisible	P-4g	5.13	154.9 – 155.2
P-2c	The reaction did not take place.		P-5a	4.99	peak is invisible
P-2d	The reaction did not take place.		P-5b	The reaction did not take place.	
P-2e	5.09	153.5 – 153.9	P-5f	4.71	154.8 – 155.1
P-2f	4.72	153.3 – 153.8	P-5g		155.0 – 155.4
P-2g	5.07	154.6 – 155.0	P-6a	5.11	peak is invisible
P-2h	The reaction did not take place.		P-6c	5.05	peak is invisible
P-3a	4.72	154.6 – 155.0	P-6g	4.71	154.9 – 155.2
P-3b		154.6 – 155.0	P-7a	4.72	154.9 – 155.2
P-3c	5.09	154.8 – 155.1	P-7c	4.72	154.9 – 155.2
P-3d	4.72	153.5 – 153.6	P-7f	4.73	154.9 – 155.2
P-3e	4.72	154.6 – 155.0	P-7g	4.74	154.9 – 155.2

Table 37 *The chemical shifts of hydrogen atom located in the closest to carbonate groups (methine hydrogens) and carbon atoms in carbonate groups.*

The general lack of selectivity copolymerisation vs. homopolymerization, already reported for other aluminium alkoxides¹²⁸, is due, on the one hand, to the high Lewis acidity of the aluminium derivatives (compared to the literature known zinc- or cobalt-based catalysts) and

on the other hand to an a complex, hard to control fragmentation of the starting oligomeric aluminium alkoxide which leads to several active species in the solution and consequently to a bad control of the selectivity. As a typical example, aluminium isopropoxide is found as a dimer A_2 in the gas phase, as a symmetric Mitsubishi logo-shaped tetramer in apolar solvents A_4 and as a trimer A_3 in freshly distilled samples. These oligomers are too labile to allow an efficient control of the reaction of CO_2 with epoxides.⁸⁵ Considering the bidentate, chelating 2,2-methylenebisphenols, the flexibility inherent to the backbone of a bisphenol yields aluminium bisphenoxides with an insufficient shielding of the reactive aluminium centre. Additionally, the resulting tetrahedral (resp. trigonal bipyramidal) coordination geometry found around the aluminium atom makes a broad docking site available for the epoxide/ CO_2 monomers. This fact, together with the high Lewis acidity of the aluminium center, means that the coordination of the epoxide would be statistically favoured and, consequently, the formation of polyether regions in the copolymer. A more constrained geometry as found in the case of the salen or porphyrin derivatives cannot be achieved with a 2,2-methylenebisphenol, even though the bisphenol is purposely substituted at carbon 6 and 4.

6 Conclusion and outlook

The goal of this work was to “design” co-polymerization catalysts displaying a “single site” feature in order to have a good control of the reaction and to be able to establish quite easily some structure-reactivity correlations between structures of the catalysts and reactivities observed and thus optimise the overall catalytic system. This target was reached through the use of handy bulky substituted 2,2'-methylenebisphenol as ligands. The ideal catalytic system should have only one definite reaction site at the metal centre (i.e. a narrow docking site) remaining accessible to the two co-monomers: epoxide and carbon dioxide. During the course of this research project, a rich variety of differently coordinated aluminum bisphenoxides with either “bare” bisphenols or different sterically demanding substituents were synthesised. The isolated bisphenoxides were obtained in course of reactions of aluminium precursors (AlEt_3 , AlEt_2Cl , AlEt_2I made *in situ* or $\text{Al}(\text{OPr}^i)_3$) with bisphenols. Reacting alkyl aluminium precursors with bulky *ortho*-substituted bisphenols in coordinating solvents (THF or Et_2O) the products formed were monomers (**1-4 a-d**, **5a-b**), the same reactions performed in non-coordinating hexane yielded dimeric compounds (**1-4 e-f**, **5f**). The geometry around aluminium atoms in the discussed methylene bridged complexes displayed distorted, only tetragonal features and was independent on the solvent used. The presence of an additional Me substituents (**4 a-g**) in the *meta*-position of the phenyl rings does not influence the coordination number of aluminium atom, also decrease of the *ortho*- substituents to methyl groups afforded complexes with fourfold coordinated aluminium atom (**5**-based compounds). For comparison, using methylene bridged ligands without any substituents at the *ortho* positions of the phenyl rings afforded complexes **6a** and **6c** with different coordination numbers of aluminium atoms depending on the ether used. Performing this reaction in THF the binuclear product **6a** with fivefold coordinated aluminium atoms and coordinated solvent molecules was obtained, using another solvent (Et_2O) it afforded a trinuclear compound **6c** with four- and fivefold coordinated metal cores. A significant change in the structures of the obtained aluminium complexes was attained through the replacement of the bridging methylene group by a sulphide moiety. Reacting AlEt_3 in THF with a such potentially tridentate (O,S,O)-ligand carrying no *ortho*-substituents it yielded aluminium alkoxide **7a** displaying the trigonal bipyramidal geometry, a dative bond (Al-S) and coordinated solvent molecule. The same reaction realised in a weak Lewis base such as Et_2O or non-coordinating hexane yielded the dimeric compounds (**7c**, **7f**) having the same coordination as this noted for monomer. In case of aluminium isopropoxide-bisphenoxides (**1-7g**) this mentioned above impact of the bridging agent has also a key importance for the coordination number of the metal core(s) in the isolated products. All products were structurally

characterised via X-ray diffraction on single crystals, and spectroscopically studied via NMR and IR spectroscopy.

Isolated compounds could be successfully employed as catalysts for the copolymerisation of CHO with CO₂, although despite several attempts of optimisation of the reactions parameters to have a possibly the highest amounts of carbonate linkages in the final copolymers, formation of pure poly(cyclohexene carbonate) did not occur. The reactivity of these aluminium 2,2'-methylenebisphenoxide is generally high and clearly more reactive than the pioneering monodentate aluminium alkoxides catalyst of Beckman (**I-14**, **I-15**, CHO / Al = 100 / 1).¹²⁸

Considering our aluminium 2,2'-methylenebisphenoxide-based catalytic system, we found that the use of a supercritical medium was not a prerequisite for an optimal carbon dioxide incorporation into the copolymer, that means working in a so-called "CO₂-expanded" liquid phase is enough to observe an optimum in the formation of poly(ether-carbonate) from CO₂ and cyclohexene oxide. A poor solubility of these aluminum bisphenoxide catalysts in a CO₂-rich phase or in supercritical CO₂ might be the cause for this general low reactivity at higher pressure; improving the solubility of the aluminium 2,2'-methylenebisphenoxide through a specific ligand design according to the works of Beckman and Darenbourg (e.g. grafting of fluorinated chains to the bisphenol backbone) might be the key to a better CO₂-insertion in the final aliphatic polycarbonates and should be assessed more in detail.

The gathered copolymerisation results indicate that the most reactive aluminium complexes relative to a discussed process seem to be the bisphenoxides bearing a sterically demanding groups at location 6 and methyl groups at location 4 of the phenyl rings – **2**- and **3**-based ones. In frames of this research project the latter group seems to be the most versatile, only in case of **3c** a significant decrease of polymer yield was observed.

Considering the catalytic activities of the monomeric compounds, the nature of the coordinated solvent (strong or weak Lewis base) or its absence in the coordination sphere of the catalyst plays a role in the catalysis. Within the same bisphenol ligand class, Et₂O-aluminium alkoxide adducts (weak Lewis base / strong Lewis acid) should not be as stable as a THF-aluminium alkoxide adduct (strong Lewis base/strong Lewis acid), we expected a higher catalytic activity of these bisphenoxides. The tests showed that the compounds with coordinated THF molecule display better selectivities than those having Et₂O molecule in the coordination sphere. However in one case Et₂O-adducts of **1**-based complexes are more selective than their "strong Lewis base / strong Lewis acid" counterparts (**1a** – yield: 39 %, -

CO₃⁻: 6.81 %, M_n: 16156 < **1c** – yield: 46 %, -CO₃⁻: 20.49 %, M_n: 6030; **1b** – yield: 52 %, -CO₃⁻: 11.36 %, M_n: 10472 < **1d** – yield: 50 %, -CO₃⁻: 11.47 %, M_n: 8190).

Surprisingly, in the solid state **4b** displayed an unusual ionic feature and a completely different molecular structure than its Al-Et counterpart, **4a**. This can be tentatively explained by the fact that bisphenoxide **4b**, originally existing as a neutral, monomeric aluminium-THF adduct, slowly rearrange in the solution to give the crystalline, more stable ionic specie. This is confirmed by the similar catalytic activities found for both complexes **4a** and **4b**. Interestingly during the course of our studies with the monomeric compounds, we found the same ligand's trends concerning the reactivities of the Al-Cl and Al-C bonds. Catalysts displaying aluminium-chlorine bond (**1b**, **3b**, **3d** and **4b** and **4d**) generally afford copolymers with a better CO₂ incorporation, than those noted for their Al-C counterparts.

Focusing now on the dimeric bisphenoxides displaying a bridging bisphenol, the analogous dependence can be found for dimeric chloro-aluminium bisphenoxides as for monomeric chloro derivatives, they seem to be generally more active than their ethyl counterparts (**1f** vs. **1e**, **2f** vs. **2e** or **4f** vs. **4e**). Moreover, it can be seen that the insertion of CO₂ in the polymer is generally better for dimeric compounds than in the case of the monomeric aluminium bisphenoxides (**1f** vs. **1b** and **1d**, **2e** vs. **2a** and **2c**, **2f** vs. **2b** and **2d**, **4e** vs. **4a** and **4c**).

The same correlation could be observed for isopropoxy-bridged dimeric bisphenoxides, they seem to be generally more active than their corresponding dimeric ethyl-aluminium counterparts. The reason of such a behaviour might be rather the better solubility of the catalysts in the CO₂-expanded liquid phase than the direct impact of the bulkiness of the substituents.

Dimeric compounds with isopropoxy-bridged structure display generally comparable or even better selectivities than the organometallic bridged bisphenoxides. As anticipated, owing to the presence of a pre-formed aluminium-alkoxide (isopropoxide) ready to react with CO₂ and the first epoxide the catalytic activity of most of these compounds is higher than the dimeric alkyl- and chloro-aluminium bisphenoxides. The most reactive aluminium complexes were anew the bisphenoxide **2g** having sterically demanding groups at location 6 of the phenyl rings and small group at location 4 of ones. **1g** afforded polymer with comparable properties, but the copolymerisation process took place at higher temperature/pressure than usually, suggesting once more for unclear reasons deactivating character of bulky *tert*-Bu groups located in 4 position of phenyl rings. The change of coordination around aluminium atom, involving thiophenol in place of bisphenol afforded catalyst, **7g**, yielding one of the highest CO₂ incorporation (yield: 37 %, -CO₃⁻: 24.21 %; M_n: 4542). Taking this compound as a

model for the future catalyst design, the use of bulky donating substituents would be a natural consequence and moreover would complete our “catalyst library”.

In attempts to modify and optimise the catalytic activity of the synthesized aluminium bisphenoxides, we have investigated these compounds in conjunction with a series of ionic salts and neutral Lewis bases co-catalysts. As model compounds two catalysts – a monomeric and a bridging dimeric one were chosen. Our preliminary studies have shown that the use of co-catalysts, contrary to the literature known system, does not improve the CO₂-incorporation into the polymer, because of the unfavourable, tetrahedral geometry found around aluminium atoms. As a results of the co-catalysts use, a deactivation of the catalytic system, probably via the formation of stable Lewis Acid/base pairs was noted. However, in some cases both catalyst and co-catalyst seem to “co-operate“ to produce “selectively“ the monomeric *cis*-cyclohexene carbonate in significant quantities.

This work shows that the aluminium bisphenoxides are easy to synthesize, giving access quite easily to a broad class of Lewis acid catalyst able to promote the copolymerisation of cyclohexene oxide. This suggest that these aluminium compounds shall have a rich chemistry in different polymerisation and terpolymerisation involving CO₂ and epoxides. The use of ligands with electron-donating bulky substituents at location 6 of the phenyl rings as well as the use of a sulphur atom as bridging agent instead of a methylene group should provide aluminium thio-bisphenoxides with a rather narrow docking site for all the monomers and potentially a better efficiency of the CO₂-insertion.

7 Experimental part

7.1 General remarks

All manipulations were carried out under an atmosphere of argon using standard Schlenk techniques. IR spectra were recorded with a BIORAD FTS 175 C apparatus, measured in the range of 4000 – 400 cm^{-1} either as a thin film between KBr pallets (aluminium complexes) or as mixture of very small amount of polymer with KBr. NMR spectra were recorded on a Bruker Avance 250 spectrometer (^1H 250 MHz, ^{13}C 62.9 MHz) and a Varian Inova 400 spectrometer (^1H 399.81 MHz, ^{13}C 100.54 MHz) at 293 K, respectively. The ^{27}Al NMR (104.207 MHz) spectra of the aluminium catalysts as solutions in different deuterated solvents were recorded at the following operating conditions: sweep width (25 kHz, non-decoupling mode, relaxation delay 0.4 s, pulse width 8.4 μs and number of scans 3000. The FIDs were processed using an exponential multiplication. For all measurements the chemical shifts were reported relative to a saturated solution of $\text{Al}(\text{NO}_3)_3$ in D_2O used as standard. Elemental analyses were performed in a Vario EL III, CHNOS-elemental analyser from Elementar Analysesysteme GmbH, and the results are obtained as average of three measurements. The X-ray structures were obtained by collecting the intensity data for the compounds on a Siemens Smart CCD 1000 diffractometer using graphite-monochromated Mo-K_α radiation. The X-ray analyses were performed with an irradiation time of 10 to 40 s per frame, collecting a full sphere of data using an ω -scan technique with $\Delta\omega$ ranging from 0.3 to 0.45°. Data were corrected for Lorentz and polarisation effects, an experimental absorption correction were performed with SADABS.¹²⁹ Structures' solutions and refinement were performed with SHELX-97.¹³⁰ For searches relating to single-crystal X-ray diffraction data, the Cambridge Structural Database was used. Molecular weights and polydispersities of isolated polymers were measured using a Merck gel permeation chromatograph (Lichograph Gradient pump L-6200 with thermostat, LaChrom RI detector L-7490, equipped with a pre-column and two different columns (PSS SDV 5m 1000 Å and 100 Å. THF was used as eluent, and calibration was performed using polystyrene as internal standard.

All reactions were performed in stoichiometrical ratios: 1.2–1.0 (Et_3Al – bisphenol ligand); 1.3–1.0 (Et_2AlCl – bisphenol ligand) and 1.0–1.0 ($\text{Al}(\text{OPr}^i)_3$ bisphenol ligand).

The following chemicals were used, most of them were obtained commercially: **Aluminium compounds:** Et_2AlCl – Stream Chemical, USA, purity 97 %, used as received; Et_3Al – Aldrich, USA, purity 93 %, used as received; $\text{Al}(\text{OPr}^i)_3$ – Aldrich, Germany, pure, 98+ %, used as received; Et_2AlI – obtained *in situ* in reaction of Et_3Al and I_2 . **Phenols and diols:** 2,4-

di-*t*-butylphenol – Aldrich, Germany, 99+ % pure, recrystallised in hexane; 2,4-dimethylphenol – Aldrich, Germany, 99+ % pure, recrystallised in hexane; 2,2'-methylenebis(4,6-di-*t*-butylphenol) – synthesised according to literature⁹⁶; 2,2'-methylenebis(4-methyl-6-*t*-butylphenol) – Merck, Germany, 99 % pure, used as received; 2,2'-methylenebis(4-chloro-6-isopropyl-3-methylphenol) – synthesised according to literature⁹⁰; 2,2'-methylenebis(4-chlorophenol) – Aldrich, Germany, 99+ % pure, washed with Et₂O and dried; 2,2'-methylenebis(4-methyl-2-(1-methylcyclohexyl)phenol) – Lancaster, Germany, 90 % (tech.), recrystallised in hexane; 2,2'-methylenebis(4,6-di-methylphenol) synthesised analogous to literature⁹⁶; 2,2'-thiobis(4-*tert*-octylphenol) – Aldrich, Germany, 97 %, used as received. All **solvents** – diethyl ether, THF, *n*-pentane, *n*-hexane, benzene, toluene were used as received from Fluka (CH) and stored over molecular sieves in inert conditions. **Mineral oil** (nujol) (for IR spectroscopy) - Fluka, (CH), was dried with the melt sodium and stored in inert conditions. All **deuterated solvents**: CDCl₃ d₁, CD₂Cl₂ d₂, benzene d₆, THF d₈ contained 99,9 % D, were purchased from Chemotrade, Germany and stored over molecular sieves in inert conditions. D₂O – Chemotrade, Germany, 99,8 % D was used to determine the peaks of hydroxy group in ligands.

The following compounds were already described in the literature: 2,2'-methylenebis(4,6-di-*t*-butylphenol)^{93,96} **1**; 2,2'-methylenebis(4-chloro-6-isopropyl-3-methylphenol) **4**^{90,94}; 2,4-di-*t*-butyl-6-(hydroxymethyl)phenol **8**⁹³; (Diethyl ether)-ethyl-{2,2'-methylenebis(4,6-di-*t*-butylphenato)}aluminium(III) **1c**⁸⁶; (Tetrahydrofuran)-chloro-{2,2'-methylenebis(4,6-di-*t*-butylphenato)}aluminium(III) **1b**⁸⁶; (Diethyl ether)-ethyl-{2,2'-methylenebis(4-methyl-6-*t*-butylphenato)}aluminium(III) **2c**⁸⁶; (Diethyl ether)-chloro-{2,2'-methylenebis(4-methyl-6-*t*-butylphenato)}aluminium(III) **2d**⁸⁶; Bis[ethyl-{2,2'-methylenebis(4-methyl-6-*t*-butylphenato)}aluminium(III)] **2e**⁸⁹. The following components: **2f**, **3f** and **3g** were mentioned in the literature¹⁰⁰, but to our best knowledge, their spectroscopic descriptions were not published.

The following designation of carbon atoms in the ¹³C NMR spectroscopy description was used. Contrary to the monomers, where signals of carbons located in two phenols rings overlap themselves and are equivalent – in the case of dimers the chemical shifts of the signals generated by the same carbons of two ligands could differ, hence the detailed designation is necessary (see Figure 39).

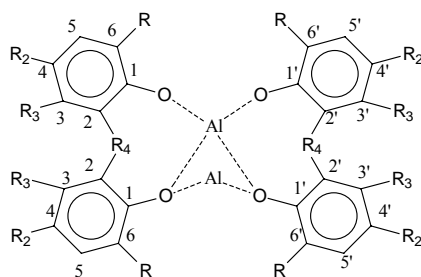


Figure 39 Designation of carbon atoms in ligands moieties of catalysts – general schema.

7.2 Syntheses of bisphenols ligands

General procedure for the synthesis of the ligands:

This synthesis path was taken over from the Pastor's publication and the following compounds were synthesised according to it: 2,2'-methylenebis(4,6-di-*t*-butylphenol) **1**, 2,2'-methylenebis(4-chloro-6-isopropyl-3-methylphenol) **4** and 2,2'-methylenebis(4,6-dimethylphenol) **5**. Below is presented in its general case.

To a mixture of 0.5 mole of substituted phenol and 0.25 mole of paraformaldehyde in 100 cm³ of heptane at 0°C, 0.37 g (3,78 mmol) of concentrated sulphuric acid was added. The reaction mixture was stirred at room temperature for 5 hours and subsequently was heated to 60°C and than stirred overnight. Then it was heated to reflux, removing the water azeotropically using Dean – Stark trap. The reaction mixture was filtered hot and cooled overnight. The resultant precipitate was filtered to give ca. 88 % yield of crystals.

7.2.1 Synthesis of 2,2'-methylenebis(4,6-di-*tert*-butylphenol) **1**

2,2'-methylenebis(4,6-di-*tert*-butylphenol) **1** was already described in the literature, values of chemical shifts in NMR spectroscopy (¹H, ¹³C), IR data and elementary analysis agree with the data reported by Pastor.⁹⁶

Sulphuric acid (0.25g, 18 mmol) was added dropwise to the solution 4,6-di-*t*-butylphenol (65.0 g, 0.31 mol) and paraformaldehyde (4.73 g, 0.16 mol) in heptane (110 cm³). The reaction mixture was refluxed overnight and was quenched by an aqueous NaOH solution (70 cm³, 0.1 M). The organic layer was dried over MgSO₄ and filtered, and the filtrate was concentrated under vacuum to give an orange solid which was washed with hexane (100 cm³) and then dried under vacuum. Yield: 55.1 g, 83 %.

7.2.2 Synthesis of the 2,2'-methylenebis(4-chloro-6-isopropyl-3-methylphenol) **4**

2,2'-methylenebis(4-chloro-6-isopropyl-3-methylphenol) **4** was already described in the literature, values of chemical shifts in NMR spectroscopy (¹H, ¹³C), IR data and elementary analysis agree with the data reported by Lin.⁹⁰

Sulphuric acid (0.15g, 15 mmol) was added dropwise to the solution of 4-chloro-2-isopropyl-5-methylphenol (36.9 g, 0.20 mol) and paraformaldehyde (3.00 g, 0.1 mol) in heptane (100 cm³). The reaction mixture was refluxed overnight and was quenched by an aqueous NaOH solution (60 cm³, 0.1 M). The organic layer was dried over MgSO₄ and filtered, and the filtrate was concentrated under vacuum to give an orange solid which was washed with hexane (75 cm³) and then dried under vacuum. Yield: 31.3 g, 82 %.

7.2.3 Synthesis of 2,2'-methylenebis(4,6-di-methylphenol) 5

This synthesis was performed analogously to synthesis of **1**.

2,4-dimethylphenol (32.47 g, 0.27 mol) and paraformaldehyde (4.00 g, 0.13 mol), the isolated compound forms very small colourless crystals, yield 29.30 g, 85.2 %.

IR (nujol, cm⁻³): 3471 (s), 3302 (s), 3013 (s), 2971 (s), 2861 (s), 1485 (s), 1379 (m), 1235 (s), 1185 (s), 1151 (s), 1021 (s), 933 (s), 856 (s), 776 (s), 629 (s); ¹H NMR: δ (ppm) = 2.20 (s, 6 H, C₆-CH₃), 2.23 (s, 6 H, C₄-CH₃), 3.85 (s, 2 H, C₂-CH₂-), 5.25 (s, 2 H, C₁-OH), 6.80 (s, 2 H, C₃-H), 6.94 (s, 2 H, C₅-H); ¹³C NMR: δ (ppm) = 32.6 (-CH₂-), 34.4 (C₆-CH₃), 34.7 (C₄-CH₃), 122.6 (C₃-H), 125.3 (C₅-H), 126.1 (C₂-CH₂-), 135.6 (C₆-CH₃), 143.1 (C, C₄-CH₃)₃, 150.0 (2 C, C₁-OH); Anal. Calcd for C₁₇H₂₀O₂: C, 79.65; H, 7.86. Found C, 79.68; H, 7.92.

7.2.4 Synthesis of 2,4-di-*t*-butyl-6-(hydroxymethyl)phenol 8

8 was already described in the literature, values of chemical shifts in NMR spectroscopy (¹H, ¹³C), IR data and elementary analysis agree with the data reported by Ohba.⁹³

To a solution of 2,4-di-*t*-butylphenol in methanol (33 g, 160 mmol) in 20 cm³ of methanol, 10 % aqueous NaOH (100 cm³) was added with ice cooling. Then a formaldehyde solution (37%, 40 g) was added dropwise over a period of 10 min. and the solution was stirred at 45°C for 5 h under argon atmosphere. After being cooled to room temperature, the reaction mixture was acidified by adding 10 % HCl (200 cm³) and was extracted with CHCl₃. The organic layer was washed with saturated NaHCO₃ and then water, and dried over MgSO₄. The solvent was removed and the residue (ca. 30 g) was crystallised from hexane (150 ml) giving **8** as a colourless prism. Yield of isolated solid: 20.1 g, 53.4 %.

7.3 Syntheses of the aluminium complexes

Aluminium alkyl and halide compounds were synthesised according to C. C. Lin's procedures^{86,97}, aluminium isopropoxy-bisphenoxide were isolated according to Okuda's one-step procedure.⁸⁹

General procedure for the synthesis of the aluminium complexes in polar solvents:

To an ice-cold solution (0°C) of ligand in 60 cm³ of anhydrous solvent (THF or Et₂O), a solution of the aluminium compound (Et₃Al or Et₂AlCl) in the same solvent was added. The mixture was stirred for 3 h and then dried in vacuum. The solid was washed twice with a small amount of the solvent, concentrated and stored in -20°C to furnish crystals.

General procedure for the synthesis of the aluminium complexes in non-polar solvents:

To an ice-cold solution (0°C) of ligand in 60 cm³ of anhydrous, a solution of the aluminium compound (Et₃Al or Et₂AlCl) in hexane was added. The mixture was stirred for 4 h and dried in vacuum. The residue was washed once with 20 cm³ of hexane dried in vacuum and then dissolved in hot toluene (25 cm³, 85°C) and allowed to cool to room temperature, giving crystals.

General procedure for the synthesis of the aluminium complexes with isopropoxy group:

The mixture of the ligand and aluminium isopropoxide Al(OPrⁱ)₃ in 50 cm³ of anhydrous toluene was stirred overnight under the reflux (85°C). After that the solvent was slowly distilled off and the residue was washed with 20 cm³ of toluene and dried in vacuum. This residue was dissolved in hot toluene (25 cm³, 85°C) and allowed to cool to room temperature, giving colourless crystals.

7.3.1 Syntheses of the aluminium complexes with 2,2'-methylenebis(4,6-di-*t*-butylphenol) **1**

7.3.1.1 (Tetrahydrofuran)-ethyl-{2,2'-methylenebis(4,6-di-*t*-butylphenato)} aluminium(III) **1a**

1 (2.81 g, 6.64 mmol) and 2.0 M solution of Et₃Al (0.98 g, 8.63 mmol), yield of isolated colourless crystals: 3.02 g, 83.0 %.

IR (nujol, cm⁻³): 2932 (s), 2860 (s), 1457 (s), 1362 (s), 1293 (s), 1240 (m), 1001 (m), 920 (m), 856 (s), 770 (m), 668 (m), 650 (m), 599 (m); ¹H NMR: δ (ppm) = 0.08 (q, 2 H, AlCH₂CH₃), 1.07 (t, 3 H, AlCH₂CH₃), 1.22 (s, 18 H, C₆-C(CH₃)₃), 1.31 (s, 18 H, C₄-C(CH₃)₃), 2.01 (O(CH₂CH₂-) in THF), 3.39 (d, 1 H, -CH₂-, J_{H-H} = 13.55 Hz, H_{EXO}), 3.88 (d, 1 H, -CH₂-, J_{H-H} = 13.70 Hz, H_{ENDO}), 4.18 (O(CH₂CH₂-) in THF), 7.05 (s, 2 H, C₃-H), 7.20 (s, 2 H, C₅-H); ¹³C NMR: δ (ppm) = 1.1 (AlCH₂CH₃), 8.8 (AlCH₂CH₃), 25.5 (O(CH₂CH₂-) in THF), 30.0 (C₆-C(CH₃)₃), 31.8 (C₄-C(CH₃)₃), 33.2 (-CH₂-), 34.2 (C₆-C(CH₃)₃), 35.3 (C₄-C(CH₃)₃), 70.13 (O(CH₂CH₂-), 122.0 (C₃-H), 125.1 (C₅-H), 129.9 (C₂-CH₂-bridge), 137.4 (C₆-C(CH₃)₃), 139.9 (C₄-C(CH₃)₃), 152.9 (C₁-O-Al); Anal. Calcd for C₃₅H₅₅O₃Al: C, 76.31; H, 10.07. Found: C, 76.26; H, 10.27.

7.3.1.2 (Tetrahydrofuran)-chloro-{2,2'-methylenebis(4,6-di-*t*-butylphenato)}aluminium (III) **1b**

1b was already described in the literature, values of chemical shifts in NMR spectroscopy (^1H , ^{13}C), IR data and elementary analysis agree with the data reported by Lin.⁸⁶

1 (3.55 g, 8,37 mmol) and 2.0 M solution of Et_2AlCl (1.21 g, 10.0 mmol) in THF, twice extracted with 50 cm³ of THF and concentrated to ca. 15 cm³, yield of isolated crystals: 3.67g, 79.0 %.

7.3.1.3 (Diethyl ether)-ethyl-{2,2'-methylenebis(4,6-di-*t*-butylphenato)}aluminium(III) **1c**

1c was already described in the literature, values of chemical shifts in NMR spectroscopy (^1H , ^{13}C), IR data and elementary analysis agree with the data reported by Lin.⁸⁶

1 (3.49 g, 8.22 mmol) and 2.0 M solution of Et_2AlCl (1.17 g, 10.3 mmol), yield of isolated colourless crystals: 4.12 g, 91.0 %.

7.3.1.4 (Diethyl ether)-chloro-{2,2'-methylenebis(4,6-di-*t*-butylphenato)}aluminium(III) **1d**

1d was already described in the literature, values of chemical shifts in NMR spectroscopy (^1H , ^{13}C), IR data and elementary analysis agree with the data reported by Lin.⁸⁶

1 (3.54 g / 8.36 mmol) and 2.0 M solution of Et_2AlCl (1.05 g / 8.78 mmol), yield of isolated crystals: 3.76 g / 80.5%.

7.3.1.5 Bis[ethyl-{2,2'-methylenebis(4,6-di-*t*-butylphenato)}aluminium(III)] **1e**

1 (2.58 g, 6.10 mmol) and the solution of Et_3Al (0.83 g, 7.31 mmol), colourless crystals 2.47g, 85.0 %.

IR (nujol, cm⁻¹): 2926 (s), 2853 (s), 1462 (s), 1379 (m), 1310 (m), 1293 (m), 1279 (m), 240 (m), 1163 (m), 1099 (m), 938 (m), 880 (m), 821 (m), 774 (m), 742 (m), 660 (m), 632 (m); ^1H NMR: δ (ppm) = 0.11, 0.15 (m, 2*2 H, AlCH_2CH_3), 0.51 (t, 2*3 H, AlCH_2CH_3 , $J = 8.0$ Hz), 1.24, 1.28 (s, 2*18 H, $\text{C}_{6,6'}\text{-C}(\text{CH}_3)_3$), 1.32, 1.38 (s, 2*18 H, $\text{C}_{4,4'}\text{-C}(\text{CH}_3)_3$), 3.48 (d, 2*1 H, $-\text{CH}_2-$, $J_{\text{H-H}} = 13.64$ Hz, H_{EXO}), 4.39 (d, 2*1 H, $-\text{CH}_2-$, $J_{\text{H-H}} = 13.64$ Hz, H_{ENDO}), 7.05 (s, 2*2 H, $\text{C}_{5,5'}\text{-H}$); 7.19 (s, 2*2 H, $\text{C}_{3,3'}\text{-H}$); ^{13}C NMR: δ (ppm) = 7.4 (AlCH_2CH_3), 21.6 (AlCH_2CH_3), 30.2 ($\text{C}_6\text{-C}(\text{CH}_3)_3$), 31.4 ($\text{C}_{6'}\text{-C}(\text{CH}_3)_3$), 31.8 ($\text{C}_4\text{-C}(\text{CH}_3)_3$), 32.1 ($\text{C}_{4'}\text{-C}(\text{CH}_3)_3$), 34.2 ($\text{C}_6\text{-C}(\text{CH}_3)_3$), 34.5 ($\text{C}_{6'}\text{-C}(\text{CH}_3)_3$), 35.0 ($\text{C}_4\text{-C}(\text{CH}_3)_3$), 35.5 ($\text{C}_{4'}\text{-C}(\text{CH}_3)_3$), 36.1 ($-\text{CH}_2-$), 123.7 ($\text{C}_3\text{-H}$), 124.1 ($\text{C}_{3'}\text{-H}$), 126.5 ($\text{C}_5\text{-H}$), 130.4 ($\text{C}_5'\text{-H}$), 133.1 ($\text{C}_{2,2'}$), 140.2 ($\text{C}_6\text{-C}(\text{CH}_3)_3$), 140.8 ($\text{C}_{6'}\text{-C}(\text{CH}_3)_3$), 144.7 ($\text{C}_4\text{-C}(\text{CH}_3)_3$), 147.4 ($\text{C}_{4'}\text{-C}(\text{CH}_3)_3$), 151.2 ($\text{C}_{1,1'}\text{-O-Al}$); elem. Anal. Calcd for $[\text{C}_{31}\text{H}_{47}\text{O}_2\text{Al}]_2$: C, 77.78; H, 9.90; Found: C, 75.26; H, 10.15.

7.3.1.6 Bis[chloro-{2,2'-methylenebis(4,6-di-*t*-butylphenato)}aluminium(III)] 1f

1 (1.95 g, 4.60 mmol) and the solution of Et₂AlCl (0.72 g, 5.98 mmol), a white amorphous residue yielded 1.82 g, 82.0 %.

IR (nujol, cm⁻¹): 2923 (s), 2857 (s), 1460 (s), 1377 (s), 1307 (sm), 1293 (m), 1200 (sm), 1154 (sm), 1099 (m), 986 (sm), 932 (sm), 883 (sm), 820 (m), 802 (m), 779 (sm), 732 (m), 667 (m), 638 (m); ¹H NMR: δ (ppm) = 1.21 (s, 2*18 H, C_{6,6'}-C(CH₃)₃), 1.38 (s, 2*18 H, C_{4,4'}-C(CH₃)₃), 3.65 (d, 2*1 H, -CH₂-, J_{H-H} = 13.42 Hz, H_{EXO}), 4.38 (d, 2*1 H, -CH₂-, J_{H-H} = 14.88 Hz, H_{ENDO}), 7.18 (s, 2*2 H, C_{5,5'}-H), 7.24 (s, 2*2 H, C_{3,3'}-H); ¹³C NMR: δ (ppm) = 30.2 (C_{6,6'}-C(CH₃)₃), 30.6 (-CH₂-), 32.0 (C_{4,4'}-C(CH₃)₃), 33.6 (C_{6,6'}-C(CH₃)₃), 35.1 (C₄-C(CH₃)₃), 35.2 (C_{4'}-C(CH₃)₃), 124.8 (C₃-H), 125.1 (C_{3'}-H), 125.7 (C₅-H), 125.9 (C_{5'}-H), 132.8, (C₂-CH₂-), 133.1 (C_{2'}-CH₂-), 139.2 (C₆-C(CH₃)₃), 139.3 (C_{6'}-C(CH₃)₃), 143.7 (C_{4,4'}-C(CH₃)₃), 148.2 (C_{1,1'}-O-Al); Anal. Calcd for [C₂₉H₄₂O₂AlCl]₂: C, 71.81; H, 8.73. Found C, 71.94; H, 8.77.

7.3.1.7 Bis[isopropoxy-{2,2'-methylenebis(4,6-di-*t*-butylphenato)}aluminium(III)] 1g

1 (2.00 g, 4.73 mmol) and aluminium isopropoxide Al(OPrⁱ)₃ (0.96 g, 4.73 mmol), colourless crystals: 1.81 g, 75.5 %.

IR (nujol, cm⁻³): 2927 (s), 2855 (s), 1457 (s), 1380 (m), 1281 (m), 1202 (m), 1115 (m), 939 (m), 864 (m), 837 (m), 691 (m), 537 (m); ¹H NMR: δ (ppm) = 1.23, (s, 2*18 H, C_{6,6'}-C(CH₃)₃), 1.33 (s, 2*18 H, C_{4,4'}-C(CH₃)₃), 1.55 (d, 2*6 H, ³J_{HH} = 6.25 Hz, -OCH(CH₃)₂), 3.77 (d, 2*1 H, -CH₂-, J = 13.55 Hz, H_{EXO}), 3.97 (d, 2*1 H, -CH₂-, J = 13.70 Hz, H_{ENDO}), 4.62 (m, 2*1 H, ³J_{HH} = 6.25 Hz, -OCH(CH₃)₂) 7.11 (s, 2*2 H, C_{3,3'}-H), 7.25 (s, 2*2 H, C_{5,5'}-H); ¹³C NMR: δ (ppm) = 24.2 (-OCH(CH₃)₂), 29.0 (C₆-C(CH₃)₃), 29.2 (C_{6'}-C(CH₃)₃), 30.5 (C₄-C(CH₃)₃), 30.6 (C_{4'}-C(CH₃)₃), 31.5 (-CH₂-), 33.1 (C₆-C(CH₃)₃), 33.2 (C_{6'}-C(CH₃)₃), 34.2 (C₄-C(CH₃)₃), 34.3 (C_{4'}-C(CH₃)₃), 70.7 (-OCH(CH₃)₂), 121.5, 121.6 (C_{3,3'}-H), 123.8 (C_{5,5'}-H), 127.4, 127.6 (C_{2,2'}-CH₂-) 136.4, 136.5 (C_{6,6'}-C(CH₃)₃), 140.0 (C_{4,4'}-C(CH₃)₃) 150.0 (C_{1,1'}-O-Al); Anal. Calcd for C₆₄H₉₈O₆Al₂: C, 75.55; H, 9.71. Found C, 75.60; H, 9.77.

7.3.2 Syntheses of the aluminium complexes with 2,2'-methylenebis(4-methyl-6-*t*-butylphenol) 2

7.3.2.1 (Tetrahydrofuran)-ethyl-{2,2'-methylenebis(4-methyl-6-*t*-butylphenato)}aluminium(III) 2a

2 (0.71 g, 2.11 mmol) and the solution of Et₃Al (0.27 g, 2.42 mmol), colourless crystals were isolated in quantitative yield, 0.97 g.

IR (nujol, cm^{-3}): 2930 (s), 2858 (s), 1462 (s), 1377 (m), 1275 (s), 1046 (m), 859 (s), 803 (sm), 672 (m); ^1H NMR: δ (ppm) = 0.01 (q, 2 H, AlCH_2CH_3), 1.08 (t, 3 H, AlCH_2CH_3), 1.29 (s, 18 H, $\text{C}_6\text{-C}(\text{CH}_3)_3$), 1.99 (b, 4 H, $\text{O}(\text{CH}_2\text{CH}_2\text{-})$ of THF), 2.16 (s, 3 H, $\text{C}_4\text{-CH}_3$), 3.31 (d, 1 H, $-\text{CH}_2\text{-}$, $J_{\text{H-H}}=13.72$ Hz, H_{EXO}), 3.85 (d, 1 H, $-\text{CH}_2\text{-}$, $J_{\text{H-H}}=13.72$ Hz, H_{ENDO}), 4.13 (b, 4 H, $\text{O}(\text{CH}_2\text{CH}_2\text{-})$ of THF), 6.91 (s, 2 H, $\text{C}_3\text{-H}$), 7.07 (s, 2 H, $\text{C}_5\text{-H}$); ^{13}C NMR: δ (ppm) = 1.1 (C, AlCH_2CH_3), 8.8 (AlCH_2CH_3), 24.4 ($\text{O}(\text{CH}_2\text{CH}_2\text{-})$ in THF), 28.7 ($\text{C}_6\text{-C}(\text{CH}_3)_3$), 29.1 ($\text{C}_6\text{-C}(\text{CH}_3)_3$), 32.1 ($-\text{CH}_2\text{-}$), 33.7 ($\text{C}_4\text{-CH}_3$), 72.0 ($\text{O}(\text{CH}_2\text{CH}_2\text{-})$ in THF), 124.5 ($\text{C}_3\text{-H}$), 125.8 ($\text{C}_4\text{-CH}_3$), 127.8 ($\text{C}_2\text{-CH}_2\text{-}$), 129.3 ($\text{C}_6\text{-C}(\text{CH}_3)_3$), 137.0 ($\text{C}_5\text{-H}$), 151.9 ($\text{C}_1\text{-O-Al}$); Anal. Calcd for $\text{C}_{29}\text{H}_{45}\text{O}_3\text{Al}$: C, 74.32; H, 9.68. Found: C, 74.22; H, 9.75.

7.3.2.2 (Tetrahydrofuran)-chloro-{2,2'-methylenebis(4-methyl-6-*t*-butylphenato)} aluminium(III) 2b

2 (1.66 g, 4.88 mmol) and the solution of Et_2AlCl (0.70 g, 5.85 mmol), reaction resulted in formation of the yellow viscous oil. Further attempts of the solid's isolation were unsuccessful. Quantitative yield 2.30 g.

IR (nujol, cm^{-3}): 2934 (s), 2866 (s), 1473 (s), 1306 (s), 1277 (s), 1291 (s), 1280 (m), 997 (s), 919 (s), 855 (s), 634 (s); ^1H NMR: δ (ppm) = 1.40 (s, 18 H, $\text{C}_6\text{-C}(\text{CH}_3)_3$), 2.13 (b, 4 H, $\text{O}(\text{CH}_2\text{CH}_2\text{-})$ of THF), 2.26 (s, 3 H, $\text{C}_4\text{-CH}_3$), 3.42 (d, 1 H, $-\text{CH}_2\text{-}$, $J_{\text{H-H}}=13.72$ Hz, H_{EXO}), 3.95 (d, 1 H, $-\text{CH}_2\text{-}$, $J_{\text{H-H}}=13.72$ Hz, H_{ENDO}), 4.29 (b, 4 H, $\text{O}(\text{CH}_2\text{CH}_2\text{-})$ of THF), 6.91 (s, 2 H, $\text{C}_3\text{-H}$), 7.07 (s, 2 H, $\text{C}_5\text{-H}$); ^{13}C NMR: δ (ppm) = 24.4 ($\text{O}(\text{CH}_2\text{CH}_2\text{-})$ in THF), 28.7 ($\text{C}_6\text{-C}(\text{CH}_3)_3$), 28.9 ($\text{C}_6\text{-C}(\text{CH}_3)_3$), 32.1 ($-\text{CH}_2\text{-}$), 33.8 ($\text{C}_4\text{-CH}_3$), 70.6 ($\text{O}(\text{CH}_2\text{CH}_2\text{-})$ in THF), 124.6 ($\text{C}_3\text{-H}$), 125.6 ($\text{C}_4\text{-CH}_3$), 127.8 ($\text{C}_2\text{-CH}_2\text{-}$), 129.3 ($\text{C}_6\text{-C}(\text{CH}_3)_3$), 137.0 ($\text{C}_5\text{-H}$), 151.9 ($\text{C}_1\text{-O-Al}$); Anal. Calcd for $\text{C}_{27}\text{H}_{40}\text{O}_3\text{AlCl}$: C, 68.26; H, 8.49. Found: C, 68.30; H, 8.47.

7.3.2.3 (Diethyl ether)-ethyl-{2,2'-methylenebis(4-methyl-6-*t*-butylphenato)}aluminium (III) 2c

2c was already described in the literature, values of chemical shifts in NMR spectroscopy (^1H , ^{13}C), IR data and elementary analysis agree with the data reported by Lin.⁸⁶

2 (1.63 g, 4.82 mmol) and the solution of Et_3Al (0.56 g, 5.12 mmol), yield of colourless crystals: 2.00 g, 89.0 %.

7.3.2.4 (Diethyl ether)-chloro-{2,2'-methylenebis(4-methyl-6-*tert*-butylphenato)} aluminium(III) 2d

2d was already described in the literature, values of chemical shifts in NMR spectroscopy (^1H , ^{13}C), IR data and elementary analysis agree with the data reported by Lin.⁸⁶

2 (0.84 g, 2.48 mmol) and the solution of Et₂AlCl (0.33 g, 2.74 mmol), colourless crystals 0.98 g, 82.5 %.

7.3.2.5 Bis[ethyl-{2,2'-methylenebis(4-methyl-6-*t*-butylphenato)}aluminium(III)] **2e**

2e was already described in the literature, values of chemical shifts in NMR spectroscopy (¹H, ¹³C), IR data and elementary analysis agree with the data reported by Okuda.⁸⁹

2 (1.57 g, 4.62 mmol) and the solution of Et₃Al (0.58 g, 5.08 mmol), yield of isolated crystals: 1.48 g, 86.7 %.

7.3.2.6 Bis[chloro-{2,2'-methylenebis(4-methyl-6-*t*-butylphenato)}aluminium(III)] **2f**

2f was described elsewhere, values of chemical shifts in NMR spectroscopy (¹H, ¹³C), wave numbers of IR spectrum and an elementary analysis agree with those reported by Chisholm.¹⁰⁷

2 (1.99 g, 5.88 mmol) and the solution of Et₂AlCl (0.99 g, 8.231 mmol), yield of isolated crystals: 2.20 g, 94.0 %

7.3.2.7 Bis[isopropoxy-{2,2'-methylenebis(4-methyl-6-*t*-butylphenato)} aluminium (III)] **2g**

2g was described elsewhere, values of chemical shifts in NMR spectroscopy (¹H, ¹³C), wave numbers of IR and elementary analysis agree with these reported by Okuda.⁸⁹

2 (2.55 g, 7.50 mmol) and aluminium isopropoxide Al(OPrⁱ)₃ (1.53 g, 7.50 mmol), yield of isolated crystals: 2.75 g, 72.1 %.

7.3.2.8 Bis[iodo-{2,2'-methylenebis(4-methyl-6-*t*-butylphenato)}aluminium(III)] **2h**

To an ice-cold solution (0°C) of iodine (1.91 g, 7.52 mmol) in 60 cm³ of toluene, a solution of 1.02 cm³ (1.22 g, 7.52 mmol) Et₃Al in 6 cm³ of toluene was added slowly. After the solution became colourless, a solution of **2** (2.55 g, 7.52 mmol) in 20 cm³ of toluene was dropped slowly. The mixture was stirred for 4 h and then dried in vacuum. The residue was washed by 25 cm³ of anhydrous hexane. Yield of isolated powder: 1.91 g, 69.2 %

IR (nujol, cm⁻³): 2930 (s), 2858 (s), 1457 (s), 1377 (m), 1273 (m), 1185 (sm), 1145 (sm), 1093 (m), 943 (m), 867 (m), 783 (m), 662 (m), 650 (m), 557 (m); ¹H NMR: δ (ppm) = 1.22, 1.24 (s, 2*18 H, C_{6,6'}-C(CH₃)₃), 2.17, 2.25 (d, 2*6 H, C_{4,4'}-CH₃), 3.58 (d, 2*1 H, -CH₂-, J = 14.65 Hz, H_{EXO}), 4.34 (d, 2*1 H, -CH₂-, J = 14.41 Hz, H_{ENDO}), 6.93, 6.98 (s, 2*2 H, C_{6,6'}-H), 7.11, 7.17 (s, 2*2 H, C_{4,4'}-H); ¹³C NMR: δ (ppm) = 28.2, 28.9 (C_{6,6'}-C(CH₃)₃), 30.5, 30.6 (C_{4,4'}-CH₃), 32.2 (-CH₂-), 33.5, 33.6 (C_{6,6'}-C(CH₃)₃), 125.7, 125.8 (C_{3,3'}-H), 127.0, 127.4 (C_{5,5'}-H), 128.7, 128.9 (C_{2,2'}-CH₂-), 129.9, 130.2 (C_{6,6'}-C(CH₃)₃), 138.9, 139.0 (C_{4,4'}-CH₃), 152.2 (C_{1,1'}-O-Al); Anal. Calcd for C₅₀H₆₀O₄Al₂I₂: C, 58.14; H, 8.85. Found: C, 58.21; H, 8.81.

7.3.3 Syntheses of the aluminium complexes with 2,2'-methylenebis(4-methyl-2-(1-methylcyclohexyl)phenol) **3**

7.3.3.1 Tetrahydrofuran)-ethyl-{2,2'-methylenebis(4-methyl-2-(1-methylcyclohexyl)phenato)} aluminium (III) **3a**

3 (0.98 g, 2.34 mmol) and the solution of Et₃Al (0.32 g, 2.80 mmol), yield of colourless crystals: 0.99 g, 77.5 %.

IR (nujol, cm⁻³): 2940 (s), 2850 (s), 1459 (s), 1376 (m), 1286 (s), 1173 (m), 1039 (m), 1001 (s), (m), 855 (s), 651 (s); ¹H NMR: δ (ppm) = 0.05 (q, 2 H, AlCH₂CH₃), 1.04 (t, 3 H, AlCH₂CH₃), 1.28 (s, 6 H, -CH₃ in Cy), 1.42 (b, 4 H, O(CH₂CH₂- of THF), 1.64 (br, ax. H in Cy), 1.88 (br, eq. H in Cy), 2.17 (s, 6 H, C₄-CH₃), 3.31 (s, 1 H, -CH₂-, J = 13.60 Hz H_{EXO}), 3.83 (s, 1 H, -CH₂-, J = 13.60 Hz, H_{ENDO}), 4.1 (b, 4 H, O(CH₂CH₂- of THF), 6.82 (d, 2 H, C₅-H), 6.97 (d, 2 H, C₃-H). ¹³C NMR: δ (ppm) = 7.6 (AlCH₂CH₃), 16.6 (AlCH₂CH₃), 19.9 (C₄-CH₃), 21.8, 21.9, 23.9, 24.5, 25.8 (carbons 3, 4, 5 and Me in Cy, THF partly overlapping); 32.4 (C₂-CH₂- and carbons 1 in Cy overlapping), 35.6, 36.1 (carbons 2 and 6 in Cy), 69.5 (O(CH₂CH₂-), 125.4 (C₅-H); 127.6 (C₃-H); 128.0 (C₄-CH₃); 129.6 (C₂-CH₂-); 136.5 (C₆); 152.1 (C₁-O-Al). Anal. Calcd for C₃₅H₅₁O₃Al: C, 78.88; H, 9.40. Found: C, 78.92; H, 9.32.

7.3.3.2 (Tetrahydrofuran)-chloro-{2,2'-methylenebis(4-methyl-2-(1-methylcyclohexyl)phenato)} aluminium(III) **3b**

3 (0.72 g, 1.72 mmol) in 30 cm³ of anhydrous THF, the solution of Et₂AlCl (0.27 g, 2.24 mmol) in 2 cm³ of THF was added, yield of colourless crystals: 0.79 g, 83.2 %.

IR (nujol, cm⁻³): 2930 (s), 2857 (s), 1458 (s), 1372 (m), 1301 (m), 1291 (s), 1176 (sm), 999 (sm), 931 (m), 854 (m), 672 (sm); ¹H NMR: δ (ppm) = 1.21 (s, 6 H, -CH₃ in Cy), 1.42 (b, 4 H, O(CH₂CH₂- of THF); 1.55-1.67 (br, ax. H in Cy), 1.99 (br, eq. H in Cy), 2.19 (s, 6 H, C₄-CH₃), 3.42 (d, 1 H, -CH₂-, J_{H-H}=14.25 Hz, H_{EXO}), 3.80 (d, 1 H, -CH₂-, J_{H-H}=14.25 Hz, H_{ENDO}), 4.07 (b, 4 H, O(CH₂CH₂- of THF), 6.84 (2 H, C₅-H); ¹³C NMR: δ (ppm) = 21.8 (C₄-CH₃); 21.9, 22.0 (carbons 3 and 5 in Cy); 24.4 (Me in 1-Me-Cy), 25.6 (O(CH₂CH₂-)₂); 25.9 (carbons 4 in Cy); 31.6 (carbons 1 in Cy); 32.2 (C₂-CH₂-); 36.7, 37.2 (carbons 2 and 6 in Cy); 66.1 (O(CH₂CH₂-)₂); 125.9 (C₅-CH₃); 127.6 (C₃-CH₃); 128.6 (C₄-H); 129.0 (C₂-CH₂-); 136.5 (C₆); 150.7 (C₁-O-Al); Anal. Calcd for C₃₃H₄₆O₃AlCl: C, 71.65; H, 6.32. Found: C, 71.84; H, 6.40.

7.3.3.3 (Diethyl ether)-ethyl-{2,2'-methylenebis(4-methyl-2-(1-methylcyclohexyl)phenato)} aluminium(III) 3c

3 (2.62 g, 6.23 mmol) in 30 cm³ of anhydrous Et₂O and the solution of Et₃Al (0.85 g, 7.48 mmol) in Et₂O was added. Yield of colourless crystals: 2.94 g, 86.0 %.

IR (nujol, cm⁻³): 2933 (s), 2865 (s), 1652 (sm), 1558 (sm), 1541 (sm), 1461 (s), 1377 (s), 1301 (m), 1271 (m), 1002 (sm), 865 (sm), 795 (sm), 772 (sm), 670 (sm); ¹H NMR: δ (ppm): 0.05 (q, 2 H, AlCH₂CH₃); 1.05 (t, 3 H, AlCH₂CH₃); 1.19 (s, 6 H, -CH₃ in Cy), 1.34 (q, 4 H, O(CH₂CH₃)₂); 1.42, 1.62 (br, ax. H in Cy); 1.91 (br, eq. H in Cy); 2.20 (s, 6 H, C₄-CH₃); 3.29 (d, 1 H, -CH₂-, J_{H-H}=13.74 Hz, H_{EXO}); 3.87 (d, 1 H, -CH₂-, J_{H-H}=13.74 Hz, H_{ENDO}); 4.21 (q, 4 H, O(CH₂CH₃)₂); 6.81 (s, 2 H, C₃-H); 6.96 (s, 2 H, C₅-H); ¹³C NMR: δ (ppm) = 7.5 (AlCH₂CH₃), 12.6 (O(CH₂CH₃)₂), 19.9 (AlCH₂CH₃), 21.7 (C₄-CH₃), 22.0 (carbons 3 and 5 in Cy), 24.2 (Me in 1-Me-Cy), 25.7 (carbons 4 in Cy), 32.1 (C₂-CH₂- and carbons 1 in Cy overlapping), 37.2 (carbons 2 and 6 in Cy), 66.8 (O(CH₂CH₃)₂), 125.6 (C₄-CH₃), 127.6 (C₅-H), 129.0 (C₃-H), 129.7 (C₂-CH₂-), 136.5 (C₆), 151.8 (C₁- O-Al); Anal. Calcd for C₃₅H₅₃O₃Al: C, 76.60; H, 9.73. Found: C, 76.68; H, 9.84.

7.3.3.4 (Diethyl ether)-chloro-{2,2'-methylenebis(4-methyl-2-(1-methylcyclohexyl)phenato)} aluminium(III) 3d

3 (1.49 g, 3.55 mmol) in 30 cm³ of anhydrous Et₂O and the solution of Et₂AlCl (0.55 g, 4.61 mmol) in Et₂O was added. Yield of colourless crystals: 2.25 g, 77.6%.

IR (nujol, cm⁻³): 2935 (s), 2872 (s), 1471 (s), 1311 (s), 1299 (s), 1289 (s), 1281 (m), 1000 (s), 920 (s), 850 (s), 660 (m); ¹H NMR: δ (ppm) = 1.21 (s, 6 H, -CH₃ in Cy); 1.40, 1.56 (br, ax. H in Cy); 2.03 (br, eq. H in Cy); 2.18 (s, 6 H, C₄-CH₃); 3.36 (d, 1 H, -CH₂-, J_{H-H}=13.74 Hz, H_{EXO}); 3.76 (d, 1 H, -CH₂-, J_{H-H}=13.74 Hz, H_{ENDO}); 4.35 (b, 2 H, O(CH₂CH₃)₂); 6.86 (d, 2 H, C₅-H); 6.98 (d, 2 H, C₃-H); ¹³C NMR: δ (ppm) = 15.38 (O(CH₂CH₃)₂); 21.38 (C₄-CH₃); 23.2 (carbons 3 and 5 in Cy); 26.3 (Me in 1-Me-Cy); 27.0 (carbons 4 in Cy); 33.4 (C₂-CH₂- and carbons 1 in Cy overlapping); 37.7, 38.7 (carbons 2 and 4 in Cy); 68.3 (O(CH₂CH₃)₂); 127.5 (C₄-CH₃); 128.3, (C₅-H); 129.0 (C₃-H); 130.6 (C₂-CH₂-); 138.2 (C₆); 151.9 (C₁- O-Al). Anal. Calcd for C₃₃H₄₈O₃AlCl: C, 71.39; H, 8.71. Found: C, 71.49; H, 8.77.

7.3.3.5 Bis[ethyl-{2,2'-methylenebis(4-methyl-2-(1-methylcyclohexyl)phenato)} aluminium (III)] 3e

3 (1.65 g, 3.93 mmol) in 40 cm³ of n-hexane and the solution of Et₃Al (0.56 g, 4.91 mmol) in 4 cm³ of n-hexane, yield of light yellow crystals: 0.99 g, 77.5 %.

IR (nujol, cm^{-1}): 2926 (s), 2855 (s), 1469 (s), 1377 (s), 1302 (m), 1262 (m), 1190 (m), 1139 (m), 1097 (m), 937 (m), 888 (sm), 786 (s), 665 (s), 555 (m). ^1H NMR: δ (ppm) = 0.25 (q, 2*2 H, AlCH_2CH_3), 0.84 (t, 2*3 H, AlCH_2CH_3), 1.11 (s, 2*6 H, $-\text{CH}_3$ in Cy), 1.19 (s, 2*6 H, $-\text{CH}_3$ in Cy), 1.20-1.38 (br, ax. H in Cy), 1.65-1.75 (br, eq. H in Cy), 2.15 (s, 2*3 H, C_4-CH_3), 2.25 (s, 2*3 H, $\text{C}_4'-\text{CH}_3$), 3.55 (d, 2*1 H, $-\text{CH}_2-$, $J_{\text{H-H}}=13.74$ Hz, H_{EXO}), 4.40 (d, 2*1 H, $-\text{CH}_2-$, $J_{\text{H-H}}=13.74$ Hz, H_{ENDO}), 6.88 (s, 2*1 H, C_3-H), 6.96 (s, 2*1 H, $\text{C}_3'-\text{H}$), 7.01 (s, 2*2 H, C_5-H); ^{13}C NMR: δ (ppm) = 8.7 (AlCH_2CH_3); 14.2 (AlCH_2CH_3); 21.0 (C_4-CH_3); 23.1 (carbons 3 and 5 in Cy); 26.3 (Me in 1-Me-Cy); 27.8 (carbons 4 in Cy); 33.5 (C_2-CH_2- and carbons 1 in Cy overlapping); 37.2, 38.2 (carbons 2 and 6 in Cy); 126.6, 126.8 ($\text{C}_{4,4'}-\text{CH}_3$); 128.7, 128.9 ($\text{C}_{5,5'}-\text{H}$); 129.1 ($\text{C}_{3,3'}-\text{H}$); 130.7, 130.8 ($\text{C}_{2,2'}-\text{CH}_2-$); 137.6, 137.7 ($\text{C}_{6,6'}$); 153.3 ($\text{C}_{1,1'}-\text{O-Al}$); Anal. Calcd for $\text{C}_{62}\text{H}_{86}\text{O}_4\text{Al}_2$: C, 78.44; H, 9.13. Found: C, 78.94; H, 9.01.

7.3.3.6 Bis[chloro-{2,2'-methylenebis(4-methyl-2-(1-methylcyclohexyl)phenato)} aluminium (III)] 3f

3f was described elsewhere, values of chemical shifts in NMR spectroscopy (^1H , ^{13}C), wave numbers of IR and elementary analysis agree with these reported by Braune.¹⁰⁰

3 (0.70 g, 1.67 mmol) in 40 cm^3 of n-hexane and the solution of Et_2AlCl (0.26 g, 2.71 mmol) in 4 cm^3 of n-hexane, yield of light yellow crystals: 0.63 g, 78.3 %.

IR (nujol, cm^{-1}): 2926 (s), 2855 (s), 1486 (s), 1377 (m), 1302 (m), 1261 (m), 1190 (m), 1139 (m), 1097 (m), 982 (sm), 936 (m), 788 (m), 655 (m), 555 (m). ^1H NMR: δ (ppm) = 1.11, 1.19 (s, 2*6 H, $-\text{CH}_3$ in Cy); 1.35 (br, ax. H in Cy); 1.69 (br, eq. H in Cy); 2.18, 2.26 (s, 2*6 H, $\text{C}_{4,4'}-\text{CH}_3$), 3.55 (d, 2*1 H, $-\text{CH}_2-$, $J_{\text{H-H}} = 13.72$ Hz, H_{EXO}); 4.40 (d, 2*1 H, $-\text{CH}_2-$, $J_{\text{H-H}} = 13.72$ Hz, H_{ENDO}); 6.92, 6.94 (d, 2*2 H, $\text{C}_{5,5'}-\text{H}$), 6.99, 7.02 (d, 2*2 H, $\text{C}_{3,3'}-\text{H}$); ^{13}C NMR: δ (ppm) = 20.1, 20.2 ($\text{C}_{4,4'}-\text{CH}_3$); 21.3, 21.3, 21.6, 21.9 (broad signal, carbons 3, 5 in Cy); 24.9, 25.5 (Me in 1-Me-Cy); 26.3, 26.6 (carbons 4 in Cy); 35.3 (C_2-CH_2-); 35.3, 36.0, 36.7, 37.2, 37.8, 37.6 (carbons 2, 6, 1 in Cy); 126.5 (C_4-CH_3); 126.6 ($\text{C}_4'-\text{CH}_3$); 127.3 (C_5-CH_3); 127.8 ($\text{C}_5'-\text{H}$); 129.5 (C_3-H); 129.8 ($\text{C}_3'-\text{CH}_2-$); 134.8 ($\text{C}_{2,2'}-\text{CH}_2-$); 137.1 ($\text{C}_{6,6'}$); 149.0 ($\text{C}_{1,1'}-\text{O-Al}$); Anal. Calcd for $\text{C}_{58}\text{H}_{76}\text{O}_4\text{Al}_2\text{Cl}_2$: C, 72.41; H, 7.96. Found: C, 72.49; H, 7.79

7.3.3.7 Bis[isopropoxy-{2,2'-methylenebis(4-methyl-2-(1-methylcyclohexyl)phenato)} aluminium (III)] 3g

3g was described elsewhere, values of chemical shifts in NMR spectroscopy (^1H , ^{13}C), wave numbers of IR and elementary analysis agree with these reported by Braune.¹⁰⁰

3 (1.50 g, 3.57 mmol) and aluminium isopropoxide $\text{Al}(\text{OPr}^i)_3$ (0.76 g, 3.57 mmol), colourless crystals: 1.23 g, 68.2 %.

IR (nujol, cm^{-1}): 2926 (s), 2855 (s), 1460 (s), 1376 (m), 1265 (s), 1106 (m), 931 (m), 858 (m), 834 (m), 691 (s), 888 (sm), 789 (sm), 691 (s), 541 (sm); ^1H NMR: δ (ppm) = 1.12 (s, 2*3 H, - CH_3 in Cy), 1.20 (s, 2*3 H, - CH_3 in Cy), 1.20-1.38 (br, ax. H in Cy), 1.49 (d, 4*3 H, - $\text{OCH}(\text{CH}_3)_2$, $^3J_{\text{HH}} = 6.2$ Hz), 1.65-1.75 (br, eq. H in Cy), 2.19 (s, 2*3 H, C_4 - CH_3), 2.25 (s, 2*3 H, C_4 - CH_3), 3.55 (d, 2*1 H, - CH_2 -, $J_{\text{H-H}}=13.74$ Hz, H_{EXO}), 4.40 (d, 2*1 H, - CH_2 -, $J_{\text{H-H}}=13.74$ Hz, H_{ENDO}); 4.54 (d, 2*1 H, - $\text{OCH}(\text{CH}_3)_2$, $^3J_{\text{HH}} = 6.2$ Hz); 6.96 (s, 2*2 H, $\text{C}_{3,3'$ -H), 7.01 (s, 2*2 H, $\text{C}_{5,5'$ -H); ^{13}C NMR: δ (ppm) = 21.05 (C_4 - CH_3); 23.05, (carbons 3 and 5 in Cy); 24.9 (- $\text{OCH}(\text{CH}_3)_2$); 26.3 (Me in 1-Me-Cy); 27.8 (carbons 4 in Cy); 33.36 (C_2 - CH_2 -); 37.2, 38.2 (carbons 2, 6, 1 in Cy); 71.8 (- $\text{OCH}(\text{CH}_3)_2$); 126.6, 126.8 ($\text{C}_{4,4'}$ - CH_3); 128.7 129.0 ($\text{C}_{5,5'$ -H); 129.3, 129.5 ($\text{C}_{3,3'$ -H); 130.7 ($\text{C}_{2,2'}$ - CH_2 -); 137.8 ($\text{C}_{6,6'}$); 153.3 ($\text{C}_{1,1'}$ -O-Al); Anal. Calcd for $\text{C}_{62}\text{H}_{86}\text{O}_4\text{Al}_2$: C, 78.44; H, 9.13. Found: C, 78.94; H, 9.01.

7.3.4 Syntheses of the aluminium complexes with 2,2'-methylenebis(4-chloro-6-isopropyl-3-methylphenol) 4

7.3.4.1 Tetrahydrofuran)-ethyl-{2,2'-methylenebis(4-chloro-6-isopropyl-3-methylphenato)} aluminium(III) 4a

4 (1.04 g, 2.74 mmol) and the solution of Et_3Al (0.37 g, 3.29 mmol). The residue was dissolved in 5 cm^3 of hexane, giving after 30 minutes colourless crystals. Yield of isolated crystals: 0.99 g, 71.1 %.

IR (nujol, cm^{-3}): 2910 (s), 1464 (s), 1399 (s), 1339 (s), 1282 (s), 1205 (s), 1038 (s), 992 (s), 864 (s), 813 (s), 781 (s), 666 (s);

^1H NMR: δ (ppm) = 0,0 (2 H, Al-(CH_2CH_3), 0.94 (3 H, Al-(CH_2CH_3), 1.06, 1.08 (s, 12 H, - $\text{CH}(\text{CH}_3)_2$), 1.84 (b, 4 H, OCH_2CH_2 - in THF), 2.28 (s, 6 H, C_3 - CH_3), 3.39 (m, 2 H, - $\text{CH}(\text{CH}_3)_2$), 3.98 (b, 4 H, $\text{O}(\text{CH}_2\text{CH}_2)_2$ in THF partly overlapping - CH_2 -), 6.94 (s, 1 H, C_5 -H); ^{13}C NMR: δ (ppm) = 7.5 (Al- CH_2CH_3), 16.1 (Al- CH_2CH_3), 21.1 (C_3 - CH_3), 24.7 ($\text{O}(\text{CH}_2\text{CH}_2)_2$); 26.0 (- $\text{OCH}(\text{CH}_3)_2$); 27.9 (- CH_2 -); 69.8 (- $\text{OCH}(\text{CH}_3)_2$); 75.0 ($\text{O}(\text{CH}_2\text{CH}_2)_2$); 123.3 (C_5 -H); 123.6 (C_3 - CH_3); 128.2 (C_2 - CH_2 -); 131.4 (C_4 -Cl); 135.8 (C_6 -Prⁱ); 153.4 (C_1 -O-Al); Anal. Calcd for $\text{C}_{27}\text{H}_{37}\text{O}_3\text{AlCl}_2$: C, 60.90; H, 7.35. Found: C, 60.87; H, 7.29.

7.3.4.2 Dichlorotetrakis(tetrahydrofuran)aluminium di(2,2'-methylenebis(4-chloro-6-isopropyl-3-methylphenato)aluminate 4b

To an ice-cold solution (0°C) of **4** (0.97 g, 2.56 mmol) in 30 cm^3 of anhydrous THF, the solution of Et_2AlCl (0.40 g, 3.29 mmol) in 3 cm^3 of THF was added slowly. The mixture was stirred for 3 h, became colourless and then was dried in vacuum. The residue was dissolved in

5 cm³ of THF and stored in -20°C, giving colourless crystals. Yield of isolated crystals: 1.01g, 67.76 %.

IR (nujol, cm⁻³): 2924 (s), 2862 (s), 1459 (s), 1396 (s), 1340 (s), 1277 (sm), 1201 (m), 1040 (m), 991 (m), 953 (sm), 846 (s), 818 (s), 777 (m), 659 (sm), 622 (sm).

¹H NMR: δ (ppm) = 1.07, 1.08 (s, 4*3 H, -CH(CH₃)₂), 1.85 (b, 4 H, OCH₂CH₂- in THF), 2.29 (s, 2*3 H, C₃-CH₃), 3.17 (m, 2*2 H, -CH(CH₃)₂), 3.89 (d, 1 H, -CH₂-, H_{EXO}), 3.95 (d, 1 H, -CH₂-, H_{ENDO}), 4.13 (b, 2*2 H, O(CH₂CH₂)₂- in THF), 6.98 (s, 2*2 H, C₅-H); ¹³C NMR: δ (ppm) = 21.4 (C₃-CH₃), 24.5 (Al(2)-O(CH₂CH₂)₂); 25.9 (-CH(CH₃)₂); 27.5 (-CH₂-), 69.6 (Al(2)-O(CH₂CH₂)₂ and carbons of -CH(CH₃)₂); 123.4 (C₅-H); 124.0 (C₃-CH₃); 127.6 (C₂-CH₂-); 131.6 (C₄-Cl); 135.3 (C₆-Prⁱ); 150.5 (C₁-O-Al(1)); Anal. Calcd for C₃₇H₇₆O₈Al₂Cl₆: C, 48.53; H, 8.37. Found: C, 48.91; H, 8.69.

7.3.4.3 (Diethyl ether)-ethyl-{2,2'-methylenebis(4-chloro-6-isopropyl-3-methylphenato)} aluminium(III) 4c

4 (1.15 g, 3.03 mmol) and the solution of Et₃Al (0.41 g, 3.64 mmol). Reaction was performed quantitatively.

IR (nujol, cm⁻³): 2924 (s), 2857 (s), 1460 (s), 1402 (m), 1378 (m), 1346 (sm), 1260 (sm), 1178 (m), 1087 (sm), 1033 (m), 847 (m), 773 (m), 653 (m);

¹H NMR: δ (ppm) = 0.00 (2 H, AlCH₂CH₃); 1.00 (3 H, AlCH₂CH₃); 1.06, 1.08 (s, 6 H, -CH(CH₃)₂); 1.18 (4 H, O(CH₂CH₃)₂); 2.26 (s, 6 H, C₃-CH₃); 3.16 (6 H, O(CH₂CH₃)₂); 3.19 (2H, -CH(CH₃)₂); 3.27 (d, 1 H, -CH₂-, H_{EXO}), 3.70 (d, 1 H, -CH₂-, J_{H-H} = 13, 42 Hz, H_{ENDO}), 3.88 (2 H, -CH₂-); 3.95 (6 H, O(CH₂CH₃)₂); 6.98 (s, 2 H, C₅-H); ¹³C NMR: δ (ppm) = 7.5 (Al-CH₂CH₃); 14.1 (Al-CH₂CH₃); 14.8 (O(CH₂CH₃)₂); 24.5 (-CH(CH₃)₂); 25.2 (C₃-CH₃); 27.9 (-CH₂-); 66.7 (O(CH₂CH₃)₂); 69.1 (-CH(CH₃)₂); 125.2 (C₅-H); 125.8 (C₃-CH₃); 126.3 (C₂-CH₂-); 133.3 (C₄-Cl); 138.8 (C₆-Prⁱ); 152.4 (C₁-O-Al); Anal. Calcd for C₂₇H₃₉O₃AlCl₂: C, 63.65; H, 7.71. Found: C, 63.74; H, 7.91.

7.3.4.4 (Diethyl ether)-chloro-{2,2'-methylenebis(4-chloro-6-isopropyl-3-methylphenato)} aluminium(III) 4d

4 (0.95 g, 2.50 mmol) and the solution of Et₂AlCl (0.39 g, 3.25 mmol). Yield of isolated crystals: 0.98 g, 76.7 %.

IR (nujol, cm⁻³): 2923 (s), 2856 (s), 1460 (s), 1378 (m), 1343 (sm), 1088 (sm), 1031 (sm), 877 (sm), 846 (sm), 772 (sm), 723 (sm), 618 (sm); ¹H NMR: δ (ppm) = 1.10, 1.12 (s, 12 H, C₆-CH(CH₃)₂), 1.34 (b, 6 H, O(CH₂CH₃)₂), 2.28 (s, 6 H, C₃-CH₃), 3.00 (d, 2 H, -CH₂-, J_{H-H} = 13.80 Hz H_{EXO}), 3.16 (m, 2 H, C₆-CH(CH₃)₂), 3.45, 3.54 (d, 2 H, -CH₂-, J_{H-H} = 13.80 Hz,

H_{ENDO}), 3.77, 3.95 (b, 4 H, $O(\underline{C}_2\underline{C}H_2\underline{C}H_3)_2$), 6.98 (s, 1 H, $C_5-\underline{H}$); ^{13}C NMR: δ (ppm) = 7.6 ($Al-\underline{C}H_2\underline{C}H_3$), 15.9 ($Al-\underline{C}H_2\underline{C}H_3$), 16.1 ($O(\underline{C}_2\underline{C}H_2\underline{C}H_3)_2$); 22.1 ($C_3-\underline{C}H_3$); 26.5 ($-\underline{C}H(\underline{C}H_3)_2$); 27.6 ($-\underline{C}H_2-$); 67.4 ($-\underline{C}H(\underline{C}H_3)_2$); 69.0 ($O(\underline{C}_2\underline{C}H_2\underline{C}H_3)_2$); 123.8 ($C_5-\underline{H}$); 124.1 ($C_3-\underline{C}H_3$); 128.2 ($C_2-\underline{C}H_2-$); 131.7 ($C_4-\underline{Cl}$); 136.2 ($C_6-\underline{Pr}^i$); 152.4 ($C_1-\underline{O}-Al$); Anal. Calcd for $C_{25}H_{34}O_3AlCl_3$: C, 58.20; H, 6.64. Found: C, 58.41; H, 6.97.

7.3.4.5 Bis[ethyl-{2,2'-methylenebis(4-chloro-6-isopropyl-3-methylphenato)}aluminium (III)] 4e

4 (3.00 g, 7.87 mmol) in 30 cm³ of anhydrous hexane, the solution of Et_3Al (1.08 g, 9.45 mmol) in 3 cm³ of hexane was added slowly. Yield of isolated solid: 2.87 g, 84.0 %

IR (nujol, cm⁻³): 2940 (s), 2868 (s), 1461 (s), 1397 (s), 1205 (m), 1156 (m), 1064 (m), 1022 (m), 882 (m), 840 (m), 763 (s), 663 (s), 619 (s); 1H NMR: δ (ppm) = 0.11 and 0.21 (m, 2*2 H, $Al\underline{C}H_2\underline{C}H_3$), 0.51 (t, 2*3 H, $Al\underline{C}H_2\underline{C}H_3$, $J = 8.07$ Hz), 1.16 (s, 2*12 H, $C_6-\underline{C}H(\underline{C}H_3)_2$); 2.36 (s, 2*6 H, $C_3-\underline{C}H_3$); 3.23 (sept., 2*2 H, $-\underline{C}H(\underline{C}H_3)_2$); 3.51 (d, 2*1 H, $-\underline{C}H_2-$, $J_{H-H} = 13.68$ Hz, H_{ENDO}); 4.35 (d, 2*1 H, $-\underline{C}H_2-$, $J_{H-H} = 13.42$ Hz, H_{ENDO}); 7.04 (s, 2*2 H, $C_5-\underline{H}$); ^{13}C NMR: δ (ppm) = 7.9 ($Al-\underline{C}H_2\underline{C}H_3$), 16.2 ($Al-\underline{C}H_2\underline{C}H_3$); 26.0 ($-\underline{C}H(\underline{C}H_3)_2$); 26.2 ($C_3-\underline{C}H_3$); 31.3 ($C_2-\underline{C}H_2-$); 67.8 ($-\underline{C}H(\underline{C}H_3)_2$); 124.6 ($C_5-\underline{H}$); 124.8 ($C_5'-\underline{H}$); 125.6 ($C_3-\underline{C}H_3$); 125.7 ($C_3'-\underline{C}H_3$); 128.2 ($C_2-\underline{C}H_2-$); 128.3 ($C_2'-\underline{C}H_2-$); 133.1 ($C_4-\underline{Cl}$); 133.3 ($C_4'-\underline{Cl}$); 136.5 ($C_6-\underline{Pr}^i$); 136.6 ($C_6'-\underline{Pr}^i$); 153.4 ($C_{1,1'}-\underline{O}-Al$); Calcd for $C_{42}H_{48}O_4Al_2Cl_6$: C, 68.43; H, 6.53. Found C, 68.57; H, 6.86.

7.3.4.6 Bis[chloro-{2,2'-methylenebis(4-chloro-6-isopropyl-3-methylphenato)}aluminium (III)] 4f

4 (0.90 g, 2.37 mmol) in 30 cm³ of anhydrous hexane, the solution of Et_2AlCl (0.37 g, 3.08 mmol), yield of isolated crystals: 0.89 g, 85.3 %

IR (nujol, cm⁻¹): 2923 (s), 2856 (s), 1461 (s), 1401 (m), 1378 (m), 1344 (sm), 1151 (sm), 1031 (sm), 879 (sm), 765 (m), 722 (sm), 669 (m); 1H NMR: δ (ppm) = 1.18 (s, 2*12 H, $-\underline{C}H(\underline{C}H_3)_2$); 2.23 (2*6 H, $C_3-\underline{C}H_3$); 3.31 (d, 2*1 H, $-\underline{C}H_2-$, $J_{H-H} = 13.42$ Hz, H_{EXO}); 3.52 (m, 2*2 H, $-\underline{C}H(\underline{C}H_3)_2$); 4.40 (d, 2*1 H, $-\underline{C}H_2-$, $J_{H-H} = 13.42$ Hz, H_{ENDO}); 7.04 (2*2 H, $C_5-\underline{H}$); ^{13}C NMR: δ (ppm) = 25.8 ($-\underline{C}H(\underline{C}H_3)_2$); 26.08, 28.68 ($C_3-\underline{C}H_3$); 30.56, ($C_2-\underline{C}H_2-$); 67.07 ($-\underline{C}H(\underline{C}H_3)_2$); 124.2 ($C_5-\underline{H}$); 125.0 ($C_3-\underline{C}H_3$); 125.2 ($C_3'-\underline{C}H_3$); 128.0 ($C_{2,2'}-\underline{C}H_2-$); 132.5 ($C_{4,4'}-\underline{Cl}$); 136.5 ($C_6-\underline{Pr}^i$); 136.7 ($C_6'-\underline{Pr}^i$); 152.4 ($C_{1,1'}-\underline{O}-Al$); Anal. Calcd for $C_{42}H_{48}O_4Al_2Cl_6$: C, 57.10; H, 5.48. Found C, 57.48; H, 5.56.

7.3.4.7 Bis[chloro-{2,2'-methylenebis(4-chloro-6-isopropyl-3-methylphenato)}aluminium (III)] 4g

4g was already described in the literature, values of chemical shifts in NMR spectroscopy (^1H , ^{13}C), IR data and elementary analysis agree with the data reported by Lin.⁹⁰

4 (2.60 g, 6.83 mmol) and $\text{Al}(\text{OPr}^i)_3$ (1.39 g, 6.83 mmol) in 55 cm³ of anhydrous toluene, yield of isolated crystals: 2.04 g, 66.2 %

7.3.5 Syntheses of the aluminium complexes with 2,2'-methylenebis(4-chlorophenol) 5

7.3.5.1 (Tetrahydrofuran)-ethyl-{2,2'-methylenebis(4,6-di-methylphenato)}aluminium (III) 5a

5 (1.53 g, 5.96 mmol) in 30 cm³ of anhydrous THF, the solution of Et_3Al (0.81 g, 7.15 mmol), Yield of isolated light yellow solid: 1.85 g, 84.6 %.

IR (nujol, cm⁻³): 2927 (s), 2855 (s), 1460 (s), 1377 (s), 1320 (m), 1265 (m), 1206 (m), 1155 (m), 1007 (m), 856 (m), 634 (m), 604 (m); ^1H NMR: δ (ppm) = 0.12 (q, 2 H, AlCH_2CH_3), 0.98 (t, 3 H, AlCH_2CH_3), 1.77 (O(CH_2CH_2 -) in THF), 2.14 (s, 6 H, $\text{C}_6\text{-CH}_3$), 2.19 (s, 6 H, $\text{C}_4\text{-CH}_3$), 3.29 (d, 1 H, $-\text{CH}_2$ -, $J_{\text{H-H}} = 13.55$ Hz, H_{EXO}), 3.90 (d, 1 H, $-\text{CH}_2$ -, $J_{\text{H-H}} = 13.70$ Hz H_{ENDO}), 4.57 (O(CH_2CH_2 -) in THF), 6.70 (s, 2 H, $\text{C}_3\text{-H}$), 6.86 (s, 2 H, $\text{C}_5\text{-H}$); ^{13}C NMR: δ (ppm) = 7.1 (AlCH_2CH_3), 16.5 (AlCH_2CH_3), 19.6 ($\text{C}_6\text{-CH}_3$), 24.2 ($\text{C}_4\text{-CH}_3$), 24.3 (O(CH_2CH_2 -) in THF), 32.2 ($-\text{CH}_2$ -), 68.0 (O(CH_2CH_2 -) in THF), 126.2 ($\text{C}_5\text{-H}$), 127.2 ($\text{C}_3\text{-H}$), 130.0 ($\text{C}_2\text{-CH}_2$ -), 133.6 ($\text{C}_6\text{-CH}_3$), 136.3 ($\text{C}_4\text{-CH}_3$), 151.1 ($\text{C}_1\text{-O-Al}$); Anal. Calcd for $\text{C}_{23}\text{H}_{31}\text{O}_3\text{Al}$: C, 72.22; H, 8.17. Found: C, 72.40; H, 8.35.

7.3.5.2 (Tetrahydrofuran)-chloro-{2,2'-methylenebis(4,6-di-methylphenato)}aluminium (III) 5b

5 (1.526 g, 5.96 mmol) in 30 cm³ of anhydrous THF, the solution of Et_2AlCl (0.86 g, 7.15 mmol), yield of isolated white solid: 2.10 g, 78.15 %.

IR (nujol, cm⁻³): 2927 (s), 2855 (s), 1465 (s), 1373 (s), 1273 (m), 1192 (m), 1150 (m), 1012 (m), 862 (m); ^1H NMR: δ (ppm) = 1.75 (O(CH_2CH_2 -) in THF), 2.14 (s, 6 H, $\text{C}_6\text{-CH}_3$), 2.19 (s, 6 H, $\text{C}_4\text{-CH}_3$), 3.32 (d, 2 H, $-\text{CH}_2$ -, $J_{\text{H-H}} = 13.55$ Hz, H_{EXO}), 3.89 (O(CH_2CH_2 -) in THF); 4.46 (d, 2 H, $-\text{CH}_2$ -, $J_{\text{H-H}} = 13.70$ Hz, H_{ENDO}), 6.71 (s, 2 H, $\text{C}_3\text{-H}$), 6.87 (s, 2 H, $\text{C}_5\text{-H}$); ^{13}C NMR: δ (ppm) = 20.1 ($\text{C}_6\text{-CH}_3$), 24.0 ($\text{C}_4\text{-CH}_3$), 24.5 (O(CH_2CH_2 -) in THF), 32.1 ($-\text{CH}_2$ -), 68.0 (O(CH_2CH_2 -) in THF), 125.0 ($\text{C}_5\text{-H}$), 127.9 ($\text{C}_3\text{-H}$), 130.1 ($\text{C}_2\text{-CH}_2$ -), 133.4 ($\text{C}_6\text{-CH}_3$), 136.5 ($\text{C}_4\text{-CH}_3$), 152.5 ($\text{C}_1\text{-O-Al}$); Anal. Calcd for $\text{C}_{21}\text{H}_{26}\text{O}_2\text{AlCl}$: C, 67.65; H, 7.03. Found: C, 67.40; H, 7.35.

7.3.5.3 Bis[chloro-{2,2'-methylenebis(4,6-di-methylphenato)}aluminium(III)] 5f

5 (2.68 g, 10.47 mmol) and the solution of Et₂AlCl (1.77 g, 13.60 mmol), yield of a white amorphous solid: 2.75 g, 83.01 %.

IR (nujol, cm⁻³): 2925 (s), 2862 (s), 1445 (s), 1378 (s), 1267 (m), 1192 (m), 1025 (m), 862 (m); ¹H NMR: δ (ppm) = 2.13-2.20 (2*12 H, C_{4,6}-CH₃), 3.76 (d, 2*1 H, -CH₂-, J_{H-H} = invisible, H_{EXO}), 4.50 (d, 2*1 H, -CH₂-, J_{H-H} = invisible, H_{ENDO}), 6.75-6.80 (s, 2*2 H, C₃-H), 7.01 (s, 2*2 H, C₅-H); ¹³C NMR: δ (ppm) = 19.54, 19.63 (C_{6,6'}-CH₃), 24.17 (C_{4,4'}-CH₃), 33.60 (-CH₂-), 127.0 – 136.5 (carbons C_{2,2'}, C_{3,3'}, C_{4,4'}, C_{5,5'}, C_{6,6'} of phenyl rings), 149.6 (C_{1,1'}-O-Al); Anal. Calcd for C₃₄H₃₆O₄Al₂Cl₂: C, 64.46; H, 5.73. Found: C, 65.50; H, 5.61.

7.3.5.4 Bis[isopropoxy-{2,2'-methylenebis(4-chlorophenato)} aluminium (III)] 5g

5 (1.25 g, 4.88 mmol) and Al(OPrⁱ)₃ (1.00 g, 4.88 mmol) in 60 cm³ of anhydrous toluene. The yield of isolated white solid: 1.09 g, 65.5 %.

IR (nujol, cm⁻³): 2924 (s), 2856 (s), 1649 (sm), 1460 (s), 1379 (s), 1311 (sm), 1152 (sm), 1087 (sm), 1024 (sm), 802 (sm), 666 (sm); ¹H NMR: δ (ppm) = 1.30 (d, 2*6 H, -OCH(CH₃)₂), 2.00-2.05 (br, 2*12 H, C_{4,4',6,6'}-CH₃); 3.50-3.55 (d, 2*1 H, -CH₂-, H_{EXO}); H_{ENDO} is invisible, 4.54 (m, 2*1 H, -OCH(CH₃)₂); 6.84 (d, 2*2 H, C₃-H); 7.02 (d, 2*2 H, C₅-H); ¹³C NMR: δ (ppm) = 24.35 (carbons C_{4,4'}-CH₃, C_{6,6'}-CH₃ as well as (-OCH(CH₃)₂) overlapping); 31.84 (-CH₂-); 63.45 (-OCH(CH₃)₂); 120.3–130.6 (carbons C_{2,2'}, C_{3,3'}, C_{4,4'}, C_{5,5'}, C_{6,6'} of phenyl rings); 150.7 (C_{1,1'}-O-Al); Anal. Calcd for C₄₀H₅₀O₆Al₂: C, 70.57; H, 7.40. Found: C, 70.89; H, 7.83.

7.3.6 Syntheses of the aluminium complexes with 2,2'-methylenebis(4-chlorophenol) 6

7.3.6.1 Bis[(Tetrahydrofuran)-ethyl-{2,2'-methylenebis(4-chlorophenato)} aluminium (III)] 6a

6 (2.30 g, 8.55 mmol) and the solution of Et₃Al (1.08 g, 9.83 mmol), yield of isolated crystals: 2.42 g, 71.3 %.

IR (nujol, cm⁻³): 2925 (s), 2857 (s), 1462 (s), 1379 (m), 1276 (m), 1243 (m), 1043 (m), 861 (m), 768 (m), 648 (m); ¹H NMR: δ (ppm) = -0.01 (s, 4 H, AlCH₂CH₃), 0.77 (s, 6 H, AlCH₂CH₃), 1.72 (br s, 8 H, O(CH₂CH₂)₂- in THF overlapping s, 2 H, -CH₂-, H_{EXO}); 3.57 (br s, 8 H, O(CH₂CH₂)₂- in THF), 3.75 (s, 2 H, -CH₂-, H_{ENDO}); 6.67 (d, 4 H, C_{6,6'}-H), 6.99 (d, 4 H, C_{5,5'}-H), 7.13 (d, 4 H, C_{3,3'}-H); ¹³C NMR: δ (ppm) = 1.55 (AlCH₂CH₃), 7.26 (AlCH₂CH₃), 26.31 (O(CH₂CH₂-) in THF), 31.12 (-CH₂-), 68.62 (O(CH₂CH₂-) in THF), 118.0, 118.1 (C_{5,5'}-H), 126.3, 126.5 (C_{4,4'}-Cl), 128.6, 128.7 (C_{2,2'}-CH₂-), 128.9 (C_{6,6'}-H), 131.0, 131.4 (C_{3,3'}-H)

152.7 (C_{1,1}-O-Al); Anal. Calcd for C₃₈H₄₂O₆Al₂Cl₄: C, 57.74; H, 5.35. Found: C, 57.94; H, 5.60.

The interaction between hydrogen atoms in the methylene bridge and the aluminium atom are invisible in the ¹H NMR spectrum, confirming the structure was attained by the interpretation of the X-ray structure.

7.3.6.2 Aluminium (III), bis[μ-3[2,2'-methylenebis(4-chlorophenato(2-)O:O':O'':O''] pentaethyltristereoisomer **6c**

To an ice-cold solution (0°C) of **6** (1.72 g, 6.38 mmol) in 60 cm³ of anhydrous Et₂O, the solution of Et₃Al (0.76g, 6.70 mmol) in Et₂O was added. The mixture was stirred for 3 h and then dried under vacuum to give a colourless powder, which was extracted three times with 90 cm³ of Et₂O, and concentrated to ca. 15 cm³, stored in -20°C to furnish colourless crystals. Yield of isolated crystals: 1.29 g, 50.0 %.

IR (nujol, cm⁻³): 2930 (s), 2855 (s), 1467 (s), 1375 (s), 1230 (m), 1172 (m), 1118 (m), 926 (m), 818 (m), 788 (m), 685 (m); ¹H NMR: δ (ppm) = -0.69 and -0.41 (doublet of multiplets, 4*2 H, Al_(1 and 3)CH₂CH₃), -0.25 and -0.21 (doublet of multiplets, 2 H, Al₍₂₎CH₂CH₃), 0.20 (t, 2*3 H, Al_(1 and 3)CH₂CH₃), 0.47 (t, 3 H, Al₍₂₎CH₂CH₃), 0.69 (t, 2*3 H, Al_(1 and 3)CH₂CH₃), 0.85 (t, 3 H, Al₍₂₎CH₂CH₃); 3.32 (d, 2*1 H, -CH₂-, J = 13.70 Hz, H_{EXO}), 4.05 (d, 2*1 H, -CH₂-, J = 13.55 Hz, H_{ENDO}), 6.85, 6.88 (d, 4 H, C_{6,6'}-H), 6.93, 6.95 (d, 4 H, C_{5,5'}-H); 7.11, 7.14, 7.17, (4 H, C_{3,3'}-H); ¹³C NMR: δ (ppm) = -0.92 (Al₍₂₎CH₂CH₃), -0.17 (Al_(1 and 3)CH₂CH₃), 6.64 and 7.20 (Al_(1 and 3)CH₂CH₃), 8.50 (Al₍₂₎CH₂CH₃), 31.47 (-CH₂-); 118.4, 119.4 (C₃-H) 120.2 (C_{3'}-H), 126.3, 126.5 (C_{4,4'}-Cl); 127.4, 127.8 (C₂-CH₂-), 129.0 (C₆-H), 129.4 (C_{6'}-H), 130.0 (C₅-H), 130.3 (C_{5'}-H). 150.5 (C_{1,1}-O-Al); Anal. Calcd for C₃₆H₄₁O₄Al₃Cl₄: C, 56.86; H, 5.43. Found: C, 56.80; H, 5.39.

7.3.6.3 Bis[isopropoxy-{2,2'-methylenebis(4-chlorophenato)} aluminium (III)] **6g**

6 (1.56 g, 5.85 mmol) and Al(OPrⁱ)₃ (1.19 g, 5.85 mmol) in 60 cm³ of anhydrous toluene. The yield of isolated white solid: 1.29 g, 65.4 %.

IR (nujol, cm⁻³): 2924 (s), 2856 (s), 1651 (sm), 1460 (s), 1377 (s), 1311 (sm), 1285 (sm), 1152 (sm), 1092 (sm), 1024 (sm), 799 (sm), 772 (m), 670 (sm); ¹H NMR: δ (ppm) = 1.13, 1.15 (d, 12 H, -OCH(CH₃)₂); 3.24 (d, 2 H, -CH₂-, H_{ENDO}); 4.11, 4.13 (m, 2 H, -OCH(CH₃)₂); 6.92, (d, 4 H, C₃-H); 7.09, (d, 4 H, C₅-H); 7.12 (d, 4 H, C₆-H); ¹³C NMR: δ (ppm) = 24.3 (-OCH(CH₃)₂); 31.8 (-CH₂-); 63.4 (-OCH(CH₃)₂); 118.3 (C_{5,5'}-H); 126.7 (C_{4,4'}-Cl); 128.0 (C_{2,2'}-CH₂-); 128.1 (C_{6,6'}-H); 130.6 (C_{3,3'}-H); 151.2 (C_{1,1}-O-Al); Anal. Calcd for C₃₂H₃₀O₆Al₂Cl₄: (calc.) C (%) 54.41, H (%) 4.28; (found) C (%) 54.35, H (%) 4.24.

7.3.7 Syntheses of the aluminium complexes with 2,2'-thiobis(4-tert-octylphenol) 7

7.3.7.1 [(Tetrahydrofuran)-ethyl-{2,2'-thiobis(4-tert-octylphenato)}aluminium (III)] 7a

7 (1.38 g, 3.11 mmol) and the solution of Et₃Al (0.43 g, 3.73 mmol) Yield of isolated powder: 1.43 g, 80.3 %. An attempt of crystal's isolation was unsuccessful.

IR (nujol, cm⁻³): 2957 (s), 2862 (s), 1601 (sm), 1491 (s), 1459 (s), 1361 (m), 1299 (s), 1239 (s), 1059 (m), 894 (m), 831 (s), 738 (m), 741 (m), 693 (m), 666 (m); ¹H NMR: δ (ppm) = 0.03 (q, 2 H, AlCH₂CH₃), 0.53-0.07 (s, 18 H, C₄-C(CH₃)₂CH₂C(CH₃)₃), 1.01 (t, 3 H, AlCH₂CH₃), 1.21-1.32 (s, 12 H, C₄-C(CH₃)₂CH₂C(CH₃)₃), 1.53-1.67 (s, 4 H, C₄-C(CH₃)₂CH₂C(CH₃)₃), 1.75 (br s, 4 H, O(CH₂CH₂-) in THF), 3.65 (br s, 4 H, O(CH₂CH₂-) in THF), 6.55-7.70 (singlets, 6 H, C₃-H, C₅-H, C₆-H); ¹³C NMR: δ (ppm) = 8.2 (AlCH₂CH₃); 25.0 (O(CH₂CH₂-) in THF); 25.6 (AlCH₂CH₃); 31.4 (C₄-C(CH₃)₂CH₂C(CH₃)₃), 37.9 (C₄-C(CH₃)₂CH₂C(CH₃)₃), 57.0 (C₄-C(CH₃)₂CH₂C(CH₃)₃), 68.0 (O(CH₂CH₂-in THF), 117.2-145.2 (carbons C₂, C₃, C₄, C₅, C₆ of phenyl rings), 152.0 (C₁-O-Al); ²⁷Al NMR: δ (ppm) = 55.80; Anal. Calcd for C₃₄H₅₃O₃AlS: C, 71.79; H, 9.39. Found: C, 71.92; H, 9.35.

7.3.7.2 Bis[ethyl-{2,2'-thiobis(4-tert-octylphenato)}aluminium (III)] 7c

To an ice-cold solution (0°C) of 7 (1.66 g, 3.78 mmol) in 50 cm³ of anhydrous Et₂O, the solution of Et₃Al (1.03 g, 9.03 mmol) in 2 cm³ of Et₂O was added. During the 3 h, when the mixture was stirred white precipitate was formed; later it was dried in vacuum. The residue was washed twice with 35 cm³ of Et₂O, the volume of solvent was reduced to ca. 7 cm³ and stored in -20°C. Yield of isolated powder: 3.85 g, 92.5 %.

IR (nujol, cm⁻³): 2932 (s), 2860 (s), 1598 (m), 1457 (s), 1395 (m), 1364 (m), 1302 (s), 1238 (s), 1150 (m), 1102 (m), 1061 (s), 980 (sm), 894 (s), 827 (s), 767 (s), 629 (s); ¹H NMR: δ (ppm) = 0.06 (q, 4 H, AlCH₂CH₃), 1.00 (t, 6 H, AlCH₂CH₃), 0.55-0.63 (s, 2*18 H, C₄-C(CH₃)₂CH₂C(CH₃)₃), 1.19-1.30 (s, 2*12 H, C₄-C(CH₃)₂CH₂C(CH₃)₃), 1.76, 1.81 (s, 2*4 H, C₄-C(CH₃)₂CH₂C(CH₃)₃), 6.57-7.73 (singlets, 12 H, C_{3,3'}-H, C_{5,5'}-H, C_{6,6'}-H); ¹³C NMR: δ (ppm) = 7.5 (AlCH₂CH₃), 24.9 (AlCH₂CH₃), 30.5 (C_{4,4'}-C(CH₃)₂CH₂C(CH₃)₃); 30.9 (C_{4,4'}-C(CH₃)₂CH₂C(CH₃)₃); 31.0-31.5 (C_{4,4'}-C(CH₃)₂CH₂C(CH₃)₃); 37.1-37.6 (C_{4,4'}-C(CH₃)₂CH₂C(CH₃)₃); 57.0 (C_{4,4'}-C(CH₃)₂CH₂C(CH₃)₃); 116.45-144.44, (carbons C_{2,2'}, C_{3,3'}, C_{4,4'}, C_{5,5'}, C_{6,6'} of phenyl rings), 151.20 (C_{1,1'}-O-Al); Anal. Calcd for C₅₆H₉₀O₄S₂Al₂: C, 71.14; H, 9.60. Found: C, 71.24; H, 9.80.

7.3.7.3 Bis[chloro-{2,2'-thiobis(4-tert-octylphenato)}aluminium (III)] 7f

To an ice-cold solution (0°C) of **7** (1.80 g, 4.072 mmol) in 50 cm³ of anhydrous hexane, the solution of Et₂AlCl (0.54 g, 4.47 mmol) in 2 cm³ of hexane was added. During the 3 h, when the mixture was stirred white precipitate was formed; later it was dried in vacuum. The residue was washed twice with 30 cm³ of hexane, the volume of solvent was reduced to ca. 6 cm³ and stored in -20°C. Yield of the isolated solid: 1.71 g, 83.6 %.

IR (nujol, cm⁻³): 2932 (s), 2860 (s), 1598 (m), 1457 (s), 1364 (m), 1302 (s), 1150 (m), 1102 (m), 1061 (s), 894 (s), 767 (s); ¹H NMR: δ (ppm) = 0.58-0.65 (s, 2*18 H, C₄-C(CH₃)₂CH₂C(CH₃)₃), 1.22-1.28 (s, 2*12 H, C₄-C(CH₃)₂CH₂C(CH₃)₃), 1.63-1.71 (s, 2*4 H, C₄-C(CH₃)₂CH₂C(CH₃)₃), 6.77-7.53 (singlets, 12 H, C_{3,3'}-H, C_{5,5'}-H, C_{6,6'}-H); ¹³C NMR: δ (ppm) = 30.7 (C_{4,4'}-C(CH₃)₂CH₂C(CH₃)₃); 30.9 (C_{4,4'}-C(CH₃)₂CH₂C(CH₃)₃); 31.3-31.9 (C_{4,4'}-C(CH₃)₂CH₂C(CH₃)₃); 37.3-37.9 (C_{4,4'}-C(CH₃)₂CH₂C(CH₃)₃); 56.8 (C_{4,4'}-C(CH₃)₂CH₂C(CH₃)₃); 118.2-142.0, (carbons C_{2,2'}, C_{3,3'}, C_{4,4'}, C_{5,5'}, C_{6,6'} of phenyl rings), 152.3 (C_{1,1'}-O-Al); Anal. Calcd for C₅₆H₈₀O₄S₂Cl₂Al₂: C, 66.84; H, 8.01. Found: not measured.

7.3.7.4 Bis[isopropoxy-{2,2'-thiobis(4-tert-octylphenato)}aluminium(III)] 7g

7 (4.17 g, 9.43 mmol) and Al(OPrⁱ)₃ (1.75 g, 8.57 mmol), yield of isolated crystals: 3.50 g, 70.5 %.

IR (nujol, cm⁻³): 2924 (s), 2858 (s), 1603 (s), 1489 (s), 1364 (s), 1313 (s), 1246 (m), 1148 (m), 1116 (m), 933 (s), 899 (s), 835 (s), 736 (s), 705 (s), 675 (s); ¹H NMR: δ (ppm) = 0.61 (s, 2*18 H, C₄-C(CH₃)₂CH₂C(CH₃)₃); 1.24 (s, 2*12 H, C₄-C(CH₃)₂CH₂C(CH₃)₃); 1.40, 1.43 (d, 2*6 H, -OCH(CH₃)₂); 1.61 (s, 2*4 H, C₄-C(CH₃)₂CH₂C(CH₃)₃); 4.77 (m, 2 H, -OCH(CH₃)₂); 6.72, 6.75, (d, 2*2 H, C_{5,5'}-H); 7.12, 7.16, 7.19 (d, 2*2 H, C_{6,6'}-H); 7.52 (d, 2*2 H, C_{3,3'}-H); ¹³C NMR: δ (ppm) = 24.4 (-OCH(CH₃)₂); 30.5 (C₄-C(CH₃)₂CH₂C(CH₃)₃); 30.9 (C₄-C(CH₃)₂CH₂C(CH₃)₃); 31.4 (C₄-C(CH₃)₂CH₂C(CH₃)₃); 36.9 (C₄-C(CH₃)₂CH₂C(CH₃)₃); 55.9 (C₄-C(CH₃)₂CH₂C(CH₃)₃); 69.6 (-OCH(CH₃)₂); 119.8, 120.0 (C_{6,6'}); 124.3, 124.5 (C_{5,5'}-H); 127.2, 127.5 (C_{4,4'}); 130.2, 130.5 (C_{3,3'}-H); 139.9 (C_{2,2'}-S-); 151.2 (C_{1,1'}-O-Al); Anal. Calcd for C₆₂H₉₄O₆Al₂S₂: C, 70.69; H, 8.99. Found: C, 70.92; H, 9.12.

7.3.8 Syntheses of the aluminium complexes with 2-hydroxy-3,5-di-tert-butylbenzyl alcohol, **8**

7.3.8.1 Aluminium (III), bis[μ -3[2,4-di-*t*-butyl-6-(hydroxymethyl)phenolate (2-)]O:O:O':O']-pentaethyltristereoisomer, **8c**

To an ice-cold solution (0°C) of 2,4-di-*t*-butyl-6-(hydroxymethyl)phenol (1.99 g, 8.44 mmol) in 50 cm³ of anhydrous Et₂O, the solution of Et₃Al (0.86 g, 10.13 mmol) was added. The mixture was stirred for 3 h and then dried in vacuum. The residue was washed three times with 60 cm³ of Et₂O, and concentrated to ca. 5 cm³, stored in -20°C to furnish colorless crystals. Yield of colorless crystals: 1.55 g / 51.8 %.

IR (nujol, cm⁻³): 2926 (s), 2862 (s), 1464 (s), 1376 (m), 1279 (m), 1249 (m), 1044 (m), 687 (m), 645 (m); ¹H NMR: δ (ppm) = -0.28 (q, 8 H, Al_(1 and 3)CH₂CH₃), 0.17 (q, 2 H, Al₍₂₎CH₂CH₃), 0.34 (t, 6 H, Al_(1 and 3)CH₂CH₃), 0.77 (t, 3 H, Al₍₂₎CH₂CH₃), 0.89 (t, 6 H, Al_(1 and 3)CH₂CH₃) partly overlapping 0.94 (t, 3 H, Al₍₂₎CH₂CH₃); 1,20 (br s, 2*9 H, C₆-C(CH₃)₃); 1,39 (s, 2*9 H, C₄-C(CH₃)₃); 4,28 (d, 2 H, -CH₂-, J_{H-H} = 13,55 Hz, H_{EXO}); 4,98 (d, 2 H, -CH₂-, J_{H-H} = 13,55 Hz, H_{ENDO}); 6,83 (s, 2 H, C₅-H); 7,26 (s, 2 H, C₃-H); ¹³C NMR: δ (ppm) = -0.12, 1.1 (AlCH₂CH₃), 8.8 (AlCH₂CH₃), 30.2 (C₆-C(CH₃)₃), 31.7 (C₄-C(CH₃)₃), 33.7 (-CH₂-), 34.2 (C₆-C(CH₃)₃), 35.2 (C₄-C(CH₃)₃), 122.1 (C₅-H), 125.2 (C₃-H), 130.1 (C₂-CH₂-bridge), 137.5 (C₆-C(CH₃)₃), 139.9 (C_{4,4'}-C(CH₃)₃), 152.6 (C₁-O-Al); Anal. Calcd for C₄₀H₆₉O₄Al₃: C, 69.13; H, 10.00. Found: C, 69.22; H, 10.12.

7.3.8.2 Bis[isopropoxy-{2-oxo-3,5-di-*tert*-butylbenzyl alcoholate}aluminium(III)], **8g**

8 (2.50 g, 10.60 mmol) and Al(OPrⁱ)₃ (2.16 g, 10.60 mmol), yield of isolated crystals: 2.13 g, 65.3 %.

IR (nujol, cm⁻³): 2935 (s), 2859 (s), 1459 (s), 1368 (m), 1281 (m), 1251 (m), 1043 (m), 933 (s), 899 (m), 687 (m), 645 (m); ¹H NMR: δ (ppm) = 1.22 (br s, 2*9 H, C₆-C(CH₃)₃); 1.40 (s, 2*9 H, C₄-C(CH₃)₃); 1.45 (d, 12 H, -OCH(CH₃)₂); 4.41 (d, 2 H, -CH₂-, J_{H-H} = 13.55 Hz, H_{EXO}); 4.93 (d, 2 H, -CH₂-, J_{H-H} = 13.55 Hz, H_{ENDO}); 7.05 (s, 2 H, C₅-H); 7.26 (s, 2 H, C₃-H); ¹³C NMR: δ (ppm) = 24.9 (-OCH(CH₃)₂); 30.6 (C₆-C(CH₃)₃), 31.4 (C₄-C(CH₃)₃), 33.1 (-CH₂-), 33.9 (C₆-C(CH₃)₃), 35.4 (C₄-C(CH₃)₃), 69.2 (-OCH(CH₃)₂); 122.4 (C₅-H), 125.4 (C₃-H), 129.8 (C₂-CH₂-bridge), 137.5 (C₆-C(CH₃)₃), 140.0 (C_{4,4'}-C(CH₃)₃), 153.5 (C₁-O-Al); Anal. Calcd for C₄₀H₆₉O₄Al₃: C, 68;65 H, 8.79. Found: C, 68.72; H, 8.82.

7.4 Synthesis of polymers

7.4.1 Purification of the polymer

The exact description of polymer syntheses as well as the whole equipment is presented in the Chapter 3.3.1. The extracted copolymer was dissolved in methylene dichloride, the catalyst was decomposed using $\text{HCl}_{(\text{aq})}$, then the traces of HCl in the organic layer were treated with NaHCO_3 . So obtained polymer solution was dried and then the large quantity of methanol was added in order to separation of short-chain polymer. The methanol-insoluble polymer was dried in vacuum at 40 °C till constant weight.

7.4.2 Spectroscopic data of polymers

In order to distinguish the different hydrogen and carbon atoms in polymer chain, they are signed as follow:

H_{CHO} – hydrogen atoms in cyclohexene cycle, located the farthest and in the middle from both ether and carbonate groups,

H_{ether} – hydrogen atoms in cyclohexene cycle, located the nearest to oxygen in ether,

$\text{H}_{\text{carbonate}}$ – hydrogen atoms in cyclohexene cycle, located the nearest from carbonate group,

$\text{C}_{\text{CHO-1}}$ – carbons in cyclohexene cycle, located the farthest from both ether and carbonate groups,

$\text{C}_{\text{CHO-2}}$ – carbons in cyclohexene cycle, located in the middle of one

C_{ether} – carbons in ether part, located the nearest to oxygen in ether's bridge

$\text{C}_{\text{carbonate}}$ – carbon of carbonate group.

Detailed NMR and IR spectra of isolated crude and long-chain polymers are presented below. As a short-chain polymer fraction CHO and two-three members cyclohexene rings oligomers were isolated and because of that were not described.

7.4.3 Copolymers synthesised with catalysts having 1 as the ligand

7.4.3.1 Copolymer P-1a

Crude copolymer: (Al / CHO) = 1 / 1000

$^1\text{H NMR}$: δ (ppm) = H_{CHO} : 0.72, 1.07, 1.24, 1.54, 1.82, 1.91, 2.03; H_{ether} : 3.28, 3.37; $\text{H}_{\text{carbonate}}$: 4.65; $^{13}\text{C NMR}$: δ (ppm) = $\text{C}_{\text{CHO-1}}$: 19.59, 22.60, 24.18; $\text{C}_{\text{CHO-2}}$: 29.38, 30.05; C_{ether} : 76.40, 77.80, 78.34; $\text{C}_{\text{carbonate}}$: 154.60; IR (KBr, cm^{-3}): 2935 (s), 2860 (s), 2672 (sm), 1741 (sm), 1438 (m), 1367 (sm), 1260 (m), 1158 (m), 1088 (s), 966 (m), 892 (m), 781 (m).

Long-chain polymer: $^1\text{H NMR}$: δ (ppm) = H_{CHO} : 1.44, 1.66, 1.83, 2.19; H_{ether} : 3.66, 3.76; $\text{H}_{\text{carbonate}}$: 5.09; $^{13}\text{C NMR}$: δ (ppm) = $\text{C}_{\text{CHO-1}}$: 23,24; $\text{C}_{\text{CHO-2}}$: 29,69; C_{ether} : 77.07, 78.26, 78.97;

$C_{\text{carbonate}}$: peak is invisible; IR (KBr, cm^{-3}): 3457 (m), 2933 (s), 2869 (m), 1737 (m, very br.), 1459 (s), 1263 (m), 1159 (m), 1087 (s), 1020 (m), 836 (m), 692 (m).

Crude copolymer: (Al / CHO) = 1 / 300

^1H NMR: δ (ppm) = H_{CHO} : 0.72, 1.07, 1.24, 1.54, 1.82, 1.91, 2.03; H_{ether} : 3.28, 3.37; $H_{\text{carbonate}}$: 4.65; ^{13}C NMR: δ (ppm) = $C_{\text{CHO-1}}$: 19.59, 22.60, 24.18; $C_{\text{CHO-2}}$: 29.38, 30.05; C_{ether} : 76.40, 77.80, 78.34; $C_{\text{carbonate}}$: 154.60; IR (KBr, cm^{-3}): 2935 (s), 2860 (s), 2672 (sm), 1741 (sm), 1438 (m), 1367 (sm), 1260 (m), 1158 (m), 1088 (s), 966 (m), 892 (m), 781 (m).

Long-chain polymer: ^1H NMR: δ (ppm) = H_{CHO} : 1.42, 1.67, 1.79, 2.25; H_{ether} : 3.76; $H_{\text{carbonate}}$: 5.09; ^{13}C NMR: δ (ppm) = $C_{\text{CHO-1}}$: 23,22; $C_{\text{CHO-2}}$: 29,91; C_{ether} : 77.12, 78.58, 78.75; $C_{\text{carbonate}}$: peak is invisible.; IR (KBr, cm^{-3}): 3457 (m), 2933 (s), 2869 (m), 1737 (m, very br.), 1459 (s), 1263 (m), 1159 (m), 1087 (s), 1020 (m), 836 (m), 692 (m).

7.4.3.2 Polymer P-1b

Crude copolymer: ^1H NMR: δ (ppm) = H_{CHO} : 1.37, 1.64, 1.84; 2.25; H_{ether} : 3.66; 3.75; $H_{\text{carbonate}}$: 5.09; ^{13}C NMR: δ (ppm) = $C_{\text{CHO-1}}$: 22.21, 22.98; $C_{\text{CHO-2}}$: 29.48, 30.01; C_{ether} : 76.97, 77.88, 78.41; $C_{\text{carbonate}}$: 154.95; IR (KBr, cm^{-3}): 3449 (m), 2935 (s), 2860 (s), 1743 (s), 1450 (m), 1366 (m), 1260 (s), 1160 (m), 1089 (s), 1020 (m), 859 (sm), 730 (sm).

Long-chain polymer: ^1H NMR: δ (ppm) = H_{CHO} : 1.36, 1.42, 1.82, 2.20; H_{ether} : 3.67, 3.76; $H_{\text{carbonate}}$: 5.10; ^{13}C NMR: δ (ppm) = $C_{\text{CHO-1}}$: 19.59, 22.97, 23.34, 24.61, 25,26; $C_{\text{CHO-2}}$: 29.55, 30.04, 33.07, 34.90; C_{ether} : 67.37, 74.94, 76.48, 74.73, 76.92, 77.83, 78.43; $C_{\text{carbonate}}$: 154.61, 154.73, 154.83, 154.94; IR (KBr, cm^{-3}): 3447 (sm), 2936 (s), 2861 (s), 2665 (sm), 1743 (s), 1450 (s), 1366 (s), 1260 (s), 1159 (s), 1087 (s), 1020 (m).

7.4.3.3 Copolymer P-1c

Crude copolymer: ^1H NMR: δ (ppm) = H_{CHO} : 1.03, 1.29, 1.49, 1.84, 1.87; H_{ether} : 3.31; 3.40; $H_{\text{carbonate}}$: 4.73; ^{13}C NMR: δ (ppm) = $C_{\text{CHO-1}}$: 19.57, 22.70, 24.80; $C_{\text{CHO-2}}$: 29.88, 32.54; C_{ether} : 76.50, 77.64, 78.17; $C_{\text{carbonate}}$: 154.30; IR (KBr, cm^{-3}): 2935 (s), 2860 (s), 2672 (sm), 1741 (m), 1438 (s), 1367 (m), 1260 (m), 1160 (m), 1087 (s), 966 (m), 891 (m), 781 (m).

Long-chain polymer: ^1H NMR: δ (ppm) = H_{CHO} : 1.26, 1.48, 1.64, 1.67, 2.03; H_{ether} : 3.50, 3.60; $H_{\text{carbonate}}$: 4.93; ^{13}C NMR: δ (ppm) = $C_{\text{CHO-1}}$: 22.99, 23.70; $C_{\text{CHO-2}}$: 29.50, 30.13; C_{ether} : 76.80, 77.88, 78.49; $C_{\text{carbonate}}$: 154.85; IR (KBr, cm^{-3}): 3449 (m), 2935 (s), 2862 (s), 1743 (s), 1446 (m), 1367 (m), 1261 (s), 1160 (m), 1089 (s), 1021 (m).

7.4.3.4 Copolymer P-1d

Crude copolymer: ^1H NMR: δ (ppm) = H_{CHO} : 1.28, 1.35, 1.47, 1.69, 1.73, 2.03; H_{ether} : 3.50, 3.58; $\text{H}_{\text{carbonate}}$: 4.92; ^{13}C NMR: δ (ppm) = $\text{C}_{\text{CHO-1}}$: 22.19, 22.98; $\text{C}_{\text{CHO-2}}$: 29.47, 30.09; C_{ether} : 76.78, 77.83, 78.43; $\text{C}_{\text{carbonate}}$: 152.94; IR (KBr, cm^{-3}): 3449 (sm), 2935 (s), 2862 (s), 2667 (sm), 1743 (s), 1451 (s), 1367 (s), 1260 (s), 1160 (m), 1089 (s), 1021 (m), 859 (m), 730 (m), 695 (sm).

Long-chain polymer: ^1H NMR: δ (ppm) = H_{CHO} : 1.45, 1.68, 1.86, 2.24; H_{ether} : 3.80; $\text{H}_{\text{carbonate}}$: 5.13; ^{13}C NMR: δ (ppm) = $\text{C}_{\text{CHO-1}}$: 22.99, 23.70; $\text{C}_{\text{CHO-2}}$: 29.50, 30.13; C_{ether} : 76.85, 77.91; $\text{C}_{\text{carbonate}}$: 154.86; IR (KBr, cm^{-3}): 3452 (sm), 2936 (s), 2863 (s), 2665 (sm), 1744 (s), 1455 (m), 1366 (m), 1260 (s), 1160 (m), 1089 (s), 1020 (m).

7.4.3.5 Copolymer P-1e

Crude copolymer: ^1H NMR: δ (ppm) = H_{CHO} : 1.03, 1.44, 1.66, 1.87, 2.23; H_{ether} : 3.68, 3.78; $\text{H}_{\text{carbonate}}$: 5.11; ^{13}C NMR: δ (ppm) = $\text{C}_{\text{CHO-1}}$: 23.22; $\text{C}_{\text{CHO-2}}$: 29.54, 30.72; C_{ether} : 76.47, 77.50, 78.50; $\text{C}_{\text{carbonate}}$: 154.18; IR (KBr, cm^{-3}): 2935 (s), 2862 (s), 1743 (s), 1451 (s), 1365 (s), 1260 (s), 1160 (s), 1083 (s), 1020 (m), 895 (s), 859 (s), 783 (m).

Long-chain polymer: ^1H NMR: δ (ppm) = H_{CHO} : 1.46, 1.69, 1.88, 2.23; H_{ether} : 3.70, 3.80; $\text{H}_{\text{carbonate}}$: 5.13; ^{13}C NMR: δ (ppm) = $\text{C}_{\text{CHO-1}}$: 23.00; $\text{C}_{\text{CHO-2}}$: 29.50, 30.22; C_{ether} : 76.97, 77.97, 78.43; $\text{C}_{\text{carbonate}}$: 154.96; IR (KBr, cm^{-3}): 2935 (s), 2862 (s), 1743 (s), 1451 (m), 1367 (m), 1260 (s), 1160 (m), 1089 (s), 1020 (m), 859 (m), 738 (m).

7.4.3.6 Copolymer P-1f

Crude copolymer: ^1H NMR: δ (ppm) = H_{CHO} : 1.43, 1.66, 1.82, 2.20; H_{ether} : 3.75; $\text{H}_{\text{carbonate}}$: 5.10; ^{13}C NMR: δ (ppm) = $\text{C}_{\text{CHO-1}}$: 22.21, 22.91; $\text{C}_{\text{CHO-2}}$: 29.47, 30.12; C_{ether} : 76.46, 76.75, 77.90, 78.51; $\text{C}_{\text{carbonate}}$: 154.72; IR (KBr, cm^{-3}): 3434 (m), 2936 (s), 2862 (s), 1743 (s), 1457 (s), 1365 (m), 1260 (s), 1160 (m), 1089 (s), 895 (m), 859 (m), 783 (m), 736 (m).

Long-chain polymer: ^1H NMR: δ (ppm) = H_{CHO} : 1.44, 1.68, 1.86, 2.24; H_{ether} : 3.71, 3.79; $\text{H}_{\text{carbonate}}$: 5.13; ^{13}C NMR: δ (ppm) = $\text{C}_{\text{CHO-1}}$: 22.44, 23.13; $\text{C}_{\text{CHO-2}}$: 29.67, 30.26; C_{ether} : 76.78, 78.17, 78.72; $\text{C}_{\text{carbonate}}$: 155.15; IR (KBr, cm^{-3}): 3436 (m), 2935 (s), 2864 (m), 1743 (s), 1457 (s), 1365 (m), 1260 (s), 1160 (m), 1089 (s), 895 (m), 860 (m), 784 (m), 736 (m).

7.4.3.7 Copolymer P-1g

Crude product: ^1H NMR: δ (ppm) = H_{CHO} : 1.00, 1.34; 1.39; 1.63, 2.19; H_{ether} : 3.66, 3.75; $\text{H}_{\text{carbonate}}$: 5.08; ^{13}C NMR: δ (ppm) = $\text{C}_{\text{CHO-1}}$: 22.85; $\text{C}_{\text{CHO-2}}$: 29.52; C_{ether} : 77.58, 78.14; $\text{C}_{\text{carbonate}}$: 154.19; IR (KBr, cm^{-3}): 3448 (m), 2940 (s), 2868 (s), 1741 (m), 1449 (s), 1266 (s), 1089 (s), 892 (m), 762 (s).

Long-chain polymer: ^1H NMR: δ (ppm) = H_{CHO} : 1.27, 1.42, 1.66, 1.82, 2.20; H_{ether} : 3.66, 3.77; $\text{H}_{\text{carbonate}}$: 5.09; ^{13}C NMR: δ (ppm) = $\text{C}_{\text{CHO-1}}$: 23.23; $\text{C}_{\text{CHO-2}}$: 29.83; C_{ether} : 77.05, 78.70; $\text{C}_{\text{carbonate}}$: 153.85; IR (KBr, cm^{-3}): 2936 (s), 2864 (s), 1745 (s), 1453 (m), 1367 (m), 1260 (s), 1159 (m), 1090 (s).

7.4.4 Copolymers synthesised with catalysts having 2 as the ligand

7.4.4.1 Copolymer P-2a

Crude product: ^1H NMR: δ (ppm) = H_{CHO} : 1.03, 1.36, 1.53, 1.75, 1.86, 2.09, 2.19; H_{ether} : 3.57, 3.66, 3.76; $\text{H}_{\text{carbonate}}$: 4.95; ^{13}C NMR: δ (ppm) = $\text{C}_{\text{CHO-1}}$: 18.42; $\text{C}_{\text{CHO-2}}$: 23.43; C_{ether} : 77.25; $\text{C}_{\text{carbonate}}$: 153.33; IR (KBr, cm^{-3}): 2935 (s), 2861 (s), 1741 (m), 1439 (m), 1260 (m), 1089 (s), 966 (m), 891 (m), 837 (m), 781 (m).

Long-chain polymer: ^1H NMR: δ (ppm) = H_{CHO} : 1.34, 1.43, 1.47, 1.70, 1.89, 2.24; H_{ether} : 3.70, 3.79; $\text{H}_{\text{carbonate}}$: 5.11; ^{13}C NMR: δ (ppm) = $\text{C}_{\text{CHO-1}}$: 22.43, 23.13; $\text{C}_{\text{CHO-2}}$: 29,60; C_{ether} : 77.14, 78.43, 78.90; $\text{C}_{\text{carbonate}}$: 155.16; IR (KBr, cm^{-3}): 2940 (s), 2864 (s), 1459 (s), 1374 (sm), 1260 (s), 853 (sm), 678 (sm).

7.4.4.2 Copolymer P-2b

Crude product: ^1H NMR: δ (ppm) = H_{CHO} : 1.03, 1.34, 1.55, 1.75, 1.81, 1.83, 2.09, 2.20; H_{ether} : 3.55, 3.64, 3.75; $\text{H}_{\text{carbonate}}$: 4.83, 4.93; ^{13}C NMR: δ (ppm) = $\text{C}_{\text{CHO-1}}$: 18.42; $\text{C}_{\text{CHO-2}}$: 23.43; C_{ether} : 75.19, 76.59, 77.14; $\text{C}_{\text{carbonate}}$: 153.33; IR (KBr, cm^{-3}): 2935 (s), 2860 (s), 1741 (m), 1441 (m), 1260 (m), 1089 (s), 967 (sm), 892 (m), 837 (m), 781 (m).

Long-chain polymer: ^1H NMR: δ (ppm) = H_{CHO} : 1.44, 1.69, 1.88, 2.24; H_{ether} : 3.70, 3.80; $\text{H}_{\text{carbonate}}$: 5.12; ^{13}C NMR: δ (ppm) = $\text{C}_{\text{CHO-1}}$: 22.81, 23.25; $\text{C}_{\text{CHO-2}}$: 29.95, 30.62; C_{ether} : 77.06, 78.10, 78.50; $\text{C}_{\text{carbonate}}$: 155.30.

IR (KBr, cm^{-3}): 3443 (m), 2935 (s), 2862 (m), 1745 (s), 1454 (s), 1368 (m), 1264 (s), 1161 (m), 1088 (s), 897 (sm), 856 (sm), 784 (sm).

7.4.4.3 Copolymerisation with 2c catalyst

As a result of the copolymerisation process 19,35 g of a yellow, viscous, transparent solution was obtained, which was identified as unreacted cyclohexene oxide. Owing to this fact further analysis were abandoned.

^1H NMR: δ (ppm) = 0.96, 1.25, 1.50, 1.76, 2.83(signals were identified as coming from CHO); IR (KBr, cm^{-3}): 2939 (m), 2862 (sm), 1438 (sm), 1257 (v-sm), 1084 (v-sm), 967 (v-sm), 891 (v-sm), 837 (sm), 781 (sm).

7.4.4.4 Copolymerisation with 2d catalyst

As a result of the copolymerisation process 16,90 g of a yellow, viscous, transparent solution was obtained, which was identified as unreacted cyclohexene oxide. Owing to this fact further analysis were abandoned.

$^1\text{H NMR}$: δ (ppm) = 0.96, 1.25, 1.50, 1.76, 2.83 (signals were identified as coming from CHO); IR (KBr, cm^{-3}): 2939 (m), 2862 (sm), 1438 (sm), 1257 (v-sm), 1084 (v-sm), 967 (v-sm), 891 (v-sm), 837 (sm), 781 (sm).

7.4.4.5 Copolymer P-2e

Crude product: $^1\text{H NMR}$: δ (ppm) = H_{CHO} : 1.04, 1.37, 1.75, 1.86, 2.19; H_{ether} : 3.67, 3.75 ; $\text{H}_{\text{carbonate}}$: 5.09; $^{13}\text{C NMR}$: δ (ppm) = $\text{C}_{\text{CHO-1}}$: 22.89, 23.45; $\text{C}_{\text{CHO-2}}$: 30.50, 30.82; C_{ether} : 77.28, 78.51; $\text{C}_{\text{carbonate}}$: 155.25, 155.32; IR (KBr, cm^{-3}): 2935 (s), 2860 (m), 2578 (vs, b), 1742 (m), 1441 (m), 1260 (m), 1089 (m), 967 (m), 895 (sm), 781 (sm), 752 (m).

Long-chain polymer: $^1\text{H NMR}$: δ (ppm) = H_{CHO} : 1.38, 1.60, 1.77, 2.16; H_{ether} : 3.71; $\text{H}_{\text{carbonate}}$: 5.04; $^{13}\text{C NMR}$: δ (ppm) = $\text{C}_{\text{CHO-1}}$: 22.72, 22.91; $\text{C}_{\text{CHO-2}}$: 30.73, 30.82; C_{ether} : 77.43, 78.21; $\text{C}_{\text{carbonate}}$: 155.18, 155.35, 155.47; IR (KBr, cm^{-3}): 2938 (s), 2864 (m), 1744 (s), 1454 (m), 1366 (m), 1260 (s), 1160 (m), 1089 (s).

7.4.4.6 Copolymer P-2f

Crude product: $^1\text{H NMR}$: δ (ppm) = H_{CHO} : 1.40, 1.53, 1.64, 1.85, 2.19; H_{ether} : 3.67, 3.75; $\text{H}_{\text{carbonate}}$: 4.72, 5.19; $^{13}\text{C NMR}$: δ (ppm) = $\text{C}_{\text{CHO-1}}$: 21.83, 23.43; $\text{C}_{\text{CHO-2}}$:, 28.98; C_{ether} : 76.31; $\text{C}_{\text{carbonate}}$: 153.68, 156.41; IR (KBr, cm^{-3}): 2931 (s), 2860 (s), 2578 (s), 1741 (m), 1459 (m), 1261 (m), 1089 (m), 753 (m).

Long-chain polymer: $^1\text{H NMR}$: δ (ppm) = H_{CHO} : 1.06, 1.28, 1.45, 1.84, 2.16; H_{ether} : 3.38; $\text{H}_{\text{carbonate}}$: 4.72; $^{13}\text{C NMR}$: δ (ppm) = $\text{C}_{\text{CHO-1}}$: 23.51; $\text{C}_{\text{CHO-2}}$:, 30.51, 30.76; C_{ether} : 77.16, 79.09; $\text{C}_{\text{carbonate}}$: 155.16, 155.20, 155.26, 155.37, 155.50; IR (KBr, cm^{-3}): 2983 (s), 2864 (m), 1744 (s), 1454 (m), 1366 (m), 1260 (s), 1160 (m), 1089 (s), 1020 (m).

7.4.4.7 Copolymer P-2g

Crude product: $^1\text{H NMR}$: δ (ppm) = H_{CHO} : 1.04, 1.42, 1.62, 1.66, 1.89, 2.23; H_{ether} : 3.75, 3.80; $\text{H}_{\text{carbonate}}$: 5.13; $^{13}\text{C NMR}$: δ (ppm) = $\text{C}_{\text{CHO-1}}$: 22.94; $\text{C}_{\text{CHO-2}}$: 28.93, 29.40, 30.12; C_{ether} : 77.89, 77.67; $\text{C}_{\text{carbonate}}$: 155.12; IR (KBr, cm^{-3}): 3458 (m), 2937 (s), 2862 (m), 1743 (s), 1452 (m), 1365 (m), 1260 (s), 1160 (m), 1089 (s), 894 (m), 782 (m).

Long-chain polymer: $^1\text{H NMR}$: δ (ppm) = H_{CHO} : 1.47, 1.61, 1.64, 1.79; H_{ether} : 3.75; $\text{H}_{\text{carbonate}}$: 5.07; $^{13}\text{C NMR}$: δ (ppm) = $\text{C}_{\text{CHO-1}}$: 19.54, 22.88, 24.54; $\text{C}_{\text{CHO-2}}$: 29.25, 29.99; C_{ether} : 76.50, 77.69;

$C_{\text{carbonate}}$: 154.84; IR (KBr, cm^{-3}): 3446 (m), 2939 (s), 2864 (m), 1744 (s), 1455 (m), 1366 (m), 1260 (s), 1160 (m), 1089 (s), 898 (m), 785 (m), 736 (m).

7.4.4.8 Copolymerisation with 2h catalyst

As a result of the copolymerisation process a yellow, viscous, transparent solution was obtained, which was identified as unreacted cyclohexene oxide. Owing to this fact further analysis were abandoned.

^1H NMR: δ (ppm) = 0.96, 1.25, 1.50, 1.76, 2.83 (signals were identified as coming from CHO); IR (KBr, cm^{-3}): 2939 (m), 2862 (sm), 1438 (sm), 1257 (v-sm), 1084 (v-sm), 967 (v-sm), 891 (v-sm), 837 (sm), 781 (sm).

7.4.5 Copolymers synthesised with catalysts having 3 as the ligand

7.4.5.1 Copolymer P-3a

Crude product: ^1H NMR: δ (ppm) = H_{CHO} : 0.86, 1.20, 1.36, 1.44, 1.66, 1.91, 2.00; H_{ether} : 3.45, 3.55, 3.61; $\text{H}_{\text{carbonate}}$: 4.75, 4.87; ^{13}C NMR: δ (ppm) = $\text{C}_{\text{CHO-1}}$: 19.60, 22.96, 23.43, 24.61; $\text{C}_{\text{CHO-2}}$: 29.50, 29.98; C_{ether} : 76.59, 77.93; $\text{C}_{\text{carbonate}}$: 154.67; IR (KBr, cm^{-3}): 3429 (m), 2940 (s), 2864 (s), 1742 (s), 1459 (m), 1366 (m), 1266 (s), 1163 (m), 1095 (s), 1019 (m), 893 (sm), 840 (sm), 786 (sm).

Long-chain polymer: ^1H NMR: δ (ppm) = H_{CHO} : 1.02, 1.23, 1.46, 1.83, 2.20; H_{ether} : 3.30, 3.38; $\text{H}_{\text{carbonate}}$: 4.72; ^{13}C NMR: δ (ppm) = $\text{C}_{\text{CHO-1}}$: 22.90, 22.97; $\text{C}_{\text{CHO-2}}$: 29.26; C_{ether} : 76.27, 77.88; $\text{C}_{\text{carbonate}}$: 154.95; IR (KBr, cm^{-3}): 3458 (m), 2940 (s), 2868 (s), 2665 (sm), 1752 (s), 1454 (s), 1378 (s), 1261 (s), 1158 (s), 1091 (s), 1015 (m), 790 (sm).

7.4.5.2 Copolymer P-3b

Crude product: ^1H NMR: δ (ppm) = H_{CHO} : 0.86, 1.20, 1.36, 1.44, 1.66, 1.91, 2.00; H_{ether} : 3.45, 3.55, 3.61; $\text{H}_{\text{carbonate}}$: 4.87; ^{13}C NMR: δ (ppm) = $\text{C}_{\text{CHO-1}}$: 22.40, 22.96, 23.83; $\text{C}_{\text{CHO-2}}$: 29.57, 29.98; C_{ether} : 77.59, 77.93; $\text{C}_{\text{carbonate}}$: 155.67; IR (KBr, cm^{-3}): 3429 (m), 2940 (s), 2864 (s), 1742 (s), 1459 (m), 1366 (m), 1266 (s), 1163 (m), 1095 (s), 1019 (m), 893 (sm), 840 (sm), 786 (sm).

Long-chain polymer: ^1H NMR: δ (ppm) = H_{CHO} : 1.12, 1.23, 1.44, 1.86, 2.19; H_{ether} : 3.36, 3.38; $\text{H}_{\text{carbonate}}$: 4.72; ^{13}C NMR: δ (ppm) = $\text{C}_{\text{CHO-1}}$: 22.20, 22.87; $\text{C}_{\text{CHO-2}}$: 29.86; C_{ether} : 76.27, 77.27; $\text{C}_{\text{carbonate}}$: 155.86; IR (KBr, cm^{-1}): 2935 (s), 2870 (s), 1749 (s), 1452 (s), 1382 (s), 1259 (s), 1191 (s), 1089 (s), 1021 (m).

7.4.5.3 Copolymer P-3c

Crude polymer: ^1H NMR: δ (ppm) = H_{CHO} : 1.06, 1.18, 1.40, 1.56, 1.85, 2.05, 2.18; H_{ether} : 3.21, 3.31, 3.56, 3.68, 3.79; $\text{H}_{\text{carbonate}}$: 4.24, 4.44, 4.83, 5.10, 5.14, 5.34, 5.77, 5.90; ^{13}C NMR: δ (ppm) =

$C_{\text{CHO-1}}$: 24.74, 25.23; $C_{\text{CHO-2}}$: 30.12, 30.66, 33.35; C_{ether} : 75.92, 77.77, 78.59, 80.49, 81.69, 81.88, 84.01, 85.22, 86.09; $C_{\text{carbonate}}$: 153.09, 155.24, 155.63; IR (KBr, cm^{-3}): 3434 (m), 2930 (s), 2861 (s), 1735 (s), 1450 (s), 1369 (m), 1261 (m), 1087 (s), 966 (m), 891 (m), 838 (m), 782 (m), 745 (m).

Long-chain polymer: ^1H NMR: δ (ppm) = H_{CHO} : 1.42, 1.62, 2.20; H_{ether} : 3.67; 3.75; $\text{H}_{\text{carbonate}}$: 5.10; ^{13}C NMR: δ (ppm) = $C_{\text{CHO-1}}$: 22,20, 22,67; $C_{\text{CHO-2}}$: 29,26, 30.18; C_{ether} : 76,82, 77,59; $C_{\text{carbonate}}$: 153.09, 155.24, 155.63; IR (KBr, cm^{-3}): 3445 (m), 2931 (m), 2864 (sm), 1735 (sm), 1699 (sm), 1652 (m), 1559 (m), 1542 (m), 1458 (m), 1260 (m), 1095 (m), 668(sm).

7.4.5.4 Copolymer P-3d

Crude polymer: ^1H NMR: δ (ppm) = H_{CHO} : 1.15; 1.20; 1.42. 1.67; 1.75; 1.83; H_{ether} : 3.30; 3.36; $\text{H}_{\text{carbonate}}$: 4.60; ^{13}C NMR: δ (ppm) = $C_{\text{CHO-1}}$: 19.50; 22.50; 24.60 ; $C_{\text{CHO-2}}$: 29.88; 32.54 ; C_{ether} : 76.54; 77.68; 78.22; $C_{\text{carbonate}}$: 154.33; 154.45; 154.55; IR (KBr, cm^{-3}): 2934 (s), 2862 (s), 1743 (s), 1452 (s), 1365 (m), 1260 (s), 1159 (m), 1089 (s), 894 (m), 782 (m).

Long-chain polymer: ^1H NMR: δ (ppm) = H_{CHO} : 1,04, 1,27, 1,45, 1,84, 1,94; H_{ether} : 3,29, 3,40; $\text{H}_{\text{carbonate}}$: 4,72; ^{13}C NMR: δ (ppm) = $C_{\text{CHO-1}}$: 21.47, 21.78; $C_{\text{CHO-2}}$: 28.22; C_{ether} : 75.74, 76.73; $C_{\text{carbonate}}$: 153.65; IR (KBr, cm^{-3}): 3452 (m), 2935 (s), 2863 (s), 1743 (s), 1454 (s), 1365 (m), 1260 (s), 1160 (s), 1090 (s), 1018 (m), 895 (m), 840 (m), 83 (m), 746 (m).

7.4.5.5 Copolymer P-3e

Crude polymer: ^1H NMR: δ (ppm) = H_{CHO} : 1.08; 1.26; 1.45. 1.82; 1.86; H_{ether} : 3.30. 3.39; $\text{H}_{\text{carbonate}}$: 4.72; ^{13}C NMR: δ (ppm) = $C_{\text{CHO-1}}$: 19.60; 22.99; $C_{\text{CHO-2}}$: 29.57; 30.17; C_{ether} : 76.73; 77.93; 78.45; $C_{\text{carbonate}}$: 154.85; IR (KBr, cm^{-3}): 3452 (m), 2938 (s), 2863 (s), 1744 (s), 1457 (m), 1371 (m), 1260 (s), 1160 (m), 1089 (s), 1017 (m), 853 (sm), 735 (sm).

Long-chain polymer: ^1H NMR: δ (ppm) = H_{CHO} : 1.04, 1.27, 1.45, 1.82; H_{ether} : 3.30, 3.39; $\text{H}_{\text{carbonate}}$: 4.72; ^{13}C NMR: δ (ppm) = $C_{\text{CHO-1}}$: 22.23, 22.86; $C_{\text{CHO-2}}$: 29.24, 29.55, 30.00; C_{ether} : 76.46, 78.38; $C_{\text{carbonate}}$: 154.83; IR (KBr, cm^{-3}): 3452 (m), 2940 (s), 2863 (s), 1745 (s), 1457 (s), 1371 (s), 1260 (s), 1160 (m), 1089 (s), 1015 (m), 785 (sm).

7.4.5.6 Copolymer P-3f

Crude polymer: ^1H NMR: δ (ppm) = H_{CHO} : 1.44, 1.56, 1.67, 1.88, 2.22; H_{ether} : 3.69, 3.78; $\text{H}_{\text{carbonate}}$: 5.11; ^{13}C NMR: δ (ppm) = $C_{\text{CHO-1}}$: 22.71, 23.40; $C_{\text{CHO-2}}$: 29.90, 30.72; C_{ether} : 76.75, 77.40; $C_{\text{carbonate}}$: 154.59; IR (KBr, cm^{-3}): 3447 (m), 2935 (s), 2861 (s), 1743 (s), 1450 (s), 1367 (s), 1261 (s), 1159 (s), 1088 (s), 893 (sm), 838 (sm), 782 (sm), 746 (sm), 610 (sm).

Long-chain polymer: ^1H NMR: δ (ppm) = H_{CHO} : 1.40, 1.61, 1.83, 2.19; H_{ether} : 3.67, 3.75, $\text{H}_{\text{carbonate}}$: 5.07; ^{13}C NMR: δ (ppm) = $C_{\text{CHO-1}}$: 22.63, 23.48; $C_{\text{CHO-2}}$: 30.04, 30.56; C_{ether} : 76.89, 78.25;

$C_{\text{carbonate}}$: 154.93, 155.54; IR (KBr, cm^{-3}): 2942 (s), 2875 (s), 1749 (s), 1456 (s), 1379 (s), 1260 (s), 1160 (s), 1089 (s), 1015 (m), 787 (sm).

7.4.5.7 Copolymer P-3g

Crude polymer: ^1H NMR: δ (ppm) = H_{CHO} : 1.45, 1.68, 1.86, 2.24; H_{ether} : 3.71, 3.79; $\text{H}_{\text{carbonate}}$: 5, 13; ^{13}C NMR: δ (ppm) = $\text{C}_{\text{CHO-1}}$: 23.22, 23.65; $\text{C}_{\text{CHO-2}}$: 29.32, 29.74, 30.31....; C_{ether} : 76.92, 77.16, 78.11, 78.61, 78.80; $\text{C}_{\text{carbonate}}$: 154.82, 154.90, 155.03, 155.11; IR (KBr, cm^{-3}): 2935 (s), 2860 (s), 1739 (s), 1459 (m), 1371 (m), 1260 (s), 1158 (m), 1088 (s), 1017 (m), 893 (m), 837 (m), 781 (m), 666 (m).

Long-chain polymer: ^1H NMR: δ (ppm) = H_{CHO} : 1.46, 1.69, 1.87, 2.25; H_{ether} : 3.72, 3.81,...; $\text{H}_{\text{carbonate}}$: 5.14; ^{13}C NMR: δ (ppm) = $\text{C}_{\text{CHO-1}}$: 22.87, 23.11; $\text{C}_{\text{CHO-2}}$: 29.27, 29.65, 30.226; C_{ether} : 76.886, 77.962, 78.663; $\text{C}_{\text{carbonate}}$: 154.94, 155.05, 155.16; IR (KBr, cm^{-3}): 3457 (sm), 2935 (s), 2864 (s), 1743 (s), 1458 (s), 1368 (s), 1262 (s), 1158 (s), 1089 (s).

7.4.6 Copolymers synthesised with catalysts having 4 as the ligand

7.4.6.1 Copolymer P-4a

Crude product: ^1H NMR: δ (ppm) = H_{CHO} : 1.08, 1.10, 1.48, 1.83; H_{ether} : 3.29, 3.39; 3.51; $\text{H}_{\text{carbonate}}$: 4.71; ^{13}C NMR: δ (ppm) = $\text{C}_{\text{CHO-1}}$: 19.76, 23.43, 24.77; $\text{C}_{\text{CHO-2}}$: 30.17; C_{ether} : 76.51, 78.09; $\text{C}_{\text{carbonate}}$: 154.91; IR (KBr, cm^{-3}): 3447 (s), 2935 (s), 2860 (m), 1743 (s), 1457 (m), 1371 (m), 1260 (m), 1159 (m), 1087 (s), 894 (m), 839 (m), 782 (m), 745 (sm).

Long-chain polymer: ^1H NMR: δ (ppm) = H_{CHO} : 1.05, 1.27, 1.47, 1.89; H_{ether} : 3.40, 3.53; $\text{H}_{\text{carbonate}}$: 4.93; ^{13}C NMR: δ (ppm) = $\text{C}_{\text{CHO-1}}$: 19.76, 23.44, 24.77, 25.43; $\text{C}_{\text{CHO-2}}$: 30.33, 33.24, 35.07; C_{ether} : 67.56, 76.92, 78.55; $\text{C}_{\text{carbonate}}$: 154.92; IR (KBr, cm^{-3}): 3440 (m), 2940 (s), 2859 (s), 1751 (s), 1459 (m), 1374 (m), 1257 (s), 1163 (m), 1086 (s), 1019 (m).

7.4.6.2 Copolymer P-4b

Crude polymer: ^1H NMR: δ (ppm) = H_{CHO} : 1.28, 1.48, 1.65, 1.80, 2.22; H_{ether} : 3.81; $\text{H}_{\text{carbonate}}$: 4.97; ^{13}C NMR: δ (ppm) = $\text{C}_{\text{CHO-1}}$: 21.98, 23.37; $\text{C}_{\text{CHO-2}}$: 29.19; C_{ether} : 77.03; $\text{C}_{\text{carbonate}}$: 154.94; IR (KBr, cm^{-3}): 2984 (s), 2965 (s), 1744 (s), 1444 (s), 1371 (s), 1267 (s), 1160 (s), 1089 (s), 966 (s), 892 (s), 842 (s), 741 (s), 637 (sm).

Long-chain polymer: ^1H NMR: δ (ppm) = H_{CHO} : 1.49, 1.71, 1.90, 2.28, 2.37; H_{ether} : 3.82; $\text{H}_{\text{carbonate}}$: 5.06; ^{13}C NMR: δ (ppm) = $\text{C}_{\text{CHO-1}}$: 23.88; $\text{C}_{\text{CHO-2}}$: 30.06; C_{ether} : 78.40; $\text{C}_{\text{carbonate}}$: invisible; IR (KBr, cm^{-3}): 2937 (s), 2865 (s), 1744 (m), 1651 (m), 1458 (m), 1367 (m), 1262 (m), 1085 (s), 895 (sm), 863 (sm), 785 (sm), 736 (sm).

7.4.6.3 Copolymer P-4c

Crude polymer: ^1H NMR: δ (ppm) = H_{CHO} : 1.08, 1.38, 1.60, 1.80, 2.14; H_{ether} : 3.60, 3.69, 3.81; $\text{H}_{\text{carbonate}}$: 4.97; ^{13}C NMR: δ (ppm) = $\text{C}_{\text{CHO-1}}$: 21.98, 22.40, 23.37; $\text{C}_{\text{CHO-2}}$: 29.19, 30.97; C_{ether} : 77.87, 78.53; $\text{C}_{\text{carbonate}}$: 154.84; IR (KBr, cm^{-3}): 3052 (sm), 2987 (s), 2935 (s), 2861 (s), 1740 (s), 1440 (s), 1367 (s), 1267 (s), 1158 (s), 1088 (s), 966 (s), 892 (s), 837 (s), 782 (s), 738 (s), 637 (sm), 534 (m).

Long-chain polymer: ^1H NMR: δ (ppm) = H_{CHO} : 1.41, 1.64, 1.81, 2.18, 2.37; H_{ether} : 3.66, 3.75; $\text{H}_{\text{carbonate}}$: 5.06; ^{13}C NMR: δ (ppm) = $\text{C}_{\text{CHO-1}}$: 23.18, 23.52; $\text{C}_{\text{CHO-2}}$: 30.06, 30.53; C_{ether} : 78.40; $\text{C}_{\text{carbonate}}$: 154.69; IR (KBr, cm^{-3}): 2931 (s), 2860 (s), 1739 (m), 1651 (m), 1457 (m), 1368 (m), 1263 (m), 1093 (s), 896 (sm), 859 (sm), 791 (sm).

7.4.6.4 Copolymer P-4d

Crude polymer: ^1H NMR: δ (ppm) = H_{CHO} : 1.07, 1.41, 1.58, 1.86, 2.15; H_{ether} : 3.62, 3.72; $\text{H}_{\text{carbonate}}$: 4.98; ^{13}C NMR: δ (ppm) = $\text{C}_{\text{CHO-1}}$: 23.25; $\text{C}_{\text{CHO-2}}$: 29.99; C_{ether} : 78.55, 79.12; $\text{C}_{\text{carbonate}}$: peak is invisible; IR (KBr, cm^{-3}): 3448 (m), 2932 (sm), 2869 (sm), 1741 (sm), 1455 (sm), 1379 (sm), 1263 (sm), 1089 (m).

Long-chain polymer: ^1H NMR: δ (ppm) = H_{CHO} : 1.46, 1.68, 1.88, 2.24; H_{ether} : 3.71, 3.81; $\text{H}_{\text{carbonate}}$: 5.15; ^{13}C NMR: δ (ppm) = $\text{C}_{\text{CHO-1}}$: 23.40; $\text{C}_{\text{CHO-2}}$: 30.76; C_{ether} : 78.43, 79.11; $\text{C}_{\text{carbonate}}$: peak is invisible; IR (KBr, cm^{-3}): 3448 (m), 2923 (sm), 2875 (sm), 1738 (sm), 1458 (sm), 1382 (sm), 1260 (sm), 1095 (m).

7.4.6.5 Copolymer P-4e

Crude polymer: ^1H NMR: δ (ppm) = H_{CHO} : 1.45, 1.68, 1.88, 2.23; H_{ether} : 3.70, 3.79...; $\text{H}_{\text{carbonate}}$: 5.12; ^{13}C NMR: δ (ppm) = $\text{C}_{\text{CH-1}}$: 22.23, 23.16; $\text{C}_{\text{CHO-2}}$: 29.39, 29.93, 30.32; C_{ether} : 78.71; $\text{C}_{\text{carbonate}}$: 149.16; IR (KBr, cm^{-3}): 3437 (m), 2934 (s), 2861 (s), 1743 (s), 1457 (s), 1367 (m), 1261 (s), 1160 (m), 1087 (s), 1020 (m), 895 (sm), 859 (sm), 783 (sm), 736 (sm).

Long-chain polymer: ^1H NMR: δ (ppm) = H_{CHO} : 1.42, 1.66, 1.86, 2.19; H_{ether} : 3.67; 3.76...; $\text{H}_{\text{carbonate}}$: 5.08; ^{13}C NMR: δ (ppm) = $\text{C}_{\text{CHO-1}}$: 23.18; 23.49; 23.54; $\text{C}_{\text{CHO-2}}$: 29.65; 29.95; 30.52; C_{ether} : 77.01; 78.40; $\text{C}_{\text{carbonate}}$: 155.33; IR (KBr, cm^{-3}): 3434 (m), 2931 (s), 2861 (m), 1743 (s), 1450 (s), 1368 (m), 1261 (s), 1160 (m), 1089 (s).

7.4.6.6 Copolymer P-4f

Crude polymer: ^1H NMR: δ (ppm) = H_{CHO} : 1.42, 1.51, 1.65, 1.87, 2.21; H_{ether} : 3.67, 3.79; $\text{H}_{\text{carbonate}}$: 5.09; ^{13}C NMR: δ (ppm) = $\text{C}_{\text{CHO-1}}$: 23.16, 24.81; $\text{C}_{\text{CHO-2}}$: 30.15; C_{ether} : 77.10, 78.68; $\text{C}_{\text{carbonate}}$: 155.10; IR (KBr, cm^{-3}): 3445 (sm), 2933 (sm), 1741 (sm), 1463 (sm), 1270 (sm), 1097 (sm).

Long-chain polymer: ^1H NMR: δ (ppm) = H_{CHO} : 1.46, 1.68, 1.87, 2.24; H_{ether} : 3.70, 3.80; $\text{H}_{\text{carbonate}}$: 5.13; ^{13}C NMR: δ (ppm) = $\text{C}_{\text{CHO-1}}$: 22.40, 22.69, 22.85, 23.21, 23.48; $\text{C}_{\text{CHO-2}}$: 29.33, 29.68, 30.16; C_{ether} : 76.67, 78.11, 78.65; $\text{C}_{\text{carbonate}}$: 154.83, 154.92, 154.97, 155.04, 155.14; IR (KBr, cm^{-3}): 3445 (m), 2933 (s), 2660 (s), 1744 (s), 1457 (s), 1367 (sm), 1261 (s), 1160 (s), 1099 (s), 857 (sm), 788 (sm).

7.4.6.7 Copolymer P-4g

Crude polymer: ^1H NMR: δ (ppm) = H_{CHO} : 1.44, 1.64, 1.82, 2.20; H_{ether} : 3.66, 3.74; $\text{H}_{\text{carbonate}}$: 5.10; ^{13}C NMR: δ (ppm) = $\text{C}_{\text{CHO-1}}$: 19.83, 21.97, 23.13, 24.85; $\text{C}_{\text{CHO-2}}$: 29.66; C_{ether} : 76.71, 78.12; $\text{C}_{\text{carbonate}}$: 155.08; IR (KBr, cm^{-3}): 3452 (sm), 2934 (s), 2864 (s), 1743 (s), 1457 (m), 1354 (m), 1260 (s), 1161 (m), 1094 (s), 1027 (m), 782 (m).

Long-chain polymer: ^1H NMR: δ (ppm) = H_{CHO} : 1.45, 1.68, 1.89, 2.24; H_{ether} : 3.70, 3.79; $\text{H}_{\text{carbonate}}$: 5.13; ^{13}C NMR: δ (ppm) = $\text{C}_{\text{CHO-1}}$: 23.00, 23.24, 23.58; $\text{C}_{\text{CHO-2}}$: 29.38, 29.76, 30.51; C_{ether} : 76.72, 78.10, 78.70; $\text{C}_{\text{carbonate}}$: 154.92, 155.04, 155.14, 155.25; IR (KBr, cm^{-3}): 3435 (m), 2933 (s), 2860 (s), 1740 (s), 1458 (s), 1369 (m), 1261 (s), 1164 (m), 1087 (s), 895 (m), 859 (m), 785 (m), 736 (m).

7.4.7 Copolymers synthesised with catalysts having 5 as the ligand

7.4.7.1 Copolymer P-5a

Crude polymer: ^1H NMR: δ (ppm) = H_{CHO} : 1.08, 1.40, 1.56, 1.84, 2.15, 2.23; H_{ether} : 3.61, 3.71; $\text{H}_{\text{carbonate}}$: 4.99; ^{13}C NMR: δ (ppm) = $\text{C}_{\text{CHO-1}}$: 21.80, 22.37, 25.13, 30.03; $\text{C}_{\text{CHO-2}}$: 29.47, 30.09; C_{ether} : 76.40, 77.80, 78.32; the signal of carbon in carbonate group is invisible; IR (KBr, cm^{-3}): 2866 (m), 2669 (sm), 1744 (m), 1449 (m), 1267 (m), 1157 (m), 1076 (br, s), 1021 (m), 859 (m), 782 (s).

Long-chain polymer: ^1H NMR: δ (ppm) = H_{CHO} : 1.45, 1.68, 1.87, 2.40; H_{ether} : 3.70, 3.80; $\text{H}_{\text{carbonate}}$: 5.11; ^{13}C NMR: δ (ppm) = $\text{C}_{\text{CHO-1}}$: 22.68, 22.99, 23.23; $\text{C}_{\text{CHO-2}}$: 29.08, 29.62, 29.99; C_{ether} : 76.50, 77.88, 78.42; signal of carbon in carbonate group is invisible; IR (KBr, cm^{-3}): 3431 (m), 2935 (s), 2862 (m), 1744 (sm), 1454 (m), 1367 (m), 1267 (m), 1162 (m), 1087 (s), 1020 (m).

Owing to the very small content of carbonate in isolated polymer, further purification of one was abandoned.

7.4.7.2 Copolymer P-5c

Crude polymer: ^1H NMR: δ (ppm) = H_{CHO} : 0.74, 1.00, 1.09, 1.17, 1.27, 1.50, 1.82, 2.15, 2.23; H_{ether} : 3.28, 3.38; $\text{H}_{\text{carbonate}}$: 4.63; IR (KBr, cm^{-3}): 2984 (m), 2936 (s), 2861 (m), 1743 (sm), 1439 (m), 1366 (sm), 1260 (sm), 1159 (sm), 1089 (m), 966 (m), 891 (m), 837 (m), 781 (m).

Long-chain polymer: ^1H NMR: δ (ppm) = H_{CHO} : 1.05, 1.28, 1.47, 1.83; H_{ether} : 3.29, 3.40; $\text{H}_{\text{carbonate}}$: 4.74; ^{13}C NMR: δ (ppm) = $\text{C}_{\text{CHO-1}}$: 22.88, 23.19, 23.45; $\text{C}_{\text{CHO-2}}$: 29.35, 29.70, 29.86, 30.23, 30.38; C_{ether} : 75.15, 76.67, 78.11, 78.68; $\text{C}_{\text{carbonate}}$: 153.63; IR (KBr, cm^{-3}): 3462 (sm), 2949 (sm), 2858 (sm), 1736 (sm), 1451 (sm), 1368 (sm), 1260 (sm), 1158 (sm), 1090 (sm).

7.4.7.3 Copolymer P-5f

Crude polymer: ^1H NMR: δ (ppm) = H_{CHO} : 1.03, 1.18, 1.27, 1.48, 1.82; H_{ether} : 3.29, 3.40, 3.50; $\text{H}_{\text{carbonate}}$: 4.71; ^{13}C NMR: δ (ppm) = $\text{C}_{\text{CHO-1}}$: 19.74, 24.76; $\text{C}_{\text{CHO-2}}$: 29.42, 32.88; C_{ether} : 77.03; $\text{C}_{\text{carbonate}}$: 154.58; IR (KBr, cm^{-3}): 3432 (m), 2933 (s), 2862 (s), 1744 (s), 1458 (s), 1371 (m), 1263 (s), 1160 (m), 1092 (s), 1017 (m), 784 (sm).

Long-chain polymer: ^1H NMR: δ (ppm) = H_{CHO} : 1.03, 1.29, 1.45, 1.83, 2.50, 2.73; H_{ether} : 3.29, 3.40; $\text{H}_{\text{carbonate}}$: 4.71; ^{13}C NMR: δ (ppm) = $\text{C}_{\text{CHO-1}}$: 19.76, 22.22, 22.86, 23.15, 24.77; $\text{C}_{\text{CHO-2}}$: 29.85, 30.34; C_{ether} : 77.94, 78.10; $\text{C}_{\text{carbonate}}$: 154.91; IR (KBr, cm^{-3}): 3460 (sm), 2935 (s), 2862 (s), 1744 (s), 1453 (s), 1368 (m), 1261 (s), 1158 (m), 1090 (s), 790 (m).

7.4.7.4 Copolymer P-5g

Crude polymer: ^1H NMR: δ (ppm) = H_{CHO} : 1.42; 1.68; 1.85; 2.21; H_{ether} : 3.76; 3.79; $\text{H}_{\text{carbonate}}$: 5.11; ^{13}C NMR: δ (ppm) = $\text{C}_{\text{CHO-1}}$: 23.28; $\text{C}_{\text{CHO-2}}$: 29.54, 30.58; C_{ether} : 77.15, 78.59; $\text{C}_{\text{carbonate}}$: 155.67; IR (KBr, cm^{-3}): 2945 (s), 2867 (s), 1740 (s), 1457 (sm), 1260 (s), 1091 (s).

Long-chain polymer: ^1H NMR: δ (ppm) = H_{CHO} : 1.45; 1.67; 1.85; 2.22; H_{ether} : 3.72; 3.79; $\text{H}_{\text{carbonate}}$: 5.12; ^{13}C NMR: δ (ppm) = $\text{C}_{\text{CHO-1}}$: 23.54; $\text{C}_{\text{CHO-2}}$: 29.74, 30.31; C_{ether} : 77.12, 78.12; $\text{C}_{\text{carbonate}}$: 155.06; IR (KBr, cm^{-3}): 2933 (s), 2860 (s), 1741 (sm), 1653 (sm), 1557 (sm), 1458 (sm), 1260 (s), 1091 (s).

7.4.8 Copolymers synthesised with catalysts having 6 as the ligand

7.4.8.1 Copolymer P-6a

Crude polymer: ^1H NMR: δ (ppm) = H_{CHO} : 1.08, 1.40, 1.56, 1.84, 2.15, 2.23; H_{ether} : 3.61, 3.71; $\text{H}_{\text{carbonate}}$: 4.99; ^{13}C NMR: δ (ppm) = $\text{C}_{\text{CHO-1}}$: 21.80, 22.37, 25.13, 30.03; $\text{C}_{\text{CHO-2}}$: 29.47, 30.09; C_{ether} : 76.40, 77.80, 78.32; the signal of carbon in carbonate group is invisible; IR (KBr, cm^{-3}): 2866 (m), 2669 (sm), 1744 (m), 1449 (m), 1267 (m), 1157 (m), 1076 (br, s), 1021 (m), 859 (m), 782 (s).

Long-chain polymer: ^1H NMR: δ (ppm) = H_{CHO} : 1.45, 1.68, 1.87, 2.40; H_{ether} : 3.70, 3.80; $\text{H}_{\text{carbonate}}$: 5.11; ^{13}C NMR: δ (ppm) = $\text{C}_{\text{CHO-1}}$: 22.68, 22.99, 23.23; $\text{C}_{\text{CHO-2}}$: 29.08, 29.62, 29.99. ; C_{ether} : 76.50, 77.88, 78.42; signal of carbon in carbonate group is invisible; IR (KBr, cm^{-3}): 3431 (m), 2935 (s), 2862 (m), 1744 (sm), 1454 (m), 1367 (m), 1267 (m), 1162 (m), 1087 (s), 1020 (m).

7.4.8.2 Copolymer P-6c

Crude polymer: ^1H NMR: δ (ppm) = H_{CHO} : 0.74, 1.00, 1.09, 1.17, 1.27, 1.50, 1.82, 2.15, 2.23; H_{ether} : 3.28, 3.38; $\text{H}_{\text{carbonate}}$: 4.63; IR (KBr, cm^{-3}): 2984 (m), 2936 (s), 2861 (m), 1743 (sm), 1439 (m), 1366 (sm), 1260 (sm), 1159 (sm), 1089 (m), 966 (m), 891 (m), 837 (m), 781 (m).

7.4.8.3 Copolymer P-6g

Crude polymer: ^1H NMR: δ (ppm) = H_{CHO} : 1.03, 1.18, 1.27, 1.48, 1.82; H_{ether} : 3.29, 3.40, 3.50; $\text{H}_{\text{carbonate}}$: 4.71; ^{13}C NMR: δ (ppm) = $\text{C}_{\text{CHO-1}}$: 19.74, 24.76; $\text{C}_{\text{CHO-2}}$: 29.42, 32.88; C_{ether} : 77.03; $\text{C}_{\text{carbonate}}$: 154.58; IR (KBr, cm^{-3}): 3432 (m), 2933 (s), 2862 (s), 1744 (s), 1458 (s), 1371 (m), 1263 (s), 1160 (m), 1092 (s), 1017 (m), 784 (sm).

Long-chain polymer: ^1H NMR: δ (ppm) = H_{CHO} : 1.03, 1.29, 1.45, 1.83, 2.50, 2.73; H_{ether} : 3.29, 3.40; $\text{H}_{\text{carbonate}}$: 4.71; ^{13}C NMR: δ (ppm) = $\text{C}_{\text{CHO-1}}$: 19.76, 22.22, 22.86, 23.15, 24.77; $\text{C}_{\text{CHO-2}}$: 29.85, 30.34; C_{ether} : 77.94, 78.10; $\text{C}_{\text{carbonate}}$: 154.91; IR (KBr, cm^{-3}): 3460 (sm), 2935 (s), 2862 (s), 1744 (s), 1453 (s), 1368 (m), 1261 (s), 1158 (m), 1090 (s), 790 (m).

7.4.9 Copolymers synthesised with catalysts having 7 as the ligand

7.4.9.1 Copolymer P-7a

Crude polymer: ^1H NMR: δ (ppm) = H_{CHO} : 1.02, 1.27, 1.47, 1.84; H_{ether} : 3.37; $\text{H}_{\text{carbonate}}$: 4.71; ^{13}C NMR: δ (ppm) = $\text{C}_{\text{CHO-1}}$: 19.75, 21.82, 24.76; $\text{C}_{\text{CHO-2}}$: 29.15; C_{ether} : 77.19; $\text{C}_{\text{carbonate}}$: 155.13; IR (KBr, cm^{-3}): 2938 (s), 2863 (s), 1743 (s), 1456 (m), 1367 (m), 1260 (s), 1160 (m), 1093 (s), 1017 (m), 894 (sm), 840 (sm), 783 (sm).

Long-chain polymer: ^1H NMR: δ (ppm) = H_{CHO} : 1.07, 1.25, 1.82; H_{ether} : 3.39; $\text{H}_{\text{carbonate}}$: 4.72; ^{13}C NMR: δ (ppm) = $\text{C}_{\text{CHO-1}}$: 21.76; $\text{C}_{\text{CHO-2}}$: 29.59; C_{ether} : 76.63, 78.12; $\text{C}_{\text{carbonate}}$: 155.02; IR (KBr, cm^{-3}): 3453 (m), 2935 (s), 2864 (s), 1743 (s), 1452 (s), 1364 (m), 1329 (m), 1260 (s), 1160 (s), 1090 (s), 956 (m), 897 (sm), 855 (sm), 788 (sm), 735 (sm).

7.4.9.2 Copolymer P-7c

Crude polymer: ^1H NMR: δ (ppm) = H_{CHO} : 0.63, 1.02, 1.27, 1.47, 1.85; H_{ether} : 3.38; $\text{H}_{\text{carbonate}}$: 4.72; ^{13}C NMR: δ (ppm) = $\text{C}_{\text{CHO-1}}$: 19.75, 21.82, 24.76; $\text{C}_{\text{CHO-2}}$: 29.15; C_{ether} : 77.19; $\text{C}_{\text{carbonate}}$: 155.13; IR (KBr, cm^{-3}): 3447 (m), 2938 (s), 2863 (s), 1743 (s), 1456 (m), 1367 (m), 1260 (s), 1160 (m), 1093 (s), 894 (m), 840 (m), 783 (m).

Long-chain polymer: ^1H NMR: δ (ppm) = H_{CHO} : 1.07; 1.29; 1.82; H_{ether} : 3.67; 3.39; $\text{H}_{\text{carbonate}}$: 4.72; ^{13}C NMR: δ (ppm) = $\text{C}_{\text{CHO-1}}$: 23.09; $\text{C}_{\text{CHO-2}}$: 29.75, 30.18; C_{ether} : 77.17, 78.67; $\text{C}_{\text{carbonate}}$: 155.15; IR (KBr, cm^{-3}): 3434 (m), 2934 (s), 2861 (s), 1743 (sm), 1456 (m), 1367 (m), 1267 (m), 1159 (m), 1088 (s), 897 (sm), 860 (sm), 787 (sm).

7.4.9.3 Copolymer P-7f

Crude polymer: $^1\text{H NMR}$: δ (ppm) = H_{CHO} : 0.65, 1.05, 1.31, 1.42, 1.79; H_{ether} : 3.42; $\text{H}_{\text{carbonate}}$: 4.73; $^{13}\text{C NMR}$: δ (ppm) = $\text{C}_{\text{CHO-1}}$: 21.51, 23.99; $\text{C}_{\text{CHO-2}}$: 30.10; C_{ether} : 78.10; $\text{C}_{\text{carbonate}}$: 154.28; IR (KBr, cm^{-3}): 2938 (s), 2867 (s), 1747 (s), 1453 (s), 1368 (m), 1261 (s), 1161 (m), 1089 (s), 894 (m), 840 (m), 783 (m).

Long-chain polymer: $^1\text{H NMR}$: δ (ppm) = H_{CHO} : 1.11; 1.25; 1.79; H_{ether} : 3.39, 3.58; $\text{H}_{\text{carbonate}}$: 4.74; $^{13}\text{C NMR}$: δ (ppm) = $\text{C}_{\text{CHO-1}}$: 23.09; $\text{C}_{\text{CHO-2}}$: 29.75, 30.81; C_{ether} : 77.74, 78.77; $\text{C}_{\text{carbonate}}$: 154.92; IR (KBr, cm^{-3}): 2945 (s), 2868 (s), 1747 (sm), 1460 (m), 1369 (m), 1268 (m), 1160 (m), 1089 (s), 860 (sm), 787 (sm).

7.4.9.4 Copolymer P-7g

Crude polymer: $^1\text{H NMR}$: δ (ppm) = H_{CHO} : 1.02, 1.07, 1.12, 1.29, 1.47, 1.84; H_{ether} : 3.14, 3.28, 3.39; $\text{H}_{\text{carbonate}}$: 4.70; $^{13}\text{C NMR}$: δ (ppm) = $\text{C}_{\text{CHO-1}}$: 22.68, 23.15; $\text{C}_{\text{CHO-2}}$: 29.91, 30.57; C_{ether} : 77.44, 78.47; $\text{C}_{\text{carbonate}}$: 154.67; IR (KBr, cm^{-3}): 3750 (m), 3452 (m), 2938 (s), 2863 (s), 1736 (m), 1651 (m), 1458 (m), 1264 (m), 1160 (m), 1090 (s).

Long-chain polymer: $^1\text{H NMR}$: δ (ppm) = H_{CHO} : 1,17, 1,22, 1,86; H_{ether} : 3.32, 3,42; $\text{H}_{\text{carbonate}}$: polyether only; $^{13}\text{C NMR}$: δ (ppm) = $\text{C}_{\text{CHO-1}}$: 21,74; $\text{C}_{\text{CHO-2}}$: 29,22; C_{ether} : 76,73, 78,78; $\text{C}_{\text{carbonate}}$: polyether only; IR (KBr, cm^{-3}): 3440 (m), 2933 (s), 2860 (m), 1745 (sm), 1460 (s), 1368 (m), 1260 (m), 1159 (m), 1088 (s), 1020 (m).

7.4.10 Copolymers synthesised with catalysts having 8 as the ligand

7.4.10.1 Copolymer P-8c

As a result of the copolymerisation process a yellow, viscous, transparent solution was obtained, which was identified as unreacted cyclohexene oxide. Owing to this fact further analysis were abandoned.

$^1\text{H NMR}$: δ (ppm) = 0.96, 1.25, 1.50, 1.76, 2.83 (signals were identified as coming from CHO); IR (KBr, cm^{-3}): 2939 (m), 2862 (sm), 1438 (sm), 1257 (v-sm), 1084 (v-sm), 967 (v-sm), 891 (v-sm), 837 (sm), 781 (sm).

7.4.10.2 Copolymer P-8g

Crude polymer: $^1\text{H NMR}$: δ (ppm) = H_{CHO} : 1.06, 1.45, 1.68, 1.88, 2.23; H_{ether} : 3.70, 3.79; $\text{H}_{\text{carbonate}}$: 5.11; $^{13}\text{C NMR}$: δ (ppm) = $\text{C}_{\text{CHO-1}}$: 22.15, 22.35, 22.77, 22.95, 23.17, 23.57; $\text{C}_{\text{CHO-2}}$: 28.853, 29.419, 29.555, 29.767, 30.296; C_{ether} : 76.97, 78.18, 78.34; $\text{C}_{\text{carbonate}}$: 155.08; IR (KBr, cm^{-3}): 3447 (m), 2939 (s), 2859 (s), 1742 (s), 1453 (m), 1364 (m), 1261 (s), 1160 (m), 1089 (s), 893 (m), 839 (m), 779 (m).

Long-chain polymer: ^1H NMR: δ (ppm) = H_{CHO} : 1.07; 1.29; 1.82; H_{ether} : 3.67; 3.39; $\text{H}_{\text{carbonate}}$: 4.72; ^{13}C NMR: δ (ppm) = $\text{C}_{\text{CHO-1}}$: 23.09.... ; $\text{C}_{\text{CHO-2}}$: 29.75, 30.18.... ; C_{ether} : 77.17, 78.67... ; $\text{C}_{\text{carbonate}}$: 155.15; IR (KBr, cm^{-3}): 3434 (m), 2934 (s), 2861 (s), 1743 (sm), 1456 (m), 1367 (m), 1267 (m), 1159 (m), 1088 (s), 897 (sm), 860 (sm), 787 (sm).

7.5 The use of catalyst-cocatalyst system as an initiator of copolymerisation

7.5.1 1b with 1 eq. of N-MeIm

^1H NMR: δ (ppm) = 1.08, 1.40, 1.59, 1.85; IR (KBr, cm^{-3}): 3447 (m), 2985 (s), 2937 (s), 2860 (s), 1824 (m), 1652 (m), 1541 (m), 1501 (sm), 1457 (s), 1261 (s), 1160 (sm), 1093 (sm), 966 (s), 891 (s), 837 (m), 781 (m), 745 (m), 534 (sm).

Only non-reacted CHO was identified.

7.5.2 1b with 1 eq. of PPh₃

^1H NMR: δ (ppm) = 0.90, 1.18, 1.39, 1.65, 4.61; IR (KBr, cm^{-3}): 2937 (s), 2861 (s), 1805 (s), 1458 (m), 1438 (m), 1355 (m), 1260 (m), 1166 (m), 1034 (s), 966 (s), 891 (s), 837 (m), 781 (m), 745 (m), 534 (sm).

7.5.3 1b with 1 eq. of TEAPTS

^1H NMR: δ (ppm) = 0.90, 1.18, 1.39, 1.65, 4.75; IR (KBr, cm^{-3}): 3748 (sm), 2985 (s), 2937 (s), 2861 (s), 199 (sm), 1651 (m), 1558 (m), 1541 (m), 1521(m), 1458 (s), 1438 (s), 1260 (m), 1184 (m), 1087 (m), 966 (s), 891 (s), 837 (m), 781 (m), 745 (m), 534 (sm).

7.5.4 1b with 1 eq. of NEt₄Br

^1H NMR: δ (ppm) = 0.89, 1.17, 1.43, 1.63; IR (KBr, cm^{-3}): 3751 (sm), 2985 (m), 2937 (s), 2861 (m), 1806 (m), 1699 (m), 1651 (m), 1541 (m), 1457 (s), 1438 (s), 1359 (sm), 1261 (m), 1167 (m), 1035 (s), 966 (s), 891 (s), 837 (s), 743 (s).

7.5.5 1b with 1 eq. of PPNCI

^1H NMR: δ (ppm) = 0.99, 1.09, 1.27, 1.40, 1.61, 1.86, 4.14; IR (KBr, cm^{-3}): 2937 (s), 2861 (s), 1805 (s), 1458 (m), 1438 (m), 1355 (m), 1260 (m), 1166 (m), 1034 (s), 966 (s), 891 (s), 837 (m), 781 (m), 745 (m), 534 (sm).

7.5.6 2g with 10 ml CH₂Cl₂

Crude polymer: ^1H NMR: δ (ppm) = H_{CHO} : 0.99, 1.25, 1.45, 1.85; H_{ether} : 3.37, 3.54; $\text{H}_{\text{carbonate}}$: 4.71; ^{13}C NMR: δ (ppm) = $\text{C}_{\text{CHO-1}}$: 19.78, 21.57, 24.69; $\text{C}_{\text{CHO-2}}$: 29.58; C_{ether} : 77.98; $\text{C}_{\text{carbonate}}$: 154.01; IR (KBr, cm^{-3}): 2941 (s), 2861 (s), 1741 (s), 1457 (m), 1366 (m), 1261 (s), 1162 (m), 1093 (s), 1022 (m), 894 (sm), 840 (sm), 783 (sm).

Long-chain polymer: ^1H NMR: δ (ppm) = H_{CHO} : 0.99, 1.33, 1.47, 1.80; H_{ether} : 3.83; $\text{H}_{\text{carbonate}}$: 4.71; ^{13}C NMR: δ (ppm) = $\text{C}_{\text{CHO-1}}$: 21.12, 21.58; $\text{C}_{\text{CHO-2}}$: 29.88; C_{ether} : 78.00; $\text{C}_{\text{carbonate}}$: 154.21; IR (KBr, cm^{-3}): 2942 (s), 2861 (s), 1741 (s), 1457 (m), 1366 (m), 1261 (s), 1162 (m), 1093 (s), 1022 (m), 894 (sm), 840 (sm), 783 (sm).

7.5.7 2g without solvent

Crude polymer: ^1H NMR: δ (ppm) = H_{CHO} : 1.01, 1.25, 1.45, 1.85; H_{ether} : 3.37, 3.54; $\text{H}_{\text{carbonate}}$: 4.71; ^{13}C NMR: δ (ppm) = $\text{C}_{\text{CHO-1}}$: 19.78, 21.57, 24.69; $\text{C}_{\text{CHO-2}}$: 29.58; C_{ether} : 77.98; $\text{C}_{\text{carbonate}}$: 154.01; IR (KBr, cm^{-3}): 2941 (s), 2861 (s), 1741 (s), 1457 (m), 1366 (m), 1261 (s), 1162 (m), 1093 (s), 1022 (m), 894 (sm), 840 (sm), 783 (sm).

Long-chain polymer: ^1H NMR: δ (ppm) = H_{CHO} : 1.12, 1.35, 1.57, 1.82; H_{ether} : 3.84; $\text{H}_{\text{carbonate}}$: 5.13; ^{13}C NMR: δ (ppm) = $\text{C}_{\text{CHO-1}}$: 21.15, 21.48; $\text{C}_{\text{CHO-2}}$: 30.48; C_{ether} : 78.05; $\text{C}_{\text{carbonate}}$: 154.05; IR (KBr, cm^{-3}): 2942 (s), 2861 (s), 1745 (s), 1456 (m), 1367 (m), 1260 (s), 1160 (m), 1090 (s), 1018 (m), 894 (sm), 842 (sm), 783 (sm).

7.5.8 2g with 3 ml CH_2Cl_2

Crude polymer: ^1H NMR: δ (ppm) = H_{CHO} : 1.15, 1.28, 1.47, 1.87; H_{ether} : 3.77, 3.84; $\text{H}_{\text{carbonate}}$: 5.14; ^{13}C NMR: δ (ppm) = $\text{C}_{\text{CHO-1}}$: 22.14, 21.69; $\text{C}_{\text{CHO-2}}$: 29.58, 30.54; C_{ether} : 77.48; $\text{C}_{\text{carbonate}}$: 154.41; IR (KBr, cm^{-3}): 2941 (s), 2861 (s), 1741 (s), 1457 (m), 1364 (m), 1260 (s), 1160 (m), 1091 (s), 1024 (m), 894 (sm), 840 (sm), 783 (sm).

Long-chain polymer: ^1H NMR: δ (ppm) = H_{CHO} : 1.12, 1.29, 1.62, 1.82; H_{ether} : 3.74; $\text{H}_{\text{carbonate}}$: 5.13; ^{13}C NMR: δ (ppm) = $\text{C}_{\text{CHO-1}}$: 22.25, 22.58; $\text{C}_{\text{CHO-2}}$: 29.56; C_{ether} : 78.05; $\text{C}_{\text{carbonate}}$: 154.05; IR (KBr, cm^{-3}): 2942 (s), 2861 (s), 1745 (s), 1456 (m), 1367 (m), 1260 (s), 1160 (m), 1090 (s), 1018 (m), 894 (sm), 842 (sm), 783 (sm).

7.5.9 2g with 10 ml CH_2Cl_2

^1H NMR: δ (ppm) = 1.08, 1.40, 1.59, 1.85; IR (KBr, cm^{-3}): 3447 (m), 2985 (s), 2937 (s), 2860 (s), 1824 (m), 1652 (m), 1541 (m), 1501 (sm), 1457 (s), 1261 (s), 1160 (sm), 1093 (sm), 966 (s), 891 (s), 837 (m), 781 (m), 745 (m), 534 (sm).

7.5.10 2g with 1 eq. of TEAPTS

Crude polymer: ^1H NMR: δ (ppm) = H_{CHO} : 1.46, 1.70, 1.88, 2.24; H_{ether} : 3.71, 3.80; $\text{H}_{\text{carbonate}}$: 5.13; ^{13}C NMR: δ (ppm) = $\text{C}_{\text{CHO-1}}$: 23.02; $\text{C}_{\text{CHO-2}}$: 30.36; C_{ether} : 77.18, 78.14; $\text{C}_{\text{carbonate}}$: 155.13; IR (KBr, cm^{-3}): 3450 (m), 2933 (s), 2863 (s), 1743 (s), 1456 (m), 1369 (m), 1262 (s), 1160 (m), 1090 (s), 894 (m), 855 (m), 784 (m), 736 (m).

Long-chain polymer: ^1H NMR: δ (ppm) = H_{CHO} : 1.48, 1.68, 1.85, 2.24; H_{ether} : 3.75, 3.80; $\text{H}_{\text{carbonate}}$: 5.14; ^{13}C NMR: δ (ppm) = $\text{C}_{\text{CHO-1}}$: 22.98, 23.02; $\text{C}_{\text{CHO-2}}$: 29.88, 30.36; C_{ether} : 77.25, 78.15;

$C_{\text{carbonate}}$: 154.13; IR (KBr, cm^{-3}): 3450 (m), 2935 (s), 2865 (s), 1741 (s), 1457 (m), 1370 (m), 1260 (s), 1162 (m), 1093 (s), 894 (m), 855 (m), 784 (m), 736 (m).

7.5.11 2g with 1 eq. of PPNCI – [Al] / [CHO] =1 / 1000 / 1

^1H NMR: δ (ppm) = 1.08, 1.40, 1.59, 1.85; IR (KBr, cm^{-3}): 3447 (m), 2985 (s), 2937 (s), 2860 (s), 1824 (m), 1652 (m), 1541 (m), 1501 (sm), 1457 (s), 1261 (s), 1160 (sm), 1093 (sm), 966 (s), 891 (s), 837 (m), 781 (m), 745 (m), 534 (sm).

7.5.12 2g with 1 eq. of PPNCI – [Al] / [CHO] =1 / 300 / 1

Crude polymer: ^1H NMR: δ (ppm) = H_{CHO} : 1.35, 1.59, 1.79, 2.20; H_{ether} : 3.74, 3.41 ^{13}C NMR: δ (ppm) = $C_{\text{CHO-1}}$: 24.35, 24.64; $C_{\text{CHO-2}}$: 30.54, C_{ether} : 76.88, 78.70, 78.78; IR (KBr, cm^{-3}): 3447 (m), 2945 (s), 2865 (s), 1457 (m), 1367 (m), 1260 (s), 1160 (m), 1090 (s), 897 (m), 835 (m), 784 (m).

7.5.13 2g with 1 eq. of [PPN]Cl – [Al] / [CHO] =1 / 300 / 1 + 1 ml toluene

^1H NMR: δ (ppm) = 1.08, 1.40, 1.59, 1.85; IR (KBr, cm^{-3}): 3447 (m), 2985 (s), 2937 (s), 2860 (s), 1824 (m), 1652 (m), 1541 (m), 1501 (sm), 1457 (s), 1261 (s), 1160 (sm), 1093 (sm), 966 (s), 891 (s), 837 (m), 781 (m), 745 (m), 534 (sm).

7.5.14 2g with 3 eq. of [PPN]Cl – [Al] / [CHO] =1 / 300 / 3 + 1 ml toluene

^1H NMR: δ (ppm) = H_{CHO} : 1.47, 1.70, 1.88, 2.25, 4.12; IR (KBr, cm^{-3}): 2863 (s), 1810 (s), 1456 (m), 1367 (m), 1260 (s), 1160 (m), 1093 (s), 894 (m), 840 (m), 783 (m).

7.5.15 2g with 1 eq. of N-MeIm – [Al] / [CHO] =1 / 1000 / 1 (AJN 686)

^1H NMR: δ (ppm) = 1.08, 1.40, 1.59, 1.85; IR (KBr, cm^{-3}): 3447 (m), 2985 (s), 2937 (s), 2860 (s), 1824 (m), 1652 (m), 1541 (m), 1501 (sm), 1457 (s), 1261 (s), 1160 (sm), 1093 (sm), 966 (s), 891 (s), 837 (m), 781 (m), 745 (m), 534 (sm).

7.5.16 2g with 1 eq. of N-MeIm – [Al] / [CHO] =1 / 300 / 1

Crude polymer: ^1H NMR: δ (ppm) = H_{CHO} : 1.10, 1.40, 1.69, 1.84, 2.23; H_{ether} : 3.71, 3.79; $H_{\text{carbonate}}$: 5.13; ^{13}C NMR: δ (ppm) = $C_{\text{CHO-1}}$: 22.17, 23.57; $C_{\text{CHO-2}}$: 28.84, 29.49, 30.29, C_{ether} : 76.97, 78.34, $C_{\text{carbonate}}$: 155.08; IR (KBr, cm^{-3}): 2939 (s), 2863 (s), 1747 (s), 1453 (m), 1364 (m), 1261 (s), 1160 (m), 1089 (s), 893 (m), 839 (m), 779 (m).

Long-chain polymer: ^1H NMR: δ (ppm) = H_{CHO} : 1.07; 1.29; 1.82; H_{ether} : 3.47; 3.59; $H_{\text{carbonate}}$: 4.72; ^{13}C NMR: δ (ppm) = $C_{\text{CHO-1}}$: 23.09; $C_{\text{CHO-2}}$: 29.74, 30.28; C_{ether} : 77.17, 78.18; $C_{\text{carbonate}}$: 155.15; IR (KBr, cm^{-3}): 2934 (s), 2861 (s), 1741 (s), 1457 (m), 1367 (m), 1267 (m), 1160 (m), 1093 (s), 894 (sm), 860 (sm), 787 (sm).

7.5.17 2g with 1 eq. of N-MeIm – [Al] / [CHO] =1 / 300 / 1 + 1 ml toluene

$^1\text{H NMR}$: δ (ppm) = 1.08, 1.40, 1.59, 1.85; IR (KBr, cm^{-3}): 3447 (m), 2985 (s), 2937 (s), 2860 (s), 1824 (m), 1652 (m), 1541 (m), 1501 (sm), 1457 (s), 1261 (s), 1160 (sm), 1093 (sm), 966 (s), 891 (s), 837 (m), 781 (m), 745 (m), 534 (sm).

7.5.18 2g with 1 eq. of NBu₄Br – [Al] / [CHO] =1 / 1000 / 1

$^1\text{H NMR}$: δ (ppm) = 0.98, 1.24, 1.51, 1.61, 4.51; IR (KBr, cm^{-3}): 2937 (s), 2861 (s), 1805 (s), 1458 (m), 1438 (m), 1355 (m), 1260 (m), 1167 (m), 1034 (s), 966 (s), 891 (s), 837 (m), 781 (m), 748 (m), 534 (sm).

7.5.19 2g with 1 eq. of N+[Bu]₄ Br- – [Al] / [CHO] =1 / 300 / 1 (AJN 691)

$^1\text{H NMR}$: δ (ppm) = 1.08, 1.40, 1.59, 1.85; IR (KBr, cm^{-3}): 3447 (m), 2985 (s), 2937 (s), 2860 (s), 1824 (m), 1652 (m), 1541 (m), 1501 (sm), 1457 (s), 1261 (s), 1160 (sm), 1093 (sm), 966 (s), 891 (s), 837 (m), 781 (m), 745 (m), 534 (sm).

7.5.20 2g with 1 eq. of DMAP – [Al] / [CHO] =1 / 1000 / 1

$^1\text{H NMR}$: δ (ppm) = 1.08, 1.40, 1.59, 1.85; IR (KBr, cm^{-3}): 3447 (m), 2985 (s), 2937 (s), 2860 (s), 1824 (m), 1652 (m), 1541 (m), 1501 (sm), 1457 (s), 1261 (s), 1160 (sm), 1093 (sm), 966 (s), 891 (s), 837 (m), 781 (m), 745 (m), 534 (sm).

7.5.21 2g with 1 eq. of DMAP – [Al] / [CHO] =1 / 300 / 1

Crude polymer: $^1\text{H NMR}$: δ (ppm) = H_{CHO} : 1.14, 1.44, 1.61, 1.81, 2.23; H_{ether} : 3.71, 3.79; $\text{H}_{\text{carbonate}}$: 5.13; $^{13}\text{C NMR}$: δ (ppm) = $\text{C}_{\text{CHO-1}}$: 22.47, 23.47; $\text{C}_{\text{CHO-2}}$: 28.74, 30.29, C_{ether} : 78.34, $\text{C}_{\text{carbonate}}$: 154.45; IR (KBr, cm^{-3}): 2939 (s), 2863 (s), 1747 (s), 1453 (m), 1364 (m), 1261 (s), 1160 (m), 1089 (s), 893 (m), 839 (m), 779 (m).

Long-chain polymer: $^1\text{H NMR}$: δ (ppm) = H_{CHO} : 1.07; 1.31; 1.82; H_{ether} : 3.47; 3.53; $\text{H}_{\text{carbonate}}$: 4.72; $^{13}\text{C NMR}$: δ (ppm) = $\text{C}_{\text{CHO-1}}$: 23.09; $\text{C}_{\text{CHO-2}}$: 29.74, 30.28; C_{ether} : 77.17, 78.18; $\text{C}_{\text{carbonate}}$: 153.91; IR (KBr, cm^{-3}): 2934 (s), 2861 (s), 1741 (s), 1457 (m), 1367 (m), 1267 (m), 1160 (m), 1093 (s), 894 (sm), 860 (sm), 787 (sm).

7.5.22 2g with 3 eq. of DMAP- – [Al] / [CHO] =1 / 300 / 3

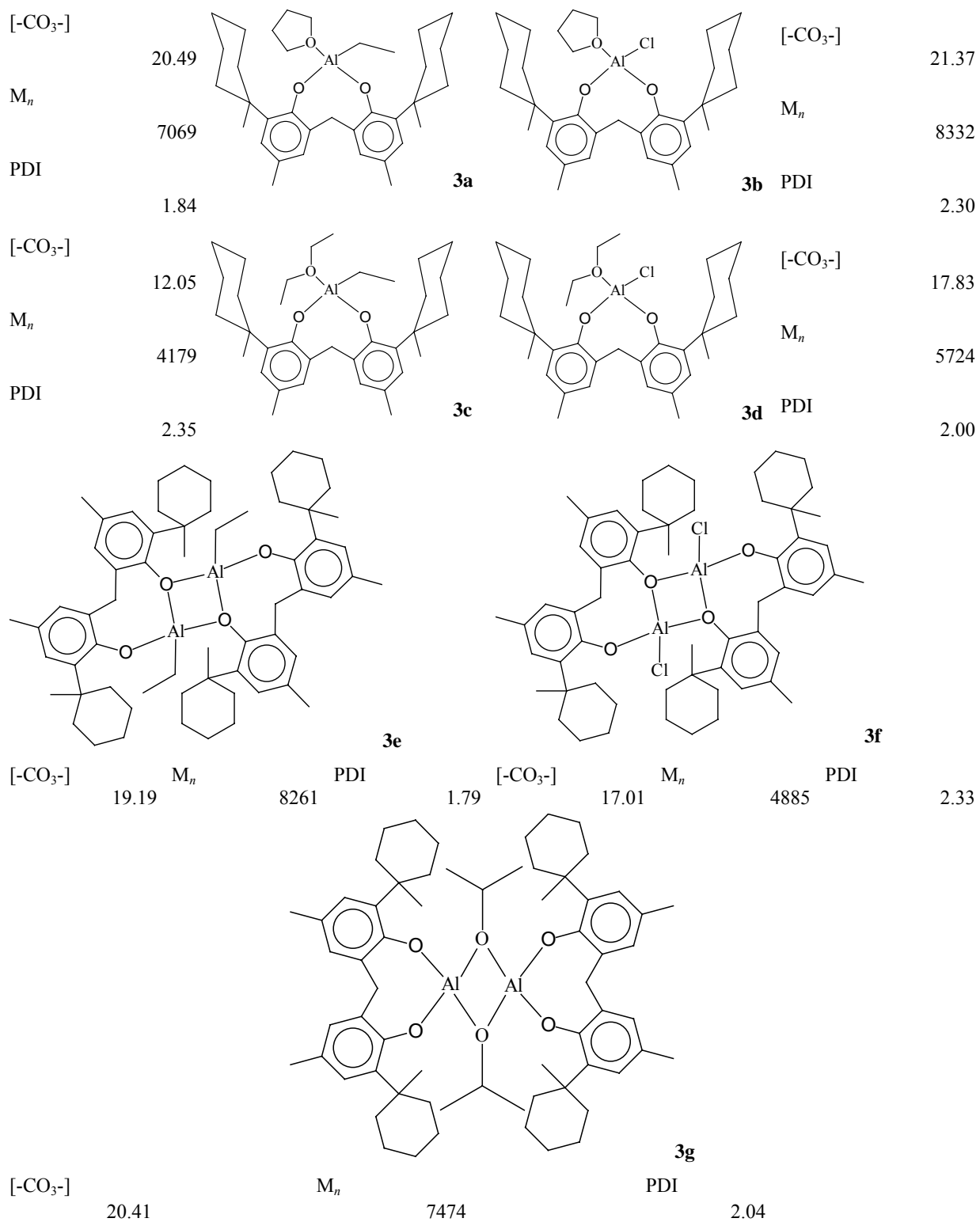
$^1\text{H NMR}$: δ (ppm) = 1.08, 1.40, 1.59, 1.85; IR (KBr, cm^{-3}): 3447 (m), 2985 (s), 2937 (s), 2860 (s), 1824 (m), 1652 (m), 1541 (m), 1501 (sm), 1457 (s), 1261 (s), 1160 (sm), 1093 (sm), 966 (s), 891 (s), 837 (m), 781 (m), 745 (m), 534 (sm).

8 Structural formulas

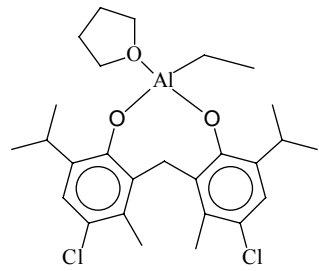
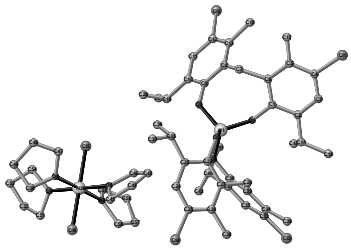
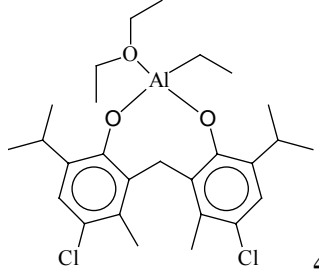
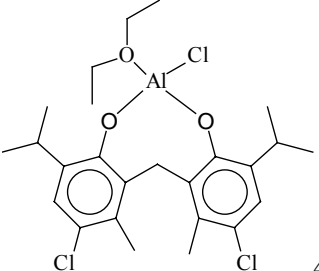
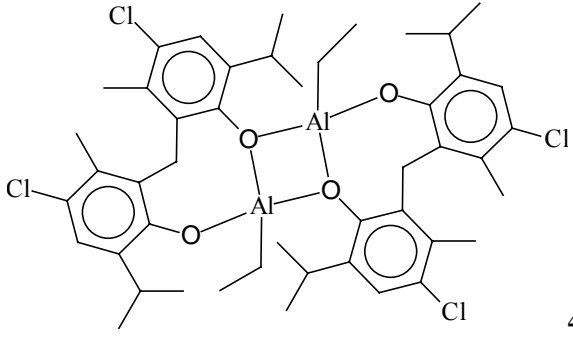
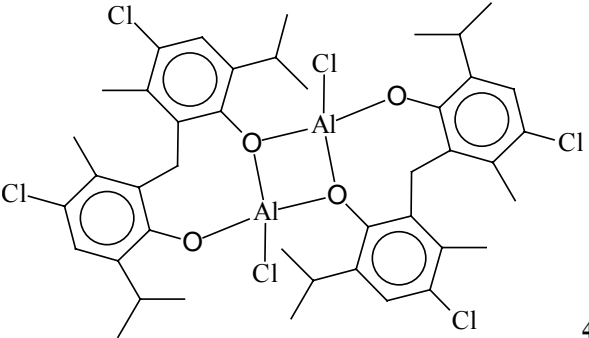
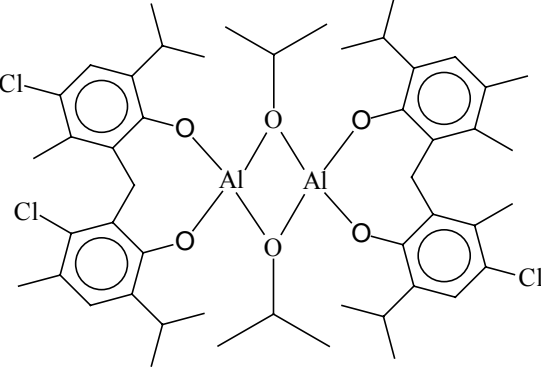
8.1 Structural formulas of 1-based complexes

	6.81								
$[-CO_3^-]$									
M_n									11.36
	16156								10472
PDI									1.77
	1.58								
			1a						
$[-CO_3^-]$									
M_n									11.47
	20.49								8190
PDI									1.61
	6030								
	2.40								
			1c						
$[-CO_3^-]$									
M_n									11.47
	20.49								8190
PDI									1.61
	6030								
	2.40								
			1c						
$[-CO_3^-]$									
M_n									11.47
	16.95								8190
PDI									1.61
	5649								
	2.43								
			1e						
$[-CO_3^-]$									
M_n									11.47
	19.46								8190
PDI									1.99
	10585								
	1.99								
			1f						
$[-CO_3^-]$									
M_n									11.47
	18.76								8604
PDI									1.94
	8604								
	1.94								
			1g						

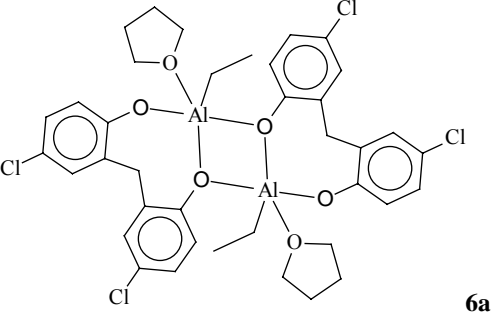
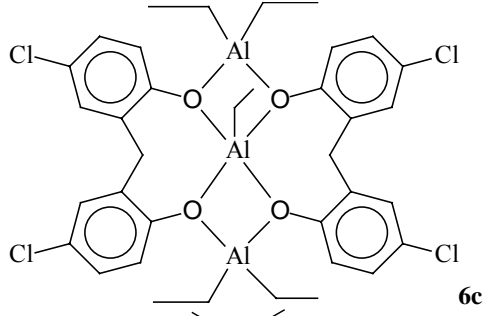
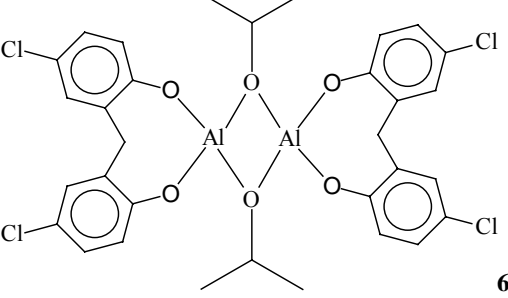
8.3 Structural formulas of 3-based complexes



8.4 Structural formulas of 4-based complexes

$[-CO_3^-]$	12.03			$[-CO_3^-]$	14.81
M_n	10255			M_n	10160
PDI	2.41			PDI	2.41
		4a	4b		
$[-CO_3^-]$	4.11			$[-CO_3^-]$	11.14
M_n	19789			M_n	34543
PDI	1.57			PDI	1.28
		4c	4d		
		4e	4f		
$[-CO_3^-]$	12.82	M_n	9004	PDI	2.43
				$[-CO_3^-]$	13.97
				M_n	12159
				PDI	2.34
			4g		
$[-CO_3^-]$	15.58	M_n	11289	PDI	1.91

8.6 Structural formulas of 6-based complexes

 <p style="text-align: right;">6a</p>	[-CO ₃ -]	The reaction did not take a place.
M _n		
PDI		
 <p style="text-align: right;">6c</p>	[-CO ₃ -]	1.98
M _n		19663
PDI		1.53
 <p style="text-align: right;">6g</p>	[-CO ₃ -]	11.53
M _n		6059
PDI		2.95

8.7 Structural formulas of 7-based complexes

	[-CO ₃ ⁻]	4.57
	<i>M_n</i>	14937
	PDI	1.57
7a		
	[-CO ₃ ⁻]	24.39
	<i>M_n</i>	6243
	PDI	1.50
7c		
	[-CO ₃ ⁻]	22.42
	<i>M_n</i>	6377
	PDI	1.51
7f		
	[-CO ₃ ⁻]	24.21
	<i>M_n</i>	4542
	PDI	1.46
7g		

9 Bibliography

1. W. H. Carothers, F. J. van Natta in *J. Am. Chem. Soc.* 1930, 52(1), 314,
2. J. W. Hill, W. H. Carothers, in *J. Am. Chem. Soc.* 1933, 55(12), 5033
3. H. Schnell in *Ind. Eng. Chem.* 1959, 51(2), 157
4. J. E. Hallgren, G. M. Lucas in *J. Organometal. Chem.*, 1981, 212, 135;
5. M. Goyal, R. Nagahata, J. Sugiyama, M. Asai, M. Ueda, K. Takeuchi in *Polymer*, 2000, 41, 2289;
6. R. V. Chaudhari R. V. et. al. in *US Pat.* 6,222,002,
7. W. B. Kim, J. S. Lee in *J. Appl. Polym. Sci.* 2002, 86, 937
8. K. Okuyama, J. Sugiyama, R. Nagahata, M. Asai, M. Ueda, K. Takeuchi in *Macromolecules*, 2003, 36, 6953
9. W. Kuran, in "Polymeric Material Encyclopedia", Vol. 9, CRC Press, 1996
10. P. T. Anastas, J. C. Warner, *Green Chemistry, Theory and Practice*, Oxford University Press, New York, 1998, p.30
11. E. J. Beckman in *J. Supercritical Fluids*, 2004, 28, 121
12. S. Inoue, H. Koinuma, T. Tsuruta in *J. Polym. Sci. Polym. Lett.*, 1969, 7, 287
13. S. Inoue, H. Koinuma, T. Tsuruta in *Macromol. Chem.*, 1969, 130, 210
14. B. S. Kim, D. J. Mooney in *Trends in Biotechnology*, 1998, 16, 224
15. S.-Y. Yang, X.-G. Fang, L.-B. Chen in *Polymers for advanced Technologies*, 1996, 7, 605
16. M. Okada in *Prog. Polym. Sci. Sci.*, 2002, 27, 87
17. A. Rokicki, W. Kuran in *J. Macromol. Sci. Rev. Macromol. Chem. Phys.*, 1981, C21, 135
18. S. Inoue, H. Koinuma, T. Tsuruta in *Polymer J.*, 1971, 2, 220;
19. T. Hirano, S. Inoue, T. Tsuruta in *Die Makromolekulare Chemie*, 1975, 176, 1913
20. Z. W. Liu, M. Torrent, K. Morokuma in *Organometallics*, 2002, 21, 1056
21. A. Rokicki, W. Kuran in *Makromol. Chem.*, 1979, 180, 2153
22. P. Gorecki, W. Kuran in *J. Polym. Sci. Part C*, 1985, 23, 299
23. W. Kuran, S. Pasykiewicz, J. Skupinska, A. Rokicki in *Makromol. Chem* 1976, 177, 11
24. W. Kuran, S. Pasykiewicz, J. Skupinska in *Makromol. Chem* 1976, 177, 1283;
25. W. Kuran, S. Pasykiewicz, J. Skupinska in *Makromol. Chem* 1977, 178, 2149;
26. Y. Hino, Y. Yoshida, S. Inoue, in *Polym J* 1984, 16, 159
27. M. Kobayashi, S. Inoue, T. Tsuruta, in *J. Polym. Sci. Polym. Chem. Ed.*, 1973, 11, 2383
28. D. J. Darensbourg, M. W. Holtcamp in *Macromolecules*, 1995, 28, 7577
29. D. J. Darensbourg, M. W. Holtcamp, G. E. Struck, M. S. Zimmer, S. A. Niezgoda, P. Rainey, J. B. Robertson, J. D. Draper, J. H. Reibenspies. in *J. Am. Chem. Soc.*, 1999, 121, 107

30. D. J. Darensbourg, J. R. Wildeson, J. C. Yarbrough, J. H. Reibenspies in *J. Am. Chem. Soc.*, 2000, 122, 12487
31. D. J. Darensbourg, M. S. Zimmer, P. Rainey, D. L. Larkins in *Inorg. Chem.*, 1998, 37, 2852
32. D. J. Darensbourg, M. S. Zimmer, P. Rainey, D. L. Larkins in *Inorg. Chem.*, 2000, 39, 1578
33. A. Rokicki in US Pat. 4,943,677
34. D. J. Darensbourg, N. W. Stafford, T. Katsurao in *J. Molecular Cat. A, Chem.*, 1995, 104, L1
35. S. A. Motika, T. L. Pickering, A. Rokicki, B. K. Stein in US Pat. 5,026,676
36. M. Ree, J. Y. Bae, J. H. Jung, T. J. Shin in *J. Polym. Sci. Part A*, 1999, 37, 1863
37. K. Soga, E. Imai, I. Hattori in *Polymer J.*, 1981, 13, 407
38. S. A. Motika, T. L. Pickering, A. Rokicki, B. K. Stein in U.S. Pat. 5,026,676
39. S. Inoue in *Prog. Polym. Sci. Jpn.* 1982, 8, 1
40. H. Kawachi, S. Minami, J. N. Armor, A. Rokicki, B. K. Stein in U.S. Pat. 4,981,948
41. D. J. Darensbourg, M. S. Zimmer in *Macromolecules*, 1999, 32, 2137
42. M. Super, E. Berluche, C. Costello, E. J. Beckman in *Macromolecules*, 1997, 30, 368
43. T. Aida, S. Inoue in *Macromolecules*, 1982, 15, 682
44. S. Inoue in *J. Polym. Sci., Part A: Polym. Chem.*, 2000, 38, 2861
45. T. Norikazu, S. Inoue et. al. in *Makromol. Chem.*, 1978, 179, 1377
46. T. Aida, S Inoue in *Macromolecules*, 1986, 19, 8
47. Copolymerisation of EO and CO₂: J. H. Jung, M. Ree, T. Chang in *J. Polym. Sci., Part A: Polym. Chem.* 1999, 37, 1863
48. W. J. Kruper, D. V. Dellar in *J. Org. Chem.*, 1995, 60, 725
49. W. J. Kruper, D. V. Dellar, US Pat. 4,663,467
50. S. Mang, A. I. Cooper, M. E. Colclough, N. Chauhan, A. B. Holmes in *Macromolecules* 2000, 33, 303
51. H. Sugimoto, H. Ohshima, S. Inoue in *J Pol. Sci, A, Polym. Chem.* 2003, 41, 3549
52. A large variety of carbonates could be synthesised, for instance propylene carbonate was synthesised with TON as high as 916 with addition of one DMAP equivalent. Other epoxides used were styrene oxide, epichlorohydrin and butadiene monoepoxide.
53. Z. Qin, C. L. Thomas, S. Lee, G. W. Coates in *J. Am. Chem. Soc.*, 2002, 124, 6335
54. D. J. Darensbourg, R. A. Mackiewicz, A. L. Phelps, D. R. Billodeaux in *Acc. Chem. Res.*, 2004, 37, 836
55. D. J. Darensbourg, R. M. Mackiewicz, J. L. Rodgers, A. L. Phelps in *Inorg. Chem.*, 2004, 43, 1831
56. D. J. Darensbourg, R. M. Mackiewicz, D. R. Billodeaux in *Organometallics*, 2005, 24, 144
57. R. Eberhardt, M. Allmendinger, B. Rieger in *Macr. Rapid Com.*, 2003, 24, 194
58. R. L. Paddock, SB. T. Nguyen in *J. Am. Chem. Soc.*, 2001, 123, 11498

59. Y. M. Shen, W. L. Duan, M. Shi, in *J. Org. Chem.*, 2003, 68, 1559
60. Z. Qin, C. M. Thomas, S. Lee, G. W. Coates in *Angew. Chem. Int. Ed.*, 2003, 42, 5484
61. X. B. Lu, Y. Wang in *Angew. Chem.*, 2004, 116, 3658
62. D. J. Darensbourg, J. L. Rodgers, C. C. Fang in *Inorg. Chem.*, 2003, 42, 4498
63. T. Sarbu, T. Styranec, E. J. Beckman in *Nature*, 2000, 405, 165
64. Darensbourg reported system affording polymer with TOF as high as 2685.5, what was obtained using Cr-salen – PPNN₃ system. Coates' catalytic systems do not require the use of cocatalyst to get such result, see Ref. 56.
65. K. Yiu, C. W. Jones in *Organometallics*, 2003, 22, 2571
66. M. Cheng, D. R. Moore, J. J. Reczek, B. M. Chamberlain, E. B. Lobkovsky, G. W. Coates in *J. Am. Chem. Soc.*, 2001, 123, 8738
67. M. Cheng, A. B. Attygalle, E. B. Lobkovsky, G. W. Coates in *J. Am. Chem. Soc.*, 1999, 121, 11583
68. L. R. Rieth, D. R. Moore, E. B. Lobkovsky, G. W. Coates in *J. Am. Chem. Soc.*, 2002, 124, 15239
69. K. Nozaki, K. Nakano, T. Hiyama in *J. Am. Chem. Soc.*, 1999, 121, 11008
70. K. Nakano, K. Nozaki, T. Hiyama in *J. Am. Chem. Soc.*, 2003, 125, 5501
71. M. Cheng, N. A. Darling, E. B. Lobkovsky and G. W. Coates in *Chem. Commun.*, 2000, 2007
72. M. Kröger, C. Folli, O. Walter, M. Döring in *Adv. Synth. Cat.*, 2005, 347, 1325
73. M. H. Chisholm, D. Navarro-Lobet, Z. Zhou in *Macromolecules*, 2002, 35, 6494
74. M. H. Chisholm, C. C. Lin, J. C. Gallucci, B. T. Ko in *Dalton Trans.*, 2003, 406
75. M. H. Chisholm, D. Navarro-Llobet in *Macromolecules*, 2002, 35, 2389
76. M. J. Byrnes, M. H. Chisholm, D. Navarro-Llobet, C. M. Hadad, Z. Zhou in *Macromolecules*, 2004, 37, 4139
77. M. H. Chisholm, D. Navarro-Llobet, W. J. Simonsick Jr. in *Macromolecules*, 2001, 34, 8851
78. T. Mole, E. A. Jeffery in *Organoaluminium Compounds*, Elsevier, Amsterdam, 1972, p 214
79. D. C. Bradley, R. C. Mehrotra, D. P. Gaur in *Metal Alkoxides*, Academic Press, London, 1978, p 74 and 122
80. J. J. Eisch in Chapter "Aluminium" in "Comprehensive Organometallic Chemistry", C. Wilkinson, F. G. A. Stone, E. W. Abel (Eds), Pergamon Press, Oxford, U K., 1982; Vol. I, p 583.
81. V. J. Shiner Jr., D. Whittaker in *J. Am. Chem. Soc.*, 1969, 91, 394
82. A. Duda, St Penczek in *Macromolecules*, 1995, 28, 5981
83. Ph. Dubois, N. Ropson, R. Jérôme, Ph. Teyssié in *Macromolecules*, 1996, 29, 1965
84. A. Duda, St. Penczek in *Macromol. Rapid Commun.*, 1995, 16, 67
85. T. A. Zevaco, A. Janssen, J. Sypień, E. Dinjus in *Green Chemistry*, 2005, 7, 659

86. C-H. Lin, L-F. Yan, F-C. Wang, Y-L. Sun, C-C. Lin in *J. Organometallic Chem.*, 1999, 587, 151
87. B. T. Ko, C. C Wu, C. C. Lin in *Organometallics*, 2000, 19, 1864
88. Y. C. Liu, B. T. Ko, B. H. Huang, C. C. Lin in *Organometallics*, 2002, 21, 2066
89. I. Taden, H.-C. Kang, W. Massa, T. P. Spaniol, J. Okuda in *Eur. J. Inorg. Chem.*, 2000, 441
90. H-L. Chen, B-T. Ko, B-H. Huang, and C-C. Lin in *Organometallics*, 2001, 20, 5076
91. T-C. Liao, Y-L. Huang, B-H Huang, C-C. Lin in *Macromol. Chem. Phys.* 2003, 204, 885
92. M. Miyamoto, Y. Saeki, C. W. Lee, Y. Kimura, H. Maeda, K. Tsutsui in *Macromolecules*, 1997, 30, 6067
93. Y. Ohba, K. Ito, H. Maeda, H. Ebara, S. Takaki, T. Nagasawa in *Bull. Chem. Soc. Jpn.*, 1998, 71(10), 2393
94. S. Rantsordas et. al. in *Acta Cryst.*, 1978, B34, 1198
95. D. J. Beaver P. J. Stoffel in *J. Am. Chem. Soc.*, 1952, 74, 3410
96. P. A. Odorisio, S. D. Pastor, D. J. Spivack, D. Bimi, R. K. Rodebaugh in *Phosphorus and Sulphur*, 1984, 19, 285
97. B-T. Ko, Y-C. Chao, C. C. Lin et. al. in *Inorg. Chem.*, 2000, 39, 1463
98. Y. Takashima, Y. Nakayama, T. Hirao, H. Yasuda, A. Harada in *J. Organometallic Chem.*, 2004, 689, 612
99. J. A. Moore, F. A. L. Anet, in: W. Lwowshi (Ed.), "Comprehensive Heterocyclic Chemistry", vol. 7, Pergamon, Oxford, 1984, pp 653 – 707
100. W. Braune, PhD. Thesis, 2003, Johannes Gutenberg University, Mainz, Germany
101. Trialkyl aluminium, dialkyl halide aluminium, di-halide alkyl aluminium and tri-halide aluminium form dimers, see Ref. 80
102. S. G. Bott, H. Elgamal, J. L. Atwood in *J. Am. Chem. Soc.*, 1985, 107, 1796
103. R. Sluka, M. Necas and P. Sindelár in *Acta Cryst. Sec. E*, 2004, E60, m447
104. N. C. Means, C. M. Means, S. G. Bott, J. L. Atwood in *Inorg. Chem.*, 1987, 26, 1466
105. [(EDBP)AlMe]₂ (analogue of **1e**): see Ref. 97
106. [(MDBP)AlBuⁱ]₂ (analogue of **1e**): see Ref. 86.
107. [(EDBP)AlCl]₂ (analogue of **1f**) was described by: Ref. 86. and by B. Antelmann, M. H. Chisholm, S. S. Iyer, J. C. Huffman, D. Navaro-Llobet, M. Pagel, W. J. Simonsick, W. Zhong in *Macromolecules*, 2001, 34, 3159
108. G. Barraclough, D. C. Bradley, J. Lewis, I. M. Thomas in *J. Chem. Soc.*, 1961, 2601
109. F. F. Bentley, L. D. Smithson and A. L. Rozek in "Infrared Spectra and Characteristic Frequences ~700–300 cm⁻¹", J. Wiley & Sons, New York, 1968
110. H. Günzler, H. U. Gremlich in "IR Spectroscopy", Wiley-VCH, Weinheim, 2002

111. There is a number of publications of Ziemkowska, where Al complexes were synthesised in stoichiometry 3:2 (Al : Ligand) with Et₂O used as reactants solvent. She has worked with aliphatic and aromatic diols. a.) W. Ziemkowska, S. Pasynekiewicz in *J. Organometal. Chem.* 1996, 508, 243; b.) W. Ziemkowska, A. Sawicki in *Main Group Metal Chem.*, 2001, 24, 111; c.) W. Ziemkowska in *Main Group Metal Chem.*, 2000, 23, 337 and some others.
112. W. Ziemkowska in *Polyhedron*, 2001, 21, 281
113. Synthesis of polyethylene and other polyolefins: a.) Ti- and Zr-based catalysts: A. van der Linden, C. J. Schaverien, N. Meijboom, C. Ganter, A. G. Orpen in *J. Am. Chem. Soc.*, 1995, 117, 3008 and references therein; b.) Ti- and Zr-based catalysts, theoretical studies: R. D. J. Froese, D. G. Musaev, T. Matsubara, K. Morokuma in *J. Am. Chem. Soc.*, 1997, 119, 7190; c.) Ti- and Al-based catalysts: Z. Janas, L. B. Jerzykiewicz, P. Sobota, K. Szczegot, D. Wiśniewska in *Organometallics*, 2005, 24, 3987; d.) L. Porri, A. Ripa, P. Colombo, E. Miano, S. Capelli, S. V. Meille in *J. Organometal. Chem.* 1996, 514, 213; e.) R. D. J. Froese, D. G. Musaev, K. Morokuma in *Organometallic*, 1999, 18, 373; f.) R. D. J. Froese, D. G. Musaev, T. Matsubara, K. Morokuma in *J. Am. Chem. Soc.*, 1997, 119, 7190
114. ROP of cyclic ethers: a.) E. P. Wasserman, I. Annis, L. J. Chopin III, P. C. Price, J. L. Petersen, K. A. Abboud in *Macromolecules*, 2005, 38, 322; b.) see Ref. 100; c.) W. Braune, H. Ma, T. P. Spaniol, J. Okuda in *Organometallics*, 2005, 24, 1953
115. L. Oliva, T. P. Spaniol, U. Englert, J. Okuda in *Dalton Trans.* 2005, 721; b.) H. Ma, G. Melillo, L. Oliva, T. P. Spaniol and J. Okuda in *Acta Crystallogr., Sect. E* 2005, E61, m221; c.) G. H. Robinson, H. Zhang, J. L. Atwood in *Organometallics* 1987, 6, 887; d.) Z. Janas, L. B. Jerzykiewicz, S. Przybylak, R. L. Richards, P. Sobota in *Organometallics* 2000, 19, 4252
116. R. Benn, A. Rufinska, H. Lemkuhl, E. Janssen, C. Kruger, in *Angew. Chem. Int. Ed.*, 1983, 22, 779
117. M. D. Healy, J. W. Ziller, A. R. Barron in *J. Am. Chem. Soc.*, 1990, 112, 2949
118. J. J. Delpuech in "NMR of Newly Accessible Nuclei", vol. 2, Chap. 6, P. Laxxlo, Ed., Academic, New York, 1983
119. J. W. Atkin in *Progress in NMR Spectroscopy*, 1989, 21, 1
120. J. M. DeSimone, M. Strangle, J. S. Riffle, J. E. McGrath in *Macromol. Chem. Macromol. Symp.*, 1991, 42/43, 373
121. M. S. Super, R. M. Enick, and E. J. Beckman in *J. Chem. Eng. Data*, 1997, 42, 664
122. For comparison: the operation condition for (BDI)Zn(II)-based catalysts are 50°C and 7-12 bar of CO₂; M. Cheng, E. B. Lobkovsky, G. W. Coates in *J. Am. Chem. Soc.*, 1998, 120, 11018
123. G. W. Coates, D. R. Moore in *Angew. Chem. Int. Ed.*, 2004, 43, 6618

124. R. T. Morrison and R. N. Boyd in "Lehrbuch der Organische Chemie", 3rd ed. VCH, Weinheim, Germany, 1986, p. 693
125. W. Kuran, T. Listoś in *Macromol. Chem. Phys.*, 1994, 195, 1011
126. K. Nakano, K. Nozaki, T. Hiyama in *Macromolecules*, 2001, 34, 6325
127. M. H. Chisholm, W. Zhong in *J. Am. Chem. Soc.*, 2004, 126, 11030
128. T. Sarbu, E. J. Beckman in *Macromolecules*, 1999, 32, 6904
129. SADABS, Siemens area detector absorption correction programme, Siemens, 1997.
130. SHELX-97, G.M. Sheldrick, Universität Göttingen, 1997; b.) xpma, L. Zsolnai, G. Huttner, Universität Heidelberg, 1997; c.) Winray, R. Soltak, Universität Heidelberg, 1997.
131. D. J. Darensbourg, D. R. Billodeaux in *Inorg. Chem.*, 2005, 44, 1433
132. Z. Qin, C. M. Thomas, S. Lee, G. W. Coates in *Angew. Chem. Int. Ed.* 2003, 42, 5484
133. D. J. Darensbourg, J. R. Wildeson, J. C. Yarbrough in *Inorg. Chem.*, 2002, 41, 973
134. D. R. Moore, M. Cheng, E. B. Lobkovsky, G. W. Coates in *J. Am. Chem. Soc.*, 2003, 125, 11911
135. S. D. Allen, D. R. Moore, E. B. Lobkovsky, G. W. Coates in *J. Am. Chem. Soc.*, 2002, 124, 14248
136. D. R. Moore, M. Cheng, E. B. Lobkovsky, G. W. Coates in *Ang. Chem.*, 2002, 114, 2711
137. B. T. Ko, C. C. Lin in *Macromolecules*, 1999, 32, 8296
138. D. J. Darensbourg, J. L. Rodgers, R. M. Mackiewicz, A. L. Phelps, *Catalysis Today*, 2004, 98, 485
139. F. H. Allen, O. Kennard, *Chemical Design Automation News*, 1993, 8, 31
140. C-H. Huang, F-C. Wang, B-T. Ko, T-L Yu, C-C. Lin, *Macromolecules*, 2001, 34, 356
141. W. Braune, H. Ma, T. P. Spaniol, J. Okuda in *Organometallic*, **2005**, 24, 1953
142. J. Lewiński in *Encyclopedia of Spectroscopy and Spectrometry*, Ed. J. Lindon, G. Tratner, J. Holmes, Academic Press, 1999, 1, 691
143. R. Benn, A. Rufinska, H. Lemkuhl, E. Janssen in *Organometallic*, 1999, 18, 373
144. B. T. Ko, Y. C. Chao, C. C. Lin, *J. Organometallic Chem.*, 2000, 589, 13
145. S. Inoue in *J. Polymer Sci. A: Polym. Chem.*, 2000, 38, 2861
146. a) R. Bacskai, *J. Polym. Sci., A1, Polym. Chem.*, 1963, 1, 2777; b) S. L. Malhotra, L. P. Blanchard, *J. Macromol. Sci., Chem. A*, 1978, 12, 1379; c) M. Sepulchre, A. Kassamaly, N. Spassky, *Makromol. Chem., Macromol. Symp.*, 1991, 42/43, 489; d) Y. Hasebe, T. Tsuruta, *Makromol. Chem.*, 1987, 188, 1403
147. X. B. Lu, B. Liang, Y. J. Zhang, Y. Z. Tian, Y. M. Wang, C. X. Bai, H. Wang, R. Zhang, *J. Am. Chem. Soc.*, 2004, 126, 3732
148. R. Paddock, Y. Hiyama, J. McKay, S. Nguyen, *Tetrahedron Lett.*, 2004, 45, 2023

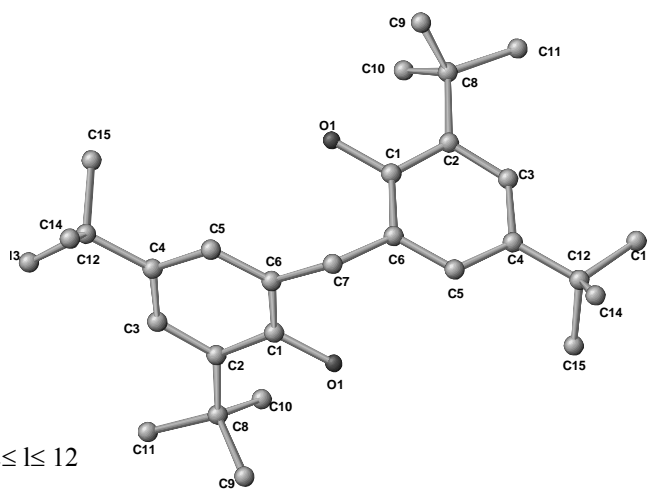
149. Y. M. Shen, W. L. Duan, M. Shi, *J. Org. Chem.*, 2003, 68, 1559
150. X. B. Lu, X. J. Feng, R. He, *Appl. Catal. A*, 2002, 234, 25
151. X. B. Lu, R. He, C. X. Bai, *J. Mol. Catal. A*, 2002, 186, 1

10 Appendix 1 - Crystal structures

10.1 Crystallographic data of the ligand 1

There is half a molecule in the independent unit of the elementary cell.

Compound	1
Empirical formula	C ₁₄ H ₂₂ O
Formula weight	212.32
Crystal size	0.7 x 0.4 x 0.08 mm ³
Crystal system	Monoclinic
Space group	C2/c (No. 15)
Unit cell dimension	a = 27,809(5) b = 10,1225(18) c = 9,2655(17) $\alpha = 90^\circ$ $\beta = 93.852(3)^\circ$ $\gamma = 90^\circ$
Cell volume	2602.3(8) x 10 ⁶ pm ³
Z	Z = 8
Density (calculated)	1.084 g/cm ³
Temperature	200 K
θ -Range	1,47 \leq θ \leq 28,30 $^\circ$
Scan	ω -Scan, $\Delta \omega = 0.3^\circ$
Index ranges	-36 \leq h \leq 36, -13 \leq k \leq 13, -12 \leq l \leq 12
Number of reflections measured	15092
Unique reflections	3194
Reflections observed	2191 (I > 2 σ)
Parameter refined	155
Residual electron density	0.790 x 10 ⁻⁶ e/pm ³
Corrections	Lorentz and polarisation, exp. absorption correction
Structure solution	direct methods
Structure refinement	full matrix least square on F ²
Programs used	SHELX-97, xpma, zortep
R indices	R1 = 0.1071 (I > 2 σ) Rw = 0.2528 (all data against F ²)



Standard deviations are given in parentheses.

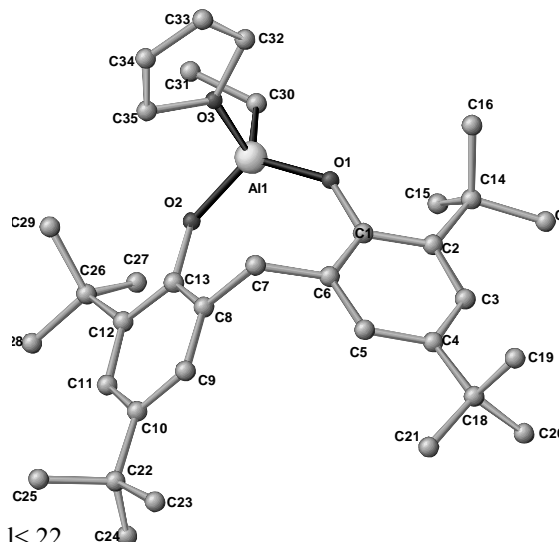
Selected bonds lengths [Å] and angles [°] for **1**.

O(1)-C(1)	1.375(3)	O(1)-C(1)-C(6)	119.5(2)
C(1)-C(6)	1.404(3)	O(1)-C(1)-C(2)	118.9(2)
C(1)-C(2)	1.408(3)	C(6)-C(1)-C(2)	121.6(2)
C(2)-C(3)	1.396(3)	C(3)-C(2)-C(1)	116.4(2)
C(2)-C(8)	1.540(3)	C(3)-C(2)-C(8)	121.5(2)
C(3)-C(4)	1.399(3)	C(1)-C(2)-C(8)	122.1(2)
C(4)-C(5)	1.394(3)	C(2)-C(3)-C(4)	124.3(2)
C(4)-C(12)	1.540(3)	C(5)-C(4)-C(12)	120.8(2)
C(5)-C(6)	1.395(3)	C(4)-C(5)-C(6)	122.0(2)
C(6)-C(7)	1.524(3)	C(5)-C(4)-C(3)	116.9(2)

10.2 Crystallographic data of the complex **1a**

It crystallises with additional 1.6 molecules of THF per unit of which the one with 60 percent occupancy is disordered.

Compound	1a
Empirical formula	AlC ₃₅ H ₅₅ O ₃ * 1,6 C ₄ H ₈ O
Formula weight	666.14
Crystal size	1.0 x 0.9 x 0.7 mm ³
Crystal system	Monoclinic
Space group	P2(1)/c (No. 15)
Unit cell dimension	a = 13.5017(13) b = 19.2244(18) c = 17.2289(17) $\alpha = 90^\circ$ $\beta = 107.8710(10)^\circ$ $\gamma = 90^\circ$
Cell volume	4256.2(7) x 10 ⁶ pm ³
Z	Z = 4
Density (calculated)	1.040 g/cm ³
Temperature	200 K
θ -Range	1,58 $\leq \theta \leq$ 28,34 $^\circ$
Scan	ω -Scan, $\Delta \omega = 0.3^\circ$
Index ranges	-18 $\leq h \leq$ 17, -24 $\leq k \leq$ 25, -22 $\leq l \leq$ 22
Number of reflections measured	49354
Unique reflections	10385
Reflections observed	7621 (I > 2 σ)
Parameter refined	494
Residual electron density	0.961 x 10 ⁻⁶ e/pm ³
Corrections	Lorentz and polarisation, exp. absorption correction
Structure solution	direct methods
Structure refinement	full matrix least square on F ²
Programs used	SHELX-97, xpma, zortep
R indices	R1 = 0.1110 (I > 2 σ) Rw = 0.2723 (all data against F ²)



Standard deviations are given in parentheses.

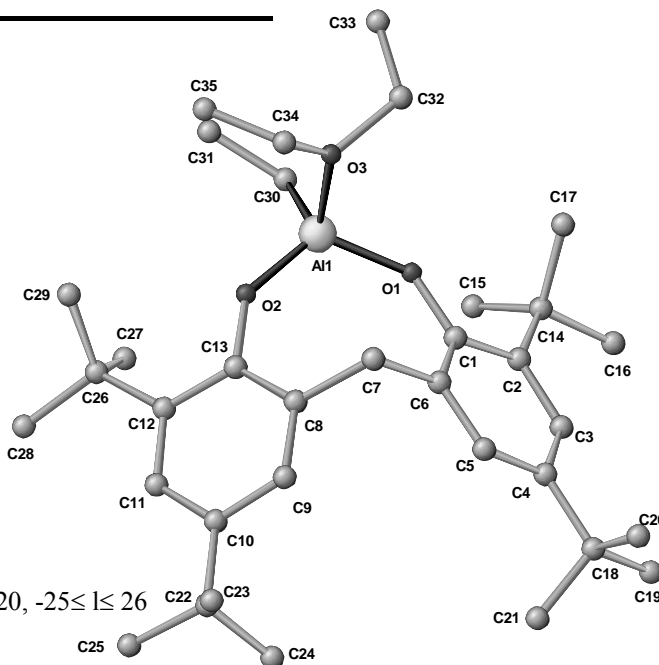
Selected bonds lengths [Å] and angles [°] for **1a**.

Al(1)-O(2)	1.7156(18)	O(2)-Al(1)-O(1)	115.76(9)
Al(1)-O(1)	1.7217(18)	O(2)-Al(1)-O(3)	100.50(9)
Al(1)-O(3)	1.8850(19)	O(1)-Al(1)-O(3)	105.22(9)
Al(1)-C(30)	1.950(3)	O(2)-Al(1)-C(30)	114.92(11)
O(1)-C(1)	1.349(3)	O(1)-Al(1)-C(30)	112.33(11)
O(2)-C(13)	1.352(3)	O(3)-Al(1)-C(30)	106.36(11)
O(3)-C(32)	1.436(4)	C(1)-O(1)-Al(1)	140.71(15)
C(1)-C(6)	1.405(3)	C(32)-O(3)-C(35)	109.2(2)
C(6)-C(7)	1.518(3)	C(35)-O(3)-Al(1)	125.08(18)
C(7)-C(8)	1.519(3)	C(3)-C(2)-C(1)	117.5(2)
H(7B)-O(3)	2.583(0)		
H(7A)-O(3)	4.079(0)		

10.3 Crystallographic data of the complex **1c**

It crystallises with one additional molecule of Et₂O per the two independent molecules in the unit of the elementary cell, one *t*-Bu-group and one coordinated Et₂O molecule are disordered.

Compound	1c
Empirical formula	2 AlC ₃₅ H ₅₇ O ₃ · 4H ₂ O
Formula weight	1179.69
Crystal size	0.8 x 0.8 x 0.6 mm ³
Crystal system	Monoclinic
Space group	Cc (No. 9)
Unit cell dimension	a = 27.734(3) b = 15.6616(17) c = 19.894(2) α = 90° β = 118.2850(10)° γ = 90°
Cell volume	7609.4(14) x 10 ⁶ pm ³
Z	Z = 4
Density (calculated)	1.030 g/cm ³
Temperature	200 K
θ-Range	1,54 ≤ θ ≤ 28,27°
Scan	ω-Scan, Δ ω=0.3°
Index ranges	-36 ≤ h ≤ 36, -20 ≤ k ≤ 20, -25 ≤ l ≤ 26
Number of reflections measured	43853
Unique reflections	18092
Reflections observed	15589 (I > 2 σ)
Parameter refined	842
Residual electron density	0.638 x 10 ⁻⁶ e/pm ³
Corrections	Lorentz and polarisation, exp. absorption correction
Structure solution	direct methods
Structure refinement	full matrix least square on F ²
Programs used	SHELX-97, xpma, zortep
R indices	R1 = 0.0739 (I > 2 σ) Rw = 0.1850 (all data against F ²)



Standard deviations are given in parentheses.

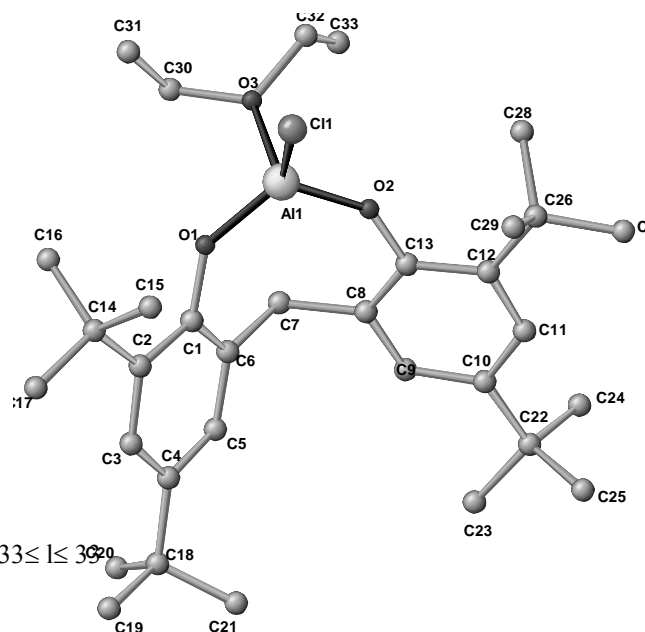
Selected bonds lengths [Å] and angles [°] for **1c**.

Al(1)-O(1)	1.721(3)	O(2)-Al(1)-O(1)	116.89(12)
Al(1)-O(2)	1.721(2)	O(2)-Al(1)-O(3)	103.17(14)
Al(1)-O(3)	1.884(3)	O(1)-Al(1)-O(3)	102.67(13)
Al(1)-C(30)	1.946(4)	O(2)-Al(1)-C(30)	114.13(16)
O(1)-C(1)	1.349(4)	O(1)-Al(1)-C(30)	112.33(11)
O(2)-C(13)	1.351(4)	O(3)-Al(1)-C(30)	111.90(17)
O(3)-C(32)	1.534(6)	C(1)-O(1)-Al(1)	142.9(2)
O(3)-C(34)	1.434(6)	C(32)-O(3)-C(35)	109.2(2)
C(6)-C(7)	1.523(5)	C(35)-O(3)-Al(1)	127.5(4)
C(7)-C(8)	1.523(5)	C(3)-C(2)-C(1)	118.1(3)
H(7A)-O(3)	2.704(0)		

10.4 Crystallographic data of the complex **1d**

There are two complex molecules in the independent unit of the elementary cell, it crystallises with one molecule of Et₂O per the two units, one coordinated Et₂O ligand is disordered.

Compound	1d
Empirical formula	2 AlC ₃₃ H ₅₂ O ₃ Cl * C ₄ H ₁₀ O
Formula weight	1190
Crystal size	0.4 x 0.3 x 0.3 mm ³
Crystal system	Monoclinic
Space group	P2(1)/n (No, 14)
Unit cell dimension	a = 15.8716(12) b = 18.7494(14) c = 25.0964(19) α = 90° β = 102.3610(10)° γ = 90°
Cell volume	7295.1(10) x 10 ⁶ pm ³
Z	Z = 4
Density (calculated)	1.086 g/cm ³
Temperature	200 K
θ-Range	1,66 ≤ θ ≤ 28,32°
Scan	ω-Scan, Δ ω=0.3°
Index ranges	-20 ≤ h ≤ 20, -24 ≤ k ≤ 24, -33 ≤ l ≤ 33
Number of reflections measured	85197
Unique reflections	17816
Reflections observed	10638 (I > 2 σ)
Parameter refined	807
Residual electron density	0.506 x 10 ⁻⁶ e/pm ³
Corrections	Lorentz and polarisation, exp. absorption correction
Structure solution	direct methods
Structure refinement	full matrix least square on F ²
Programs used	SHELX-97, xpma, zortep
R indices	R ₁ = 0.0948 (I > 2 σ) R _w = 0.1427 (all data against F ²)



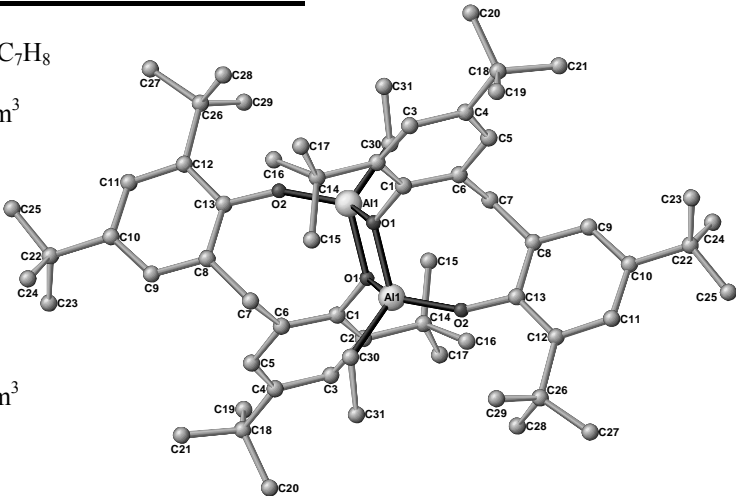
Standard deviations are given in parentheses.

Selected bonds lengths [Å] and angles [°] for **1d**.

Cl(1)-Al(1)	2.1270(8)	O(2)-Al(1)-O(1)	119.93(6)
Al(1)-O(2)	1.6912(12)	O(2)-Al(1)-O(3)	104.21(6)
Al(1)-O(1)	1.7010(12)	O(1)-Al(1)-O(3)	104.51(6)
Al(1)-O(3)	1.8498(15)	O(2)-Al(1)-Cl(1)	110.82(5)
O(1)-C(1)	1.3662(19)	O(3)-Al(1)-Cl(1)	103.52(6)
O(3)-C(30)	1.452(4)	C(13)-O(2)-Al(1)	144.01(11)
O(3)-C(32)	1.461(4)	C(1)-O(1)-Al(1)	138.34(11)
C(1)-C(6)	1.398(2)	C(30)-O(3)-Al(1)	19.66(19)
C(6)-C(7)	1.522(2)	C(32)-O(3)-Al(1)	116.46(19)
C(7)-C(8)	1.519(2)	C(1)-C(2)-C(14)	121.19(15)
H(7B)-O(3)	2.840(0)		

10.5 Crystallographic data of the complex **1e**

The independent unit cell contains one molecule of the complex and two solvent molecules.

Compound	1e	
Empirical formula	[AlC ₃₁ H ₄₇ O ₂] ₂ * 2 C ₇ H ₈	
Formula weight	1140	
Crystal size	0.3 x 0.35 x 0.1 mm ³	
Crystal system	triclinic	
Space group	P-1 (No, 2)	
Unit cell dimension	a = 10,0281(12) b = 12,3366(15) c = 14,2885(17) α = 89,875(2) $^\circ$ β = 88,721(2) $^\circ$ γ = 87,225(2) $^\circ$	
Cell volume	1765.2(4) x 10 ⁶ pm ³	
Z	Z = 2	
Density (calculated)	1.074 g/cm ³	
Temperature	200 K	
θ -Range	1,43 \leq θ \leq 28,31 $^\circ$	
Scan	ω -Scan, $\Delta \omega$ =0.3 $^\circ$	
Index ranges	-13 \leq h \leq 13, -16 \leq k \leq 14, -17 \leq l \leq 19	
Number of reflections measured	13359	
Unique reflections	8283	
Reflections observed	3431 (I > 2 σ)	
Parameter refined	407	
Residual electron density	0.532 x 10 ⁻⁶ e/pm ³	
Corrections	Lorentz and polarisation, exp. absorption correction	
Structure solution	direct methods	
Structure refinement	full matrix least square on F ²	
Programs used	SHELX-97, xpma, zortep	
R indices	R1 = 0,2020 (I > 2 σ) Rw = 0,2409 (all data against F ²)	

Standard deviations are given in parentheses.

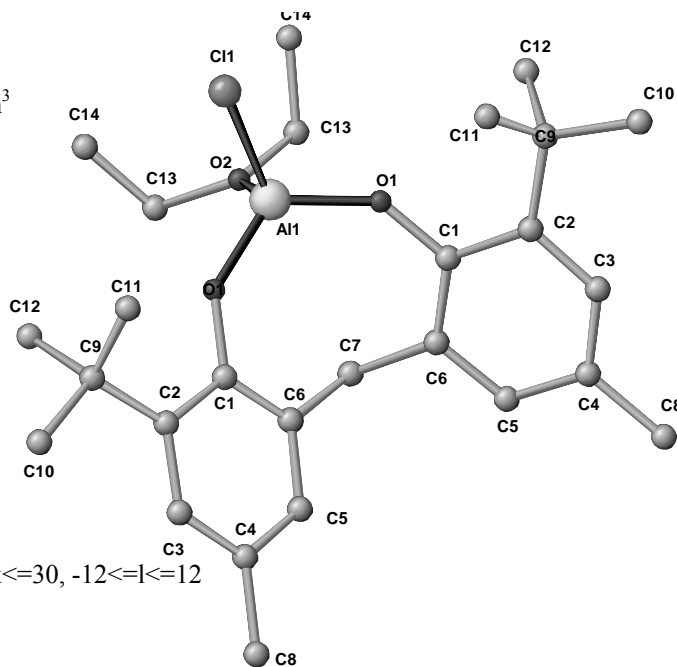
Selected bonds lengths [\AA] and angles [$^\circ$] for **1e**.

Al(1)-O(2)	1.700(2)	O(2)-Al(1)-O(1)	112.62(12)
Al(1)-O(1)	1.862(3)	O(2)-Al(1)-O(1)#1	118.26(12)
Al(1)-Al(1)#1	2.870(2)	O(1)-Al(1)-O(1)#1	79.61(12)
Al(1)-C(30)	1.938(4)	O(2)-Al(1)-C(30)	108.02(15)
O(1)-C(1)	1.428(4)	O(1)-Al(1)-C(30)	121.69(15)
O(2)-C(13)	1.363(4)	O(1)#1-Al(1)-C(30)	114.90(15)
C(4)-C(18)	1.536(5)	O(2)-Al(1)-Al(1)#1	123.96(11)
C(2)-C(14)	1.547(5)	O(1)#1-Al(1)-Al(1)#1	39.65(8)
C(6)-C(7)	1.525(5)	C(30)-Al(1)-Al(1)#1	128.00(13)
C(7)-C(8)	1.512(5)	C(1)-O(1)-Al(1)	123.9(2)

10.6 Crystallographic data of the complex 2d

There is half a molecule in the independent unit of the cell.

Compound	2d
Empirical formula	AlC ₂₇ H ₄₀ O ₃ Cl
Formula weight	474,45
Crystal size	0.2 x 0.25 x 0.05 mm ³
Crystal system	orthorhombic
Space group	Pnma (No. 62)
Unit cell dimension	a = 12.0705(7) b = 23.1724(14) c = 9.7390(6) $\alpha = 90^\circ$ $\beta = 90^\circ$ $\gamma = 90^\circ$
Cell volume	2724.0(3) x 10 ⁶ pm ³
Z	Z = 8
Density (calculated)	1.158 g/cm ³
Temperature	200 K
θ -Range	1.76 \leq θ \leq 28,29 $^\circ$
Scan	ω -Scan, $\Delta \omega = 0.3^\circ$
Index ranges	-15 \leq h \leq 16, -30 \leq k \leq 30, -12 \leq l \leq 12
Number of reflections measured	31453
Unique reflections	3456
Reflections observed	1691 (I > 2 σ)
Parameter refined	162
Residual electron density	0.227 x 10 ⁻⁶ e/pm ³
Corrections	Lorentz and polarisation, exp. absorption correction
Structure solution	direct methods
Structure refinement	full matrix least square on F ²
Programs used	SHELX-97, xpma, zortep
R indices	R ₁ = 0.1256 (I > 2 σ) R _w = 0.1317 (all data against F ²)



Standard deviations are given in parentheses.

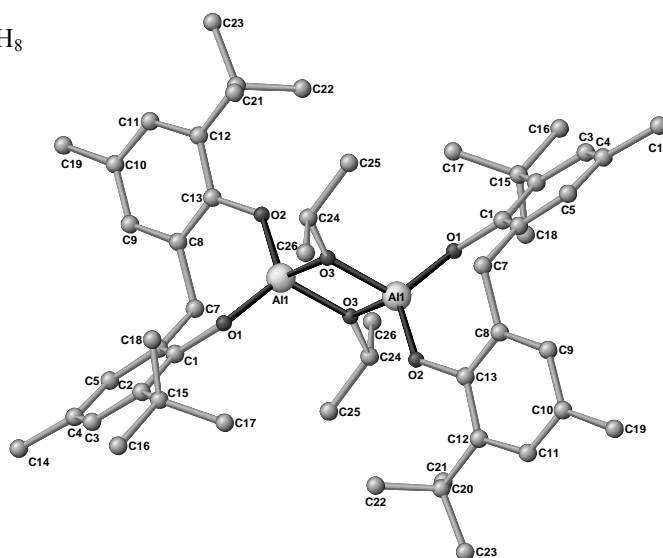
Selected bonds lengths [Å] and angles [°] for **2d**.

Cl(1)-Al(1)	2.1252(13)	O(1)-Al(1)-O(2)	104.55(7)
Al(1)-O(1)	1.6948(15)	O(1)-Al(1)-Cl(1)	110.14(6)
Al(1)-O(2)	1.849(2)	O(2)-Al(1)-Cl(1)	106.11(8)
O(1)-C(1)	1.361(2)	C(1)-O(1)-Al(1)	140.82(14)
C(1)-C(6)	1.428(4)	C(13)-O(2)-Al(1)	121.77(15)
C(6)-C(7)	1.523(3)	O(1)-C(1)-C(6)	120.08(19)
C(2)-C(3)	1.391(3)	C(1)-C(6)-C(7)	122.5(2)
C(2)-C(9)	1.536(3)	C(2)-C(9)-C(12)	109.6(2)
C(3)-C(4)	1.390(3)	C(2)-C(9)-C(11)	111.17(18)
C(4)-C(8)	1.518(3)	C(14)-C(13)-O(2)	112.0(2)
		C(7)-H(7B)-O(3)	164.7(0)

10.7 Crystallographic data of the complex **2g**

There is one molecule crystallising with one molecule toluene in the independent unit.

Compound	2g
Empirical formula	[AlC ₂₆ H ₃₇ O ₃] ₂ * 2 C ₇ H ₈
Formula weight	1033.34
Crystal size	0.6 x 0.5 x 0.2 mm ³
Crystal system	Monoclinic
Space group	P2(1)/c (No. 14)
Unit cell dimension	a = 11.5015(11) b = 16.5420(15) c = 16.0112(15) $\alpha = 90^\circ$ $\beta = 94.0440(10)^\circ$ $\gamma = 90^\circ$
Cell volume	3038.7(5) x 10 ⁶ pm ³
Z	Z = 4
Density (calculated)	1.129 g/cm ³
Temperature	200 K
θ -Range	1.77 \leq θ \leq 28.29 $^\circ$
Scan	ω -Scan, $\Delta \omega = 0.3^\circ$
Index ranges	-14 \leq h \leq 14, -21 \leq k \leq 21, -21 \leq l \leq 21
Number of reflections measured	35718
Unique reflections	7427
Reflections observed	4806 (I > 2 σ)
Parameter refined	355
Residual electron density	0.457 x 10 ⁻⁶ e/pm ³
Corrections	Lorentz and polarisation, exp. absorption correction
Structure solution	direct methods
Structure refinement	full matrix least square on F ²
Programs used	SHELX-97, xpma, zortep
R indices	R1 = 0.0474 (I > 2 σ) Rw = 0.0859 (all data against F ²)



Standard deviations are given in parentheses.

Selected bonds lengths [Å] and angles [°] for **2g**.

Al(1)-O(2)	1.7048(12)	O(1)-Al(1)-O(2)	117.53(6)
Al(1)-O(1)	1.6954(12)	O(1)-Al(1)-O(3)	115.78(6)
Al(1)-Al(1)#1	2.7573(10)	O(1)-Al(1)-O(1)#1	79.61(12)
Al(1)-O(3)	1.8156(12)	C(1)-O(1)-Al(1)	140.39(10)
C(1)-C(6)	1.400(2)	C(13)-O(2)-Al(1)	134.62(11)
O(2)-C(13)	1.412(2)	C(24)-O(3)-Al(1)	136.40(10)
C(2)-C(3)	1.389(2)	O(1)-C(1)-C(6)	119.73(14)
C(2)-C(15)	1.542(2)	O(1)-C(1)-C(2)	119.50(14)
C(4)-C(14)	1.393(2)	C(9)-C(8)-C(7)	118.33(15)
C(5)-C(6)	1.386(2)	O(2)-C(13)-C(12)	119.61(15)

10.8 Crystallographic data of the complex 3a

Compound	3a	
Empirical formula	AlC ₃₅ H ₅₁ O ₃	
Formula weight	546	
Crystal size	0.25 x 0.05 x 0.05 mm ³	
Crystal system	Monoclinic	
Space group	P2(1)/n (No, 14)	
Unit cell dimension	a = 10.5142(9) b = 15.6338(13) c = 19.4057(16) $\alpha = 90^\circ$ $\beta = 96.7870(10)^\circ$ $\gamma = 90^\circ$	
Cell volume	3167.5(5) x 10 ⁶ pm ³	
Z	Z = 4	
Density (calculated)	1.146 g/cm ³	
Temperature	200 K	
θ -Range	1.68 $\leq \theta \leq$ 28.34 $^\circ$	
Scan	ω -Scan, $\Delta \omega = 0.3^\circ$	
Index ranges	-14 $\leq h \leq$ 13, -20 $\leq k \leq$ 20, -25 $\leq l \leq$ 25	
Number of reflections measured	38034	
Unique reflections	7760	
Reflections observed	3351 (I > 2 σ)	
Parameter refined	412	
Residual electron density	0.654 x 10 ⁻⁶ e/pm ³	
Corrections	Lorentz and polarisation, exp. absorption correction	
Structure solution	direct methods	
Structure refinement	full matrix least square on F ²	
Programs used	SHELX-97, xpma, zortep	
R indices	R ₁ = 0.1710 (I > 2 σ) R _w = 0.2371 (all data against F ²)	

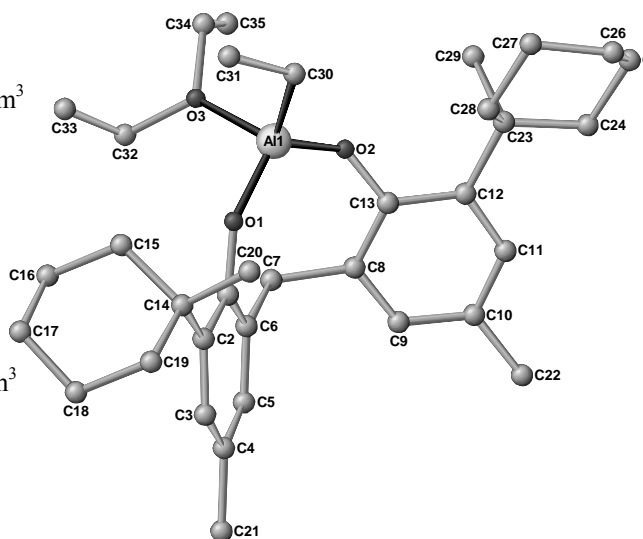
Standard deviations are given in parentheses.

Selected bonds lengths [Å] and angles [°] for **3a**.

Al(1)-O(2)	1.720(2)	O(1)-Al(1)-O(2)	117.08(11)
Al(1)-O(1)	1.713(2)	O(1)-Al(1)-O(3)	103.17(11)
Al(1)-O(3)	1.870(2)	O(2)-Al(1)-O(3)	101.11(12)
Al(1)-C(30)	1.955(4)	O(1)-Al(1)-C(30)	112.77(16)
O(1)-C(1)	1.351(3)	O(2)-Al(1)-C(30)	115.83(17)
O(2)-C(13)	1.362(4)	O(3)-Al(1)-C(30)	104.21(19)
O(3)-C(32)	1.41(2)	C(1)-O(1)-Al(1)	149.2(2)
O(3)-C(35)	1.46(2)	C(13)-O(2)-Al(1)	136.52(19)
C(1)-C(2)	1.406(4)	C(32)-O(3)-C(35)	114.7(15)
C(6)-C(7)	1.512(4)	O(1)-C(1)-C(2)	120.4(3)
H(7B)-O(3)	2.821(0)		

10.9 Crystallographic data of the complex **3c**

Compound	3c
Empirical formula	AlC ₃₅ H ₅₃ O ₃
Formula weight	548
Crystal size	0.25 x 0.2 x 0.04 mm ³
Crystal system	Orthorhombic
Space group	Pbca (No. 61)
Unit cell dimension	a = 14.8606(18) b = 20.105(3) c = 21.775(3) $\alpha = 90^\circ$ $\beta = 90^\circ$ $\gamma = 90^\circ$
Cell volume	6505.6(14) x 10 ⁶ pm ³
Z	Z = 8
Density (calculated)	1.121 g/cm ³
Temperature	200 K
θ -Range	1.87 \leq θ \leq 28.35 $^\circ$
Scan	ω -Scan, $\Delta \omega = 0.3^\circ$
Index ranges	-19 \leq h \leq 19, -26 \leq k \leq 26, -29 \leq l \leq 29
Number of reflections measured	76526
Unique reflections	8104
Reflections observed	1920 (I > 2 σ)
Parameter refined	373
Residual electron density	0.654 x 10 ⁻⁶ e/pm ³
Corrections	Lorentz and polarisation, exp. absorption correction
Structure solution	direct methods
Structure refinement	full matrix least square on F ²
Programs used	SHELX-97, xpma, zortep
R indices	R ₁ = 0.0691 (I > 2 σ) R _w = 0.3234 (all data against F ²)



Standard deviations are given in parentheses.

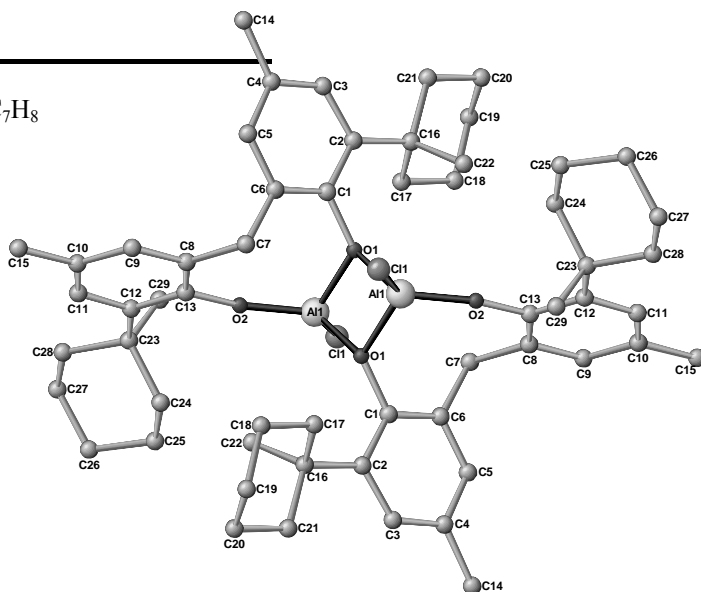
Selected bonds lengths [Å] and angles [°] for **3c**.

Al(1)-C(30)	1.945(5)	O(1)-Al(1)-O(2)	116.29(17)
Al(1)-O(1)	1.703(3)	O(1)-Al(1)-O(3)	100.79(16)
Al(1)-O(2)	1.722(3)	O(2)-Al(1)-O(3)	104.60(16)
Al(1)-O(3)	1.882(3)	O(1)-Al(1)-C(30)	113.20(19)
O(1)-C(1)	1.342(5)	O(2)-Al(1)-C(30)	114.04(19)
O(2)-C(13)	1.360(5)	O(3)-Al(1)-C(30)	105.96(19)
O(3)-C(32)	1.473(5)	C(1)-O(1)-Al(1)	147.4(3)
O(3)-C(35)	1.455(5)	C(13)-O(2)-Al(1)	138.8(3)
C(1)-C(2)	1.410(6)	C(34)-O(3)-C(32)	115.1(4)
C(6)-C(7)	1.530(6)	O(1)-C(1)-C(2)	119.8(4)
H(7B)-O(3)	2.817(0)		

10.10 Crystallographic data of the complex **3f**

There is half a molecule in the independent unit of the elementary cell crystallises with 1 molecule of toluene per half molecule.

Compound	3f
Empirical formula	[AlC ₂₉ H ₃₈ O ₂ Cl] ₂ · 2 C ₇ H ₈
Formula weight	1114,9
Crystal size	0.3 x 0.35 x 0.1 mm ³
Crystal system	monoclinic
Space group	P2(1)/c (No. 14)
Unit cell dimension	a = 10.0047(8) b = 10.6334(9) c = 30.108(3) $\alpha = 90^\circ$ $\beta = 92.0840(10)^\circ$ $\gamma = 90^\circ$
Cell volume	3200.8(5) x 10 ⁶ pm ³
Z	Z = 4
Density (calculated)	1.189 g/cm ³
Temperature	200 K
θ -Range	1.35 \leq θ \leq 28.36 $^\circ$
Scan	ω -Scan, $\Delta \omega = 0.3^\circ$
Index ranges	-13 \leq h \leq 13, -14 \leq k \leq 14, -39 \leq l \leq 40
Number of reflections measured	38502
Unique reflections	7965
Reflections observed	5005 (I > 2 σ)
Parameter refined	398
Residual electron density	0.916 x 10 ⁻⁶ e/pm ³
Corrections	Lorentz and polarisation, exp. absorption correction
Structure solution	direct methods
Structure refinement	full matrix least square on F ²
Programs used	SHELX-97, xpma, zortep
R indices	R ₁ = 0.1265 (I > 2 σ) R _w = 0.2236 (all data against F ²)



Standard deviations are given in parentheses.

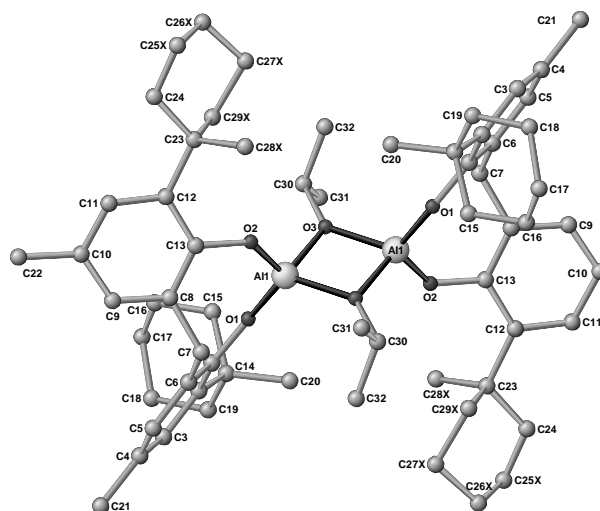
Selected bonds lengths [Å] and angles [°] for **3f**.

Al(1)-O(2)	1.674(2)	O(2)-Al(1)-O(1)	112.59(10)
Al(1)-O(1)	1.844(2)	O(2)-Al(1)-O(1)#1	125.43(11)
Al(1)-Cl(1)	2.0898(12)	O(1)-Al(1)-O(1)#1	80.20(9)
Al(1)-Al(1)#1	2.8218(17)	O(2)-Al(1)-Cl(1)	106.68(8)
O(1)-Al(1)#1	1.845(2)	O(1)-Al(1)-Cl(1)	121.47(8)
O(2)-C(13)	1.367(3)	O(2)-Al(1)-Al(1)#1	129.05(9)
C(1)-C(6)	1.393(4)	O(2)-Al(1)-Al(1)#1	40.12(6)
C(1)-C(2)	1.413(4)	O(1)#1-Al(1)-Al(1)#1	40.08(6)
C(6)-C(7)	1.525(4)	Cl(1)-Al(1)-Al(1)#1	124.26(6)
C(7)-C(8)	1.504(4)	C(1)-O(1)-Al(1)	122.11(16)
C(8)-C(9)	1.392(4)	C(1)-O(1)-Al(1)#1	128.71(16)
C(8)-C(13)	1.401(4)	C(13)-O(2)-Al(1)	155.1(2)

10.11 Crystallographic data of the complex **3g**

There is half a molecule in the independent unit of the elementary cell crystallises with 1 molecule of toluene per half molecule.

Compound	3g
Empirical formula	C ₃₂ H ₄₅ O ₃ Al
Formula weight	504.66
Crystal size	0.3 x 0.35 x 0.1 mm ³
Crystal system	monoclinic
Space group	P2(1)/c (No. 14)
Unit cell dimension	a = 10.0047(8) b = 10.6334(9) c = 30.108(3) $\alpha = 90^\circ$ $\beta = 92.0840(10)^\circ$ $\gamma = 90^\circ$
Cell volume	3200.8(5) x 10 ⁶ pm ³
Z	Z = 4
Density (calculated)	1.189 g/cm ³
Temperature	200 K
θ -Range	1.35 \leq θ \leq 28.36 $^\circ$
Scan	ω -Scan, $\Delta \omega = 0.3^\circ$
Index ranges	-13 \leq h \leq 13, -14 \leq k \leq 14, -39 \leq l \leq 40
Number of reflections measured	38502
Unique reflections	7965
Reflections observed	5005 (I > 2 σ)
Parameter refined	398
Residual electron density	0.916 x 10 ⁻⁶ e/pm ³
Corrections	Lorentz and polarisation, exp. absorption correction
Structure solution	direct methods
Structure refinement	full matrix least square on F ²
Programs used	SHELX-97, xpma, zortep
R indices	R ₁ = 0.0973 (I > 2 σ) R _w = 0.1833 (all data against F ²)



Standard deviations are given in parentheses.

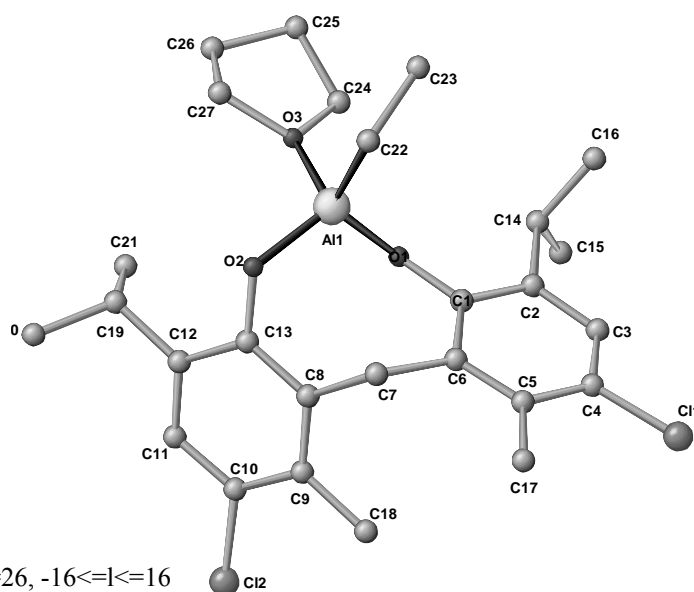
Selected bonds lengths [Å] and angles [°] for **3g**

Al(1)-O(2)	1.674(2)	O(1)-Al(1)-O(2)	118.5(2)
Al(1)-O(1)	1.844(2)	O(1)-Al(1)-O(3)	116.06(18)
Al(1)-Cl(1)	2.0898(12)	O(2)-Al(1)-O(3)	113.82(18)
Al(1)-Al(1)#1	2.8218(17)	O(1)-Al(1)-O(3)#	109.20(17)
O(1)-Al(1)#1	1.845(2)	O(2)-Al(1)-O(3)#1	112.03(19)
O(2)-C(13)	1.367(3)	C(1)-O(1)-Al(1)	144.2(3)
C(1)-C(6)	1.393(4)	C(13)-O(2)-Al(1)	130.7(3)
C(1)-C(2)	1.413(4)	C(30)-O(3)-Al(1)	133.9(4)
C(6)-C(7)	1.525(4)	C(30)-O(3)-Al(1)#1	127.0(4)
C(7)-C(8)	1.504(4)	O(1)-C(1)-C(2)	120.5(5)
C(8)-C(9)	1.392(4)	C(6)-C(1)-C(2)	120.4(5)
C(8)-C(13)	1.401(4)	Al(1)-O(3)-Al(1)#1	99.07(17)

10.12 Crystallographic data of the complex 4a

There is half a molecule in the independent unit of the elementary cell.

Compound	4a
Empirical formula	AlC ₂₅ H ₃₇ O ₃ Cl ₂
Formula weight	506,9
Crystal size	0.3 x 0.2 x 0.2 mm ³
Crystal system	monoclinic
Space group	P2(1)/c (No. 14)
Unit cell dimension	a = 11.9118(11) b = 19.9307(18) c = 12.3076(11) $\alpha = 90^\circ$ $\beta = 112.3650(10)^\circ$ $\gamma = 90^\circ$
Cell volume	2702.2(4) x 10 ⁶ pm ³
Z	Z = 4
Density (calculated)	1.242 g/cm ³
Temperature	200 K
θ -Range	1,85 \leq θ \leq 28,30 $^\circ$
Scan	ω -Scan, $\Delta \omega = 0.3^\circ$
Index ranges	-15 \leq h \leq 11, -24 \leq k \leq 26, -16 \leq l \leq 16
Number of reflections measured	19742
Unique reflections	6572
Reflections observed	3630 (I > 2 σ)
Parameter refined	324
Residual electron density	0.612 x 10 ⁻⁶ e/pm ³
Corrections	Lorentz and polarisation, exp. absorption correction
Structure solution	direct methods
Structure refinement	full matrix least square on F ²
Programs used	SHELX-97, xpma, zortep
R indices	R ₁ = 0.0595 (I > 2 σ) R _w = 0.1270 (all data against F ²)



Standard deviations are given in parentheses.

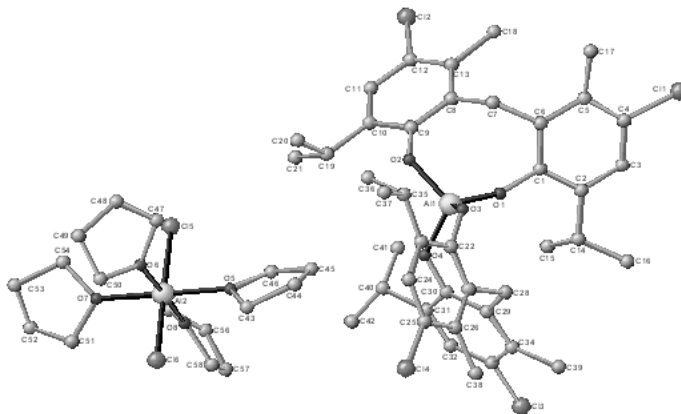
Selected bonds lengths [Å] and angles [°] for **4a**.

Cl(1)-C(4)	1.755(3)	O(1)-Al(1)-O(2)	109.16(10)
Cl(2)-C(17)	1.760(3)	O(1)-Al(1)-O(3)	98.63(10)
Al(1)-O(1)	1.728(2)	O(1)-Al(1)-C(22)	119.73(13)
Al(1)-O(2)	1.735(2)	C(27)-O(3)-Al(1)	121.56(18)
Al(1)-O(3)	1.877(2)	C(1)-C(6)-C(7)	118.7(3)
Al(1)-C(22)	1.941(3)	O(2)-C(13)-C(12)	118.0(3)
O(1)-C(1)	1.353(3)	C(8)-C(9)-C(18)	121.3(3)
O(2)-C(13)	1.364(3)	C(11)-C(10)-Cl(2)	116.7(2)
O(3)-C(24)	1.475(4)	O(3)-C(27)-C(26)	102.3(2)
O(3)-C(27)	1.484(4)	C(25)-C(26)-C(27)	102.2(3)
C(2)-C(14)	1.519(5)	C(20)-C(19)-C(21)	111.5(3)
C(5)-C(17)	1.512(5)	C(8)-C(9)-C(18)	121.3(3)
C(6)-C(7)	1.528(4)	C(3)-C(4)-Cl(1)	117.1(3)
C(8)-C(13)	1.410(4)	C(5)-C(4)-Cl(1)	120.2(3)

10.13 Crystallographic data of the complex 4b

There is one molecule of 4b crystallising with 1.1 molecules of THF per unit (0.5 THF plus 0.6 THF, latter disordered).

Compound	4b
Empirical formula	C _{62.40} H _{88.80} Al ₂ Cl
Formula weight	1251.19
Crystal size	0.4 x 0.35 x 0.2:
Crystal system	monoclinic
Space group	P2(1)/n (No. 14)
Unit cell dimension, [Å]	a = 12.4402(7) b = 24.6826(13) c = 22.2765(12) $\alpha = 90^\circ$ $\beta = 91.8210(10)$ $\gamma = 90^\circ$
Cell volume	6836.7(6) x 10 ⁶
Z	Z = 4
Density (calculated)	1.216 g/cm ³
Temperature	200 K
θ -Range	1.23 \leq θ \leq 28.29°
Scan	ω -Scan, $\Delta \omega = 0.3^\circ$
Index ranges	-16 \leq h \leq 16, -32 \leq k \leq 32, -29 \leq l \leq 29
Number of reflections measured	82505
Unique reflections	16794
Reflections observed	6105 (I > 2 σ)
Parameter refined	324
Residual electron density	0.612 x 10 ⁻⁶ e/pm ³
Corrections	Lorentz and polarisation, exp. absorption correction
Structure solution	direct methods
Structure refinement	full matrix least square on F ²
Programs used	SHELX-97, xpsa, zortep
R indices	R ₁ = 0.0978 (I > 2 σ) R _w = 0.2694 (all data against F ²)



Standard deviations are given in parentheses.

Selected bonds lengths [Å] and angles [°] for **4a**.

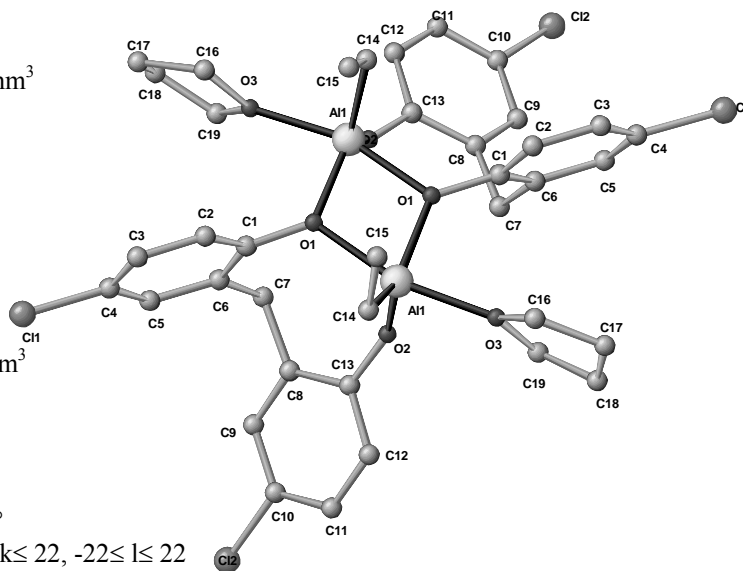
Cl(1)-C(4)	1.769(6)	O(1)-Al(1)-O(2)	108.3(2)
Cl(2)-C(12)	1.765(6)	O(1)-Al(1)-O(4)	107.9(2)
Cl(3)-C(33)	1.767(6)	O(2)-Al(1)-O(4)	111.4(2)
Cl(4)-C(25)	1.764(6)	O(1)-Al(1)-O(3)	115.7(2)
Cl(5)-Al(2)	2.246(3)	O(2)-Al(1)-O(3)	107.7(2)
Cl(6)-Al(2)	2.225(3)	O(4)-Al(1)-O(3)	105.7(2)
Al(1)-O(1)	1.726(4)	O(6)-Al(2)-O(8)	178.4(2)
Al(1)-O(2)	1.739(4)	O(6)-Al(2)-O(5)	90.4(2)
Al(1)-O(3)	1.747(4)	O(8)-Al(2)-O(5)	91.3(2)
Al(1)-O(4)	1.746(4)	O(6)-Al(2)-O(7)	89.8(2)
Al(2)-O(5)	1.955(5)	O(8)-Al(2)-O(7)	88.5(2)
Al(2)-O(6)	1.944(5)	O(5)-Al(2)-O(7)	179.8(2)
Al(2)-O(7)	1.955(5)	Cl(6)-Al(2)-Cl(5)	178.90(13)

Al(2)-O(8)	1.949(5)	C(1)-O(1)-Al(1)	144.9(4)
O(1)-C(1)	1.336(6)	C(9)-O(2)-Al(1)	126.6(4)
O(2)-C(9)	1.349(7)	C(22)-O(3)-Al(1)	123.3(4)
O(3)-C(22)	1.357(7)	C(30)-O(4)-Al(1)	129.6(4)
O(4)-C(30)	1.361(7)	C(46)-O(5)-C(43)	108.5(6)
O(5)-C(43)	1.470(10)	C(46)-O(5)-Al(2)	127.5(5)
O(5)-C(46)	1.440(9)	C(43)-O(5)-Al(2)	123.8(4)
O(6)-C(47)	1.495(9)	C(50)-O(6)-C(47)	105.5(6)
O(6)-C(50)	1.475(8)	C(50)-O(6)-Al(2)	128.2(4)
O(7)-C(51)	1.474(8)	C(51)-O(7)-Al(2)	124.8(4)
O(7)-C(54)	1.465(8)	C(58)-O(8)-C(55)	105.9(6)
O(8)-C(55)	1.495(10)	C(58)-O(8)-Al(2)	127.6(5)
O(8)-C(58)	1.453(9)	C(55)-O(8)-Al(2)	125.9(5)

10.14 Crystallographic data of the complex **6a**

There is 0.5 molecules in the independent unit of the elementary cell crystallising with 0.5 THF solvent molecules on special position.

Compound	6a
Empirical formula	C ₃₆ H ₄₁ Al ₃ Cl ₄ O ₄
Formula weight	760.43
Crystal size	0.4 x 0.5 x 0.05 mm ³
Crystal system	orthorhombic
Space group	Iba2 (No. 45)
Unit cell dimension	a = 15.0671(11) b = 16.8044(13) c = 16.8539(13) $\alpha = 90^\circ$ $\beta = 90^\circ$ $\gamma = 90^\circ$
Cell volume	4267.3(6) x 10 ⁶ pm ³
Z	Z = 8
Density (calculated)	1.343 g/cm ³
Temperature	200 K
θ -Range	1.82 \leq θ \leq 28.32 $^\circ$
Scan	ω -Scan, $\Delta \omega = 0.3^\circ$
Index ranges	-19 \leq h \leq 19, -22 \leq k \leq 22, -22 \leq l \leq 22
Number of reflections measured	25002
Unique reflections	5257
Reflections observed	3345 (I > 2 σ)
Parameter refined	264
Residual electron density	0.489 x 10 ⁻⁶ e/pm ³
Corrections	Lorentz and polarisation, exp. absorption correction
Structure solution	direct methods
Structure refinement	full matrix least square on F ²
Programs used	SHELX-97, xpma, zortep
R indices	R1 = 0.0617 (I > 2 σ) Rw = 0.1186 (all data against F ²)



Standard deviations are given in parentheses.

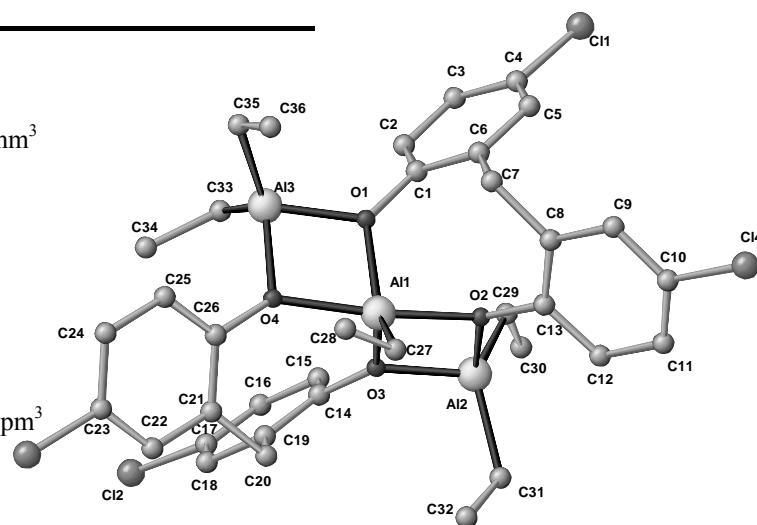
Selected bonds lengths [Å] and angles [°] for **6a**.

Cl(1)-C(4)	1.748(4)	O(2)-Al(1)-O(1)#1	112.37(15)
Cl(2)-C(10)	1.749(4)	O(2)-Al(1)-C(14)	122.71(18)
Al(1)-O(1)#1	1.829(2)	O(1)#1-Al(1)-C(14)	124.84(18)
Al(1)-C(14)	1.958(4)	O(2)-Al(1)-O(3)	88.56(15)
Al(1)-O(2)	1.729(3)	O(3)-Al(1)-O(4)	94.52(17)
O(1)-C(1)	1.375(4)	O(1)-Al(1)-O(3)	163.72(11)
O(1)-Al(1)#1	1.829(2)	C(1)-O(1)-Al(1)#1	129.2(2)
O(2)-C(13)	1.338(5)	C(1)-O(1)-Al(1)	125.0(2)
O(3)-C(16)	1.463(5)	Al(1)#1-O(1)-Al(1)	105.23(11)
O(3)-C(19)	2.938(3)	C(13)-O(2)-Al(1)	144.0(3)
C(6)-C(7)	1.521(6)	C(16)-O(3)-C(19)	108.8(3)
C(1)-C(6)	1.406(6)	C(3)-C(4)-Cl(1)	119.4(4)

10.15 Crystallographic data of the complex **6c**

There is half a molecule in the independent unit of the elementary cell.

Compound	6c
Empirical formula	Al ₃ C ₃₆ H ₄₁ O ₄ Cl ₄
Formula weight	760.43
Crystal size	0.3 x 0.3 x 0.05 mm ³
Crystal system	triclinic
Space group	P-1 (No, 2)
Unit cell dimension	a = 10,170(3) b = 12,322(4) c = 16,273(5) α = 71,32(3)° β = 86,68(3)° γ = 79,61(2)°
Cell volume	1900.0(10) x 10 ⁶ pm ³
Z	Z = 2
Density (calculated)	1.329 g/cm ³
Temperature	200 K
θ-Range	1,43 ≤ θ ≤ 28,31°
Scan	ω-Scan, Δ ω=0.3°
Index ranges	-13 ≤ h ≤ 13, -16 ≤ k ≤ 16, -21 ≤ l ≤ 21
Number of reflections measured	22330
Unique reflections	9174
Reflections observed	3978 (I > 2 σ)
Parameter refined	792
Residual electron density	0.489 x 10 ⁻⁶ e/pm ³
Corrections	Lorentz and polarisation, exp. absorption correction
Structure solution	direct methods
Structure refinement	full matrix least square on F ²
Programs used	SHELX-97, xpsa, zortep
R indices	R ₁ = 0.2086 (I > 2 σ) R _w = 0.2318 (all data against F ²)



Standard deviations are given in parentheses.

Selected bonds lengths [Å] and angles [°] for **6c**.

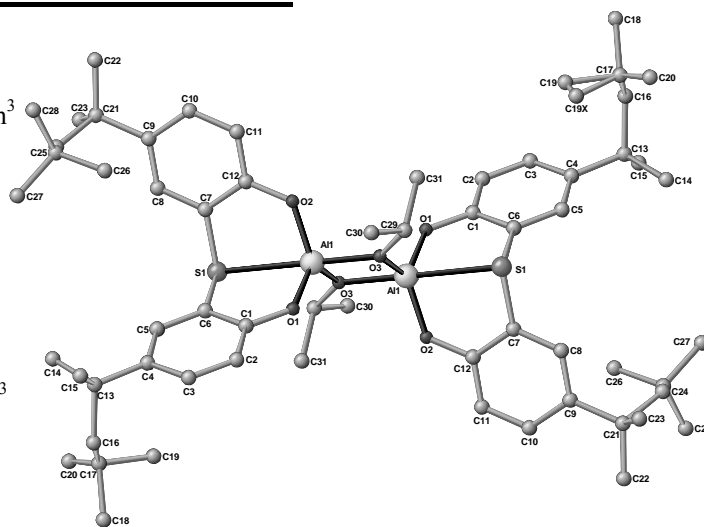
Cl(1)-C(4)	1.735(5)	O(1)-Al(1)-O(3)	103.09(17)
Cl(2)-C(17)	1.743(6)	O(1)-Al(1)-C(27)	129.9(2)
Cl(3)-C(23)	1.742(5)	O(3)-Al(1)-C(27)	127.0(2)
Cl(4)-C(10)	1.748(6)	O(1)-Al(1)-O(4)	76.29(15)
Al(1)-O(1)	1.850(4)	O(3)-Al(1)-O(4)	94.71(16)
Al(1)-O(3)	1.852(4)	C(27)-Al(1)-O(4)	99.4(2)
Al(1)-C(27)	1.958(5)	O(1)-Al(1)-O(2)	94.13(16)
Al(1)-O(4)	1.960(4)	O(3)-Al(1)-O(2)	76.76(15)
Al(1)-O(2)	1.962(4)	C(27)-Al(1)-O(2)	95.0(2)
Al(1)-Al(3)	2.938(3)	O(4)-Al(1)-O(2)	165.59(16)
Al(1)-Al(2)	2.939(2)	O(1)-Al(1)-Al(3)	37.98(11)
Al(2)-O(2)	1.853(4)	O(3)-Al(1)-Al(3)	99.65(13)
Al(2)-O(3)	1.883(4)	C(27)-Al(1)-Al(3)	122.34(18)

Al(2)-C(29)	1.945(6)	O(4)-Al(1)-Al(3)	38.38(10)
Al(2)-C(31)	1.952(6)	O(2)-Al(1)-Al(3)	130.78(12)
Al(3)-O(4)	1.856(4)	O(1)-Al(1)-Al(2)	101.64(13)
Al(3)-O(1)	1.867(4)	O(3)-Al(1)-Al(2)	38.48(11)
Al(3)-C(33)	1.989(7)	C(27)-Al(1)-Al(2)	115.44(18)
Al(3)-C(35)	1.910(7)	O(4)-Al(1)-Al(2)	132.36(12)
		O(2)-Al(1)-Al(2)	38.29(11)
		Al(3)-Al(1)-Al(2)	122.22(8)
		O(2)-Al(2)-O(3)	78.72(15)

10.16 Crystallographic data of the complex **7g**

There is half a molecule in the independent unit of the elementary cell.

Compound	7g
Empirical formula	C _{34.50} H ₄₉ AlO ₃ S
Formula weight	570.78
Crystal size	0.4 x 0.2 x 0.08 mm ³
Crystal system	triclinic
Space group	P-1 (No. 2)
Unit cell dimension	a = 8.5211(6) b = 12.0192(8) c = 18.0161(12) α = 93.3480(10) [°] β = 100.3980(10) [°] γ = 108.0640(10) [°]
Cell volume	1712.4(2) x 10 ⁶ pm ³
Z	Z = 2
Density (calculated)	1.107 g/cm ³
Temperature	200 K
θ -Range	1.80 ≤ θ ≤ 28.31 [°]
Scan	ω -Scan, $\Delta\omega=0.3^{\circ}$
Index ranges	-11 ≤ h ≤ 11, -16 ≤ k ≤ 16, -24 ≤ l ≤ 23
Number of reflections measured	20932
Unique reflections	8255
Reflections observed	4551 (I > 2 σ)
Parameter refined	618
Residual electron density	0.577 x 10 ⁻⁶ e/pm ³
Corrections	Lorentz and polarisation, exp. absorption correction
Structure solution	direct methods
Structure refinement	full matrix least square on F ²
Programs used	SHELX-97 , xpma, zortep
R indices	R ₁ = 0.0687 (I > 2 σ) R _w = 0.1905 (all data against F ²)



Standard deviations are given in parentheses.

Selected bonds lengths [Å] and angles [°] for **7g**.

S(1)-C(7)	1.777(3)	C(7)-S(1)-C(6)	105.40(13)
S(1)-C(6)	1.780(3)	C(7)-S(1)-Al(1)	89.09(9)
S(1)-Al(1)	2.6798(11)	C(6)-S(1)-Al(1)	88.43(9)
Al(1)-O(2)	1.736(2)	O(2)-Al(1)-O(1)	118.21(10)
Al(1)-O(1)	1.744(2)	O(2)-Al(1)-O(3)	122.35(10)
Al(1)-O(3)	1.813(2)	O(1)-Al(1)-O(3)	117.73(10)
Al(1)-O(3)#1	1.8428(19)	O(2)-Al(1)-O(3)#1	100.18(9)
Al(1)-Al(1)#1	2.8005(16)	O(1)-Al(1)-O(3)#1	102.93(9)
O(1)-C(1)	1.342(3)	O(3)-Al(1)-O(3)#1	79.99(9)
O(2)-C(12)	1.350(3)	O(2)-Al(1)-S(1)	81.43(7)
O(3)-C(29)	1.473(3)	O(1)-Al(1)-S(1)	81.78(7)
O(3)-Al(1)#1	1.8429(19)	O(3)-Al(1)-S(1)	93.65(6)
		O(3)#1-Al(1)-S(1)	173.32(7)
		O(3)#1-Al(1)-Al(1)#1	39.60(6)

S(1)-Al(1)-Al(1)#1	134.01(5)
O(2)-Al(1)-Al(1)#1	117.56(8)
O(1)-Al(1)-Al(1)#1	116.64(8)
O(3)-Al(1)-Al(1)#1	40.39(6)
C(1)-O(1)-Al(1)	128.21(18)
C(12)-O(2)-Al(1)	129.13(19)
C(29)-O(3)-Al(1)	128.96(16)
C(29)-O(3)-Al(1)#1	129.48(16)
Al(1)-O(3)-Al(1)#1	100.01(9)

11 Danksagung

An erster Stelle möchte ich mich bei meinen Eltern für Ihre Unterstützung während der gesamten Ausbildung bedanken.

Der Dank gilt auch für alljene, die mich während meines Aufenthaltes in Deutschland unterstützten. Ganz besonders möchte ich mich bei Herrn Prof. Dinjus bedanken. Er eröffnete mir die Möglichkeit, diese Arbeit durchzuführen.

Meinem Betreuer Herrn Dr. Thomas A. Zevaco bin ich für seine große Geduld und Verständnis, sowie für die gemeinsamen Stunden wissenschaftlicher und nicht wissenschaftlicher Diskussionen dankbar. Auf eine sehr konstruktive Art und Weise zeigte mir Dr. Zevaco die Wege der Forschungsarbeit. Meine Abschlussarbeit wäre auch nicht komplett ohne Hilfe von Frau Anette Janssen, die mich in die Autoklaventechnik einführte und mir bei den Polymeren geholfen hat. Für beide *Chapeaux bas*.

Mein herzlicher Dank gilt ebenso Herrn Dr. Albers; er hat mich in die Geheimnisse der Vakuumtechnik eingeführt.

Für die zahlreichen Röntgenstrukturanalysen danke ich Dr. Olaf Walter. Auch dafür, dass ich, dank seiner und der des Herrn Dr. Pitter Unterstützung bei den vielen Diskussionen nicht nur wissenschaftlicher Natur, meine Deutschkenntnisse verbessern konnte.

Meinen Freunden Dr. Martin Ahlman, Johannes Artner, Ortrud Aschenbrenner, Kacper Černý, Dr. Maria Debu, Dr. Erika Ember, Fengfwen Fan, Dr. Stephan Flicker, Melany Frank, Angelika Gorschinski, Cezar Ionescu, Anette Janssen, Pedro d'Jesus, Dr. Mario Kröger, Dr. Piotr Makarczyk, Constantin Maniut, Fatima Mesri, Dr. Florian Patcas, Alexander Schäfer, Sebastian Seibold, Danuta Sereżyńska, Dr. Uwe Storzer danke ich besonders herzlich für die nette Atmosphäre während und nach der Arbeit. Ihr alle habt mir sehr geholfen, die Sprache Schillers kennenzulernen.

Danke

Najznacniejszą osobą, wspierają mnie każdego dnia jest moja żona, najważniejsza dla mnie osoba. Dziękuję Ci, Agnieszko, za Twoje zrozumienie dla moich spraw zawodowych, za twoje wsparcie duchowe jakiego mi udzielałaś i cały czas udzielasz. Dzięki Twojemu przekonywaniu zdecydowaliśmy o kilku trudnych, a także istotnych dla mnie rzeczach.

Dziękuję Ci.

The most important person supporting me on a daily basis is my wife, Agnieszka. Thank you very much for your understanding concerning my professional problems, as well as your moral support. You have convinced me to take some difficult but very significant decisions.

Thank you.